THE UNIVERSITY
of EDINBURGH

The Impact of Atypical Porcine Pestivirus (APPV) in Great Britain

Holly Hill

Thesis submitted for the degree of Doctor of Philosophy

The University of Edinburgh

2021

Declaration

I hereby declare that this thesis is composed entirely by myself, and it contains no material previously submitted in substance for any other degree. The work reported in this thesis herein is my own, except where due acknowledgement or reference is made in the text.

Holly Hill

Abstract

Atypical porcine pestivirus (APPV) is a positive-sense ribonucleic acid (RNA) enveloped virus belonging to the *Pestivirus* genus, a group of viruses known for their high socio-economic impact. Since its discovery in 2015, APPV has been established as the causative agent of congenital tremor type A-II (CT A-II). The overarching aim of this study was to investigate host—pathogen interactions with regards to the clinical, pathological and immunological outcomes with a focus on the British pig industry.

As no commercially available diagnostics are currently available, it was initially necessary to establish techniques capable of detecting the virus and APPV-specific antibodies. To aid in diagnostic assay development and to characterise host—pathogen interactions in an initial in vivo viral amplification was undertaken, Three one-week-old piglets were inoculated with tissue homogenate supernatant from three British CT A-II outbreaks. Peak viraemia detected by RT-qPCR was observed by nine days post inoculation (DPI). APPV shedding was detected from seven DPI in oropharyngeal and rectal swabs and from nine DPI in nasal swabs. APPV was found in all tissue types, with the highest viral loads detected in lymphoid tissues.

To understand APPV transmission and the infection dynamics in naturally occurring CT A-II outbreaks, two farrowing groups from a Scottish CT A-II outbreak were studied. The exploratory study (first farrowing group) determined the relationship between clinical status, virus presence, and antibody response over time. There was no significant relationship between clinical status and viral load at either two or eight weeks of age, nor was there a difference between the two age groups. Similarly, no relationship was observed between clinical status and level of APPV-specific antibodies present at either age. However, there was a significant reduction in antibody levels between two and eight weeks regardless of clinical status indicating a probable maternal origin of the antibody. Viral loads among different tissue types varied

significantly: brain and Peyer's patches showed less detectable virus than lymph nodes, thymus and tonsil. APPV BaseScope ISH analysis of the CNS revealed a high concentration of APPV RNA in the cerebellum, hippocampus and the spinal cord identifying APPV cell and tissue tropism (neuronal and lymphatic).

A longitudinal cohort study followed piglets from a second farrowing group from 2.5 weeks of age until slaughter. This study aimed to understand virus-host interactions, including the potential for viral persistence. In line with establishing diagnostic techniques, ear tissue was assessed for its suitability as a diagnostic sample.

The viral load in both clinical and non-clinical animals was highly variable. APPV was detected in serum at 2.5 weeks of age, suggests either vertical transmission (most likely for clinical animals) or early postnatal horizontal transmission by direct contact. At 10 weeks, 24% of piglets were viremic for the first time, indicating horizontal transmission. Of all the initially infected animals, 97% were APPV RNA free at slaughter, indicating that none exhibited persistent viraemia. Maternally-derived APPV-specific antibodies were found to be greatly reduced in the majority of piglets (89%) at slaughter. However, APPV-specific antibody levels increased fivefold demonstrating not only exposure of the whole farrowing group to the virus and seroconversion, but also a lack of persistent infection, even in clinical animals, differentiating APPV from closely related pestiviruses.

A lack of relationship between clinical signs, APPV viral load in serum or ear tissue at 2.5 weeks and the length of time to slaughter suggests a limited impact of APPV on growth of the animals. There was also no relationship between the clinical status at 2.5 weeks and viral load in serum; however, there was a positive relationship between clinical status and APPV viral load in ear tissue. A weak positive correlation was found between viral loads in serum and ear tissue, indicating that ear tissue is a suitable sample type for the diagnosis

of APPV infection by RT-qPCR. Interestingly, APPV was also detected in high amounts in raw (non-extended) semen, indicating the potential for venereal transmission, although further investigation is needed.

In natural cases of CT A-II, APPV has been found in comorbidity with other porcine pathogens. ‘Classical’ pestiviruses are also known to induce immunosuppression of the host, which may lead to enhanced disease or increased susceptibility to co-infections. To investigate the potential effect of APPV on the immune system and to determine its contribution to disease during co-infection with another pathogen, 10-week-old piglets from the Scottish CT A-II field outbreak were co-infected with porcine respiratory and reproductive syndrome virus (PRRSV). Although no significant differences in antibody level or viral load were found between APPV positive and negative groups, there was a clear interaction between APPV and PRRSV, suggesting that although APPV did not enhance or prolong PRRSV viraemia, viral interference might have occurred. Significant differences in febrile response were observed between the APPV positive and APPV negative PRRSV challenged groups. APPV was also found to increase lung consolidation, a recognised sign of PRRSV infection, suggesting that APPV may play a role in enhancing pathology.

Following the Scottish CT A-II field outbreak investigation, a more comprehensive epidemiological survey of 108 Scottish pig farms was conducted to determine the presence of APPV and the extent of exposure to the virus within the Scottish pig population. APPV was detected by RT-qPCR in 4.7% of samples within the study, with viral ribonucleic acid (RNA) detected in one or more sample on 33 out of 108 farms. Additionally, of the 1,077 samples tested, 48.8% were antibody positive by ELISA and 93 out of 108 farms tested had at least one seropositive sample.

A broad investigation into APPV presence within semen was conducted: 475 pooled semen samples submitted from 41 commercial stud units were tested for the presence of APPV. No virus was detected in any of the pools tested.

This project is the first step to understanding APPV associated CT A-II in the British pig industry, providing insights into the pathogenesis and immunogenicity of the virus, alongside the development of validated diagnostic techniques for the detection of British APPV strains.

Lay Summary

A common condition affecting new-born piglets, congenital tremor type A-II (CT A-II), also known as shaker or dancing pigs, has been observed worldwide for over 100 years; however, until recently, the cause of the disease was unknown. Since its discovery in 2015, atypical porcine pestivirus (APPV) has been associated with CT A-II, which was reproduced by experimentally infecting pregnant sows with APPV. Piglets from these sows had tremors varying from mild twitching to constant, whole body shaking often resulting in death without intervention. Currently, there are no commercial tests available for detecting APPV, and outbreaks of CT A-II are most commonly diagnosed based on clinical signs. At present the relationship between APPV and clinical disease, and the interaction between APPV and the piglet's immune system or other common pig organisms is largely unknown. As the diagnosis is usually based on clinical manifestation, the true extent of the spread of the virus within Great Britain is unknown. There were three main aims in this work: (1) to develop diagnostic techniques to detect the virus and virus-specific antibodies, (2) to use the newly developed tools to understand how the virus interacts with the piglet and its immune system both in natural and experimental infections, and (3) to determine the level of APPV circulating within the British pig industry.

Assays capable of detecting APPV and APPV-specific antibodies were developed and subsequently used to determine the outcome of an experimental infection in one-week-old piglets. No tremors were observed during the study, virus was detected in the blood and reached a peak between seven and nine days after infection. APPV also was detected in oral, nasal and rectal swabs, suggesting that these bodily fluids/secretions pose a transmission risk.

A natural CT A-II outbreak on a commercial pig farm in Scotland was investigated to understand the relationship between the virus and the disease. The study found that the virus can be transmitted both during pregnancy and after birth between piglets via direct contact and that viral infection can persist in blood and tissue up to 8 weeks. Based on these results, studying clinically affected piglets for longer than 8 weeks of age appeared essential to determine how long the piglets remain infected.

A second group of affected and unaffected piglets was followed from 2.5 weeks of age until slaughter (between 22 and 28 weeks old) monitoring blood virus levels and APPV specific antibodies to assess whether the infection was cleared or if animals remained persistently infected. In addition, an ear notch was collected at 2.5 weeks of age to compare the virus level in this tissue type to serum and the occurrence of clinical signs, to assess the suitability of this sample type for diagnostic purposes.

Most (26/37) animals infected at 2.5 weeks of age cleared the infection by 10 weeks of age. All but 2 of the 37 animals resolved the infection by the time of slaughter. Antibody levels present in serum dropped by week 10, followed by an increase afterwards, which indicates an active antibody response to the virus. Approximately a quarter of the animals that did not have detectable virus at 2.5 weeks of age had demonstrable APPV levels at 10 weeks, supporting animal-to-animal transmission. Within the tissue collected at slaughter, the highest amount of virus was detected in the lymphatic organs including lymph node and spleen. A high concentration of virus was also detected in semen. The pattern of infection observed in this group and the ability of the animals to mount an antibody response suggests that APPV infection did not cause suppression of their immune system. Further investigation of how APPV interacts with the immune system of the piglets is required to understand its role in this disease.

When evaluating the value of ear tissue as a diagnostic sample, more animals with clinical signs had detectable levels of APPV in ear tissue compared to blood and if the amount of virus was high in ear tissue, it was also increased in the blood, indicating that ear samples are better than blood for the detection of APPV. This will allow a new diagnostic approach for APPV detection, as ear samples can be collected by the farmer using sampling ear tags, combining sample collection and piglet marking, reducing the need for a veterinary intervention, which blood sampling requires.

The potential for APPV to suppress the piglet's immune system, leaving the animals more susceptible to secondary infections, was further explored using naturally-infected animals from a Scottish field outbreak. In brief, APPV infected or non-infected piglets were challenged with porcine respiratory reproductive syndrome virus (PRRSV), an economically significant virus frequent in the UK pig industry and known to cause severe disease. Although having an active APPV infection did not affect the length or severity of PRRSV infection, there was an increase in rectal temperature, which persisted for longer and more lung damage in the APPV group indicating an increased inflammatory response. The evidence from the co-infection suggests that a simultaneous APPV infection increased susceptibility to PRRSV and could enhance disease.

As previously established by the detection of APPV in the natural CT field outbreak, the virus is present in Scotland; however, the frequency of circulating virus and the extent of national herd exposure were unknown. In order to determine this, a survey of 108 Scottish pig farms was performed. Of the farms, 30% had at least one animal with detectable levels of APPV by molecular testing, moreover 86% of farms had animals that were positive for APPV-specific antibodies, indicating previous exposure to the virus. This further highlights the level of undetected virus circulating within the Scottish pig industry.

This research highlights the significance of understanding APPV associated CT A-II within the British pig industry through the employment of diagnostic tests to investigate the distribution of the virus, how it is transmitted, and its relationship with disease to better inform future prevention, control and eradication strategies.

Acknowledgements

I am so fortunate to have had the experience to work alongside so many lovely and talented people during my PhD project, not only within the Moredun group itself, including Moredun Scientific (MSL) and the Moredun Research Institute (MRI) but also at other collaborating institutes including the Roslin Institute, University of Edinburgh (UoE), Scotland's Rural College (SRUC), the Animal and Plant Health Agency (APHA), Biomathematics and Statistics Scotland (BioSS), Quality Meat Scotland (QMS), the University of Gießen and Centre de Recerca en Sanitat Animal (CReSA).

I would like to give special thanks to MSL as the funders of my project, and John Murray and John Mackinnon for their unwavering support, and David Reddick and Cliff Rammage for their expertise in the design and implementation of animal studies carried out on site.

I would like to thank my primary supervisors Dr Tom McNeilly (MRI) and Tanja Opriessnig (UoE and the Roslin Institute), and their lab groups for their continuous support and guidance, without which I could not have completed my studies. Thank you to Dr Mara Rocchi (MRI) for her steadfast commitment to the project and agreeing to join my supervisory team. I am incredibly grateful to her for her technical support and pastoral care. I would also like to thank her lab group: Maddy Maley, Ellie Laming and Dylan Turnbull, for not only the technical training and guidance but for also giving me such a warm welcome making me feel part of the team. Thank you also to Dr Francesca Chianini for her supervision in the early stage of this project.

I would like to give special thanks to those who helped me achieve the practical and technical aspects of this project, including past and present members of the histopathology department for sample collection and processing, namely Clare Underwood, Val Hughes, Dr Mark Dagleish and fellow student Dr Gaston Caspe but also to Dr Jo Moore for her pathological expertise with regards to

the BaseScope ISH analysis. I would also like to thank SRUC's histopathology department for additional support in this area. A big thank you to Dr George Russell for help with cloning, Dr Keith Ballingall for assistance with sequencing, Dr Jennifer Thacker (SRUC) and her department for technical advice and the use of her lab and equipment at short notice, and Dr Adam Hayward for his help with R analysis software and statistics and patience with my lack of statistical knowhow. I would also like to say a special thank you to Dr David Ewing (BioSS) for his help with power calculations for the co-infection study and the Scottish sero-survey and Dr Giles Innocent (BioSS) for his modelling of positive thresholds for the NS3 indirect ELISA.

I am incredibly grateful for all of the Bioservices and High security unit department staff, without whom my animal studies on site would not have been possible, and especially to Dr Stephen Anderson for the organisational aspect and to Louise Gibbard and Dawn MacMillan-Christensen for their work with the snatch farrowed colostrum deprived piglets.

I would also like to express my deep gratitude for David Frew (MRI), Allan Ward (QMS), Calum Wilson (SRUC), Prof. Jill Thompson for their commitment to the collection of abattoir samples as part of the longitudinal Scottish cohort study without who this could not have been undertaken. Jill has been instrumental in the organisation and implementation of the later part of this study. She has also been of great help and support throughout my studies, offering her expertise in pathology and providing clinical material. In this vein, I would like to also thank the farm and the farm's veterinary team (who wish to remain anonymous) for help in the collection of samples from the piglets while on the farm. I would like to thank Dr Susanna Williamson (APHA) for her wealth of knowledge and expertise during this project and the organisation and provision of clinical material, without which I could not have established diagnostic techniques. For this reason, a thank you must also go to my collaborator Dr Benjamin Lamp and his group at the University of Gießen for the preparation and provision of material for the NS3 blocking and indirect

ELISAs. Additionally, I would like to say thank you to Dr Quim Segalés, Dr Llilianne Ganges and her group for the support and advice given to me during the project and the opportunity to visit CReSA for training and knowledge exchange.

I would like to show my appreciation for all of the love and support given by my friends and family through my PhD by dedicating my thesis to them. I would not have had the courage or determination to finish this without you. Thank you to my dad Bernard and sister Chloe for their tireless support proofreading and formatting, my best friend John Lawlor, not only for all of his counsel but for his artistic talent which features in the technical drawings presented in this work and to my father-in-law for his support and keeping me going with endless cups of tea! Lastly, no greater thank you could go to anyone but my ever-patient and long-suffering husband, Kevin: you have moved mountains to fulfil my dreams and been my rock throughout, helping me navigate the stormiest of seas.

Contents

Figures

Tables

Common abbreviations

AIC	Akaike's Information Criteria
APHA	Animal and Plant Health Agency
APPV	Atypical porcine pestivirus
ASFV	African swine fever virus
BDV	Border disease virus
BioSS	Biomathematics and Statistics Scotland
BLAST	Basic local alignment search tool
BT	Bovine turbinate
BVDV	Bovine viral diarrhoea virus
cDNA	Complementary deoxyribonucleic acid
CSFV	Classical swine fever virus
CT	Congenital tremors
Ct	Cycle threshold
CT A-I	Congenital tremors type A-I
CT A-II	Congenital tremors type A-II
CT A-III	Congenital tremors type A-III
CT A-IV	Congenital tremors type A-IV
CT A-V	Congenital tremors type A-V
CV	Coefficient of variance
DIVA	Differentiating infected from vaccinated animals
DMSO	Dimethyl sulfoxide
DNA	Deoxyribonucleic acid
DPI	Days post-inoculation
EDTA	Ethylenediaminetetraacetic acid
ELISA	Enzyme-linked immunosorbent assays
EU	European union
FBS	Fetal bovine serum
FCS	Fetal calf serum
FFPE	Formalin-fixed paraffin-embedded
FISH	Fluorescent *in situ* hybridisation
GAMM	Generalised additive mixed-effects models
GB	Great Britain
GFAP	Glial fibrillary acidic proteins
H&E	Haematoxylin and Eosin
HBSS	Hank's buffered salt solution
HCT-8	Human colorectal tumor cells-8
HRPO	Horseradish peroxidase
IFI	Indirect immunofluorescence test
IFN-γ	Interferon - Gamma

IgG	Immunoglobin G
IHC	Immunohistochemistry
IP	Interstitial pneumonia
IQR	Interquartile range
ISH	*In situ* hybridisation
KCL	Potassium Chloride
LB	Luria Bertani
LBF	Luxol fast blue fast
LCL	Lower control limits
LINDA	Lateral-shaking inducing neurodegenerative agent
LWL	Lower warning limits
MARC-145	Meat Animal Research Center-145
MDBK	Madin-darby bovine kidney
MDCK	Madin-darby canine kidney
MIQE	Minimum information for publication of quantitative real-time experiments
MRI	Moredun Research Institute
NaCl	Sodium chloride
NC	Normalised coefficient
NS	Non-structural protein
NTC	No template control
OD	Optical density
OIE	World Health Organisation of Animal Health
ORF	Open reading frame
PAstV	Porcine astrovirus
PBS	Phosphate-buffered saline
PCR	Polymerase Chain Reaction
PCV2	porcine circovirus type 2
PhoPeV	Phocoena pestivirus
PK-15	Porcine kidney-15
PM	Post mortem
PPgV	Porcine pegivirus
PPIB	Peptidylprolyl isomerase B
PRRS	Porcine reproductive and respiratory syndrome
PRRSV	Porcine reproductive and respiratory syndrome virus
PRRSV-1.2	Porcine reproductive and respiratory syndrome virus species 1 subtype 2
PTV	Porcine teschovirus
RNA	Ribonucleic Acid
RPM	Revolutions per minute
RPMI	Roswell Park Memorial Institute Medium
RT	Reverse transcriptase

RT-PCR	Reverse transcriptase polymerase chain reaction
RT-qPCR	Reverse transcriptase real time quantitative polymerase chain reaction
S/P ratio	Sample/positive ratio
s/s/y	Nucleotide substitutions per site per year
SAPO	Specified animal pathogen order
SD	Standard deviation
SIV	Swine influenza virus
SIV	Swine influenza
SK-6	Swine kidney-6
SRUC	Scotland's rural college
ST	Swine testis
STWS	Scots tap water substitute
swIAV	Swine influenza A
TMB	Tetramethylbenzidine
TWM	Transport and wash media
UCL	Upper control limit
UK	United Kingdom
UWL	Upper warning limit
VNT	Viral neutralisation assay
VTM	Virus transport medium

Chapter 1: Introduction

1.1 Congenital tremor

Congenital tremor (CT), a disease sporadically affecting neonatal piglets, was first described in the USA as “dancing pigs” (Kinsley, 1922.). The condition is also known as “shivers" (Nissley, 1932.), “myoclonia congenita" (Kernkamp, 1950), “trembles” (Brooksbank, 1955), and “shakiness” (Chapman, 1956), all named for the characteristic tremors observed in affected pigs. Over time, a number of factors have been implicated in the development of CT including infection with neurotropic viruses, hereditary genetic disorders, and nutritional deficiencies (Kernkamp, 1950; Brooksbank, 1955; Larsson, 1955; Chapman, 1956).

Subsequently, a different classification of CT has been adopted based on presence (type A) or absence (type B) of morphological lesions in the central nervous system, namely defective myelination of the spinal cord with or without cerebellar hypoplasia and/or dysplasia (Done, 1968). CT type A (referred to as CT A) has been further subdivided depending on the accepted aetiology: A-I is associated with low virulence strains of classical swine fever virus (CSFV) another pestivirus (Harding, Done and Darbyshire, 1966; Bradley *et al.*, 1983), A-III and A-IV are linked to genetic conditions where A-III is sex-linked, affecting a small proportion of male Landrace pigs, whereas A-IV is an autosomal recessive defect of saddleback pigs, usually affecting 25% of the litter (Harding *et al.*, 1973; Patterson *et al.*, 1973; Kidd *et al.*, 1986). CT A-V has been associated with trichlorfon poisoning from feed treated with organophosphates (Knox *et al.*, 1978). Until recently, the aetiology of A-II was unknown despite having long been suspected to be viral-induced (Done, 1968; Patterson *et al.*, 1976). A novel pestivirus, atypical porcine pestivirus, has now been linked to the disease and is considered the aetiologic agent (discussed further in 1.1.2)

1.1.1 Clinical signs

Clinical signs are usually observed in neonatal piglets and are characterised by constant rhythmic non-progressive tremors localised at the head, flanks and hind limbs (Yuan *et al.*, 2017). Tremors vary in intensity and in severe cases they manifest as whole-body shaking and disruption of the ability of piglets to stand, walk and nurse, leading to starvation and death (De Groof *et al.*, 2016; Yuan *et al.*, 2017). In less severe cases, the tremors resolve by the time the piglets are four weeks of age. It has been reported that mild tremors of the flank or ears can persist up to 14 weeks of age in rare cases (Schwarz *et al.*, 2017). In general, tremors are exacerbated during periods of stress and excitement and cease when the piglets are at rest (Arruda *et al.*, 2016; Hansmann *et al.*, 2017). Presently, clinical signs have not been observed in adult animals (Arruda *et al.*, 2016; De Groof *et al.*, 2016; Gatto *et al.*, 2018b).

1.1.2 Viruses associated with congenital tremors

Historically, several viral pathogens have been linked with congenital tremors type A-II (CT A-II), including porcine circovirus type 2 (PCV2) (Hines and Lukert, 1994; Stevenson *et al.*, 2001; Tummaruk and Pearodwong, 2016), porcine astrovirus (PAstV) (Blomström, Ley and Jacobson, 2014), porcine circovirus-like virus P1 (Wen *et al.*, 2018) and lateral-shaking inducing neurodegenerative agent (LINDA) virus (Lamp *et al.*, 2017). The association between PCV2 and CT is controversial (Chae, 2005), and the evidence presented conflicting, with studies finding the virus in both clinically-infected and apparently healthy piglets (Kennedy *et al.*, 2003; Tummaruk and Pearodwong, 2016). Similarly, reverse transcriptase polymerase chain reaction (RT-PCR) also detected PAstV in the brains of healthy piglets and piglets affected with CT (Blomström, Ley and Jacobson, 2014). To date, only one outbreak of LINDA virus has been reported in piglets with CT, on a farm in Austria (Lamp *et al.*, 2017). Similarly, there has only been one report of CT

where porcine circovirus-like virus P1 was detected by reverse transcriptase quantitative polymerase chain reaction (RT-qPCR) in serum, brain and lymph nodes from affected piglets on two farms in the Jiangsu Province of China (Wen *et al.*, 2018). Further investigation is warranted to understand the strength of the association between these viruses and disease.

As CSFV has been established as the causal agent of CT A-I, other pestiviruses have been investigated as potential agents involved in the aetiology of CT A-II. However, as pigs are not the natural host for bovine viral diarrhoea virus (BVDV), infections, even if present in a high proportion of the pigs in the herd, are generally without clinical signs. On very few occasions, the virus has been associated with reproductive issues, including reduced conception rate, abortion or stillbirths and, when piglets are infected *in utero*, clinical signs from birth similar to CSFV-associated CT A-I (Tao *et al.*, 2013; Kirkland, Le Potier and Finlaison, 2019). In a study by Mechler *et al.*, (2018), two gilts underwent intrauterine fetal inoculation at 45 days of gestation with BVDV-2: the sows produced a combined total of 19 piglets, including two mummified (estimated time of death 11- and 16- days post-inoculation [DPI]) and three stillborn; the remaining 14 piglets were born healthy. At post mortem (PM), the affected piglets had a cerebellar brain ratio lower than 9%, a sign of cerebellar hypoplasia associated with CT type A-I. Another experimental infection in which pregnant sows were inoculated with BVDV-1 showed that neonatal piglets displayed clinical signs of weakness, tremors, fever and diarrhoea with splay leg comorbidity consistent with those observed in CT A-I, in animals infected with a low-virulence strain of CSFV (Kulcsár *et al.*, 2001).

Similarly, border disease virus (BDV), another pestivirus affecting sheep and seldom cattle, is also capable of transplacental infection mostly without inducing clinical signs. Although, like BVDV, this is somewhat dependent on both the timing of infection and the viral strain involved, with severe cases leading to reproductive failure and clinical signs in the surviving neonates similar to CSFV (Terpstra and Wensvoort, 1988; Vannier et al., 1988;

Leforban, Vannier and Cariolet, 1992). The main clinical signs of affected neonatal lambs are tremors, abnormal body conformation and hairy appearance to the fleece (which contributes to the colloquialism 'hairy-shaker' or 'fuzzy' lambs given to affected animals) (Nettleton et al., 1998; Toplu et al., 2011). These animals commonly present with hypoplasia of the cerebellum hydranencephaly, and nonsuppurative meningoencephalomyelitis with hypomyelinogenesis (Toplu et al., 2011).

A novel pestivirus-like viral agent (also known as "agent X") with cross-reactivity with anti-BVDV antibodies was identified in neonatal piglets displaying neurological clinical signs of tremor and ataxia from an outbreak in Iowa USA (Pogranichniy, Schwartz and Yoon, 2008). Although, unlike CT A-II, clinical signs were present in weaned pigs and were progressive with head pressing, aggression and paresis leading to death within three days. Sows were also lethargic, febrile and pale before reproductive failure (embryonic/fetal death). The occurrence of progressive neurological clinical signs, presentation of clinical signs in older pigs (including high parity sows) and lack of pathology usually associated with CTs make an association between the virus and CT A-II unlikely. However, no further investigation has been conducted to date.

Since its discovery in 2015, atypical porcine pestivirus (APPV) has been detected in neonatal piglets presenting with tremors typically associated with CT A-II (Arruda *et al.*, 2016; De Groof *et al.*, 2016; Postel *et al.*, 2016; Beer *et al.*, 2017; Schwarz *et al.*, 2017), both as a sole viral agent or in co-infections with CSFV, African swine fever (ASFV), porcine pegivirus (PPgV) and porcine teschovirus (PTV) (Possatti *et al.*, 2018a; Chen *et al.*, 2019; Liu *et al.*, 2020). In a study by Arruda *et al.* (2016), pregnant sows were inoculated at either day 45 or 62 of gestation with APPV positive serum, which reproduced the disease in between 57 and 100% of litters. APPV viral ribonucleic acid (RNA) was detectable in all piglets with CT A-II and in 10 of 11 non-affected littermates. Further studies have provided additional evidence for a strong association

between the virus and the disease (De Groof *et al.*, 2016; Postel *et al.*, 2016; Schwarz *et al.*, 2017), satisfying Mokili's metagenomic Koch's postulates (Mokili, Rohwer and Dutilh, 2012). Although, Koch's postulates are yet to be fulfilled, with reproduction of the disease using a pure culture of the virus yet to be attempted (Stenberg, Jacobson and Malmberg, 2020).

1.2 Atypical porcine pestivirus

Atypical porcine pestivirus was first identified in the USA by metagenomic sequencing in serum collected from apparently healthy fattening pigs (Hause *et al.*, 2015). The 182 serum samples, from which five APPV positive samples were identified, were initially screened as part of a porcine reproductive and respiratory disease syndrome virus (PRRSV) metagenomic sequencing project (Hause *et al.*, 2015). Subsequently, the virus was identified in serum and tissue samples from piglets with CT A-II and has been reported in several countries worldwide, including Great Britain (Postel *et al.*, 2017a; Dessureault *et al.*, 2018; Mósena *et al.*, 2018; Shen *et al.*, 2018; Sutton *et al.*, 2019).

1.2.1 Atypical porcine pestivirus classification

Atypical porcine pestivirus is an enveloped, linear, non-segmented, positive-sense, RNA virus which belongs to the *Pestivirus* genus in the *Flaviviridae* family (Smith *et al.*, 2017). In 2017, the *Pestiviruses* genus was expanded to include seven new members (E—K) discovered between 2001 and 2015 (as shown in Figure 1-1): pronghorn antelope pestivirus (E), porcine pestivirus otherwise known as Bungowannah (F), giraffe pestivirus (G), HoBi-like pestivirus (H), Aydin-like pestivirus (I), rat pestivirus (J), and APPV (K) (Smith *et al.*, 2017). These novel members now share the group with the more established pestiviruses including BVDV type 1 and 2 (reclassified as pestivirus A and B respectively), CSFV (pestivirus C) and border disease virus

(BDV) (pestivirus D), that are known for their high socio-economic and welfare impact. The ‘established’ pestiviruses (pestivirus A-D) were distinguished from each other based on set criteria: a 25% or greater difference in nucleotide identity over the complete coding sequence, a difference of more than 10-fold in cross neutralisation titres and differences in the primary host. This reclassification was primarily based on genetic diversity as limited studies of cross-reactivity of novel genus member’s (such as APPV) with other pestiviruses have been performed so far. However, a study by Postel *et al.* (2017b) found no cross-reactivity of APPV-specific antibodies with commercial ELISAs routinely used to detect CSFV specific antibodies. It is likely that in future the *Pestivirus* genus will continue to expand with the inclusion of more divergent pestiviruses, such as those recently discovered in rats, bats and harbour porpoises (Z. Wu *et al.*, 2018; Jo *et al.*, 2019).

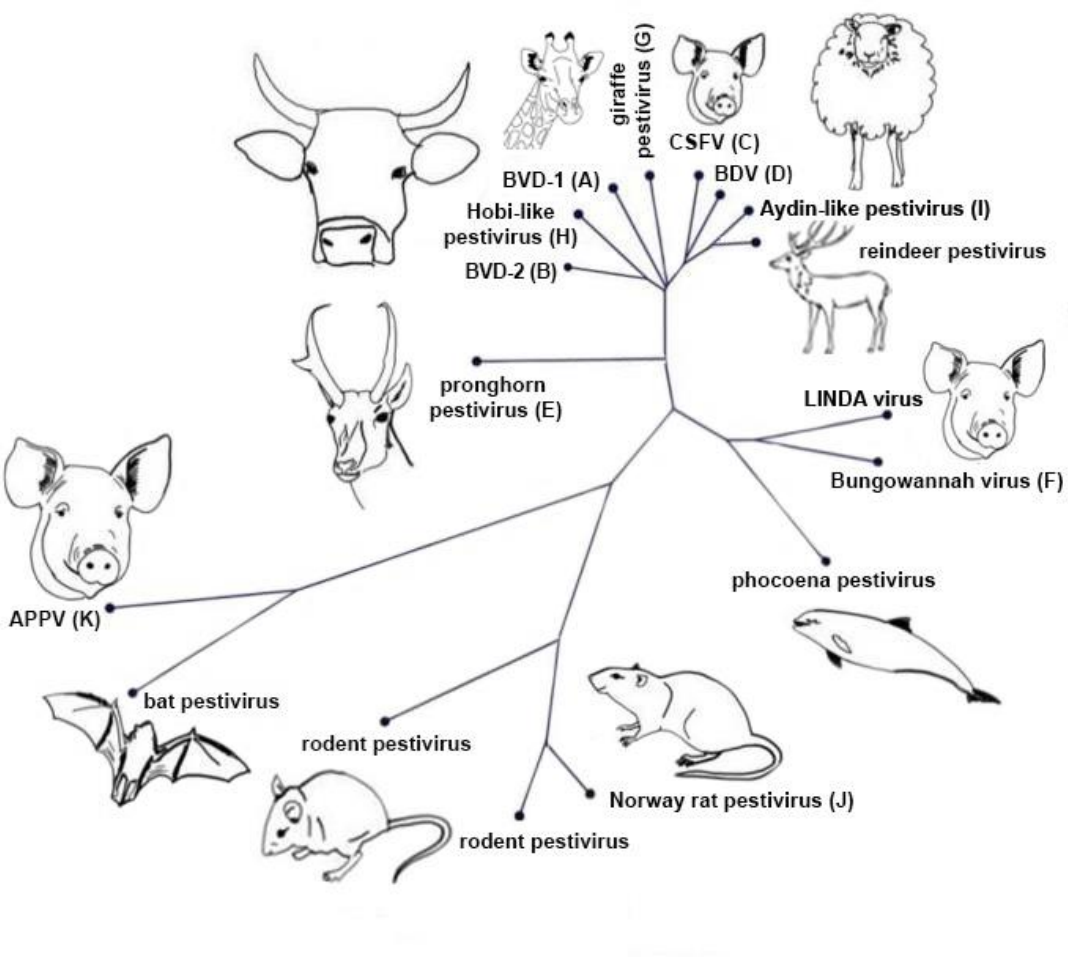

Figure 1-1: Phylogenetic tree of *Pestivirus* genus and related unclassified viruses (Riedel *et al*., 2021). Modified reproduction of the image in this thesis is covered by CC-BY-4.0 licence.

1.2.2 Structure and genetic diversity of APPV

Atypical porcine pestivirus is highly divergent from other well-known pestiviruses, sharing only a 40% amino acid identity of the complete polyprotein sequence with BVD, BDV, or CSFV. APPV is more closely related to an unclassified pestivirus discovered in Chinese bats (*Rhinolophus affinis* and *Scotophilus kuhlii*) sharing a 68% identity of the amino acid sequence of the partial polyprotein (Wu *et al.*, 2012; Hause *et al.*, 2015; Z. Wu *et al.*, 2018). Interestingly, unlike the other pestiviruses, both the unclassified bat pestivirus and APPV share a unique deletion of most of the two N-terminal domains of the E2 envelope protein. Moreover, although APPV possesses the cleavage sites in the N^{pro} amino acid sequence, it only shares a 9-18% similarity to other pestiviruses, further highlighting its divergence (Hause *et al.*, 2015; Riedel *et al.*, 2021).

In 2018, the first whole APPV genome sequence derived from the spleen of a piglet exhibiting CT was published (S. Wu *et al.*, 2018). The sequence was 11,526 base pairs long and encoded a large single open reading frame (ORF) of 10,911 nucleotides (as shown in Figure 1-2) that codes a polyprotein of 3636 amino acids. The size of the polyprotein is of similar length (3635) to the one previously predicted (Hause *et al.*, 2015). Similarly, other Chinese studies also determined that the whole APPV genome size ranges from 11,475 to 11,565 nucleotides in lengths with an ORF of 10,908 nucleotides encoding a polyprotein of 3,635 amino acids flanked by 5′ and 3′ untranslated regions (Zhang *et al.*, 2018a; Pan *et al.*, 2019; Shi *et al.*, 2021). The polyprotein structure is cleaved into four structural (C, E^{rns}, E1 and E2) and eight non-structural (NS) proteins (N^{pro}, P7, NS2, NS3, NS4A, NS4B, NS5A and NS5B) (Schirrmeier *et al.*, 2004; Pan *et al.*, 2019).

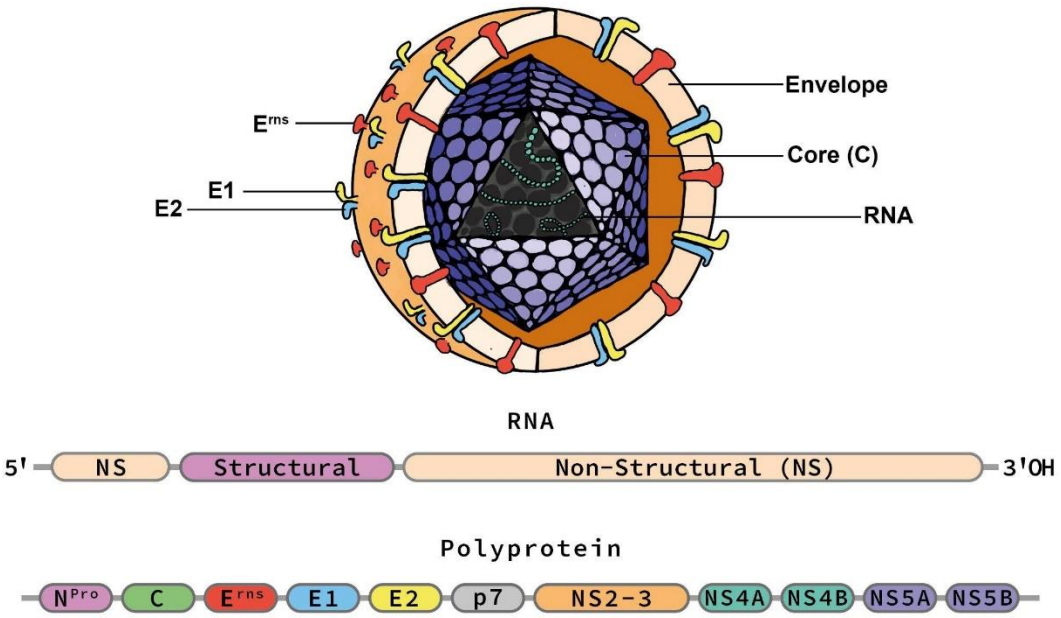

Figure 1-2: APPV virion and genomic structure showing open reading frame encoding the structural and non-structural proteins. Image prepared by John Lawlor.

Of the structural proteins, the C protein (core) has a role in assembling the nucleocapsid, in virus proliferation and it also displays antigenic epitopes that stimulate T and B lymphocyte-mediated immune responses (Hause *et al.*, 2015; Riedel *et al.*, 2017; Liu *et al.*, 2021). The envelope protein E^{rns} is unique to pestiviruses. It is known to have RNAse activity and can inhibit activation of the interferon (IFN) system (IRF3) aiding in viral replication by degrading viral dsRNA (Riedel *et al.*, 2017, 2021; Cagatay *et al.*, 2021; Liu *et al.*, 2021). The envelope glycoproteins E1 and E2 form heterodimers necessary for viral entry into host cells. E2 is responsible for binding to complement regulatory protein CD46 for receptor-mediated endocytosis. Of the non-structural proteins, N^{pro}, a non-essential non-structural protein unique to pestiviruses, is responsible for self-cleavage from the polyprotein and has a role in suppression of IFN-β production and IRF3 promoter activity (Mou *et al.*, 2021). P7 is thought to be involved in virus maturation whereas NS2 and NS3 are known to have protease activity which is responsible for polyprotein processing (with NS4A

acting as a cofactor for NS3 activity). NS3 also display RNA helicase/NTPase activity for RNA replication with NS5A regulating replication potentially through direct interaction with NS5B through modulation of its polymerase activity (King *et al.*, 2011; Tautz, Tews and Meyers, 2015; Riedel *et al.*, 2021).

Conservation of these regions within the polyprotein varies considerably among pestiviruses, with the non-structural proteins N^{pro}, P7 NS2 and NS5A having less than 5% amino acid conservation between species (Riedel *et al.*, 2021). The most conserved proteins are the envelope protein E^{rns}, sharing 23% of its amino acid identity and the non-structural proteins NS3, NS4B and NS5B (conserving 29, 20 and 22% of their amino acids, respectively) (Smith *et al.*, 2017; Riedel *et al.*, 2021). This may explain why these regions (NS3, NS5B and E^{rns}) have also proven to be the most heavily sequenced portions of the genome to date (Arruda *et al.*, 2016; Postel *et al.*, 2016; Beer *et al.*, 2017; Muñoz-González *et al.*, 2017; Yuan *et al.*, 2017; Dénes *et al.*, 2018; Possatti *et al.*, 2018b; Gatto *et al.*, 2018b; Mósena *et al.*, 2018; Cagatay *et al.*, 2019; Pan *et al.*, 2019; Sozzi *et al.*, 2019; Yuan *et al.*, 2021; Shi *et al.*, 2021).

According to a 2020 study, 58 distinct APPV whole genome sequences were deposited into NCBI GenBank from multiple countries in North and South America, Europe and Asia, sharing a nucleotide identity between 80 and 99% (Folgueiras-González *et al.*, 2020). Since this study only one further full genome sequence has been added to the collection (without altering the amount of genetic variation observed between strains). A study by Beer *et al.* (2017) described genetic diversity in NS5B sequences from tissue and serum samples collected from two neighbouring states in the North of Germany. The observed sequences form four distinct clusters with the two main regional clusters sharing a nucleotide identity of between 96 and 100% and the two other clusters sharing only an 88-90% and 92-94% identity, respectively, with one more closely related to a USA sequence (>97%). Another study by Yan *et al.* (2019) also reported considerable variability within 12 genome sequences from the Eastern province of Anhui and the South-East province of Guangdong

in China with nucleotide identity ranging between 80.5 and 99.8%. This, at the time of publication, was similar to the variability seen between all other available sequences from the USA, Austria, the Netherlands, Germany, Korea and, China which collectively shared a nucleotide identity of between 80.5% and 99.8%. Recently, a retrospective study of APPV in the Midwest of the USA determined a high level of diversity within the partial NS5B region sequences obtained from 54 samples sharing between 85.8 and 100% nucleotide identity (Yuan *et al.*, 2021). Two complete genome sequences from the USA study were also found to vary significantly (~12% across the genome) from the previously published USA sequences described in 2014. At the start of this study, only one partial NS3 sequence of APPV has been deposited for Great Britain. Hence, no information is available regarding the genetic variability of the virus in this country. Further investigation is needed to determine British strain variation and their relationship to other countries.

As observed with other pestiviruses such as BVDV and CSFV, point mutations and homologous recombinations have also been identified in Chinese APPV strains (GenBank ID: MH493895, MH493896, and MG792803) (Weber *et al.*, 2015; Smith *et al.*, 2017; Guo *et al.*, 2020). A study by Muñoz-González *et al.* (2017) identified a mutation rate (nucleotide substitutions per site per year [s/s/y]) based on 1,615 nucleotide partial sequences of the NS2-3 region of a Spanish APPV strain (LT631736) (detected between 2001 and 2015 during a retrospective serum survey), to be 2.65×10^{-3} s/s/y; moreover 3.62×10^{-3} s/s/y were found between a 2001 Spanish strain and a 2015 German strain (KU041639.1) identified in 2015 (Muñoz-González *et al.*, 2017). These rates are similar to mutation rates detected between European outbreaks of CSFV (2.7×10^{-3} s/s/y) (Díaz de Arce *et al.*, 1999). These studies together suggest not only a high level of genetic variability between APPV strains from different countries but also within countries. For this reason, it has proven difficult to definitively determine the origin and evolution of APPV which also poses a potential hurdle for molecular diagnosis. The Bayesian analysis performed by Yuan *et al.* (2017) indicates that APPV originated in Germany and diversified

into three ancestral clades which were then introduced separately to the United States, the Netherlands and China. Although, due to the novelty of the virus, the analysis was conducted with limited sequence data covering a short time period, as more sequences have become available, analyses in this area have been strengthened. Subsequent phylogenetic analyses of the whole genome, N^{pro} $E^{rns,}$ and E2 regions performed by several groups have proposed a three-genotype subdivision of APPV, loosely based on the strain's geographic distribution. Genotype 1 includes sequences from America, Asia and Europe, with genotype 2 and 3 solely including Chinese sequences (Xie *et al.*, 2019; Yan *et al.*, 2019; Choe *et al.*, 2020; Folgueiras-González *et al.*, 2020; Guo *et al.*, 2020; Shi *et al.*, 2021). Further divisions of genotype 1 into four subgroups (1.1 to1.4) have been proposed based on the level of genetic diversity within the group (Choe *et al.*, 2020; Guo *et al.*, 2020; Shi *et al.*, 2021).

1.2.3 Pestivirus replication

The entry mechanism of pestiviruses into host cells is a complex multistep process that is poorly understood, requiring a number of co-receptors and host factors to enable entry through receptor-mediated endocytosis (Grummer, Grotha and Greiser-Wilke, 2004; Shi *et al.*, 2016). Similar to BVDV and Hobi-like pestivirus, which rely on a complement regulatory protein $CD46_{(bov)}$ as one of their main receptors for cell entry, APPV also relies on $CD46_{(pig)}$ as a major receptor for binding and entry (Cagatay *et al.*, 2021). However, other porcine pestiviruses (Bungowannah and CSFV), or indeed other pestiviruses (giraffe pestivirus), can gain cytoplasmic access through CD46 independent entry mechanisms (Cagatay *et al.*, 2021; Leveringhaus *et al.*, 2022). For example, CSFV has been shown to utilise the host factor MERTK (a protein tyrosine kinase) to enable cell entry (Zheng *et al.*, 2020), suggesting that the cellular invasion process for different pestiviruses is more diverse than initially described.

Once the virus has undergone attachment and internalisation through clathrin-mediated endocytosis, endosomal membrane fusion occurs in acidic conditions triggering conformational changes of the viral envelope proteins that mediate fusion of the viral and endosomal membranes and the consequent release of the nucleocapsid into the cytoplasm (Krey, Thiel and Rümenapf, 2005; Fernández-Sainz *et al.*, 2014; Ji *et al.*, 2015; Smit *et al*., 2011). The viral RNA is released by the nucleocapsid (uncoating) into the cytosol by an unknown mechanism (Valiakos *et al*., 2013), acting as both genomic and messenger RNA for viral replication. During replication, the positive-sense RNA is used to create a negative-sense RNA template to direct the synthesis of positive-sense RNA progeny (Gong *et al.*, 1996; Ji *et al.*, 2015). Unlike Hepaciviruses (another genus of *Flaviviridae*), which form a membranous web surrounding the viral replication complex enabling viral replication, Pestiviruses are not known to induce distinct cellular membrane rearrangements during this process (Schmeiser *et al*., 2014). After replication, the core proteins bind to the progeny RNA to form histone-like protein-RNA aggregates that become enveloped as the capsid invaginates into the lumen of the endoplasmic reticulum during virion assembly (Riedel *et al*., 2010; Valiakos *et al*., 2013).

As there is no cap structure present at the 5′ end of the genome, pestiviruses exploit an internal ribosomal entry site in the 5′ untranslated region, which binds the virus to the ribosomes at the rough endoplasmic reticulum (Poole *et al.*, 1995; Moes and Wirth, 2007; Ji *et al.*, 2015). This enables cap-independent translation of the viral polyprotein precursor and co- and post-translational processing of the polyprotein assisted by both viral and cellular proteases, as previously discussed in Section 1.2.2 (Rümenapf *et al.*, 1993; Blome *et al.*, 2017b). After the synthesis of viral components, virion assembly occurs within the lumen of the endoplasmic reticulum where there is an accumulation of envelope glycoproteins. The virions are then transported to the ER-Golgi intermediate compartment for maturation of the infectious virion prior to the

release of the infectious viral particle from the infected cells via exocytosis (Schmeiser *et al.*, 2014; Blome *et al.*, 2017b).

1.2.4 Epidemiology

Several epidemiological and retrospective investigations in healthy pig populations and CT A-II cases have been conducted (see Chapter 6 for further details). These studies have established that the virus has a global distribution with reports of APPV detection in Asia, Europe and America from both healthy pigs and piglets with CT A-II (Postel *et al.*, 2017a; Dessureault *et al.*, 2018; Mósena *et al.*, 2018; Shen *et al.*, 2018; Pedersen *et al.*, 2021; Yuan *et al.*, 2021). Retrospective analysis of tissue samples (brain, cerebellum, tonsil and retropharyngeal lymph nodes) from Hungary showed presence of APPV in CT A-II cases 10 years before the first identification of the virus (Dénes *et al.*, 2018). Similarly, a serum survey of the Veterinary Pathology Diagnostic Service at the Universitat Autònoma de Barcelona biobank, discovered that APPV has been in circulation in Spain for 18 years, and the earliest report of the virus was from Switzerland, where APPV was detected in serum samples from 1986 (Muñoz-González *et al.*, 2017; Kaufmann *et al.*, 2019). APPV has not only been identified in commercial pigs but also in wild boar, which may act as a reservoir for the virus in some European and Asian countries, although transmission studies between wild and domestic pigs are yet to be performed (Cagatay *et al.*, 2018; Colom-Cadena *et al.*, 2018; Sozzi *et al.*, 2019; Choe *et al.*, 2020). At the start of this study, only one study has been conducted to investigate the presence of APPV within Great Britain using 86 serum samples from healthy domestic pigs (Postel *et al.*, 2017a). Further study is therefore needed to understand the distribution and prevalence of the virus within the British pig population, both in healthy pigs and in CT A-II outbreaks.

Classically, APPV-associated CT A-II outbreaks occur over 1 to 2 months in gilt litters or litters from naive sows Outbreaks have been reported to persist

for 6 to 7 months (Guo *et al.*, 2020; Pedersen *et al.*, 2021), affecting a large proportion of litters (16 to100%) in and between farrowing groups and with clinical signs in varying proportions within the affected litters (<10 to 100%) (Arruda *et al.*, 2016; De Groof *et al.*, 2016; Gatto *et al.*, 2018b; Pan *et al.*, 2019). Typically, the first litter from an infected sow will present with clinical signs of tremor and ataxia from birth to two months old whereby they usually self-resolve; subsequent litters from the same sow are generally subclinical (Gatto, Sonálio and de Oliveira, 2019; Pan, Mou and Chen, 2019).

As well as the usual clinical signs associated with CT A-II, splay leg have also been described as a comorbidity in several clinical cases (Arruda *et al.*, 2016; De Groof *et al.*, 2016; Schwarz *et al.*, 2017; Sutton *et al.*, 2019). Splay leg is a congenital syndrome characterised by weakness and lateral abduction of predominantly hind limbs in neonates and, in severe cases, forelimbs can also be concurrently affected (Edwards and Mulley, 1986; Schumacher, Röntgen and Maak, 2021). The causes of splay leg are currently poorly understood, and little is known pathophysiologically, with several pathogens and factors implicated in the development, including the breed, length of pregnancy and development of the skeletal muscles and motor neurons, although no definitive conclusions have been reached (Papatsiros, 2012; Schumacher, Röntgen and Maak, 2021). In a study of litters born to sows exposed at 54 days of gestation to APPV derived from fetal fluids of APPV-associated CT A-II positive piglets, there was a significant relationship between the presence of CT A-II and splay leg: the average frequency of splay leg in CT A-II affected litters was 22.4% compared to 0.5% in unaffected litters (Sutton *et al.*, 2019). Another study also found a moderate to high level (6-55%) of splay leg comorbidity in CT A-II affected litters from the four farms investigated (Gatto *et al.*, 2018b).

As with other pestiviruses, the transmission of the virus occurs vertically via the placenta, although limited information is available regarding infection in relation to gestational stage and fetal development (nervous and immune system) and how this influences the clinical, pathological and immunological

status of the piglet after birth (Schwarz *et al.*, 2017). Pestiviruses are known to be immunosuppressive agents causing prolonged infection and enhanced disease by impairing cellular immunity leading to persistent infection and increased likelihood of secondary infections or co-infections (described further in Chapter 5) (Strong *et al.*, 2015). Instances of viral persistence in bodily fluids and tissues have been reported between 6 and 8.5 months of age in both non-clinical and clinical pigs, well after the resolution of the clinical signs (Schwarz *et al.*, 2017; Dall Agnol, Alfieri and Alfieri, 2020; Yuan *et al.*, 2021). Additional studies (further explored in Chapter 6) are needed regarding APPV role as an immunosuppressive agent and viral host interactions leading to possible immune tolerance and viral persistence.

Piglets have also been reported to have contracted the virus horizontally through either direct contact with infected littermates or possibly through the faecal-oral routes, as supported by the high viral load detection in oral fluids, including saliva, nasal secretions and faeces (Arruda *et al.*, 2016; De Groof *et al.*, 2016; Postel *et al.*, 2016; Muñoz-González *et al.*, 2017; Schwarz *et al.*, 2017; Yuan *et al.*, 2017, 2021; Gatto *et al.*, 2018a). High APPV viral loads have also been detected in semen (both previously affected by CT A-II and healthy animals from commercial units) (Schwarz *et al.*, 2017; Gatto *et al.*, 2018a; Grahofer, Zeeh and Nathues, 2020). Even though no transmission studies have been performed to date, this may highlight venereal transmission as a possible route of sow infection. Further investigation should be undertaken to determine this and the extent of APPV circulation in commercial stud units within Great Britain.

1.2.5 Pathology

No consistent significant gross pathological findings have been reported in association with APPV induced CT A-II in newborn piglets (Schwarz *et al.*, 2017; Zhang *et al.*, 2017; Mósena *et al.*, 2018). However, one study that

investigated three CT affected piglets (three-day-old) reported PM findings of congestion of the cervical area of the spinal cord (C4-7) (Possatti *et al.*, 2018a). The same study also found neuronal necrosis, gliosis, neuronophagia, and satellitosis in association with APPV-induced CT A-II. Histologically, CT A-II does not present with cerebellar hypoplasia, as seen in other pestivirus infections, and is instead associated with the presence of vacuoles in the cerebellar white matter and demyelination of the white matter of the cerebellum and spinal cord (Patterson *et al.*, 1976; Postel *et al.*, 2016; Hansmann *et al.*, 2017; Schwarz *et al.*, 2017; Possatti *et al.*, 2018b). Abnormal 'swollen' oligodendrocytes have also been observed in the spinal cord of CT A-II affected piglets (Patterson *et al.*, 1976). Recent immunohistochemical investigations have found that although the number of normal oligodendrocytes were unchanged between CT A-II affected and unaffected animals, affected animals showed increased levels of oligodendrocyte transcription factor two in the central nervous system, indicating the involvement of APPV in the disruption of myelin development (Schwarz *et al.*, 2017). Currently, the pathogenesis of APPV is poorly understood, and additional investigation of the role of APPV in the development of pathology linked to clinical signs is needed.

1.2.6 Tissue tropism

Atypical porcine pestivirus is systematically distributed and is detectable by RT-qPCR in all major organs (Strong *et al.*, 2015; Blome *et al.*, 2017b). However, the viral titres are variable, with higher viral loads detected in lymphoid (lymph nodes, spleen, tonsil and thymus) and nervous tissues (brain, notably the cerebellum and spinal cord) (Gatto *et al.*, 2018b; Mósena *et al.*, 2018; Shen *et al.*, 2018; Liu *et al.*, 2019; Xie *et al.*, 2019; Guo *et al.*, 2020). This finding is in keeping with other classical pestiviruses which have a systemic distribution affecting the mucosal surfaces of most organs and also possess a predilection for lymphoid and nervous tissues (Nettleton and

Entrican, 1995; Sentsui *et al*., 2001; Blome *et al.*, 2017b). An immunohistological study of nervous and lymphoid tissue targeting the E^{rns} protein APPV described the distribution of the virus to be located predominantly in the matrix and nerve fibres in the cerebellum, brainstem and spinal cord with moderate neuronal staining in the cerebellum, endothelial cells of lymphoid tissues (spleen) and epithelial cells in all other tissue types tested (lung, liver, kidney) (Liu *et al.*, 2019). This finding was supported by a study using RNAScope *in situ* hybridisation (ISH) which also detected the N^{pro} and E^{rns} region of APPV in endothelial cells in the liver, kidney, colon, lung, lymph nodes, tonsils, thymus and thyroid as well as in vascular tunics, fibroblasts and fibromuscular stroma (Buckley *et al.*, 2021). The same study also found marked presence of APPV RNA in the cerebrum and cerebellum of CT A-II affected piglets (both infected neonates and an 11-month-old boar which has resolved clinical signs of CT A-II) with the most abundant signal detected in the granular and molecular layers of the cerebellum (Buckley *et al.*, 2021). Further work is needed to investigate tropism on both a tissue and cellular level to better understand host—pathogen interactions and viral pathogenesis.

1.2.7 Diagnosis

Historically, the primary diagnostic criteria for CT A-II were clinical signs and exclusion of other (congenital tremor) types (A-I, III, IV and V). CSFV-associated A-I and APPV-induced CT A-II present with highly similar clinical signs in neonatal piglets. Therefore, it is essential to initially exclude CSFV, which is an exotic notifiable pathogen in the UK, and which must be considered the primary differential diagnosis. Clinical signs of CT A-II are considered non-specific: tremors, ataxia and the inability to suckle are also associated with other conditions affecting piglets, such as vitamin A deficiencies, hypoxia (Madson, Arruda and Arruda., 2019) and in rare cases, toxoplasmosis and cerebellar abiotrophy, although ataxia and tremors are not usually observed in piglets until three to eight weeks of age (Madson, Arruda and Arruda., 2019).

For this reason, the identification of the viral agent in suspected cases should be conducted via laboratory testing, highlighting the importance of readily available robust diagnostic assays.

Until recently, pathological examination and histological tests performed on formalin-fixed tissue have been used to diagnose CT A-II infection without confirmation of APPV involvement. As discussed in 1.2.5, no gross pathology is observed with CT A-II. However, lesions (vacuoles) can be visualised by haematoxylin and eosin staining and demyelination of the cerebellum and spinal cord can be observed using luxol fast blue (LBF) stain (Schwarz *et al.*, 2017; Dessureault *et al.*, 2018; Possatti *et al.*, 2018a; Mósena *et al.*, 2018). The presence of vacuolisation and demyelination in association with clinical signs are indicative of CT A-II.

Currently, there are no commercial diagnostic tests available for the detection of APPV. After the discovery of the virus, the development of a small number of in-house molecular (conventional reverse transcriptase-polymerase chain reaction [RT-PCR] and RT-qPCR), serological (enzyme-linked immunosorbent assay [ELISA]) and fluorescent *in situ* hybridisation [FISH]) tests were developed targeting conserved regions of the genome (primarily NS3, NS5B and envelope proteins E^{rns} and E2) (Hause *et al.*, 2015; Arruda *et al.*, 2016; Postel *et al.*, 2016; Beer *et al.*, 2017; Schwarz *et al.*, 2017). However, these assays were based on limited sequence availability, and due to difficulties in culturing the virus, validation of these techniques was restricted. Over time, these assays have been adapted and employed in subsequent epidemiological studies for the identification and quantification of APPV in different sample types, including tissues, swab, semen and blood from APPV experimental infections and CT A-II field cases (Hause *et al.*, 2016; Hansmann *et al.*, 2017; Muñoz-González *et al.*, 2017; Postel *et al.*, 2017a; Dessureault *et al.*, 2018; Gatto *et al.*, 2018b; Mósena *et al.*, 2018; Sutton *et al.*, 2019).

Recently, new assays have also been developed for the detection and quantification of the virus, including RT-PCR, RT-qPCR, immunohistochemistry (IHC), and RNAScope *in situ* hybridisation (ISH) as well as APPV-specific antibodies used to detect virus presence and neutralising properties by in indirect and competitive ELISAs, virus neutralisation tests (VNT) and indirect immunofluorescence (IIF) test (Postel *et al.*, 2017a; Cagatay *et al.*, 2018, 2019; Possatti *et al.*, 2018b; Pfankuche *et al.*, 2018; Liu *et al.*, 2019, 2020; Michelitsch *et al.*, 2019; Sutton *et al.*, 2019; Buckley *et al.*, 2021). Further development, optimisation and validation of assays for the detection and quantification of APPV and APPV-specific antibodies are still required, not only for the accurate diagnosis of APPV at both farm and national herd level but also to investigate complex host—pathogen interactions (see Chapter 3).

1.3 Impact of APPV induced CT A-II

The precise economic impact of APPV induced CT A-II remains unknown at present. The *Pestivirus* genus contains viruses (BVDV and CSFV) notable for their high welfare and socioeconomic impact. Currently, CSFV is exotic to the UK and is considered a notifiable disease both nationally and internationally (Animal and Plant Health Agency, 2018; World Organisation for Animal Health, 2021). The virus is a persistent problem in Europe in domestic and wild boar, causing significant losses and requiring stringent control measures impacting trade and movement of animals. In a study using a model to analyse the financial losses from the 1997/1998 outbreak of CSFV in the Netherlands where a total of 429 farms were infected, and more than 60% of farms had at least one control measure imposed, financial losses were calculated to be $2.3 billion US (approximately £1.66 billion) with a direct cost to the farming sector of $423 million US (approximately £305 million) and related industries of $596 million US (approximately £430 million) (Meuwissen *et al.*, 1999).

Both BVDV and BDV are endemic in the UK and known to have a significant economic impact both directly via their effect on the animal and production (such as ill thrift and poor growth, fertility issues, immunosuppression leading to secondary infection and increased mortality rates) as well as indirectly through the need for repeated veterinary interventions and the cost of participating in control and eradication programmes (including culling of persistently infected animals and vaccination) (Yarnall and Thrusfield, 2017). The economic impact of BVD in the United Kingdom (UK) is highly variable, with between £0 and 2,370 per cow per year depending on the strain severity, herd status (whether BVD was endemic or not on farm and previous herd exposure), clinical outcomes and resulting immune status of the animals (Yarnall and Thrusfield, 2017). Recently, it was estimated the yearly cost of BVD to the UK cattle industry to be £39.6 million per year (Hardstaff *et al.*, 2020). Currently, neither BVD nor BDV are notifiable diseases in the UK. BVD requires notification by the World Organisation for Animal Health (OIE) as of 2014, requirements that has been adopted by several European countries including Austria, Belgium, Denmark, Finland, Germany, Norway, Sweden and Switzerland with implications for increased surveillance, biosecurity and trade restrictions (in the case of reported suspected cases) (Sandvik, 2014; Agri-Food and Biosciences institute, 2015).

Reports of morbidity and mortality rates for APPV-induced CT A-II outbreaks are highly variable. Outbreak morbidity has been reported anywhere between 2.5 and 100%, varying between litters, farms, regions and countries (Schwarz *et al.*, 2017; Dessureault *et al.*, 2018; Shen *et al.*, 2018). Mortality of up to 30% was described in 105 sow farms in Austria as a consequence of piglet malnutrition, with the study describing an overall decrease in weaned piglets of more than 10% per sow (Schwarz *et al.*, 2017). Similarly, a study of 91 sows exposed orally to fetal fluids collected from CT A-II-affected piglets and containing APPV antigen, found a pre-weaning mortality rate of 46.4% in clinical and 15.3% in non-clinical littermates from CT-affected litters compared to unaffected litters, where a mortality rate of 12.7% was instead recorded

(Sutton *et al.*, 2019). In contrast, an outbreak on a commercial farm in China resulted in a mortality of 60% of the weaned pigs (Shen *et al.*, 2018). Levels of mortality may depend not only on the severity of the clinical signs but also on the management of the clinically affected piglets where ensuring adequate colostrum intake may be beneficial in reducing mortality.

Co-infection of APPV with other viruses may also increase mortality in affected piglets, as observed in a co-infection study of APPV and porcine teschovirus with reported mortality rates of 100% (Possatti *et al.*, 2018a). To date, APPV has been found in co-infection with several viruses considered to have considerable welfare and socio-economic impacts, such as ASF, CSFV, porcine respiratory and reproductive syndrome virus, swine influenza A virus and porcine epidemic diarrhoea virus, among others (further detailed in Chapter 5) (Yuan *et al.*, 2021). Further investigation is needed to understand the role of APPV in concurrent infection and to determine if APPV is an immunosuppressive agent, which may lead to changes in host—pathogen interactions and enhance clinical and pathological outcomes of disease during co-infection (see Chapter 5).

As well as the direct impact of the clinical disease, production may be indirectly affected by poor weight gain of affected piglets and reduced average litter size (Arruda *et al.*, 2016; Dessureault *et al.*, 2018). In a recent study, CT-affected gilt litters were observed to be smaller (12.2 piglets per litter) when compared to unaffected gilt litter sizes (13.3 piglets per litter) (Dessureault *et al.*, 2018). Moreover, Sutton *et al.* (2019) found that of 91 litters from sows exposed in pregnancy to APPV CT affected litters had significantly lower birth weights (CT affected piglets 1.22 +/- 0.02 kg, unaffected littermates 1.09 +/- 0.03 kg) compared to birth weight of non-affected litters (1.30 +/- 0.02 kg). The same study also investigated the relationship between reproductive failure and APPV induced CT A-II, however, no difference was detected in the incidence of stillborn or mummified fetuses between CT affected and unaffected litters.

Further research is needed to understand the direct and indirect effects of APPV induced CT A-II infection on pig production (see Chapter 4).

The role of viral persistence in the maintenance of APPV in pig populations or the impact on pig production is also unclear. As previously discussed, high levels of APPV RNA have been detected in bodily fluids, including oral and nasal secretions, blood, faeces, semen and tissues from all major organs indicating possible viral persistence through life (Schwarz *et al.*, 2017). Due to the importance of persistently infected animals in BVDV and BDV transmission and maintenance cycles and their overall impact on production, additional investigation of the potential for viral persistence is required (see Chapter 4).

1.4 Control and prevention

The development and delivery of safe, efficacious vaccines for control and prevention of classical pestiviruses and their associated diseases has long presented challenges. Historically, several vaccines have been established commercially for pestiviruses, falling into three main categories: modified live virus, subunit vaccines based on the main immunogenic protein E2, and chimeric live recombinant viral vector vaccines (Madera *et al*., 2016).

Modified live virus vaccines have been developed based on either *in vitro* or *in vivo* attenuation of viral strains for CSFV. Attenuation was achieved through *in vivo* passaging methods, such as the Chinese vaccine strain (C-strain) attenuated through 480 passages of the virulent strain in rabbits in 1956 (Luo *et al*., 2014). *In vitro* techniques to attenuate viral strains have also been deployed, including serial passaging (more than 90 passes) of the low-virulence strain of Miyagi (LOM) in bovine kidney cells and the continuous propagation under low-temperature conditions (30°C) of both the ALD and Alfort virulent strains to produce the low virulent guinea-pig exaltation-negative (GPE-) and Thiverval strains respectively (Terpstra and Kroese, 1996; van

Oirschot, 2003; Coronado *et al*., 2021). Live attenuated vaccines are generally considered a safe and efficient methods of providing long-lasting immunity in at-risk groups, and have been used prophylactically to control CSFV in endemically affected countries. The GPE- and Thiveral vaccines have been found to perform similarly to the C-Strain based vaccine formulations. These vaccines offer early (72 to 96 hours post-vaccination) and long-lasting (6 months to lifelong) immunity in both pregnant sows and young piglets (Graham *et al*., 2012; Blome *et al*., 2017a; Coronado *et al*., 2021). However, the effectiveness of live attenuated vaccines may diminish in the presence of maternal antibodies or co-infection with an immunosuppressive pathogen leading to vaccination failure and the re-emergence of CSFV outbreaks in vaccinated herds (van Oirschot, 2003; Blome *et al*., 2006; Suradhat, Damrongwatanapokin, and Thanawongnuwech, 2007; Coronado *et al*., 2021). A 2015 to 2018 outbreak of LOM CSFV strain on Jeju Island (previously established as CSFV-free) was linked to a commercial CSF- swine erysipelas combined vaccine deployed on the island in 2014 (Choe *et al*., 2019). However, the lack of serological distinction between infected and vaccinated animals (DIVA), precludes the use of non-DIVA attenuated vaccines in large-scale eradication programmes and CSF-free areas including within the EU, due to trade implications (Coronado *et al*., 2021). In such cases, countries rely on non-vaccination stamping-out strategies where affected animals are culled; nevertheless, this strategy is not without ethical and economic implications.

To date, some DIVA vaccines against CSFV have been developed with varying degrees of success. These marker vaccines are used alongside diagnostic tests for differentiation between infected and vaccinated animals (van Oirschot, 2003; Blome *et al*., 2017a). Two subunit vaccines, Bayovac *CSF (*Bayer) and Porcilis Pesti (Intervet International BV), based on the E2 protein expressed in the baculovirus system were licenced within Europe (Huang *et al*., 2014). These vaccines were used in conjunction with their respective commercially available E^{rns} antibody ELISA (PrioCHECK CSFV Erns ELISA, previously Ceditest Marker ELISA and the IDEXX CSF

marker ELISA, previously Chekit CSF Marker ELISA) to differentiate between vaccinated and naturally-infected animals (Huang et al., 2014; Madera *et al*., 2016). As the vaccines elicited only transient protection (6-13 months), were unable to prevent vertical transmission of CSFV, required multiple doses to prevent horizontal transmission, and were ineffective for oral vaccination, showed a limited use within control and eradication programmes, especially when targeting wild boar populations they were subsequently withdrawn (Beer *et al*. 2007; Huang *et al*. 2014; Coronado *et al*. 2021; EMA 2018a, 2018b).

In 2015, another marker vaccine (Suvaxyn CSF Marker) with DIVA capabilities was licenced for emergency vaccination in Europe (EMA, 2018c). The vaccine was based on a pestivirus chimaera CP7-E2alf constructed from E2 envelope protein from Alfort/187 CSF strain inserted into a BVDV cytopathic type 1 backbone (CP7) (Blome *et al*., 2017c). Several studies, performed to investigate the safety and efficacy of the vaccine in both oral and intramuscular vaccinations in domestic and wild pig populations (Feliziani *et al*., 2014; Dräger *et al*., 2015, 2016; Henke *et al*., 2018) showed prevention of vertical transmission of CSFV after a single intramuscular dose. Suvaxyn CSF Marker was able to confer horizontal protection against the highly virulent Koslov strain in piglets vaccinated with two doses intramuscularly after seven days, even in the presence of pre-existing BVDV-1 antibodies (Dräger *et al*., 2016; Henke *et al*., 2018).

Protection was also conferred to animals challenged with the Koslov vaccine 14 days post oral vaccination (Blome *et al*., 2012). In a study by Dräger *et al.* (2015) investigating viral shedding and dissemination in vaccinated boars, no viral shedding was detected in saliva, faeces or urine. CP7 E2alf RNA was also not detected in reproductive organs or accessory glands, indicating that it is unlikely shedding through semen occurred. Low levels of CP7 E2alf RNA was detected up to seven days post vaccination in lymphatic tissues; however, only two of the samples (tonsil and parotid lymph node) on day four were found

to be of an infectious titre which decreased by day seven, suggesting replication was limited (Dräger *et al*., 2015).

Like the DIVA diagnostic tests designed to differentiate of Bayovac CSF/Porcilis Pesti vaccines and CSFV naturally infected animals, Erns ELISAs have also been implemented for differentiation of the Suvaxyn CSF Marker vaccine from infected animals. The double antigen ELISA (pigtype CSFV Erns Ab) developed by Meyer *et al*. (2017) is both sensitive (90.2%) and specific (93.8%) in its ability to differentiate vaccinated from infected animals. During validation of the assay, cross-reactivity was detected in BVDV and BDV experimentally infected pigs (5/20). Although no cross-reactivity was detected in any of the vaccinated wild boar serum samples tested, cross-reactivity with other pestiviruses is a common problem in Erns ELISA-based DIVA diagnostic tests, requiring further development and optimisation to address this (Meyer *et al.,* 2017).

At present, there are no commercial vaccines available for the control of APPV infection. Research on APPV vaccines is still in its infancy and is likely to face hurdles similar to BVDV vaccine development due to the high level of genetic diversity among APPV strains and the potential for APPV to cause immunosuppression and persistent infections (Griebel, 2015; Folgueiras-González *et al.*, 2020). However, recent APPV studies have shown promising results in this area: A study in which a subunit vaccine, based on purified recombinant E2 envelope glycoprotein (thought to be the main immunogenic protein of APPV) tested with two different adjuvants (ISA 201VG and IMS 1313VG) was administered to BALB/cSPF mice (Zhang *et al.*, 2018b) showed that the antigen was able to elicit a Th2-type immune response. However, the E2 protein with ISA 201VG produced significantly higher levels of APPV-specific antibodies and a greater interleukin (IL)-10 response than the E2 protein adjuvated in IMS 1313VG (Zhang *et al.*, 2018b). Recently, another vaccine study using virus-like particles (VLP) self-assembled from APPV E^{rns} and E2 purified proteins was shown to induce a strong antibody response

(determined by E^{rns} ELISA) and reduced viral titres in tissue (RT-qPCR and IHC) of BALB/c mice (Liu *et al.*, 2021). Both vaccines seem therefore promising, however, their real efficacy will be revealed when moving to evaluation in the target species.

In the absence of a vaccine, a common control strategy is to expose naïve sows and gilts to a source of the virus (usually either 8 to12 week old weaner piglets or cull sows) before service, to infect the naive pigs before breeding to ensure development of immunity to the virus through a transient infection (Williamson, 2017). Other strategies employed to reduce the incidence of disease include using in-house replacement gilts and removal of affected piglets and their littermates from production cycles to limit exposure of others to the virus (Williamson, 2017).

1.5 Aims and objectives

This project aimed to further characterise APPV and the outcomes (clinical, virological, pathological, and immunological) associated with infection using British APPV field strains. In order to study the virus for a greater understanding of host—pathogen interactions and their effect on host immunity (including the potential for immunosuppression leading to co-infection and persistent infection) and disease development it is initially necessary to develop robust diagnostic assays capable of detecting and quantifying British APPV strains. Sensitive and specific diagnostic techniques are also necessary for epidemiological investigation of APPV-associated CT A-II to accurately appraise the current risk to the British pig industry. Further research in this area will contribute to the improvement of current control and prevention strategies and ultimately eradication efforts.

More specifically the objectives were to:

- Establish methodologies for the detection, quantification and characterisation of APPV
- Identify APPV in natural CT A-II infections and characterise the clinical, virological, pathological and immunological outcomes of infection in piglets
- Evaluate the role of APPV as an immunosuppressive agent and its impact on co-infections
- Determine the prevalence of APPV within the Scottish herd and characterise British APPV field strains.

Chapter 2: Materials and Methods

2.1 Sample preparation

Samples were collected from experimentally-infected pigs, negative controls and clinical field cases. The following sample types were collected: nasal swabs, rectal swabs, oropharyngeal swabs, Ethylenediaminetetra acetic acid (EDTA) blood, coagulated blood for serum and tissues. Tissues were sectioned in half, with half stored frozen in separate bags (-20°C) until processed, and the remaining material immediately immersed in 10% buffered formalin for a minimum of 2 weeks for fixation prior to processing. Instead of storing the brain section in a bag, it was placed on a dispocut board (cell path), sealed in clingfilm then immediately frozen (-20°C) to maintain structural integrity of the sample. In some cases, only fixed or frozen material was collected from the animals. Ear notches were stored in individual Eppendorf tubes at -20°C.

2.1.1 Homogenisation of fresh tissue

Each tissue was homogenised separately at a concentration of 0.25 g /ml (25%) in virus transport medium (VTM) to preserve the virus. Depending on the amount of material available, the tissue was homogenised in one of two ways. For quantities of tissue weighing equal to or greater than 0.5 g, tissue was homogenised using dispomix tubes (M tubes, Miltenyi Biotec) in combination with the GentleMacs™ dissociator and a pre-set programme consisting of two cycles of +2000 revolutions per minute (RPM) for four seconds, -2000 RPM for four seconds, +4000 RPM for four seconds then -4000 RPM punctuated by four-second rest intervals. For smaller quantities (0.5 g or less) CK28 Precellys tubes containing ceramic beads were used in combination with high-speed centrifugation (two cycles of two, 23-second pulses at 58,000 *xg* leaving samples on ice for two minutes between cycles).

The homogenates were freeze-thawed at -80°C once to increase the release of the virus into the supernatant. The supernatant was harvested after centrifugation at 2000 *xg* for 10 minutes at 4°C to remove cell debris and stored at -20°C until further use.

2.1.2 Ear notches

Ear notches were collected using an ear punch tool capable of producing a 1 cm diameter plug; the tool was disinfected using 70% ethanol between animals. Each ear notch was shaved to remove the hair from the skin, its weight recorded and placed into an Eppendorf containing 0.2 ml of Virotype RLT lysis buffer. The Eppendorf was incubated at 65°C for 30 minutes then 98°C for an additional 15 minutes using a heat block. The samples were placed on ice to cool for five minutes prior to centrifugation in a bench top centrifuge at 800 RPM for 30 seconds. The supernatant was collected and stored at -20°C until testing.

2.1.3 Environmental samples

Five hundred milligrams of used bedding were transferred to an Eppendorf tube, and 1 ml of phosphate-buffered saline (PBS) added before vortexing vigorously for three minutes. The suspension was then centrifuged for one minute at 15,000 *xg* before the supernatant was removed and stored at -20°C until further processed. Environmental swabs taken from pens, walkways and troughs were prepared as detailed in 2.1.5

2.1.4 Serum

Whole blood was collected in vacutainers containing a silica additive and left to coagulate at 4°C until a visible clot formed. After centrifugation at 2000 *xg*

for 10 minutes at 4°C, the serum was collected and stored at -20°C until further use.

2.1.5 Swabs

One millilitre of sterile PBS was added to a bijou containing the head of the swab before vortexing the sample for one minute to release viral particles. The swab was then discarded, and the sample was transferred to an Eppendorf tube and centrifuged at 15,000 *xg* for three minutes. The supernatant was collected and stored at -20°C until needed.

2.1.6 Semen

Semen samples were obtained at slaughter from the epididymis of boars from a farrowing group naturally infected with atypical porcine pestivirus (APPV). Each semen sample was freeze-thawed once at -20°C to release the virus prior to centrifugation at 15,000 *xg* for two minutes. The supernatant was collected and stored at -20°C until required.

2.2 Molecular techniques

2.2.1 Nucleic acid extraction

Nucleic acid was extracted from tissue, serum, swabs and semen collected from experimentally-infected pigs, negative controls and clinical field cases as described below.

2.2.1.1 Manual extraction

2.2.1.1.1Extraction of RNA from tissue

Ribonucleic acid (RNA) isolation and purification were performed using QIAshredder and RNeasy mini kits (Qiagen) with the reagents provided and

following the manufacturer's instructions. For extraction of samples, 350 µl of the tissue homogenate supernatant was added to an equal volume of RLT buffer containing 1% β-Mercaptoethanol prior to loading into the QIAshredder column for centrifugation at 12,000 *xg* for 2 minutes to homogenise the sample further. The column eluate was added to 700 µl of 70% ethanol, then loaded onto a RNeasy column and centrifuged for 15 seconds at 12,000 *xg*. The column was washed once with 700 µl of buffer RWI and centrifuged for 15 seconds at 12,000 *xg*, then washed twice with 500 µl of RPE and centrifuged at 12,000 *xg* for 15 seconds for the first wash and two minutes for the second wash. To remove additional flow through and residual buffers, the column was centrifuged for a further minute at 12,000 *xg*. The purified RNA was eluted in 40 µl of molecular grade water by centrifuging at 12,000 *xg* for one minute. The RNA eluate was stored at -20°C until required.

2.2.1.1.2 Extraction of RNA from swabs, serum and cell culture

RNA isolation and purification from cell-free bodily fluids were performed using the reagents supplied as part of the QIAmp viral RNA mini kit (Qiagen) following the manufacturer's protocol. For each extraction, 140 µl of the sample was added to 560 µl of AVL buffer containing 10 ng/µl of carrier RNA (pre-diluted in AVE buffer), vortexed for 15 seconds and incubated at room temperature for 10 minutes to lyse the sample. An equal volume of 100% ethanol was added to the lysate and vortexed for 15 seconds before loading into the QIAmp viral column and centrifuged at 6,000 *xg* for one minute. The column was washed once with 500 µl of AW1 buffer (centrifuged for one minute at 6,000 *xg),* then twice with 500 µl of AW2 buffer and centrifuged at 6,000 *xg* for one minute for the first wash and three minutes for the second wash. To remove additional flow through and residual buffers, the column was then centrifuged for an extra minute at 12,000 *xg*. The elution step was performed twice using 40 µl of AVE buffer incubated within the column for one minute then centrifuged at 6,000 *xg* for one minute. The 80 µl RNA elution was stored at -20°C until further use.

2.2.1.2 Automated extraction of total nucleic acid

The MagMAX CORE nucleic acid purification kit (Life Technologies) was used in combination with the MagMax Express 96 platform (Life Technologies) for a magnetic bead-based automated extraction of total nucleic acid. This system was used in the extraction of total nucleic acid from tissue, cell culture, semen, serum, swabs and environmental samples following the manufacturer's guidelines. Briefly, two deep 96-well processing plates containing either 500 µl of wash one and wash two buffers and a 200 µl 96-well plate containing 90 µl of elution buffer were prepared in advance of loading the extraction platform. For simple samples (serum, semen, swabs, cell culture, and tissue) a deep 96-well lysis plate was also prepared to contain 30 µl of a bead/proteinase K mix (20 µl of beads with 10 µl of proteinase K reagent, supplied with the kit). The processed sample (2.1) was added to the lysis plate and mixed by pipetting. The volume of sample added for the extraction was dependent on sample type (200 µl of serum, swabs, semen supernatant, and cell culture supernatant, or 100 µl of tissue homogenate supernatant). Seven hundred millilitres of lysis mix (350 µl of lysis buffer added to 350 µl of binding solution per sample and mixed thoroughly by inversion) were then added to the lysis plate. The plates were then loaded directly on to the extraction platform.

For complex environmental samples, 450 µl lysis buffer was added to 200 µl of sample supernatant before vortexing for three minutes. The lysate was then centrifuged at 15,000 xg for two minutes. Five hundred microlitres of clarified lysate supernatant were removed and added to the lysis plate alongside the 30 µl of a bead/proteinase k mix. The solution was mixed by pipetting and incubated for two minutes at room temperature before adding 350 µl of the binding solution then loaded onto the extraction platform.

A preformed tip comb, the processing plates, and the lysis plate containing the sample were loaded into the appropriate positions within the MagMax instrument and a preloaded programme (MagMAX_ CORE_ KF-96_ no_

heat.bdz) supplied by the manufacturer was used for the extraction. The eluate, corresponding to 90 µl of total extracted nucleic acid, was stored at -20°C until processed for downstream analysis.

2.2.2 Conventional PCR and gel electrophoresis

Conventional reverse transcriptase polymerase chain reaction (RT-PCR) was performed on the TC-plus (Techne) thermal cycler using the Superscript III One-step RT-PCR system with Platinum Taq (Invitrogen) following the manufacturer's instructions as set out in Table 2-1 and Table 2-2. The reverse transcription (RT) and polymerase chain reaction (PCR) amplification steps were carried out within the same 0.2 µl tube in a closed system. Biological positive control and negative template control were included in each assay run.

Table 2-1: Master mix preparation for conventional PCR using Superscript III One-step RT-PCR system with Platinum Taq kit

Reagent	Volume (µl)
2X Reaction Mix	25
Super Script™ III RT/Platinum™ Taq Mix	2
Forward Primer (10 µM)	1
Reverse Primer (10 µM)	1
Molecular grade water	19
RNA template	2
Total	**50**

Table 2-2: Thermocycling profile for conventional PCR using Superscript III One-step RT-PCR system with Platinum Taq kit

Temperature	Time	Stage	Cycles
50°C	15 minutes	Reverse transcription cDNA synthesis and pre-denaturation	1
95°C	2 minutes		1
94°C	15 seconds	Denaturation	40
55°C	30 seconds	Annealing	
60°C	1 minute	Extension	
68°C	1 minute	Final extension	1

Agarose gel electrophoresis was used to visualise the PCR product separating the complementary deoxyribonucleic acid (cDNA) fragments by size. The gel consisted of 1.5 to 2% ultrapure agarose (Invitrogen) dissolved in a 1 x TAE solution (1 x TAE was diluted from a 50 x TAE stock solution from Thermo Fisher containing 40 mM Tris, 20 mM Acetic acid and 1 mM EDTA) with GelRed (Biotium) added for a final dilution of 1:10,000. The samples were mixed with 5 x deoxyribonucleic acid (DNA) loading buffer blue (Bioline) at a 1:5 dilution, and 10 µl loaded and run against 5 µl of either Hyperladder I or IV DNA Markers (Bioline) depending on the size of the PCR product fragment. The gel was run at 80 V for 45—60 minutes and visualised using the G: BOX F3 Automated Gel Doc system (Syngene).

2.2.3 Reverse transcriptase real time quantitative polymerase chain reaction

To detect the part of the APPV Non-structural protein (NS) 3 gene a reverse transcriptase real time quantitative polymerase chain reaction (RT-qPCR) was optimised and validated as described in 3.3.1 The finalised master mix and

thermocycling profile is outlined in Table 3-7 and Table 3-6 Samples were quantified by a standard curve (3.3.1.5) of an APPV plasmid produced using the techniques described in 2.3. The standard series, the biological positive control (3.3.1.6) the no template control (PCR master mix only) and negative extraction control (extracted sterile nuclease-free water) were included on each assay, all standards, samples and controls were tested in duplicate. Results were interpreted as described in 3.3.1.7

2.2.4 Purification of cDNA from PCR products

Purification of cDNA PCR product from the reaction reagents was achieved using either the ethanol precipitation technique or a magnetic bead method performed using the Charge switch PCR clean up kit (Invitrogen). All centrifugation steps were performed using a benchtop centrifuge. For ethanol precipitation, 100 µl of the PCR product was combined with 1 µl of 20 mg/µl glycogen, 10 µl of 3 M sodium acetate and 300 µl of 100% ethanol before chilling for one hour at -20°C to precipitate the cDNA. To pellet the cDNA, the solution was centrifuged at 14,000 RPM for 30 minutes. The supernatant was then removed, and the pellet was washed twice with 70% ethanol before air drying. The pellet was then re-suspended in 100 µl of molecular grade water.

The charge switch PCR clean up Kit was carried out per the manufacturer's protocol. Briefly, 40 µl of the PCR product is combined with an equal volume of the purification buffer provided with the kit and 10 µl of magnetic beads. The reaction is incubated at room temperature for one minute before placing the tube on the MagnaRack separation rack (Invitrogen) for one minute to form a tight bead pellet. The supernatant is removed, and the pellet is washed twice with a 150 µl wash buffer before eluting the DNA in 30 µl of elution buffer.

Purification of cDNA PCR product from agarose gel was carried out using the QIAquick gel extraction kit (Qiagen) as per the manufacturer's protocol. The

DNA fragment was visualised on gel visualiser and excised using a scalpel. The band was weighted, and 100 µl of QG buffer added for each 100 mg of gel then incubated at 50°C for 10 minutes until the agarose gel had dissolved. One hundred microlitres of isopropanol per 100 mg of the gel was added and vortexed to mix prior to loading into QIAquick column. The column was centrifuged at 13,000 RPM for one minute to bind the DNA to the column. Five hundred microlitres of QG buffer passed through the column by centrifugation at 13,000 RPM for one minute, and the flow-through was discarded. Seven hundred and fifty microlitres of PE buffer were allowed to stand in the column for two minutes prior to centrifugation at 13,000 RPM for one minute. After the flow-through was discarded, the column was centrifuged for one minute without additional reagents to remove the residual PE wash buffer. Finally, a two-step elution was performed; 20 µl of EB buffer was added to the column and left to stand for two minutes before centrifugation at 13,000 RPM for one minute, then repeated.

2.2.5 Assessment of DNA and RNA quality and quantity

The quantity and quality of RNA and DNA were assessed by spectrophotometry (Nanodrop 1000, Thermo Fisher Scientific). A blank (elution buffer) was used to calibrate the instrument before loading the sample. The purity of the sample was assessed by absorbance reading at 260 nm and 280 nm, where a ratio of 2.0 was considered acceptable, with a corresponding 260/230 ratio of 2.0 to 2.2.

2.2.6 Sanger sequencing

Sanger sequencing was completed externally by MWG-Eurofins. Forward and reverse sequences were aligned using SeqMan Pro (DNAStar) and to determine nucleotide identity with other published APPV sequences Basic

local alignment search tool BLAST, (National Centre for Biotechnology Information) analysis was performed on the consensus sequence.

2.3 Molecular cloning for standards

A 1:10 serial dilution of a known concentration of target sequence was run in duplicate on every test to create a standard curve allowing absolute quantification of samples during Real-Time PCR. For the generation of APPV plasmid standards APPV cDNA PCR product which had been previously purified and sequenced (as described in 2.2.4 and 2.2.6) was cloned as follows. This technique was also used to generate PRRSV plasmid from purified and sequenced (2.2.4 and 2.2.6) PRRSV European genotype cDNA for absolute quantification of samples when used in conjunction with the Virotype PRRSV RT-PCR kit (Indical Biosciences) as described in 5.4.4

2.3.1 Transformation of the pGEM-T easy vector plasmid

A PCR product containing the desired APPV cDNA sequence was inserted into the pGEM-T easy vector (Promega) following the manufacturer's guidelines. The ligation reaction and self-ligation control reactions were set up as detailed in Table 2-3. The reactions were incubated at room temperature for one hour preceding the transformation of JM109 competent cells.

Table 2-3: Ligation reaction preparation for pGEM-T easy vector system

Reagent	Volume (µl)
2X Rapid ligation buffer, T4 DNA ligase	5
pGEM-T easy vector (50ng)	1
T4 DNA ligase (3 Weiss units/µl)	1
Molecular grade water	1
APPV SYBR Green RT-PCR Product	2
Total Volume	**10**

2.3.2 Transformation of JM109 cells

JM109 high-efficiency competent *Escherichia coli* cells (Promega) were used in the transformation following the manufacturer's instructions. In short, Luria Bertani (LB) (reagent grade water containing 1% BactoTryptone, 1% sodium chloride and 0.5% Bacto yeast extract) enriched agar plates containing a final concentration of 100 µg/ml Ampicillin was prepared following aseptic techniques. The JM109 competent cells were thawed on ice, and 50 µl were then added to 2 µl of the ligation reaction before incubating on ice for 20 minutes. The reaction mixture was heat shocked for 45—50 seconds in a 42°C water bath followed by two minutes on ice. Nine hundred and fifty microliters of super optimal broth (SOC) media (2% Tryptone, 0.5% Yeast Extract, 10 mM NaCl, 2.5 mM KCl ,10 mM $MgCl_2$, 10 mM $MgSO_4$, 20 mM glucose (Invitrogen)) was added to the ligation reaction transformation and incubated for one hour at 37°C with shaking (150 rpm). Ten microlitres and 100 µl of the transformations were spread on the previously prepared plates. The plates were incubated at 37°C overnight.

2.3.3 Growth of bacterial cultures

Six of the pGEM-T positive colonies were selected at random and grown individually in 10 ml of LB enriched broth with a final concentration of 100 µg/ml Ampicillin. The broth was incubated at 37°C with shaking at 200 RPM for between 12 and 16 hours.

2.3.4 Long term storage of bacterial stock

To prepare surplus bacterial cultures positive for the transformed clone for long-term storage glycerol was added to the culture to a final concentration of 25% and aliquoted into 2 ml vials before storage at -80°C.

2.3.5 Plasmid DNA purification

Bacterial cultures were centrifuged at room temperature at 3,000 *g* for 10 minutes before discarding the supernatant. The plasmid DNA was then purified from the bacterial pellet using the QIAprep spin miniprep kit (Qiagen) according to the manufacturer's instructions; prior to use, all kit reagents were prepared as specified in the protocol. Centrifugation steps were performed in a bench top centrifuge. Five mililitres of the bacterial culture, grown as stated in 2.3.3, was centrifuged at 800 RPM for three minutes to form a pellet. The supernatant was discarded before resuspension of the pellet in 250 µl of P1 buffer. A total of 250 µl of P2 buffer was added to the tube then mixed by inversion until the solution became clear blue (no more than five minutes). Three hundred and fifty microlitres of N3 buffer was added to the preparation followed by mixing through inversion until it became colourless. The solution was centrifuged at 13,000 RPM for 10 minutes; the supernatant was transferred to the QIAprep spin column and centrifuged for 60 seconds at 13,000 RPM. The flow-through was discarded, and the column washed with 0.5ml of PB buffer. The wash step was repeated with a volume of 0.75 ml PE buffer. An additional centrifugation step for one minute was used to remove

residual wash buffer from the column preceding the elution in 50 µl of EB buffer (10 nM Tris-hydrochloric acid) by letting the EB-filled column stand for one minute, then centrifuging it for one minute. After purification, the concentration of DNA was quantified as detailed in 2.2.5.

2.3.6 Restriction enzyme digest

A digestion of the purified plasmid was conducted to produce linearised DNA to be used as a standard for RT-qPCR. The digestion was performed using *EcoR*I restriction enzyme (Promega) in a total reaction volume of 20 µl. The reaction mix contained 2 µl of 10x buffer H the corresponding high salt buffer to *EcoR*I, 1 µl of *EcoR*I, 7 µl of molecular grade water and 10 µl of the purified plasmid. The reaction was incubated at 37°C for 2 hours.

2.3.7 Production and storage of standards for APPV RT-qPCR

The linearised plasmid stock was aliquoted and stored at -20°C. Sets of standards were produced in batches by a 10-fold serial dilution of the stock plasmid from $3.19x10^8$ to $3.19x10^1$ copies/µl and were allowed a maximum of three freeze-thaw cycles before discarding to prevent inter-assay variation due to degradation. Each new batch of standards were tested against the in-use batch to assess variation, batches were considered acceptable for use when the difference between batches was less than 1 Ct (cycle threshold).

2.3.8 Calculation of standards copy number

To calculate the copy number of the standards, the fragment length and concentration of the APPV plasmid (ng/µl) quantified as described in 2.2.5 was first determined (109.9 ng and 3,139 bp respectively). The molecular weight for the APPV plasmid was then calculated (2,071,740 Dalton) using the

average molecular weight of one base pair (660 Dalton). The number of plasmid molecules in 1 ng was calculated based on Avogadro's constant ($6.02x10^{23}$ molecules) and assumption that one mole is equivalent to the molecular weight in grams ($6.02x10^{23}/2{,}071{,}740x10^{-9}= 2.9x10^{8}$ copies). The final copy number per µl was calculated using both the molecules of the plasmid in 1 ng and the concentration of APPV plasmid ($2.9x10^{8}$ copies x 109.9 ng/µl). The final copy number in the neat plasmid stock was found to be $3.19x10^{10}$ copies/µl and from this a set of standards with a known copy number was prepared in accordance with 2.3.7.

2.4 Serology for the detection of APPV antibodies

2.4.1 NS3H blocking enzyme-linked immunosorbent assay (ELISA)

To detect APPV antibodies present in serum, an NS3H blocking ELISA was supplied by a collaborator (Schwarz *et al.*, 2017). Briefly, the protocol was performed as follows; all stages were carried out at room temperature unless specified. Prior to the commencement of the test, a coating buffer and a wash buffer were made in house as outlined in Table 2-4.

Table 2-4: Preparation of reagents for the coating and wash buffers used in the APPV NS3H blocking ELISA.

Coating buffer *	**Wash buffer ◊**		
Reagent	Quantity	Reagent	Quantity
Sodium carbonate	3.03 g	Sodium hydrogen phosphate	1.16 g
Sodium bicarbonate	6.00 g	Potassium chloride	0.10 g
Distilled water	1000 ml	Potassium phosphate	0.10 g
		Sodium chloride	4.00 g
		Tween 20	2.5 ml
		Distilled water	500 ml

* Coating Buffer pH 9.6, ◊ Wash buffer pH 7.4

To coat the ELISA plate (Maxisorb, Nunc), 10 mg/ml antigen was diluted 1:200 in the coating buffer and 50 µl of the diluted coating antigen was added to each well and incubated at 4°C overnight. The plate was washed with 300 µl PBS three times and blocked with 5% fetal bovine serum (FBS) in the wash buffer for one hour. The wash step was repeated, and 100 µl of controls (positive pig serum as a positive control and FBS as a negative control as supplied by the collaborator) and samples, which had been prediluted 1:2 in the wash buffer, were added to the plate and incubated for 1 hour. The plate was washed with 300 µl of wash buffer three times before adding 100 µl of prediluted monoclonal antibody 1B3 (a 1:5 dilution in the wash buffer) and incubated for 30 minutes. During the incubation period the goat anti-mouse heavy and light chain conjugated with horseradish peroxidase (Jackson laboratories) was diluted 1:3,000 in the washing buffer. After repeating the previous wash step, 50 µl was added to the plate and incubated for 30 minutes. The wash step was repeated once more before adding 100 µl of SureBlue TMB 1-component

microwell peroxidase substrate (KPL). The plate was incubated for 5—10 minutes, based on reaching an optical density (OD) value of 1 in the negative control wells before stopping the reaction with 100 µl of 0.18 M sulphuric acid. The plate was read at an absorbance of 450 nm, and the results were valid if the negative control wells had an OD value greater than 1 and the positive control had a percentage inhibition of greater than 50%. The percentage inhibition of each sample was calculated using the sample and the negative control OD values. Samples were considered positive if their percentage inhibition was greater than 50%.

2.4.2 NS3 indirect ELISA

An indirect ELISA was developed and optimised for the detection of differences in APPV antibody titres in sera over time using the antigen supplied previously for the NS3H blocking ELISA (2.4.1). The test was performed under the conditions specified the NS3H blocking ELISA section (2.4.1) using the same buffers prepared in-house as described in Table 2-4.

The ELISA plate (Maxisorb, Nunc) was coated with the antigen (10 mg/ml) diluted 1:1,000 in the coating buffer, 50 µl of the diluted coating antigen was added to each well and incubated at 4°C overnight. The plate was washed three times with 300 µl PBS and blocked with 5% pestivirus-free FBS (in wash buffer) and incubated for one hour before the wash step was repeated. For all tests, excluding the sero-survey described in 6.3.1, high and low positive and negative controls were prepared as follows: high concentration controls were created by diluting positive pooled sow serum as a positive control and negative pig serum E10/18-4 as a negative control 1:200 in wash buffer while low concentration control was diluted at 1:400 in wash buffer. For the serum sample survey (6.3.1), the same controls were prepared at a dilution of 1:50 for the high concentration and 1:200 for the low concentration. The no serum control and the samples were diluted 1:200 for all tests excluding the sero-

survey for which a dilution of 1:50 was used. One hundred microlitres of all controls and samples were added in duplicate to the plate and incubated for one hour. The plate was then washed with 300 µl of wash buffer three times prior to adding 50 µl of a rabbit anti pig immunoglobulin G (IgG) whole molecule antibody conjugated with horseradish peroxidase (Sigma Aldrich) diluted 1:40,000 to the plate, followed by an incubation step for 30 minutes. The wash step was repeated once more before adding 100 µl of SureBlue TMB 1-component microwell peroxidase substrate (KPL). The plate was incubated for 10—15 minutes, reaching an OD of 0.7 in the negative control wells (read with the 405 nm filter) before stopping the reaction with 100 µl of 0.18 M sulphuric acid. The plate was then read at an absorbance of 450 nm.

Results were corrected for background based on the average OD of the no serum control wells (also referred to as blank wells) and standardised using the normalised coefficient (NC) calculated by dividing the average positive control OD of the test plate by the mean OD of the positive control from all plates from the experiment, then dividing the samples OD by the NC value.

2.5 Histopathological examination

2.5.1 Tissue preparation

Tissues were fixed in 10% buffered formalin for approximately three weeks prior to trimming and sectioning. The tissues were then dehydrated in alcohol for 24 hours prior to embedding in paraffin wax blocks. Tissue blocks were stored at room temperature. All tissue processing was carried out within the histopathology surveillance unit at Moredun Research Institute (MRI) following standard operating protocols used for diagnostic submissions. Paraffin-embedded tissue blocks were sectioned at 5 mm and mounted onto super frost plus slides (Fisher scientific) for haematoxylin and eosin staining (H&E), and for BaseScope *in situ* hybridisation (ISH) analysis. The H&E staining was

performed by the histopathology surveillance unit (MRI) following standard operating protocols used for diagnostic submissions. Stained slides were stored at room temperature, and slides prepared for BaseScope ISH were stored at 4°C until analysis.

2.5.2 BaseScope *in situ* hybridisation

The BaseScope ISH technique was used to visualise short APPV targets (single RNA molecules) in slide-mounted tissue samples. The assay was designed, optimised and validated in consultation with ACDBio (Bio-Teche) using their commercial BaseScope ISH detection reagent kit V2-RED in conjunction with the optimised protocol for formalin-fixed paraffin-embedded tissue (FFPE). Optimisation and validation of the technique for APPV detection is detailed in 3.3.4 and the finalised protocol is described below.

Slides were produced as detailed in 2.5.1 for BaseScope ISH analysis; slides were pre-treated by baking them in a dry oven for one hour at 60°C before the sections were deparaffinised at room temperature using a Shandon 24-4 Varistain (Thermo Fisher Scientific) following Programme 1 steps 1—4 with agitation; five minutes in xylene, five minutes in xylene, two minutes in 99% methylated spirit (74 O.P., Thermo Fisher Scientific) followed by two minutes in 74 O.P. The slides were then removed and left to air dry.

Once dry, the slides were placed horizontally, eight drops of hydrogen peroxide were applied to cover the tissues on each slide followed by an incubation for 10 minutes at room temperature. The excess hydrogen peroxide was removed by tapping the slide on absorbent paper before adding to a slide rack. The slides were washed by submerging the slide rack five times in distilled water before repeating the process with fresh distilled water. The antigen retrieval step was performed manually by submerging the slide rack in a covered beaker containing 700 ml of prepared target retrieval buffer (70 ml

of 10 times concentrated target retrieval buffer in 630 ml of distilled water). Depending on the level of fixation, integrity of the tissue and the tissue type, the slides were boiled in the target retrieval buffer at 98—100°C for either eight minutes for more fragile tissues (lung and spinal cord) or for an extended period of 20 minutes (brain, spleen and lymphoid tissue). The slides were then immediately washed as previously described in distilled water at room temperature before incubating them in ethanol absolute (Fisher Scientific) for three minutes. The slides were left to dry at room temperature. Once dry, a hydrophobic barrier was drawn on each slide to encircle the tissue using an Immedge hydrophobic barrier pen (Vector Laboratory). To improve adhesion, lung slides were then baked for 30 minutes at 37°C prior to protease IV treatment (provided with the kit). This additional step was not carried out for any other tissue tested as it was deemed unnecessary. The protease IV treatment was performed on the slides as follows: the slides were secured in an ACD Ez-Batch slide rack (Bio-Techne) and six drops of RNAScope protease IV added to cover the tissue section on the slide, the rack was then sealed inside a HybEZ humidity control tray (Bio-Techne) and incubated at 40°C inside the HybEZ Oven (Bio-Techne) for 15 minutes. After incubation, any reagent excess was removed as previously described on absorbent paper before washing the slides five times with distilled water.

The BaseScope ISH assay was performed in the ACD EZ batch slide rack in the HybEZ humidity control tray on pre-treated slides through an initial probe hybridisation step where six drops of the Great Britain (GB)-specific APPV probe (3.3.4) were added to the slides and incubated in the HybEZ Oven at 40°C for two hours. The slides were washed for two minutes using room temperature wash buffer (supplied with the kit), which was then repeated using fresh wash buffer. The second stage of the assay involved incubating the slides in different hybridize BaseScope V2 reagents (AMP 1-8) for various lengths of time specific to the reagent; AMP 1 and AMP 2 were incubated for 30 minutes, AMP 3 for 15 minutes, AMP 4 and AMP 5 for 30 minutes, AMP 6 for 15 minutes, AMP 7 for one hour and AMP 8 for 15 minutes all incubations

were performed in the oven at 40°C with the exception of AMP 7 and AMP 8 which were performed at room temperature. For all AMP reagent's steps, after incubation excess reagent was removed by blotting the edge of the slide on absorbent paper. The slides were washed in wash buffer for two minutes at room temperature before repeating the wash step with fresh wash buffer before proceeding with the next sequential hybridize BaseScope V2 reagent.

Assay results were visualised by adding 120 µl of red solution (supplied with the kit) to each slide in the ACD EZ batch slide rack in the HybEZ humidity control tray. The tray was sealed and incubated at room temperature for 10 minutes; excess red solution was removed from the slides and the slides washed in distilled water; the wash step was repeated using fresh, distilled water. The slides were counterstained using the Shannon Varistain (Thermo Scientific) programme 1 step 7-13 with agitation; 50% Gils No.1 haematoxylin (Merck) for two minutes, running tap water for one minute, Scott's tap water (prepared in-house as follows: 2 g sodium bicarbonate, 20 g magnesium sulphate, 1 L of distilled water) for one minute, and finally running water for one minute. The slides were left to dry overnight at room temperature before cover slipping using 24 x 50 mm #1,5 Menzel Gläser coverslips (Fisher scientific) with EcoMount (Biocare Medical).

The slides were examined using a light microscope at 40 x magnification to assess the morphology of the tissue and level of staining. The positive and negative control probe signals were evaluated at 40 x magnification, and the test determined valid if the positive control was observed as visible defined punctuated dots and the negative control had no more than one dot to every 20 cells as a level of background staining. The slides were evaluated for the presence of any APPV positive signal; APPV signal was considered to be cell associated when observed in the nucleus or cytoplasm of the cell and considered non-cell-associated when present in the extracellular matrix.

2.6 Cell culture

2.6.1 Cell splitting and maintenance

Bovine turbinate (BT) and SPEV 0008 cell lines detailed in Table 2-5 were cultured in closed cap flasks (T225, Corning) at 37°C. Porcine kidney-15 (PK-15) cells described in Table 2-5 were cultured in vented cap flasks (T225, Corning) at 37°C in 5% CO_2. Cells were passed by washing the monolayer with PBS twice before rinsing with trypsin-versene solution (4 ml of 0.25% Trypsin to 16 ml of 0.2 g/l Versene, MRI). Once the excess trypsin-versene solution was removed, the cells were left to dissociate from the flask in the incubator at 37°C for two to five minutes. Following this, 5 ml of the cell culture medium was added to cells to neutralise the effects of the trypsin-versene and pipette mixed to form a single-cell suspension. Two hundred microlitres of 2% nigrosin was added to an equal volume of the cell suspension used to count the cells using an improved Neubauer haemocytometer counting chamber using light microscopy. The cell count was used to determine the appropriate volume of the cell suspension to seed the new flask to reach 100% confluence within three days, with 75 ml of maintenance media added to the flask. The cell stock was checked daily for signs of toxicity, contamination, and changes to morphology and confluency.

Table 2-5: Density and media for the maintenance of specific cell lines used for virus isolation

Cell line	Species	Cell type	Media	Seeding density	Virus susceptibility
BT	Bovine	Turbinate	Isocove's modified media 200 nM glutamine 10% horse serum	$1.0x10^5$ cells	BVDV
PK-15	Porcine	Kidney	Dulbecco's modified Eagle medium 1% glutamax 10% horse serum	$1.5x10^6$ cells	CSFV
SPEV 0008	Porcine	Kidney	In house (Table 2-6) 5% horse serum	$3.3x10^6$ cells	CSFV APPV

Bovine viral diarrhoea virus abbreviated as BVDV and classical swine fever virus abbreviated as CSFV

Table 2-6: Preparation of SPEV 0008 cell media. Once prepared the pH of the media was adjusted to 7.3 ± 0.1, filtered at 0.22 µm and given a batch number and a 21-day expiry date.

Reagent	Quantity
Minimum essential media with Earle's salts	100 ml
Minimum essential media with Hank's salts	100 ml
Sodium bicarbonate	2.1 ml
L-glutamine (200 nm)	4 ml
Sodium pyruvate (120 mg/l)	2 ml
Non-essential amino acids	2 ml
Gentamycin (10 mg/ml)	1 ml
Penicillin (10,000 units) and streptomycin (10 mg/ml)	2 ml

2.6.2 Virus isolation

Virus isolation was attempted using the cell lines detailed in 2.6.1. Optimisation of the virus isolation protocol was conducted for each cell line individually as described in 3.4.

2.6.3 Cryopreservation and resuscitation of cells

Cells were dissociated from the flask, re-suspended and counted as described in 2.5.1. The cells were clarified at 800 RPM for five minutes at 4°C. The supernatant was discarded, and the cells were re-suspended at a concentration of $1x10^6$ to $2x10^6$ cells/ml in freezing media containing 90% cell media with 5% horse serum and 10% dimethyl sulphoxide (DMSO). One millilitre volume of the cell suspension was added to cryovials (Nunc) that were placed in a Mr Frosty freezing chamber (Thermo Fisher Scientific) containing

isopropanol precooled at -20°C prior to storing at -80°C for 24 hours to allow the temperature to cool at a rate of 1°C per minute until frozen. Once frozen, the cells were transferred to long term storage in liquid nitrogen.

Cells were resuscitated by thawing the cells quickly before mixing with 10 ml of the appropriate maintenance media and pelleting at 150 xg for five minutes at room temperature. The supernatant containing cryoprotectant (DMSO) was removed and the cells re-suspended in warm maintenance media at the required seeding density. The cells were then transferred to a flask and grown as previously described in 2.5.1.

2.7 Animal studies

Animal experiments were conducted with the approval of the MRI animal ethics review board and carried out under the animal (scientific procedures) act 1986 following home office guidelines under project licence PFA7E7AD6. Clinical samples collected from live animals from a Scottish field case study were submitted by a veterinarian as diagnostic samples for investigation of suspected APPV.

2.8 Statistical analysis

Statistical analysis was performed with the software R, version 3.6.1 (R Core Team, 2019) with consultation with in-house statistical expertise at MRI (Dr Adam Hayward) and externally from Biomathematics and Statistics Scotland (BioSS). Additional information regarding the statistical analysis and parameters to define significance is located within the respective chapters.

Chapter 3: Establishing diagnostic techniques for the detection of atypical porcine pestivirus and generation of supporting infectious material

3.1 Introduction

Robust techniques for the detection and quantification of atypical porcine pestivirus (APPV) are paramount, not only to successfully achieve diagnosis in a clinical setting but also to underpin research into the characterisation of the virus and host—pathogen interactions. Diagnostic tests are integral to both active and passive surveillance programmes to determine the prevalence and distribution of APPV both within the British pig industry and in a global context, which can inform and thus improve prevention and control strategies. At the commencement of this project in 2017, the availability of diagnostic assays for APPV was severely limited: no tests were commercially available and only a small number of in-house assays were published. Validation of the assays used in the diagnosis of APPV was also under-reported and hampered by a lack of available APPV isolates and reference samples. In this chapter, additional development, optimisation and validation of molecular and immunological techniques for the diagnosis of APPV are described to address this deficit and to establish informative, sensitive and specific diagnostic tools.

Initially, APPV real time reverse transcriptase quantitative polymerase chain reaction (RT-qPCR) assays were designed based on limited sequences available for the 5′UTR (De Groof *et al.*, 2016), non-structural protein (NS) 3 (Arruda *et al.*, 2016; Postel *et al.*, 2016) and NS5B (Beer *et al.*, 2017; Schwarz *et al.*, 2017) with subsequent assays designed for these regions (Yuan *et al.*, 2017; Gatto *et al.*, 2018b; Kaufmann *et al.*, 2019; Zhou *et al.*, 2019) as well as the NS4B (Postel *et al.*, 2016) and the NS5A (Shen *et al.*, 2018) regions after

the commencement of optimisation work conducted in this chapter. The initially designed NS3 (Arruda *et al.*, 2016; Postel *et al.*, 2016) and NS5B (Beer *et al.*, 2017; Schwarz *et al.*, 2017) assays have also been subsequently adapted and employed in other studies for the identification and quantification of APPV ribonucleic acid (RNA) in different sample types including tissues, swab samples, semen and blood/serum samples from naturally infected pigs (Muñoz-González *et al.*, 2017; Dessureault *et al.*, 2018; Gatto *et al.*, 2018a; Sozzi *et al.*, 2019; Mósena *et al.*, 2020). Since its discovery in 2015, APPV sequences for all genes have been determined to have high genetic variability even within the same geographic location (Postel *et al.*, 2016; Beer *et al.*, 2017; Postel *et al.*, 2017a; Yuan *et al.*, 2017; Dessureault *et al.*, 2018; Mósena *et al.*, 2018). For this reason, previously established assays need to be evaluated in the context of the APPV strains circulating locally. At the commencement of this thesis, only one study had been conducted to evaluate British samples for APPV; in this study only a small number (86) of serum samples were included for RT-qPCR and sequence analysis (one serum sample, GenBank accession number MF279220). No sample history (date of sample collection, age of the pigs, or geographical distribution) was reported, and interpretation of strain variability within Great Britain could not be made based on a single APPV sequence (Postel *et al.*, 2017a). Therefore, further work was urgently needed to establish effective molecular assays for the detection of British APPV strains in a range of sample types and specific to the landscape in Great Britain. Fluorescent *in situ* hybridisation (FISH) methods have also been adopted to identify viral genomes in lymphoid and central nervous tissues. One study used an in house APPV NS3 specific probe cross-validated with RT-qPCR to determine the presence of APPV in different tissues (Postel *et al.*, 2016). FISH results agreed with RT-qPCR detection results for all tissues apart from in thymus, longissimus muscle and brain stem tissues, where APPV was not detectable by FISH but APPV ribonucleic acid (RNA) was detected at low viral loads (quantification cycle between 30 and 38) by RT-qPCR, suggesting a limited sensitivity at low viral loads. Pfankuche *et al.* (2018) investigated the capability of a digoxigenin-labelled RNA probe (designed in-house) for use

with *in situ* hybridisation (ISH) techniques and a commercially available ViewRNA TYPE 1 RNA Probe Set consisting of different Z-linked probes that are designed to hybridize specific target sequences (APPV target sequence accession number: KU041638 [catalogue number VF1-19276 20, Thermo Fisher Scientific]) for use in FISH on APPV positive cerebellum. Although the in-house probe was unable to detect APPV RNA, the commercial RNA probe identified diffuse APPV within the inner granular layer of the cerebellum from an APPV positive pig (Pfankuche *et al.*, 2018). Further evaluation of the commercial probe set is needed to determine if the probes can detect other pestiviruses to discern the usefulness of the test as a differential technique.

Immunohistochemical (IHC) tests using established techniques for the detection of glial fibrillary acidic proteins (GFAP), which are found in astrocytes and oligodendrocytes, have been performed on brain and spinal cord tissue to identify possible pathology changes associated with APPV infections (Schwarz *et al.*, 2017; Possatti *et al.*, 2018b). Changes in GFAP levels are not specific to APPV infections and elevated levels are often present in tissues of a diseased or damaged state associated with a number of conditions such as porcine respiratory and reproductive syndrome virus (PRRSV) (Antonson *et al.*, 2018). To date, only one IHC test has been established for the detection of APPV specific antigen using a rabbit polyclonal antibody raised against the envelope protein E^{rns} of APPV (Liu *et al.*, 2019). The test was capable of detecting APPV in all the tissue types tested, although additional investigations are needed to rule out possible cross-reactions with other pestiviruses, especially those infecting pigs. Since the development of the BaseScope *in situ* hybridisation (ISH) technique presented in this chapter for the detection of British strains of APPV in tissue sections based on the NS3 gene, an RNAScope test (a sister test to BaseScope ISH) was developed to detect the N^{pro} and E^{rns} portions of the viral RNA in tissues from pigs with an experimental APPV infection (Buckley *et al.*, 2021). However, as the probe used by Buckley *et al.* (2021) was designed to be specific to the experimental inoculum strain, unlike the general Great Britain (GB) BaseScope ISH probe,

which was designed to be pan GB strains, it may not detect other genetically diverse strains of the virus. These relatively new techniques both employ simultaneous hybridisation of independent double Z probes to the target sequence to enable signal amplification and minimising non-specific binding and background signal. Both techniques are highly sensitive and specific alternatives to the other tests discussed and can be used to improve the diagnosis and characterisation of APPV infections.

Enzyme-linked immunosorbent tests (ELISA) have also been developed for the detection of anti-APPV immunoglobulin G (IgG) antibodies, to detect either previous exposure to the virus or passive transfer of maternally derived antibodies through colostrum. Direct (Hause *et al.*, 2015) and indirect (Postel *et al.*, 2017b) ELISAs were developed using the envelope proteins E^{rns} and E2 (Cagatay *et al.*, 2019) as antigen. Again, a lack of positive and negative APPV reference samples made it difficult to accurately define the sensitivity and specificity of the test, hampering validation (Hause *et al.*, 2015; Postel *et al.*, 2017b). These tests however have proven to be useful tools in the detection of antibodies and have been subsequently employed to study APPV seroprevalence (Postel *et al.*, 2017a; Cagatay *et al.*, 2018; Grahofer, Zeeh and Nathues, 2020). Schwarz *et al.* (2017) developed both an indirect and a blocking ELISA based on the NS3 helicase; however, the use of the indirect ELISA was discontinued due to evidence of insufficient sensitivity and specificity. Presently an IgM ELISA has not been described; it could be a useful tool in combination with an IgG ELISA in the distinction of acute infection from past exposure or chronic infection as IgM are generated in the early stages of an infection prior to class switching, which produces IgG in mid—later stage of infection.

In this chapter, additional diagnostic assay development, optimisation and validation of molecular and immunological techniques were conducted using clinical and experimentally collected samples. This was done to address the

under-reporting of optimisation and validation of previously published techniques and to establish informative, sensitive and specific diagnostic tools. As discussed in previous studies, the lack of an available tissue-culture grown APPV isolate has hampered the development and validation of diagnostic techniques (Hause *et al.*, 2015; Postel *et al.*, 2016; Postel *et al.*, 2017b; Schwarz *et al.*, 2017; Cagatay *et al.*, 2019; Gatto, Sonálio and de Oliveira, 2019), and the characterisation of the relationship between APPV and congenital tremor type A-II (CT A-II) (Gatto, Sonálio and de Oliveira, 2019; Pan, Mou and Chen, 2019; Stenberg, Jacobson and Malmberg, 2020). Concerted efforts have been made to isolate the virus using a range of well-established transformed cell lines including: MARC-145 (Meat Animal Research Center-145), Vero (African green monkey kidney), Vero 76 (African green monkey kidney 76), HCT-8 (human colorectal tumour Cells-8), BT (bovine turbinate), MDCK (Madin-Darby canine kidney) and MDBK (Madin-Darby bovine kidney) (Hause *et al.*, 2015). Other research groups have used porcine-derived lines such as SK-6 (swine kidney-6), PK-15 (porcine kidney-15), IBRS (swine kidney derived) and ST (swine testis) with limited success, even after multiple passages (Hause *et al.*, 2015; De Groof *et al.*, 2016; Postel *et al.*, 2017b; Schwarz *et al.*, 2017; Yuan *et al.*, 2017; Sozzi *et al.*, 2019).

The first isolation of APPV from positive serum collected from breeding sows and young fattening pigs was reported by Beer *et al.* (2017) using a porcine kidney cell line (SPEV, cell line 0008) and standard techniques developed for the isolation of classical swine fever virus (CSFV), as published in the European Union (EU) diagnostic manual for CSFV diagnosis and the accompanying technical annexe (2002/106/EC). Confirmation of isolation was obtained through RT-qPCR and next-generation sequencing as APPV was observed to be non-cytopathic in cell culture. Subsequently, propagation of the virus has also been reported by Postel *et al.* (2017b) and Cagatay *et al.* (2019) using the SPEV 0008 cell line and similar protocols. It should be noted that in all cases isolation was inefficient, virus could only be isolated from a small proportion of samples and isolates that were successfully propagated

achieved low viral titres even after multiple passages, suggesting infectivity of the virus may be limited. To date, cell culture-propagated APPV isolates have not been used in further studies, although Cagatay *et al.* (2019) were able to develop a viral neutralisation test (VNT) using their isolate.

Although attempts to isolate the virus from samples identified as APPV positive by reverse-transcriptase polymerase chain reaction (RT-PCR) increases the likelihood of success, there may be interfering antibodies present which reduce the efficiency of the culture of the virus. In this study, virus isolation was attempted on samples collected from colostrum deprived snatch farrowed piglets experimentally exposed to APPV, to avoid interference from maternal antibodies. Using this approach would likely have removed any effect of anti-APPV antibodies in the samples, limiting interference with virus propagation. The colostrum deprived piglet model used in this study has also been deployed in a study by De Groof *et al.* (2016). Unlike previous studies (De Groof *et al.,* 2016), the piglets in our study were snatched farrowed and only one week old at inoculation limiting the active production of anti APPV-antibodies. The model was established to generate antibody free infectious material for virus isolation and additional positive sample material of various matrices for diagnostic assay development and validation.

3.2 Aims and objectives

The main aim of this chapter was to establish methodologies for the detection and quantification of APPV and to propagate the virus to study the relationship between APPV and CT A-II in piglets with emphasis on clinical, immunological and pathological outcomes of infection and disease presentation. To achieve this, a one-week-old snatch farrowed colostrum deprived piglet model was developed and used for experimental APPV infection to study horizontal infection characteristics and host—pathogen interactions.

3.3 Establishment of APPV diagnostic techniques

3.3.1 Development of a RT-qPCR for the detection of APPV

Three previously published RT-qPCR assays developed for the detection of part of the NS5B (Beer *et al.*, 2017) and a fragment of the NS3 conserved region (Arruda *et al.*, 2016; Postel *et al.*, 2016) were reviewed as potential candidates for optimisation by conventional PCR and gel electrophoresis as described in 2.2.2. For the analysis, a panel of tissue samples consisting of brain, spleen and spinal cord from three confirmed separate clinical field cases of APPV (NOR-0616-01, NOR-0417-01, and SUF-0617-01), kindly provided by the Animal and Plant Health Agency (APHA) (Table 6-1), were subjected to conventional PCR and gel electrophoresis (2.2.2.) using the above primer sets. The final RT-qPCR assay that was included in this study, with minor modification, had been published by Arruda *et al.,* (2016). Specifically, the primer probe set was modified (listed in Table 3-1) to improve the melting temperature (lowering the predicted melting temperature from 69.5°C to 65.7°C) to reduce the difference between that of the probe and the primers. Also, an alternative fluorophore and quencher was selected to allow potential multiplexing with other target genes e.g. reference genes such as β-actin as an internal positive control or genes from other pestiviruses affecting pigs (bovine viral diarrhoea virus [BVDV] or CSFV) or notable porcine pathogens (African swine fever virus [ASFV]).

Table 3-1: Primers and modified probe (Arruda et al., 2016) used for the optimised RT-qPCR

Type	Name	Oligonucleotides
Forward Primer	Pesti_6332_F	TGCCTGGTATTCGTGGC
Reverse Primer	Pesti_6455_R	TCATCCCATGTTCCAGAGT
Probe*	Pesti_6351_P	5′-FAM◆- CTCCGTCTCCGCGGCTTCTT-BHQ▲-1-3′ *

◆FAM: 6-carboxyfluorescein ▲BHQ-1 Black hole Quencher-1
* Modifications were made to the probe of the published assay (Arruda *et al.*, 2016). The probe reporter and quencher were changed (from CY5 and BHQ-2 to FAM and BHQ-1 respectively) and three bases (TGG) were removed from the 3′ end.

All assay reagents including RT-qPCR kit master mix, probe, forward and reverse primers, were aliquoted into smaller volumes from stock and given a 6-month expiry date. The aliquots were stored at -20°C and allowed a maximum of three freeze-thaw cycles before discarding to retain reagent integrity and prevent inter-assay variation due to degradation of reaction components. New batches of primers and probes were tested alongside in use batches and deemed acceptable for use if a difference of less than one cycle threshold (Ct) was found.

The results (Figure 3-1) indicated that one of the primer sets (Beer *et al.*, 2017) produced no defined bands for the tissue samples tested. A band was observed for the spinal cord sample using the Arruda *et al.* (2016) and Postel *et al.* (2016) primer sets. However, both spleen and brain samples produced a faint double band. The spinal cord and spleen samples produced clearer bands using the primers published by Arruda *et al.* (2016) with the brain sample showing a very faint single band. Therefore, the Arruda *et al.* (2016)

primer/probe set was chosen for further optimisation and to develop into a quantitative real-time RT-PCR.

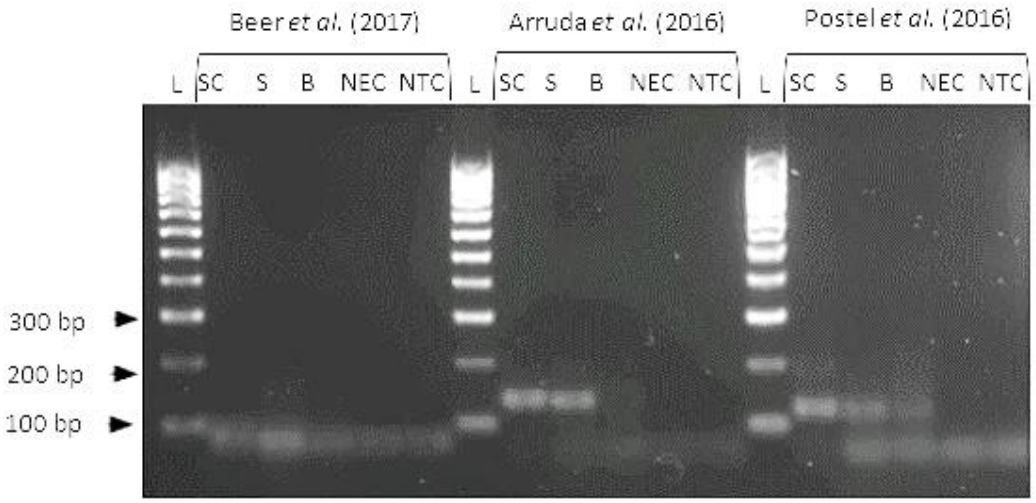

Figure 3-1: Agarose gel electrophoresis of the primer set comparisons. A comparison of published primers using APPV known positive clinical samples of spinal cord (SC), spleen (S) and brain (B). A negative extraction control (NEC), no template control (NTC), and 100—1000 bp deoxyribonucleic acid (DNA) marker ladder (L) were also included. Image corrected for brightness (+40%) and contrast (+20%) to improve clarity.

3.3.1.1 Optimisation of the RT-qPCR reaction chemistry

The forward and reverse primer concentrations were optimised simultaneously by performing a checkerboard titration of different concentrations as presented in Table 3-2 using the Power SYBR Green RNA-to-CT 1-step kit (Applied Biosystems) on an ABI Prism 7500 instrument (Applied Biosystems).

Table 3-2: Checkerboard titration showing concentrations of forward and reverse primers used for optimisation

100 nM Forward 100 nM Reverse	200 nM Forward 100 nM Reverse	400 nM Forward 100 nM Reverse
100 nM Forward 200 nM Reverse	200 nM Forward 200 nM Reverse	400 nM Forward 200 nM Reverse
100 nM Forward 300 nM Reverse	200 nM Forward 300 nM Reverse	400 nM Forward 300 nM Reverse

The one-step RT-qPCR was performed according to the manufacturer's instructions for master mix preparation and thermocycling profile as outlined in Table 3-3 and Table 3-4, respectively. Each 48 µl reaction was tested in duplicate with 2 µl of APPV RNA template (NOR-0616-01 spinal cord) in a 96-well format (Applied Biosystems); a no template control (NTC, molecular grade water) was also included. The final primer concentrations were chosen based on the lowest concentration of primers able to produce the lowest Ct values with the highest Δ Rn value (normalised reporter value).

Table 3-3: Master mix preparation for primer optimisation using the Power SYBR Green RNA-to-CT 1-step kit.

Reagent	Volume (µl)
Power SYBR Green RT-PCR Mix (2X)	25
RT Enzyme Mix (125X)	0.4
Forward primer	1
Reverse Primer	1
Molecular grade water	20.6
Template RNA	2
Total Volume	**50**

Table 3-4: Thermocycling profile for primer optimisation using the Power SYBR Green RNA-to-Ct 1-step kit.

Temperature	Time	Stage	Number of cycles
48 °C	30 minutes	Reverse transcription cDNA synthesis and pre-denaturation	1
95C	10 minutes		1
95 °C	15 seconds	Denaturation	40
60 °C	1 minute	Combined annealing and extension	
95 °C	15 seconds	Melt curve	1
60 °C	1 minute		1
95 °C	30 seconds		1
60 °C	15 seconds		1

The assay showed Ct values ranging from 26.2—28.6 (Figure 3-2). Two hundred nanomolar of each primer concentration was determined to be optimal based on the lowest concentration with the highest Ct value while retaining a sigmoidal amplification curve.

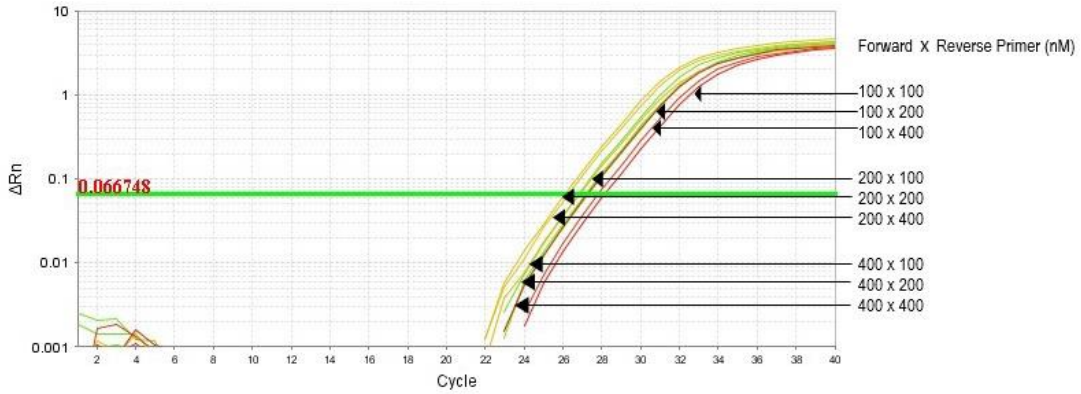

Figure 3-2: Results of primer optimisation. A known APPV positive spinal cord sample was amplified using different concentrations of forward and reverse primers in duplicate (as indicated by arrows). The threshold of the assay (green) was automatically adjusted by the software based on the passive reference dye. The no template control was undetected.

Optimisation of the probe concentration was carried out using a titration at 50 nM, 100 nM, 200 nM, and 400 nM with the optimised concentration of both forward and reverse primers. The RT-qPCR was performed as per the manufacturer's recommendations for the master mix assembly (Table 3-5) and thermocycling profile (Table 3-6) using the SuperScript III Platinum One-Step qRT-PCR Kit (Invitrogen). Reverse transcription and PCR amplification were carried out within the same well of a 96-well plate using the ABI Prism 7500 instrument (Applied Biosystems). Each 24 µl reaction was tested in duplicate with 1 µl of APPV RNA template and an NTC was also included. The Ct value ranged between 28.1 and 29.1, and the optimal concentration of the probe was determined to be 200 nM (Figure 3-3). The final primers and probe concentrations were used to establish the final master mix volumes as listed in Table 3-7.

Table 3-5: Master mix preparation for probe optimisation using SuperScript III Platinum One-Step qRT-PCR Kit.

Reagent	Volume (µl)
RT-PCR Mix (2X) with ROX	12.5
RT Enzyme Mix (2X)	0.5
Forward primer	0.5
Reverse Primer	0.5
Probe	0.5
RNase-free water	9.5
Template RNA	1
Total Volume	**25**

Table 3-6: Thermocycling profile for probe optimisation using SuperScript III Platinum One-Step qRT-PCR Kit.

Temperature	Time	Stage	Number of cycles
50 °C	15 minutes	Reverse transcription cDNA synthesis and pre-denaturation	1
95 °C	2 minutes		1
95 °C	15 seconds	Denaturation	40
60 °C	1 minute	Combined annealing and extension	

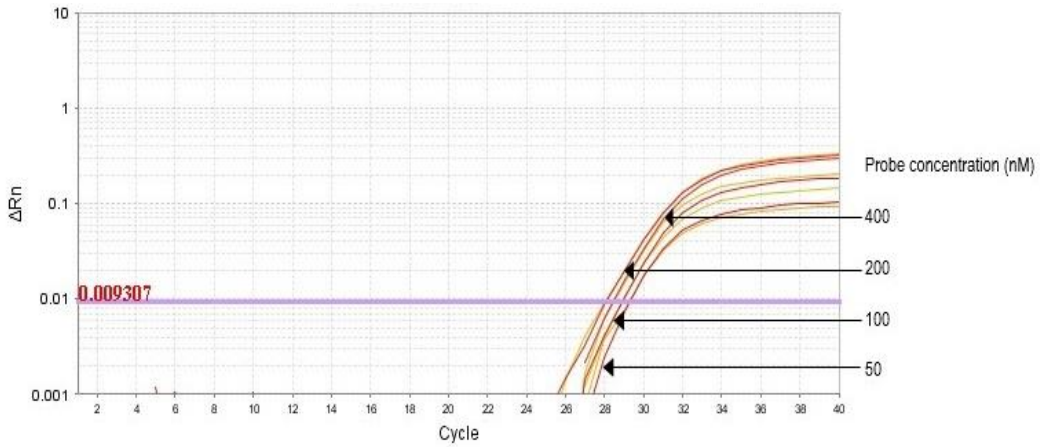

Figure 3-3: Results of the probe optimisation titration. A known APPV positive spinal cord sample was amplified in duplicate. Different concentrations of the probe (as indicated by the arrows) where tested using the optimal concentration of the primers (200 nM). The threshold of the assay (purple) was automatically adjusted by the software based on the passive reference dye. The no template control was undetected.

3.3.1.2 Optimisation of the RT-qPCR thermocycling profile

Initially, a three-step (denaturation, annealing and extension phase) thermocycling profile was optimised by conventional PCR as the real-time PCR instrument was incapable of conducting a thermo-gradient due to limitations with the heat block. A thermo-gradient PCR within a temperature range between 54.5°C and 58.5°C, chosen based on the melting temperature of the primers, was performed and visualised by gel electrophoresis (2.2.2).

The optimal annealing temperature of the primers was initially used to optimise the thermocycling conditions. A clear band was observed for temperatures ranging between 54.5°C and 58.3°C. However, a double band was observed at 55.3°C and 57.9°C. The brightest and most defined bands were found to be 54.5°C and 54.8°C (Figure 3-4); with consideration given to the predicted melting temperatures of the primers (the melting temperature of the forward and reverse primers were 55.2°C and 54.5°C respectively), the higher temperature 54.8°C was chosen. However, the assay was further optimised to

have a combined annealing extension phase based on the addition of the probe with a high predicted melting temperature (65.7°C) and the recommendations of the SuperScript III Platinum One-Step qRT-PCR Kit (Invitrogen). This resulted in in the combined annealing and extension phase being raised to 60°C.

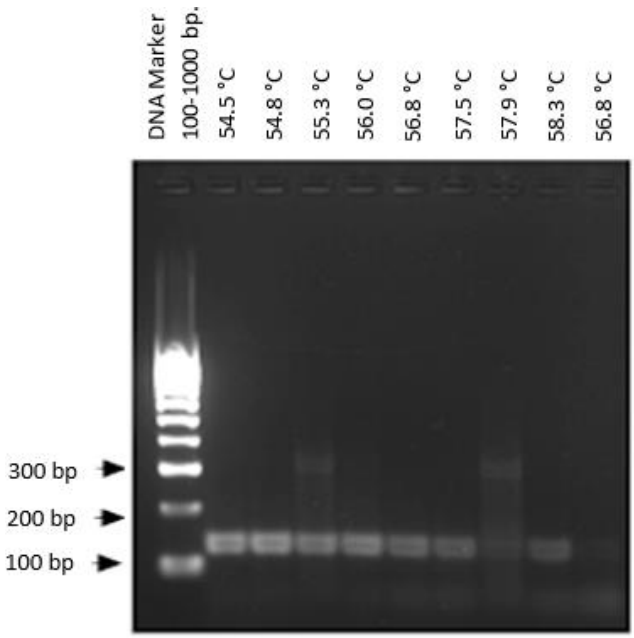

Figure 3-4: Thermo-gradient to determine the optimal annealing temperature of the primers. The thermal gradient assay was performed on a known APPV positive spinal cord sample.

3.3.1.3 Re-optimisation of APPV RT-qPCR for improved analytical sensitivity

In order to improve the analytical sensitivity and reduce the run-time of the assay, the RT-qPCR was re-optimised using the qScript™ XLT One-Step RT-qPCR ToughMix®, Low ROX kit (Quantabio) in conjunction with the QuantStudio5 instrument (Applied Biosystems). This was done in line with the recommendations of the manufacturer for reaction chemistry and thermocycling profile with consideration given to the previous optimisation where appropriate. For this reason, a forward and reverse primer

checkerboard titration was carried out with the following concentrations: 300 nM, 600 nM, and 900 nM; once a final concentration of the primers was optimised, the assay was conducted. The total reaction volume was reduced from 25 µl (24 µl master mix and 1 µl RNA template) to 20 µl (19 µl master mix and 1 µl RNA template) per reaction. All re-optimisation was conducted using the standards generated in Chapter 2, Section 2.3. Table 3-7 outlines the preparation of optimised master mix. The thermocycling profile remained as described in Table 3-6, however, the ramp times increased from 1.6°C/second to 2.74°C/second reducing the length of the run time from 1 hour 35 minutes to 1 hour 25 minutes.

Table 3-7: Master mix preparation for the optimised APPV assay using the qScript™ XLT One-Step RT-qPCR ToughMix, Low ROX.

Reagent	Volume (µl)
qScript XLT One-Step RT-qPCR ToughMix, Low ROX (2X)	10
Forward primer	1.2
Reverse Primer	1.2
Probe	0.4
RNase-free water	6.2
Template RNA	1
Total Volume	**20**

Based on the mean Ct values and the efficiency of the reaction (Table 3-8), it was determined that the optimal final concentration of each primer was 600 nM. This concentration improved the Ct values on average by five cycles and the analytical sensitivity of the assay increased 10-fold (Figure 3-5).

Table 3-8: Comparison of the average Ct values detected for standards (in duplicate) with the corresponding efficiency and R^2 value for the optimised Superscript III Platinum One-Step qRT-PCR Kit assay and the qScript XLT One-Step RT-qPCR ToughMix, Low ROX kit with primer set concentrations of 300 nM, 600 nM and 900 nM.

	Average Ct values			
Standards copies/µl	**SuperScript III**	**qScript XLT**	**qScript XLT**	**qScript XLT**
	200 nM Forward and Reverse	**300 nM Forward and Reverse**	**600 nM Forward and Reverse**	**900 nM Forward and Reverse**
$3.19x10^8$	17.6	13.141	12.394	12.633
$3.19x10^7$	21.5	16.036	16.034	15.846
$3.19x10^6$	24.8	19.711	19.690	19.742
$3.19x10^5$	28.5	23.369	23.552	22.151
$3.19x10^4$	31.8	26.708	25.935	26.553
$3.19x10^3$	35.1	29.941	28.574	29.049
$3.19x10^2$	NVD♦	33.383	33.550	31.890*
$3.19x10^1$	NVD♦	NVD♦	35.997*	37.724*
Standard curve results				
Efficiency (%)	93.584	96.374	98.181	96.674
R^2	0.997	0.997	0.984	0.988

* Single replicates with a Ct value, no virus detected in the other replicates therefore mean average is listed as the single value.
♦ No virus detected

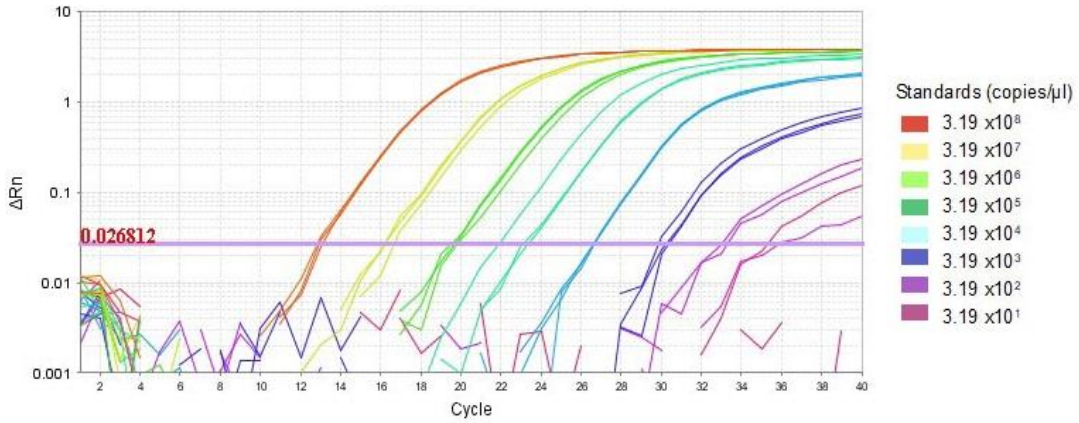

Figure 3-5: Re-optimised assay limit of detection. Each colour denotes a different standard (10-fold eight-point dilution series) from $3.19x10^8$ – $3.19x10^1$ copies /µl tested in duplicate. The threshold of the assay (purple) was automatically adjusted by the software based on the passive reference dye. The no template control was undetected.

3.3.1.4 Specificity validation

Melt curve analysis was performed on the product obtained during the primer concentration optimisation, as previously described in Table 3-3 and Table 3-4, to determine the specificity of the assay. The specificity validation assay showed one clear peak with no evidence of primer-dimer formation or non-specific product contaminants, suggesting that only APPV was amplified (Figure 3-6). The PCR product from the melt curve was purified and submitted to an external laboratory (Eurofins Genomics, Wolverhampton, UK) for Sanger sequencing. The sequences from both forward and reverse reads were aligned using Seqman Pro 15 (DNAStar) to obtain a consensus sequence, which was then checked through BLAST analysis and compared to other deposited APPV sequences (Chapter 2, Section 2.2.6). The BLAST analysis of the product

showed only identity with other APPV sequences ranging between a 98.3 and 86.4% nucleotide identity, as shown in Table 3-9.

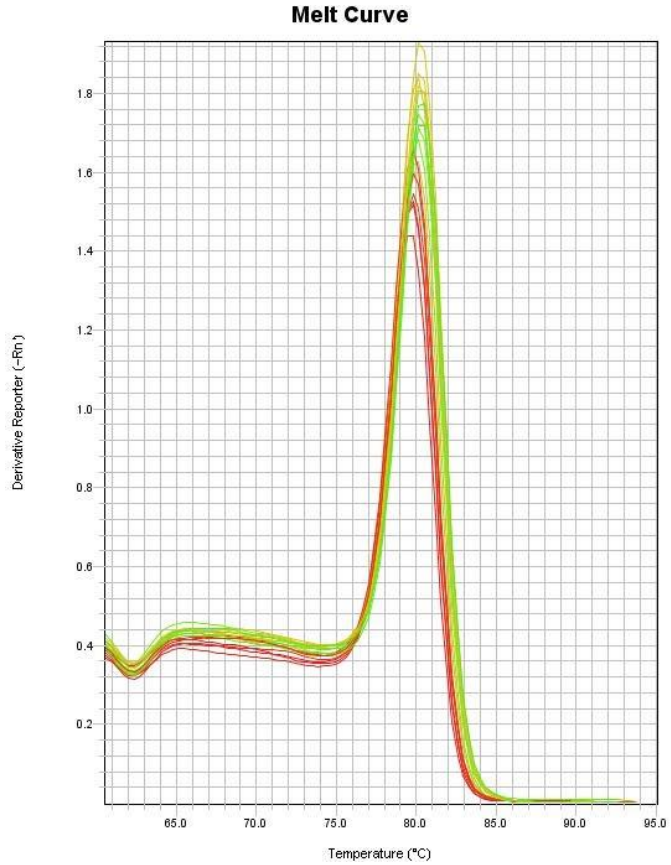

Figure 3-6: Melt curve analysis. Melt curve was performed as part of the primer concentration optimisation titration (18 technical replicates) on a known APPV positive spinal cord sample. The no template control was undetected.

Table 3-9: BLAST analysis results of the most closely related nucleotide sequences to the melt curve product (a known positive spinal cord sample from a British field case).

GenBank Accession Number	Description	Max Score	E Value	Percentage Identity
KU041637.1	Germany, 2016	207	$6x10^{-50}$	98.31%
NC_038964.1	USA, 2015	185	$3x10^{-43}$	94.92%
KU194231.1	USA, 2016	180	$1x10^{-41}$	94.07%
MH307700.1	China, 2018	174	$6x10^{-40}$	93.22%
MF377344.1	China, 2017	174	$6x10^{-40}$	93.22%
KU194230.1	USA, 2016	174	$6x10^{-40}$	93.22%
KU194229.1	USA, 2016	174	$6x10^{-40}$	93.22%
MH499643.1	China, 2018	163	$1x10^{-36}$	91.53%
LT631734.1	Spain, 2016	158	$6x10^{-35}$	90.68%
MK378661.1	China, 2018	147	$1x10^{-31}$	88.98%
MG792803.1	China, 2018	141	$6x10^{-30}$	88.14%
KY475592.1	China, 2017	141	$6x10^{-30}$	88.14%
KY652092.1	China, 2017	141	$6x10^{-30}$	88.14%
MF167292.1	China, 2017	130	$1x10^{-26}$	86.44%

Finally, a panel of common porcine pathogens and pestiviruses, outlined in Table 3-10, was tested using the RT-qPCR assay to ensure absence of cross-reactivity. The common porcine pathogens were provided by Moredun Scientific (MSL) as swabs of isolates, prepared as described in 2.2.5 and extracted using the QiAMP DNA mini kit (Qiagen) following the manufacturer's

protocol. The pestiviruses were obtained as pre-extracted RNA from archives at APHA, the Roslin Institute and the Viral Surveillance Unit at Moredun Research Institute (MRI). All pathogens, aside for APPV, were undetected.

Table 3-10: Common porcine pathogen and pestivirus panel used to determine the specificity of the APPV optimised assay.

Common porcine pathogens	Pestiviruses
Actinobacillus pleuropneumoniae	Bungowannah virus
Escherichia coli K99	Bovine viral diarrhoea virus type 1
Mycoplasma hyopneumoniae	Bovine viral diarrhoea virus type 2
Pasteurella multocida	Border disease virus
Streptococcus suis	Classical swine fever virus*
Porcine reproductive and respiratory syndrome virus species 1 subtype 2	
Porcine circovirus type 2	

*Classical swine fever virus was tested as purified RNA only (kindly provided by APHA) due to its Specified Animal Pathogen (SAPO) classification in the UK, which meant that the live virus could not be handled in the lab.

3.3.1.5Analytical sensitivity validation

APPV samples (serum, swabs, tissues and semen) either known positive supplied by APHA or tested positive by the RT-qPCR were tested to ascertain the assay ability to detect APPV in these matrices, as no APPV isolate was available to perform a spiking titration. The assay was able to detect APPV in all of the sample types initially tested (Table 3-11).

Table 3-11: Detection of APPV in different sample matrices from different clinical and experimental submissions.

Source	Sample Type	Average Ct value †
SUF-0617-01	Brain	26.0
SUF-0617-01	Spinal cord	27.0
SUF-0617-01	Tonsil	23.7
SUF-0617-01	Spleen	24.7
E10/18-1 (7 DPI*)	Oropharyngeal Swab	33.0
E10/18-1 (7 DPI*)	Rectal Swab	33.6
E10/18-1 (9 DPI*)	Nasal Swab	33.2
E10/18-1 (9 DPI*)	Serum	21.7
CSCOT-FG2-945	Semen	28.6

* Days post-inoculation.
Based on two technical replicates

The limit of detection of the assay was calculated by performing six sets of 1:10 serial dilutions (standard curve) of a known concentration of APPV plasmid ($3.19x10^8$-$3.19x10^1$ copies/µl) prepared as described in Chapter 2, Section 2.3. This standard curve was also included in duplicate in every assay to assess ongoing analytical sensitivity. The initial analytical sensitivity threshold of the assay was found to be $3.19x10^3$ copies/µl, as seen in Figure 3-7. As previously discussed, the limit of detection was eventually reassessed after the test was re-optimised (see 3.3.1.3 for the re-optimised assays analytical sensitivity threshold detection results).

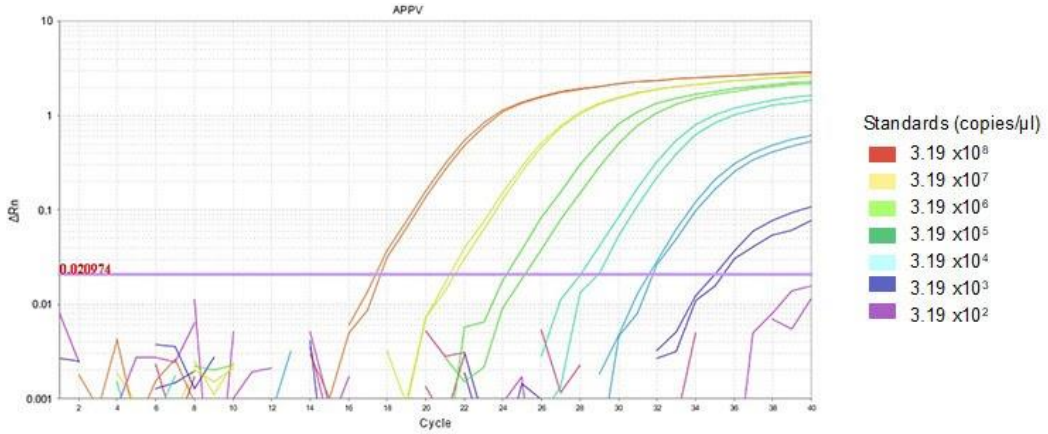

Figure 3-7: Initial limit of detection assay. Each colour denotes a different standard (10-fold eight-point dilution series) from $3.19x10^8$ – $3.19x10^1$ copies /µl tested in duplicate. The threshold of the assay (purple) was automatically adjusted by the software based on the passive reference dye. The no template control was undetected.

3.3.1.6 Reproducibility validation

A biological positive control was prepared from serum collected from APPV-infected, colostrum deprived piglets as detailed in 3.5. APPV RNA was extracted from five replicates using the automated extraction procedure defined in Chapter 2, Section 2.2.1.2. The RNA was pooled and tested 10 times to determine a mean and standard deviation (SD) which was then used to create a Shewhart chart (Simonet, 2005). The Shewhart chart defines the upper and lower warning (2 SD from the mean) and control limits (3 SD from the mean) for the assay performance. The chart was used to track the biological positive controls that were added in duplicate to each PCR run and to confirm that their performance fell within an acceptable range, enabling the monitoring of inter-assay variability over time. Those assays that had biological positive control values between the upper warning and upper control limits or, conversely, between the lower warning and lower control limits were evaluated for repeat testing based on the average of the replicates and whether they fell within the acceptable limits. Those assays that had values outside of the upper

and lower control limits were deemed unacceptable and the test repeated. Only one test had one of the biological positive control values fall between the upper warning (UWL) and upper control limit (UCL) based on evaluation of the replicates (Figure 3-8); the average was within the acceptable limits. Therefore, the test did not need to be repeated. In addition, a standard curve was created from a serial dilution of the APPV plasmid from $3.19x10^8$ copies/µl to $3.19x10^1$ copies/µl as described in 3.3.1.5 to assess the efficiency and R^2 values of each PCR run.

Figure 3-8: Shewhart chart for the biological positive control. The biological positive control was included on every APPV RT-qPCR assay in duplicate. The upper (UWL) and Lower (LWL) warning limits (red lines) show variation of 2 standard deviations from the mean (green line) whereas the Upper (UCL) and lower (LCL) control limits (orange lines) indicate 3 standard deviations variation from the mean.

3.3.1.7 Interpretation and classification of results

The APPV copy number in clinical samples was calculated per millilitre of the liquid sample (serum, swabs, semen) or per gram of solid sample (tissues) based on the quantified output of the PCR and accounting for the extraction volumes and preparation method of the different sample types (for example the homogenisation process of tissues). The samples were classified as positive if the copy number was higher than the limit of detection of the assay, equivocal if the copy number was lower than the limit of detection, or no virus detected if the sample showed no presence of nucleic acid (no amplification).

3.3.2 Optimisation of a NS3 ELISA

Originally, an NS3H blocking ELISA (2.4.1) kindly supplied by a collaborator was used as described by Schwarz *et al.* (2017) to screen for antibodies in sows' sera that had been previously naturally infected with APPV and had given birth to piglets with CT A-II (results shown in Figure 3-9), and which could be used as control material. Samples from sows deemed positive, defined as having a percentage inhibition of greater than 50% (Sows 513, 556, B729, B777, LW60 and LW89), were pooled due to the limited quantity of each sample available and retested for use as positive control. Originally, pestivirus-free FCS was used as an APPV negative control on the NS3H blocking ELISA. However, this was later substituted with serum collected from a colostrum-deprived negative control animal from the APPV infected piglets from the postnatal APPV infection study (E10/18-4).

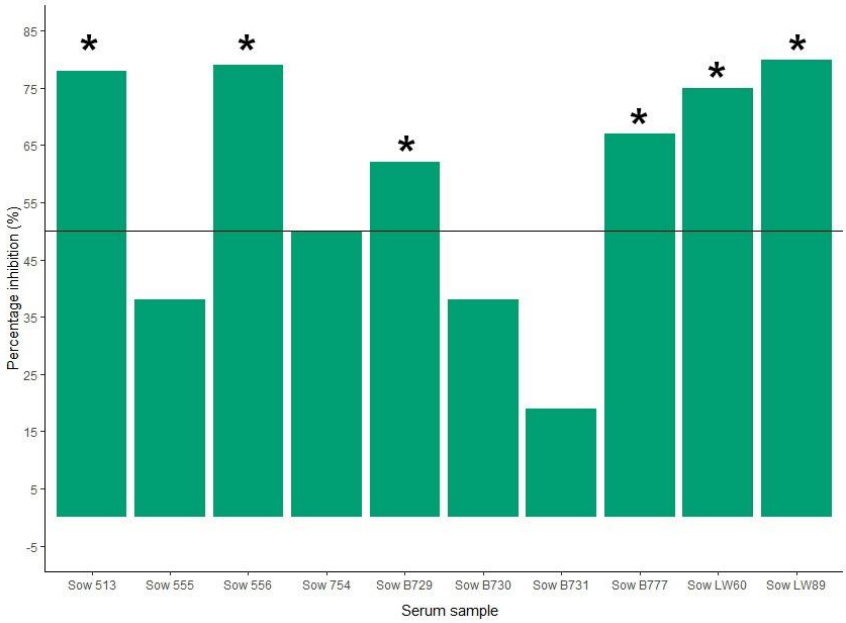

Figure 3-9: Antibody screening for positive control material. The graph shows the percentage inhibition of serum from sows previously infected naturally with APPV tested in duplicate. The horizontal line indicates the threshold for positive samples at 50% inhibition. * Indicates samples pooled for ELISA positive control.

As a result of complications with the consistency of the reagents provided, the use of this NS3H blocking ELISA was discontinued and an indirect ELISA optimised. To standardise the assays, the same antigen, coating buffer and wash buffer used in the NS3H blocking ELISA were also used for the indirect ELISA together with a modified protocol in which the competitive mouse monoclonal antibody was omitted and the secondary horseradish peroxidase (HRPO)-conjugated goat anti-mouse IgG antibody (Jackson laboratories) was substituted with a rabbit anti-pig IgG HRPO conjugated antibody (Sigma Aldrich).

For optimisation of this indirect ELISA, as a limited amount of the antigen was available, the optimal concentration for coating was tested at two dilutions of 1:250 and 1:1,000 (stock concentration of antigen 10 mg/ml). Titration curves

were obtained using both a sow serum (collected from a field case as detailed in Chapter 4, 4.5.1.1., determined as seropositive by the NS3 ELISA, serially diluted (two-fold dilution from 1:4-1:65,526) in antibody-negative serum derived from colostrum deprived piglets from the APPV postnatal infection study E10/18 (described in section 3.5). These samples subsequently became the controls for the assay to determine assay sensitivity and optimal sample dilution. The results shown in Figure 3-10 indicate that in the linear phase of the curve there are minimal differences in the OD values between either concentration for both the positive and negative control. Therefore, using a 1:1,000 dilution of antigen to coat plates did not negatively impact the OD values while allowing for conservation of the antigen stock which was limited in supply.

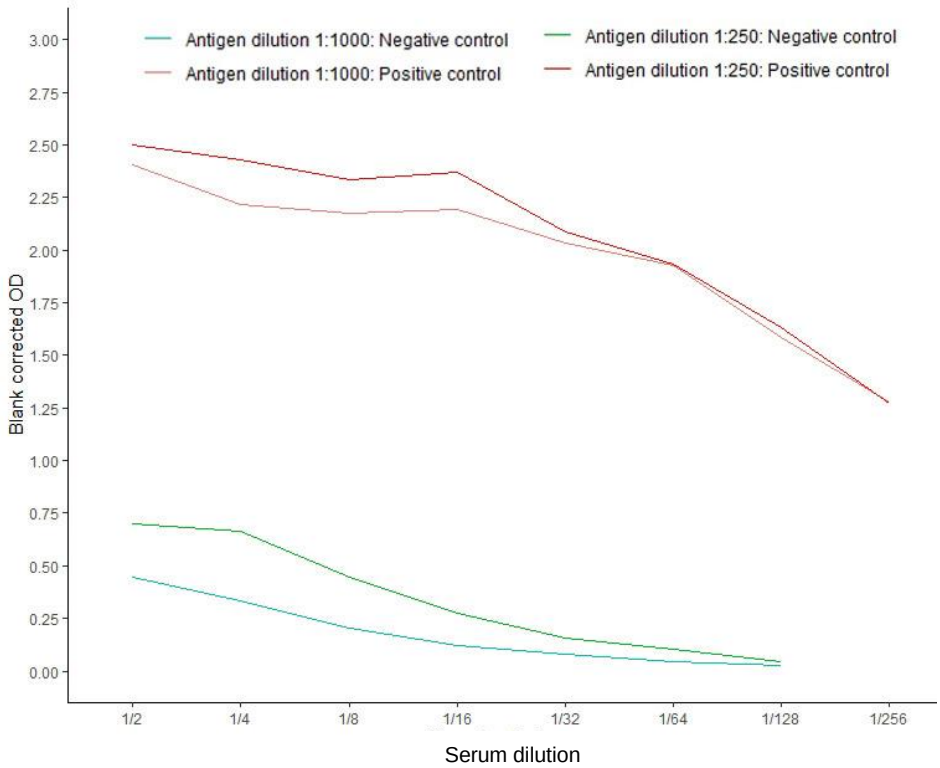

Figure 3-10: A comparison of positive and negative control titrations performed in duplicate on plates coated with antigen diluted 1:250 and 1:1,000. The average of the blank wells (n=2) was subtracted from absorbance (OD) values to correct for background.

Additionally, 1% fish gelatin and pestivirus-free fetal calf serum at 5% and 10% (FCS) were compared to determine the most suitable blocking reagent for reducing non-specific binding. No difference was observed for the OD value between blocking reagents for the negative control standards curves; however, the positive control blocked with 1% fish gelatin had much lower OD values compared to the FCS, whereas the 5% and 10% FCS blocking reagents produced comparable OD values (Figure 3-11). Therefore, the lowest concentration of FCS was considered optimal and used for further assay development.

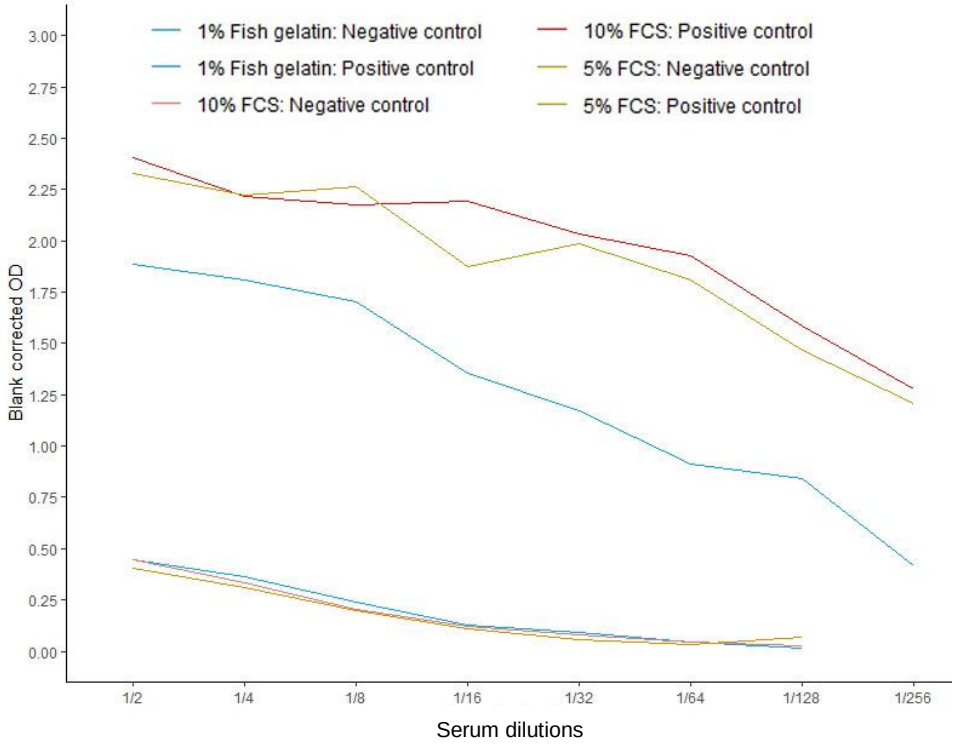

Figure 3-11: Comparison of the titrations of positive and negative control sera blocked with 1% fish gelatin, 5% FCS and 10% FCS on plates coated with antigen at a 1:1,000 dilution performed in duplicate. The average of the blank wells (n=2) was subtracted from absorbance (OD) values to correct for background.

All assay optimisation was performed using the same secondary antibody as previously detailed at the manufacturer's recommended concentration for ELISA of 1:40,000. SureBlue TMB was added as the chromogen and the plate read initially at 405 nm and stopped when the most positive well had an optical density OD value equal to 0.7. The assay was then stopped using 0.18 M sulphuric acid and reread at 450 nm. The final protocol is described in Chapter 2, Section 2.4.2.

Validation was performed to assess the sensitivity of the assay using a titration curve of a known positive sample to determine the limits of detection of the assay. The titration curve (Figure 3-12) shows that the assay reached the upper limit of detection at a dilution of 1:16 and the lower limit of detection at 1:65,526. Sample dilution was chosen based on the intended use of the assay, namely evaluation of changes in IgG antibody levels over time in animals with a known APPV status (3.5.2.4, Chapter 4 and Chapter 5); samples were used at a dilution of 1:200, which was determined suitable based on its position within the linear phase of the curve. The experiments conducted with diagnostic samples with unknown APPV status, as part of the epidemiological investigation of APPV within Great Britain (6.3.1) used a dilution of 1:50 to ensure that the samples were diluted enough that metabolites in the matrices would not interfere with the assay but over dilution of the sample would not contribute to false negative status. Positive and negative status thresholds (OD value of 0.77) were assigned based on the absorbance data from the 1:50 diluted samples tested in Chapter 6 using a Bayesian latent class model and ROC analysis provided by Biomathematics and Statistics Scotland (BioSS) as shown in Appendix B.

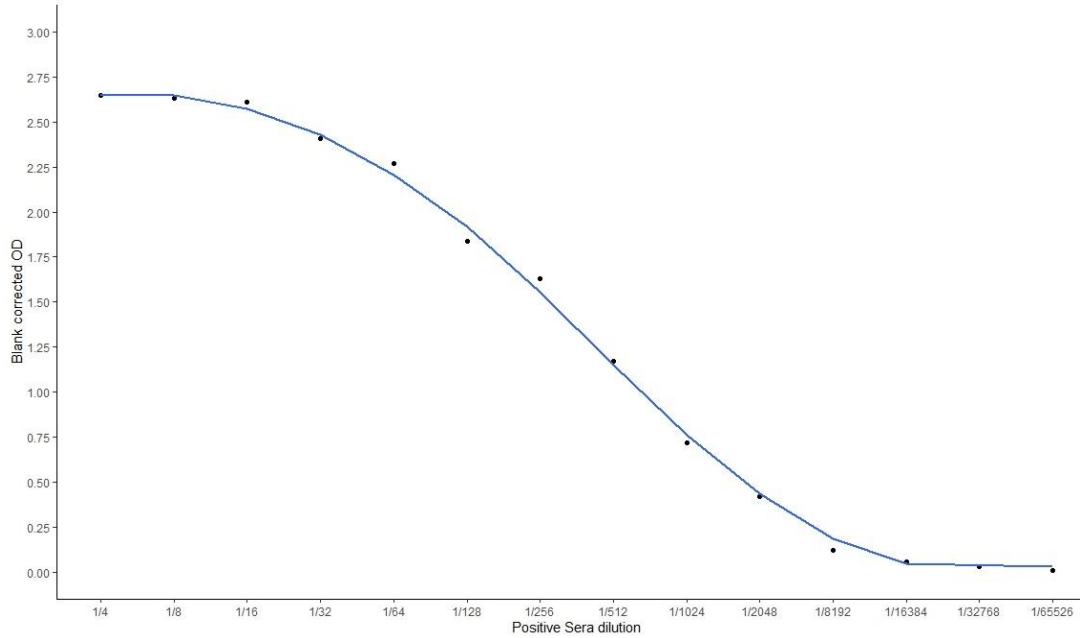

Figure 3-12: Titration of pooled positive sera to define assay limitations. The titration was performed in duplicate and the average of the blank wells subtracted from average absorbance (OD) values to correct for background.

The reproducibility of the assay was evaluated by establishing a Shewhart chart established based on the mean and SD of the first 10 positive control results to determine suitable warning and control limits (as previously explained in 3.3.1.6). The positive control was diluted at the same concentration as the sample (1:50), which was added in duplicate to each test. All of the assays had positive control replicates within 2 SD of the mean (between the upper and lower warning limits) and were considered within the acceptable parameters (Figure 3-13).

Figure 3-13: Shewhart chart for the positive control diluted 1:50 included on every ELISA assay in duplicate. The warning limits (orange lines) show a variation of 2 standard deviations from the mean (green line) whereas the control limits (red lines) indicate a variation of 3 standard deviations from the mean.

The positive control diluted at 1:50 was also used to determine the inter and intra-assay variability by calculating the percentage coefficient of variance (% CV), with the results shown in Table 3-12. Intra-assay % CV was calculated by dividing the SD of the two positive control replicates by the mean of the replicates and then averaged for the number of plates tested (n=30). The inter-assay % CV was calculated in the same way, however the mean of the positive control replicates from each plate was used to determine the SD and mean of all plates (n=30) to be used in the equation. The intra-assay % CV should not be greater than 15% whereas the inter-assay variation should be no greater than 20% to demonstrate the overall reliability of the test (Jacobson, 1998). All plates had % CV values lower than the generally accepted upper threshold of 15%. Individual tests with higher intra-assay values (greater than 10%) were likely due to human error rather than the reproducibility of the assay. The inter-assay % CV was found to be 4.58%, less than the 20% threshold considered acceptable, therefore the test was considered reproducible.

Table 3-12: Percentage coefficient of variance (% CV) for inter-and intra-assay reproducibility using a blank corrected normalised OD value of the positive control diluted at 1:50 (two technical replicates).

Assay	Replicate 1	Replicate 2	Mean	Standard deviation	Intra-assay % CV
1	2.28	2.30	2.29	0.02	0.71
2	2.23	2.34	2.29	0.08	3.56
3	2.32	2.25	2.29	0.05	2.07
4	2.26	2.31	2.29	0.03	1.39
5	2.52	2.05	2.29	0.33	14.38
6	2.07	2.50	2.29	0.31	13.45
7	2.48	2.09	2.29	0.27	11.97
8	2.43	2.15	2.29	0.20	8.75
9	2.42	2.15	2.29	0.19	8.20
10	2.30	2.27	2.29	0.02	1.05
11	2.35	2.22	2.29	0.09	3.99
12	2.10	2.48	2.29	0.27	11.69
13	2.33	2.25	2.29	0.06	2.57
14	2.26	2.32	2.29	0.04	1.89
15	2.31	2.27	2.29	0.03	1.27
16	2.31	2.26	2.29	0.03	1.52
17	2.28	2.29	2.29	0.01	0.40
18	2.22	2.35	2.29	0.09	3.87
19	2.47	2.11	2.29	0.25	11.04
20	2.27	2.30	2.29	0.02	1.05

Continuation of Table 3-12: Percentage coefficient of variance (% CV) for inter and intra assay reproducibility using a blank corrected normalised OD value of the positive control diluted at 1:50 (two technical replicates).

Assay	Replicate 1	Replicate 2	Mean	Standard deviation	Intra-assay % CV
21	2.35	2.22	2.29	0.09	3.99
22	2.10	2.48	2.29	0.27	11.69
23	2.33	2.25	2.29	0.06	2.57
24	2.26	2.32	2.29	0.04	1.89
25	2.31	2.27	2.29	0.03	1.27
26	2.31	2.26	2.29	0.03	1.52
27	2.28	2.29	2.29	0.01	0.40
28	2.22	2.35	2.29	0.09	3.87
29	2.47	2.11	2.29	0.25	11.04
30	2.27	2.30	2.29	0.02	1.05
Overall intra-assay % CV			5.07%		
Overall standard deviation			0.10		
Overall mean			2.29		
Inter-assay % CV			4.58%		

3.3.3 Evaluation of antibodies for APPV immunohistochemistry

The antibodies listed in Table 3-13 were tested for cross-reactivity to APPV as potential candidates for immunohistochemistry (IHC). The veterinary pathology Moredun (VPM) antibodies generated at MRI were lysates from cells infected with cytopathic border disease virus (BDV). These antibodies had shown cross-reactivity to non-cytopathic BDV and cross-reacted with several BVDV strains (Dutia, Entrican and Nettleton, 1990). Two dilutions of the VPM antibodies were tested: 1:50 and 1:200, alongside a pan-pestivirus antibody pre-diluted at 1:100,000 provided by APHA. APPV-positive brain sections cut and mounted onto slides (SuperFrost Plus, Fisher Scientific) from a paraformaldehyde-fixed capsular brain tissue block (from NOR-0417-01, see Chapter 6, Table 6-1 for further case details) also provided by APHA were stained to determine the presence of cross-reactivity. BVDV positive brain sections cut from paraformaldehyde-fixed tissue collected from a positive case submitted to the histopathology surveillance unit at MRI were used as a positive control for the pan pestivirus antibody test. As the pan pestivirus antibody was performed simultaneously with VPM antibody testing, a “no antibody” control for both tissue types was shared; APPV and BVDV positive slides without primary antibody were included to exclude non-specific staining due to the secondary antibody.

Table 3-13: Antibodies used to determine cross-reactivity for APPV IHC.

Antibody	Isotype	Production method
VPM 20	IgG2a	Cell culture supernatant
VPM 21	IgG1	Cell culture supernatant
VPM 22	IgG2b	Ascites fluid
VPM 25	IgG2a	Ascites fluid
VPM 26	IgG2a	Cell culture supernatant

All the steps of the IHC protocol were performed at room temperature unless otherwise specified, using an established in-house protocol for BVDV detection with a proteinase K antigen retrieval step. Briefly, the section slides were dewaxed and rehydrated using a preloaded program (slides moved through stations containing Xylene, 100% ethanol, 50% ethanol and water) on the Varistain machine. The slides were then loaded using distilled water into a Sequenza staining rack, and 100 µl of proteinase K (20 µl/ml in 1 M Tris hydrochloride) added to each slide and incubated for 5 minutes. The slides were removed from the rack and washed for 5 minutes in a Coplin jar containing phosphate-buffered saline (PBS) and 0.5% Tween 80 (forming PBST-80), before incubating the slides for 20 minutes in a Coplin jar containing PBST-80 and 0.3% hydrogen peroxide (peroxidase block). The slides were washed for 5 minutes in PBST-80 and loaded into the Sequenza rack using PBS and aspecific reactivity was blocked with 100 µl of 25% normal goat serum (diluted in PBST-80) for one hour. One hundred microlitres of the diluted antibodies were applied to the APPV and BVD positive slide-mounted tissue sections and incubated at 4°C overnight. The slides were washed twice with PBS before remounting into the rack and incubating with 100 µl of undiluted goat anti-mouse polymer-HRP from the Dako-Envision kit (Dakocytomation)

for 30 minutes. The sections were then washed twice with PBS and incubated with DAB substrate (Dakocytomation) for 7.5 minutes. After a final wash with distilled water, the slides were loaded into the Varistain to be counterstained with haematoxylin and dehydrated using a pre-set program (slides moved through stations containing haematoxylin, water, Scotts tap water substitute (STWS), water, 95% ethanol, 50% ethanol/xylene and 100% xylene). The slides were removed from the Varistain and left in a chemical safety cabinet fume hood until the excess xylene evaporated prior to the addition of a coverslip using DPX mountant (Sigma-Aldrich).

The immunohistochemistry results are shown in Figure 3-14. No staining at either 1:50 or 1:200 dilution was observed for VPM 20 or VPM 21, indicating no cross-reactivity. VPM 22 showed non-specific staining at both dilutions and no cross-reactivity with APPV. However, both VPM 25 and VPM 26 showed a limited staining in the cell cytoplasm of a few cells, indicating possible cross-reactivity with APPV. Therefore, both VPM 25 and 26 were considered as viable candidates for optimisation. VPM 25 and VPM 26 showed a slightly stronger cell-specific staining compared to the intensity of background at a 1:50 dilution, however the intensity of background staining was considered too high and differentiation between specific and non-specific staining was difficult to interpret. Conversely, VPM 25 at a dilution of 1:200 showed little background staining, however, the intensity of specific staining was much weaker, also making differentiation difficult. VPM 26 had a similar level of staining (both specific and background) at the 1:200 dilution to the 1:50 dilution. Further work is needed to determine the optimal dilution of the antibodies for the purpose of demonstrating APPV by IHC staining. The pan-pestivirus antibody provided by APHA pre-diluted at 1:100,000 (Figure 3-15) showed specific staining with no background staining on brain tissue from a cow infected with BVDV (positive control), however no staining was observed on APPV PCR positive porcine brain tissue. No staining was observed in the no primary antibody control (see Figure 3-15).

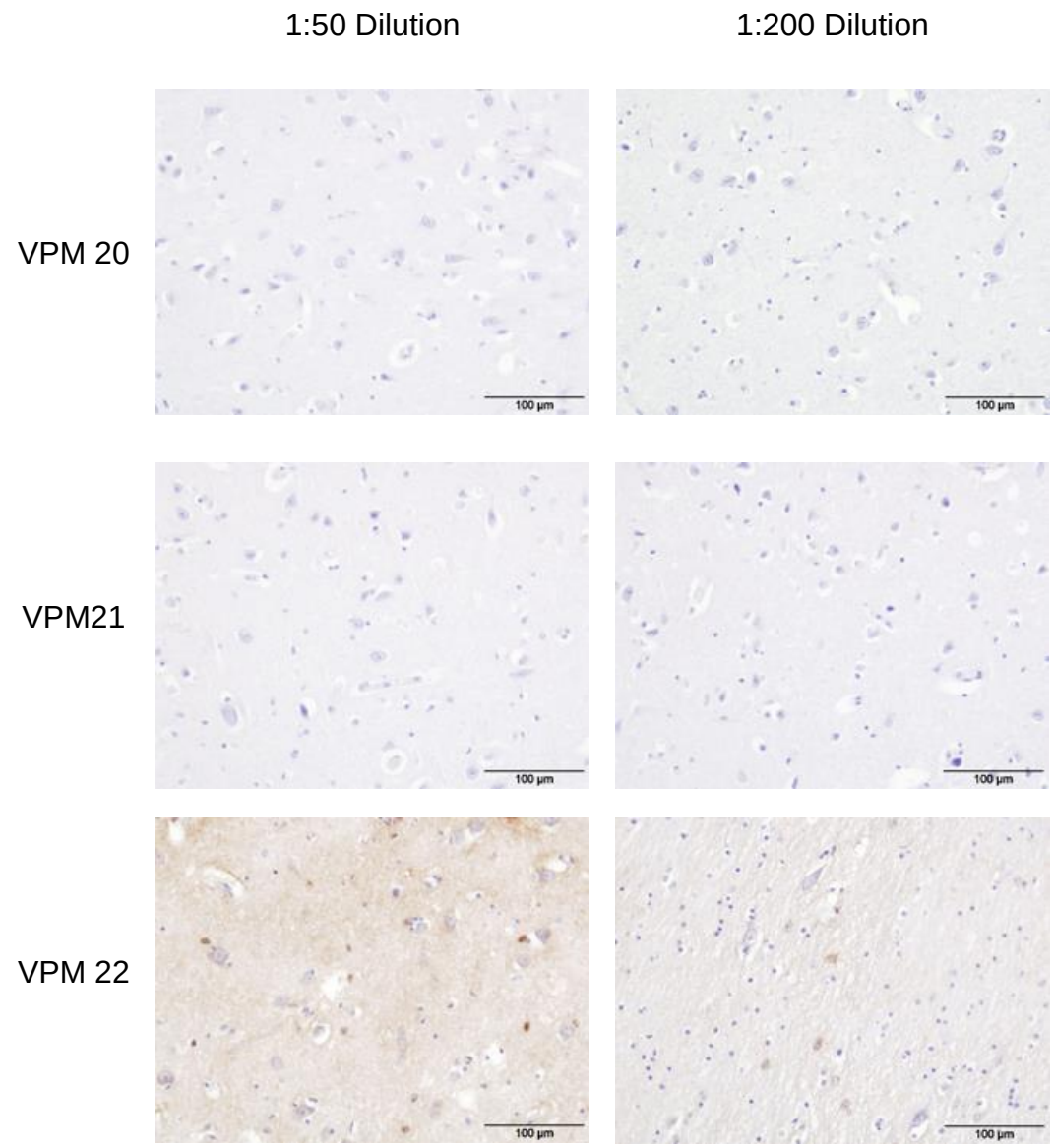

Figure 3-14: Cross-reactivity of VPM antibodies to APPV. IHC staining is shown for VPM 20, VPM 21, and VPM 22 at an antibody dilution of 1:50 and 1:200. No antibody control included for this test shown in Figure 3-15.

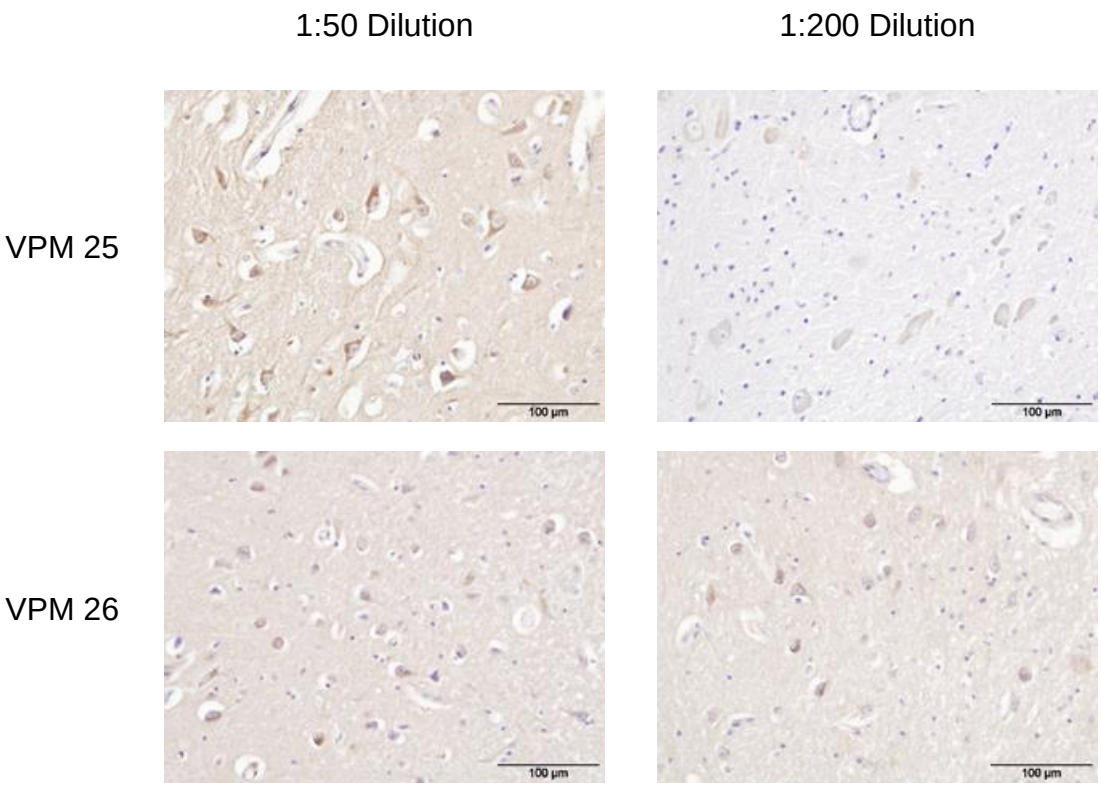

Continuation of Figure 3-14: Cross-reactivity of VPM antibodies to APPV. IHC staining is shown for VPM 25 and 26 at an antibody dilution of 1:50 and 1:200. No antibody control included for this test shown in Figure 3-15.

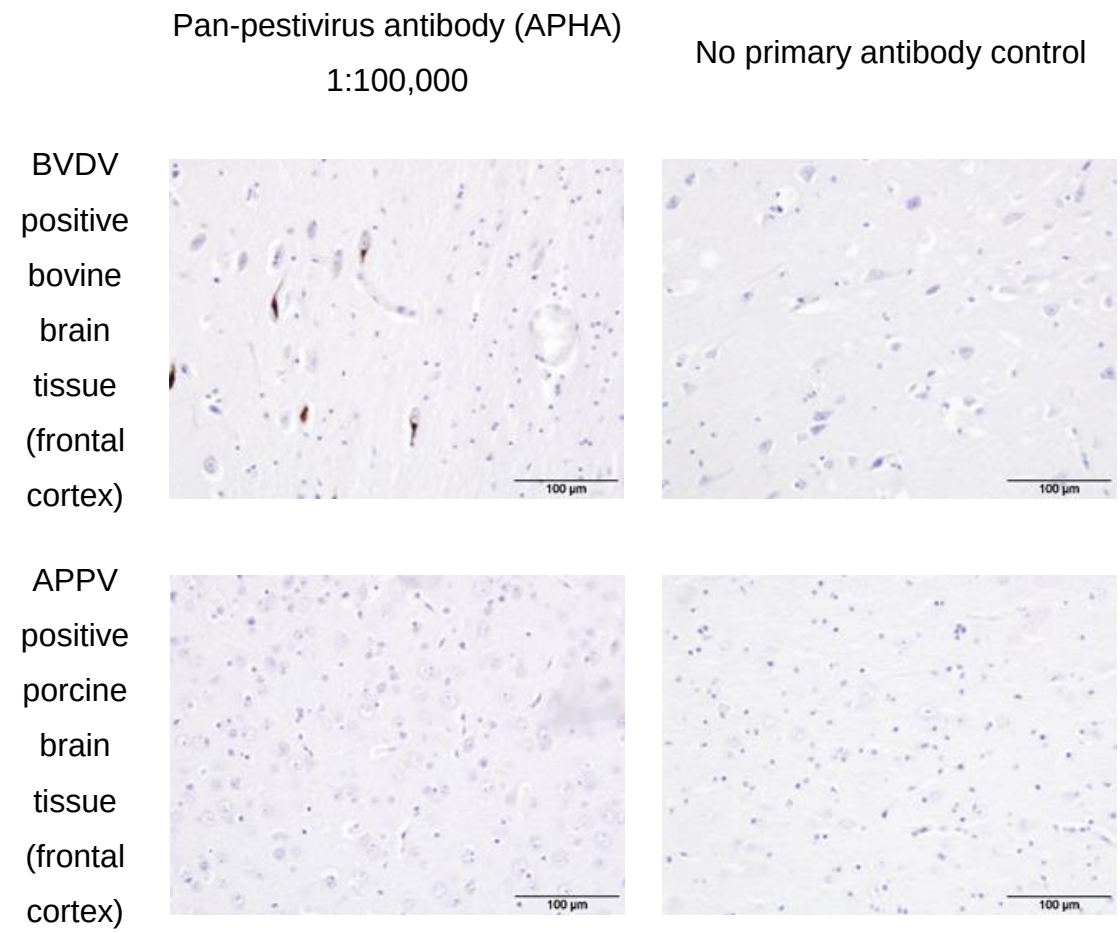

Figure 3-15: Test of cross-reactivity of the APHA pan-pestivirus antibody. The APHA pan-pestivirus antibody with APPV at a dilution of 1:100,000 on both a BVDV positive bovine brain tissue and APPV positive porcine brain tissue (left). A 'no primary antibody control' for both tissue types is shown on the right.

3.3.4 BaseScope *in situ* hybridisation

To produce a GB APPV specific BaseScope ISH assay, two probes were designed based on partial NS3 gene sequences amplified using the RT-qPCR discussed previously in this chapter. The first probe set (BA-V-APPV-2zz-st) was based on sequences of clinical field cases from Great Britain (Figure A-2) as outlined in Chapter 6, Table 6-1 and the second probe set (BA-V-APPV-2zz-st1) was designed specifically for the Perthshire farm study (Chapter 4) using positive tissue sequences from the first farrowing group and positive

semen sample sequences from the second farrowing group (Figure A-1) due to genetic diversity from the other available British strains (probes sequences are detailed in Table 3-14).

Table 3-14: BaseScope probe design based on the consensus sequences (124 bp) of the Perthshire farm case and other British field strains sequenced using the NS3 RT-qPCR primers (Arruda et al., 2016).

Name	Probe	Viral target sequences for probe design	Location within NS3 gene
BA-V-APPV-2zz-st	2ZZ	TTGCCTGGTATTCGTGGCAACCAAAGAAGCCGCGGAAACGGAGGCTAAAGAGCTGCGTGCTAGAGGAATCAACGCCACCTACTACTATTCAGGTATAGACCCCAAG	409-512
	2ZZ	TTGCCTGGTATTCGTGGCGACCAAAGAAGCCGCGGAGACAGAGGCCAAAGAGCTGCGTGCCAGAGGAATTAACGCAACCTATTACTATTCAGGTATAGACCCCAAA	409-513
BA-V-APPV-2zz-st1	2ZZ	TGCCTGGTATTCGTGGCAACCAAAGAAGCAGCGGAGACGGAGGCTAAAGAACTGCGTGCCCGAGGAATTAATGCCACATATTATT	478-554

The basic BaseScope ISH protocol (Advanced Cell Diagnostics, 2018) was optimised over four experiments as shown in Table 3-15 using a positive control (BA-Ss-PPIB-1ZZ based on *Sus scrofa* peptidylprolyl isomerase B [cyclophilin B] PPIB partial mRNA) and negative control (BaseScope ISH negative control probe DapB designed with a single ZZ probe pair) on the formalin-fixed paraffin-embedded (FFPE) tissues from the experimental postnatal APPV infection study (E10/18) described in 3.5. The APPV general GB probe (BA-V-APPV-2zz-st) was optimised using the same tissue as also used for the control optimisation process. The second APPV probe, specifically designed for the Perthshire field study (BA-V-APPV-2zz-st1), was optimised

on FFPE tissues from farrowing group 1 of the field study (Chapter 4) and right cardiac lung tissue from the co-infection study (Chapter 5). Optimisation of the pre-treatment stages for target retrieval and proteinase digest were conducted to determine the optimal protocol for the level of fixation of the tissues and to ensure preservation of the morphology of the tissue while enabling access to the probe hybridisation sequences. The optimal incubation length of the penultimate amplification stage of the BaseScope ISH protocol (AMP7) was also assessed to improve the intensity and clarity of staining. The final protocol is detailed in Chapter 2, Section 2.5.2

Table 3-15: BaseScope ISH optimisation of experimental conditions (Exp) for pre-treatment; target retrieval incubation time in minutes (mins) and temperature (temp,°C), protease treatment incubation time in minutes (mins) and amplification (stage AMP 7) incubation time (min) for different tissue types.

Exp	Probe	Tissue Type	Target retrieval temp (°C)	Target retrieval (mins)	Protease IV (mins)	AMP7 (mins)
1	BA-Ss-PPIB-1ZZ DapB	Brain Spinal cord Spleen Lymph node	100—104	25	40	15
2	BA-V-APPV-2zz-st	Spinal cord Lymph node	98—100	20	35	15
3	BA-V-APPV-2zz-st	Brain Spleen	98—100	30	25	60
3	BA-V-APPV-2zz-st BA-V-APPV-2zz-st1	Spinal cord Lymph node Lung	98—100	25	25	60
4	BA-V-APPV-2zz-st	Brain Spinal cord Spleen Lymph node	98—100	20	15	60
4	BA-V-APPV-2zz-st1	Lung	98—100	8	15	60

In the first experiment, shown in Figure 3-16, the assay results indicated that the integrity of the fixed tissue varied between tissue types, with spinal cords and lymph nodes appearing over digested. A milder protocol with a lower temperature for the target retrieval stage and shorter incubation times for both target retrieval (reduced from 25 minutes to 20 minutes) and protease digestion steps (reduced from 40 minutes to 35 minutes) was therefore developed for these tissues. The negative control probe showed no signal on any of the tissues tested indicating that the level of non-specific staining was minimal. The positive control peptidylprolyl isomerase B (PPIB) was visible within all tissue types although at lower concentration in the brain, in agreement with its natural distribution. The strength of the positive signal in all tissues appeared weak and diffuse indicating that further optimisation was needed to improve the clarity and signal strength.

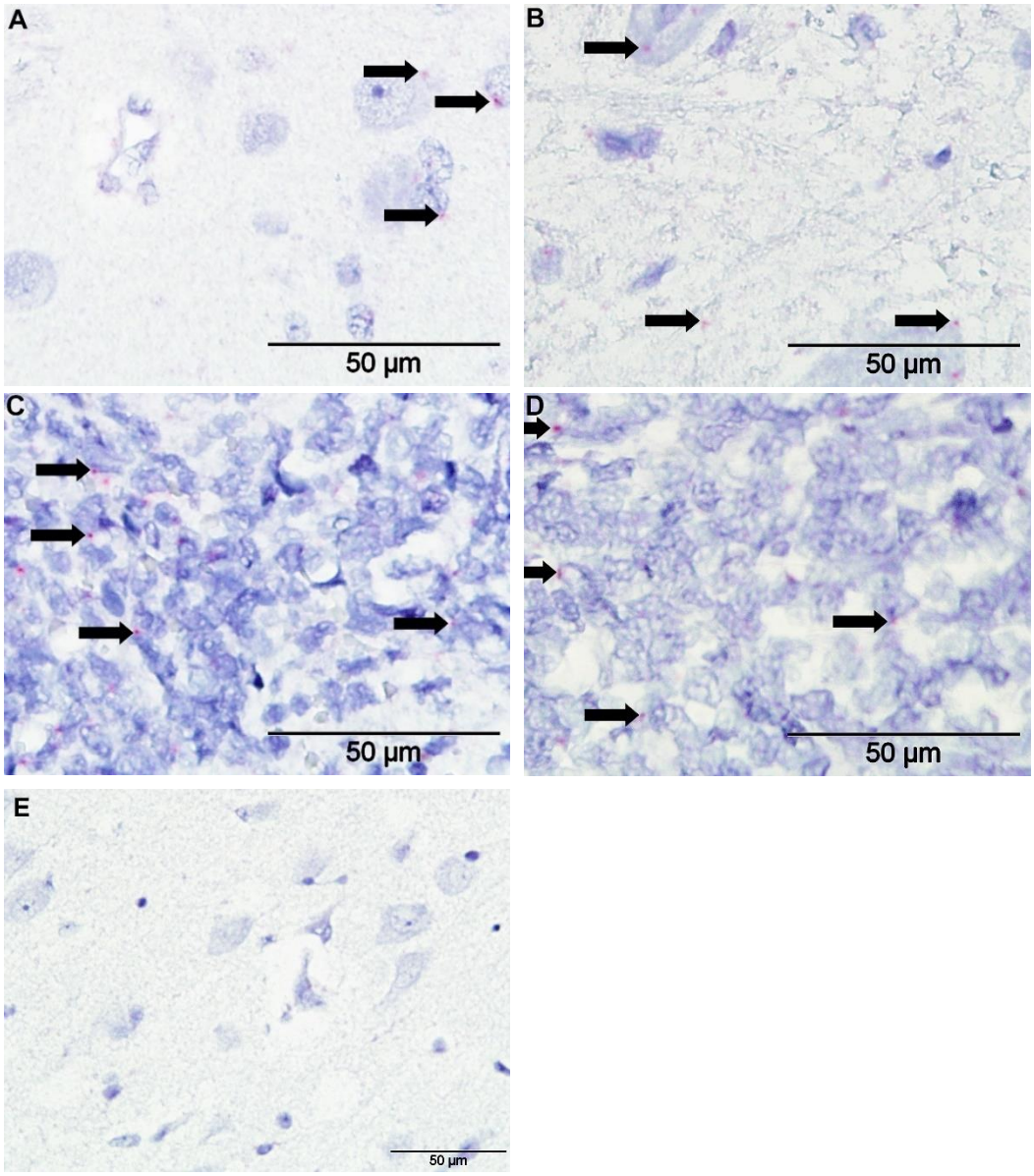

Figure 3-16: Optimisation experiment 1. BA-Ss-PPIB-1ZZ positive control probe (A) brain frontal cortex, (B) cervical spinal cord, (C) spleen and (D) submandibular lymph node. The negative control probe was tested on (E) brain frontal cortex. The experimental conditions for all tissues were a target retrieval step at 100—104°C for 25 minutes, protease IV digestion step at 40°C for 40 minutes and AMP7 amplification of the probe for 15 minutes at room temperature. APPV signal is observed as red dots indicated by arrows and tissue nuclei counterstained with haematoxylin.

The second optimisation experiment, shown in Figure 3-17, showed that the general APPV probe designed from the British field sequences was able to detect APPV RNA within all the tissue types tested from the APPV experimentally infected animals. The negative control hybridization on brain tissue showed no signal, suggesting minimal levels of non-specific binding, whereas the positive control staining of the spinal cord exhibited a stronger signal than in experiment 1, albeit diffused. To further improve sensitivity, incubation of the tissue with AMP 7 was increased from 15 minutes to 60 minutes at room temperature. Overall, there was an improvement in the tissue morphology. However, some of the tissues still remained over digested, including spinal cord and lymph node, even when tested using the milder protocol; therefore, the length of the protease IV incubation was reduced by 10 minutes for both protocols. The results of these changes are shown in Figure 3-18.

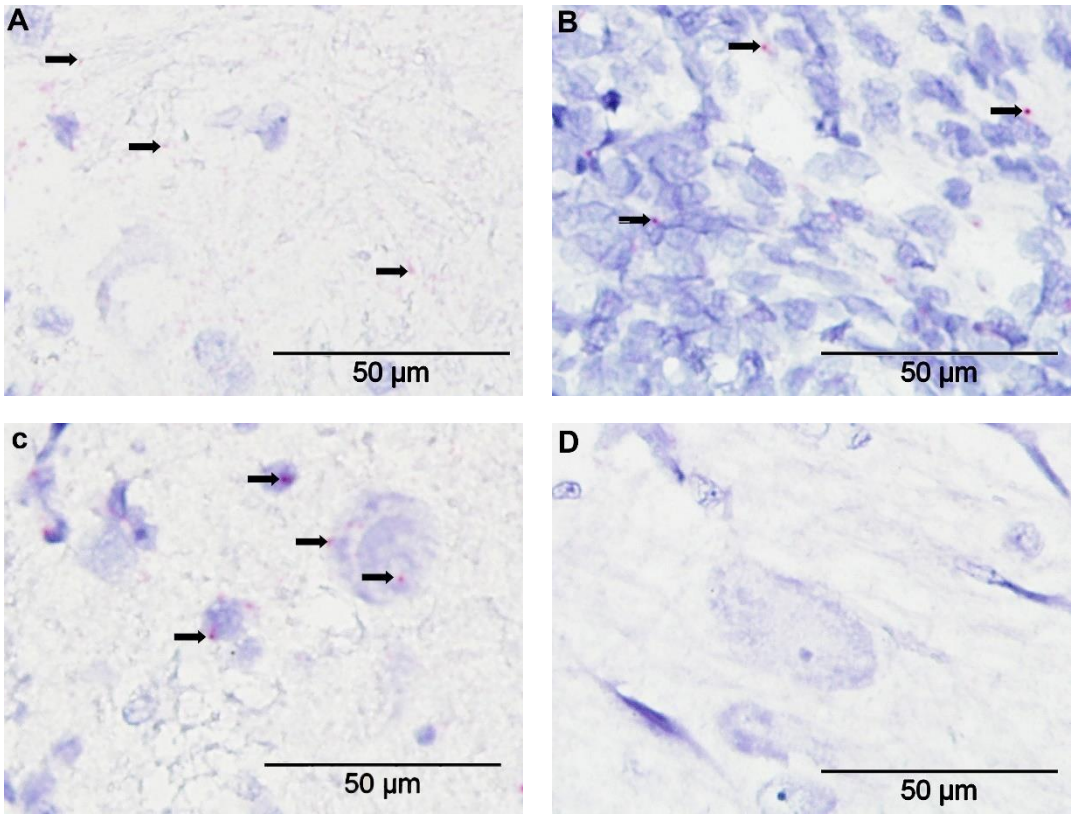

Figure 3-17: Optimisation experiment 2. BA-V-APPV-2zz-st APPV probe tested on (A) cervical spinal cord and (B) submandibular lymph node. The positive control probe was tested on (C) cervical spinal cord and the negative control probe was tested on (D) brain frontal cortex. Experimental conditions for the brain tissue were the same as used in optimisation experiment 1 where as those for the spinal cord and lymph node were as follows: target retrieval step at 98—100°C for 20 minutes, protease IV digestion step at 40°C for 35 minutes and AMP7 amplification of probe for 15 minutes at room temperature. APPV signal is observed as red dots indicated by arrows and tissue nuclei counterstained with haematoxylin.

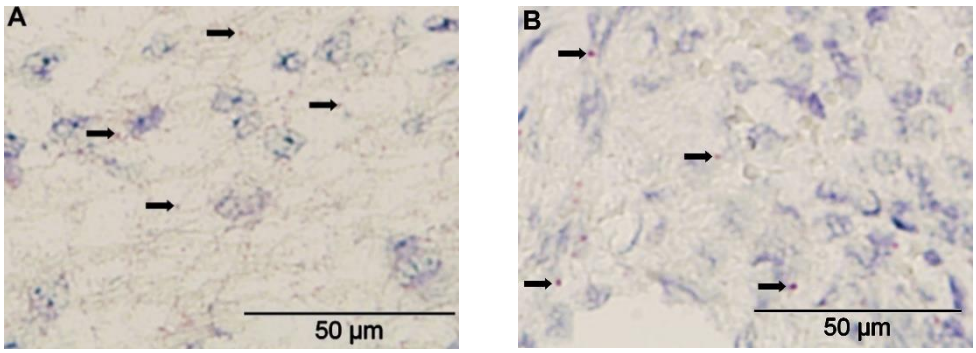

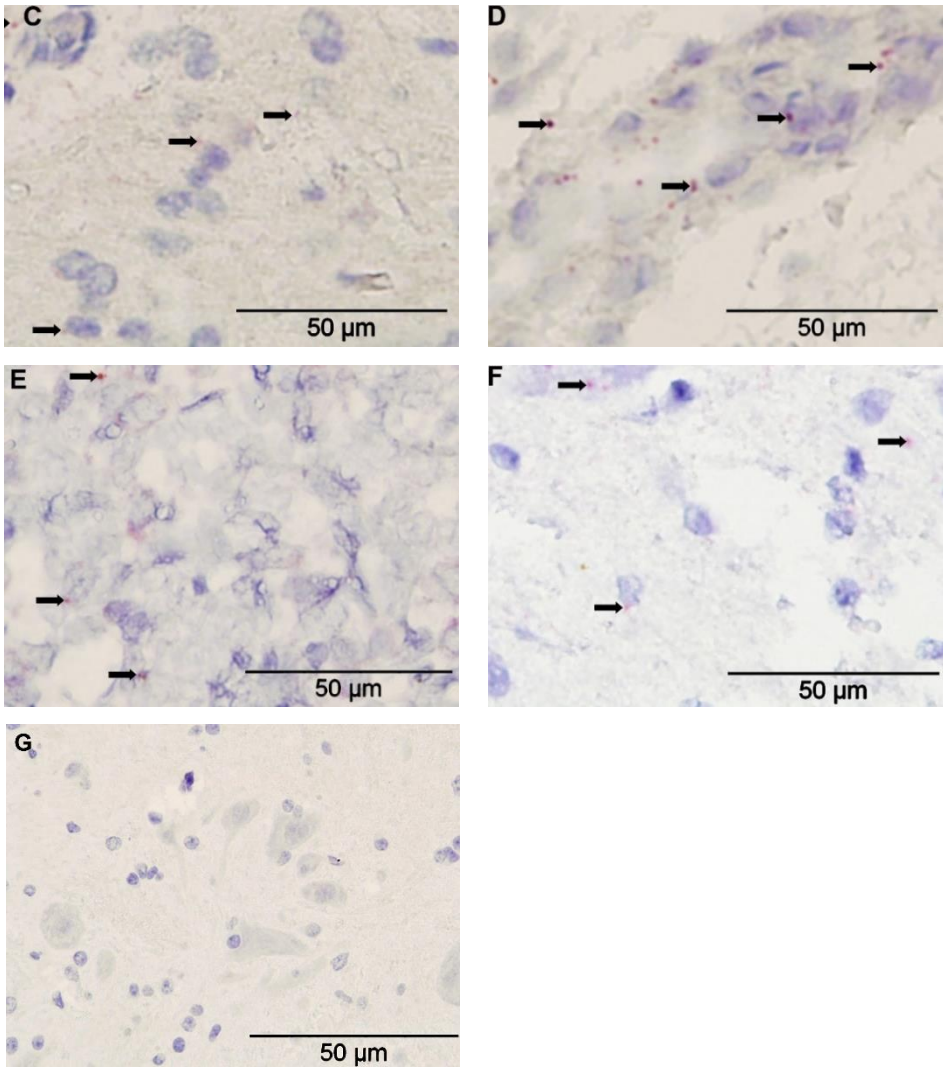

Figure 3-18: Optimisation experiment 3. BA-V-APPV-2zz-st APPV probe tested on (A) brain and (B) spleen with a target retrieval step at 98-100°C for 30 minutes, protease IV digestion step at 40°C for 25 minutes and AMP 7 incubation for 60 minutes at room temperature. BA-V-APPV-2zz-st1 APPV probe was optimised on (C) cervical spinal cord, (D) submandibular lymph node and (E) lung tissue with a target retrieval of step at 98-100°C for 25 minutes, protease IV digestion step at 40°C for 25 minutes and the same AMP7 conditions. Both the (F) positive control and (G) negative control were tested on cervical spinal cord following the milder protocol. APPV signal is observed as red dots indicated by arrows and tissue nuclei counterstained with haematoxylin.

In experiment 3, both the APPV probes were able to detect APPV in their respective tissues with an increased intensity of staining. The negative control showed no signal detection suggesting specificity. There was some background staining observed on lung tissue sections due to suboptimal adhesion which is common with areas that have a higher volume of lumen and a smaller surface area of cells available to interact with BaseScope ISH reagents, such as in the alveoli. The smaller area of cells contactable by the reagents can lead to chromogen becoming trapped between the tissue and the slide. Even though the background staining could be easily differentiated from the positive APPV signal, an additional baking step of 37°C for 30 minutes was included for lung tissue only prior to the protease IV stage to reduce this background.

The integrity of all tissues tested was still slightly compromised due to over digestion. Therefore, to reduce this further and improve the sharpness of the signal, the pre-treatment protocols were adjusted so that the final conditions used for brain, spleen and lymphoid tissue were as follows: a target retrieval incubation at 98—100°C for 20 minutes followed by a 15-minute protease IV treatment at 40°C with the extended AMP 7 step of 60 minutes at room temperature. The milder protocol for more fragile tissues (lung and spinal cord) followed the same protocol with the exception of a shortened target retrieval step of 8 minutes. The results of this final optimisation (experiment 4) are shown in Figure 3-19. The negative control had minimal signal and the background staining was greatly reduced. The positive control had a sharp, bright signal of the expected frequency and the APPV probes showed greater signal strength and clarity. All of the tissues tested showed improvement in structural integrity appearing less digested. Therefore, the assay was considered optimised.

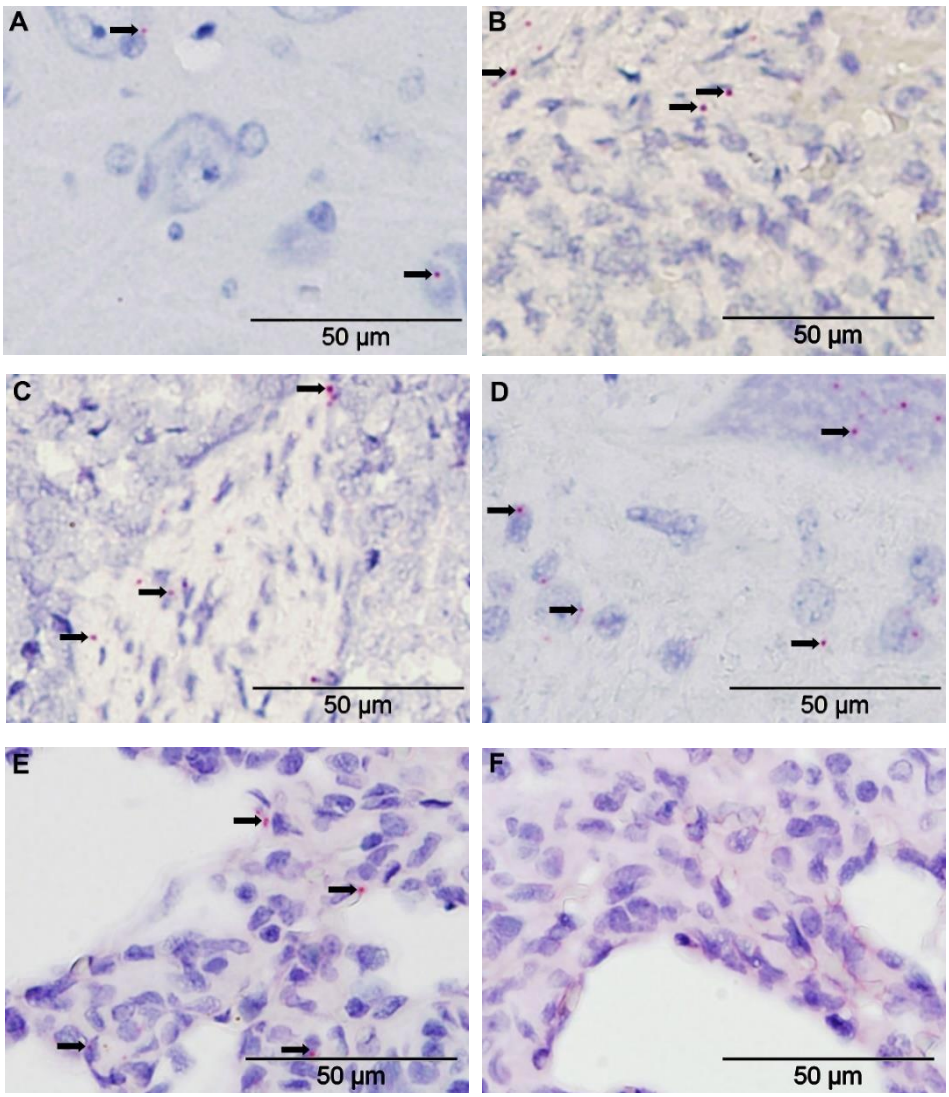

Figure 3-19: Optimisation experiment 4. BA-V-APPV-2zz-st1 APPV probe tested on (A) brain and (B) spleen and (C) submandibular lymph node tissue with a target retrieval step at 98—100°C for 20 minutes, protease IV digestion step at 40°C for 15 minutes and AMP 7 incubation for 60 minutes at room temperature. (D) cervical spinal cord and (E) lung tissue were tested using the same probe under the same conditions with the exception of a reduced target retrieval of step at 98—100°C for eight minutes. The negative control shown on lung tissue (F) was tested following the milder protocol. APPV signal is observed as red dots indicated by arrows and tissue nuclei counterstained with haematoxylin.

3.4 Virus isolation

Isolation was attempted in pre-seeded 80% confluent cells in 2 ml cell culture tubes (Cellstar) alongside a negative control (PBS only) and a cell control. The BT, PK-15 and SPEV 0008 cells were washed twice with Hank's buffered salt solution (HBSS) without calcium or magnesium prior to inoculation with 0.2 ml of the sample and incubated for one hour at 37°C. SPEV 0008 cells were inoculated with 0.5 ml of the samples following the same protocol to determine optimum inoculum dose for isolation. After incubation, either 0.8 ml or 0.5 ml (for cells inoculated with 0.2 ml or 0.5 ml respectively) of the appropriate media containing 1% horse serum and 1% Penicillin (100 units/ml final) and streptomycin (0.1 µg/ml final) was added.

Initially, BT cells were harvested after 3-, 5-, and 7-days post-inoculation (DPI) and the viral load quantified by RT-qPCR. All other cell lines were incubated for three- or five-days post-inoculation prior to harvesting. Adherent cells were removed from the culture tubes by trypsinisation and were freeze-thawed twice, and cell debris removed by centrifugation in a benchtop centrifuge at 800 RPM for 5 minutes at 4°C. Five blind passages were performed for each virus isolation attempt before quantification by RT-qPCR (described in 2.2.3). Viral load for the zero time points of each serial passage was calculated by correcting for the amount of inoculum used in respect of the total media volume. Each attempted SPEV 0008 and BT virus isolation replicate was passaged separately, however PK-15 replicates were pooled prior to re-passaging to increase uniformity of inoculum between replicates. An isolation attempt was considered successful if the virus quantity increased 10-fold (or more than three RT-qPCR Cts) over two consecutive cell culture passages.

3.4.1 Bovine turbinate cells

Virus isolation was attempted on BT cells (Chapter 2, Section 2.6.1) in duplicate using 0.22 µm filtered heart and spleen sample supernatant from the APPV subclinical infection study (E10/18) over three passages. In this study, BT cells were chosen due to their routine use for isolation of other pestiviruses. It has been found that APPV is non-cytopathic, therefore in absence of CPE or of a cytological staining, the only possibility to quantify virus growth was to follow the changes in copy number in the cultures. APPV copy number (viral load) after each passage in each of two replicates was measured by RT-qPCR on day three, five and seven post-inoculation to determine the optimal length of incubation before passages. Cultures were maintained up to day seven, then passaged to avoid carrying over a large amount of debris and toxic metabolites from older cultures. As outlined in Table 3-16, both the heart and spleen supernatant viral isolation attempts were unsuccessful as the virus copy number/µl failed to increase 10-fold (or decrease more than three Cts) over two passages. Viral load showed a general tendency to decrease but also a high variability between time points of the same cultures: in some instances, (e.g. heart two passage 3, day zero to three and spleen two, passage 1 day five to seven) a limited increase in viral copy number was observed between time points however this was not maintained over time and this increase was never substantially higher than the initial inoculum. A number of time points or replicates returned a zero value; in these samples, as the assay was performed before the re-optimisation of the RT-qPCR (described in 3.3.1.3); it is possible that the culture contained a viral load below the analytical sensitivity of the original assay ($3.19x10^3$ copies/µl) therefore the viral genomes present in these replicates might not have been detectable.

Aside from a general trend of reduction of the viral load in each culture over time, a reduction in copy number was also observed between passages, with the exception of a time point for spleen two (passage 1, day seven) which gave a viral load marginally higher than the initial inoculum.

As the viral load had essentially reduced 10-fold with each passage for both tissues, the virus isolation attempt was deemed unsuccessful and ceased. No virus was detected in either the cell control or the sham-inoculated culture throughout the isolation attempt.

Due to the time point results for each passage, and the observation that the cell line showed cellular overgrowth after seven days with acidic media, further isolation attempts were made over a maximum of five days on other epithelial cell types that were found to grow at a similar rate. As the spleen sample still retained a modest viral load at passage 3, the passage number was increased to five passages.

Table 3-16: Virus isolation attempt on BT cells. The average viral load (copies/µl, technical replicates=2) of the culture tested inoculated with E10/18-2 heart and spleen supernatant shown over 3 passages. Each passage was monitored at three-time points: day three, five and 7 post-inoculation by APPV RT-qPCR. ND = Not done.

Sample	Tube	Passage number											
		0	1			2				3			
		Days post-inoculation											
		0	3	5	7	0	3	5	7	0	3	5	7
E10/18-2 Heart	1	3.5×10^5	2.0×10^5	1.4×10^5	1.2×10^5	2.4×10^4	ND	6.3×10^3	7×10^3	1.4×10^3	0	0	0
	2		1.3×10^5	1.1×10^5	1.1×10^5	2.2×10^4	1.4×10^4	0	5.4×10^4	1.1×10^4	3.1×10^5	0	0
E10/18-2 Spleen	1	4.7×10^6	4.5×10^6	2.4×10^6	4.2×10^6	8.4×10^5	5.5×10^5	3.6×10^5	3.1×10^5	6.2×10^4	9.4×10^2	0	1.7×10^4
	2		3.0×10^6	3.0×10^6	5.3×10^6	1.6×10^6	6.0×10^5	4.1×10^5	2.4×10^5	4.8×10^4	3.7×10^4	1.4×10^4	2.0×10^4
Negative control	1	0	0	0	0	0	0	0	0	0	0	0	0
Cell control	1	0	0	0	0	0	0	0	0	0	0	0	0

3.4.2 Porcine Kidney-15 (PK-15) cells

Viral isolation was attempted using APPV positive clinical serum samples (NEE-0419-01-03, Chapter 6, Table 6-1), supplied by APHA, and serum collected on day 10 post-inoculation from the postnatal APPV infection study (E10/18 1-3). The virus isolation attempts (results outlined in Table 3-17) using the 10 DPI serum collected from the subclinical APPV infection study (E10/18 1-3) was unsuccessful, with the viral load reducing over the course of the five passages and becoming undetectable at passage three for sample E10/18-1, at passage 4 for E10/18-3 and at passage 5 for sample E10/18-2. Similarly, the virus isolation attempts using clinical serum samples from the North East England 2019 (NEE-0419) outbreak also proved unsuccessful with diminishing viral loads observed for all three samples until the virus was undetectable at passage 3 for sample one and passage 2 for sample three. Sample two was undetectable at passage 3, however 36.2 copies/µl of the virus was observed at passage 4, then load became undetectable again at passage 5. This variability could be attributed to the viral load being very close to the limit of detection of the assay ($3.19x10^2$ copies/µl).

Table 3-17: Virus isolation attempt on PK-15 cells. The average viral load (copies/µl, technical replicates=2) of the culture inoculated with 0.2 ml of serum collected either at 10 DPI from viraemic APPV positive piglets infected as part of the postnatal APPV infection study (E10/18 1-3) and or from serum collected during the North East England April-19 outbreak (NEE-0419-01-03) is shown over 5 passages. Each passage was monitored at 3 DPI by APPV RT-qPCR.

Sample	Passage number					
	0	1	2	3	4	5
E10/18-1	$2.0x10^7$	$1.9x10^4$	$7.6x10^1$	0	0	0
E10/18-2	$3.7x10^7$	$2.8x10^4$	$2.7x10^3$	$4.1x10^2$	6.7	0
E10/18-3	$2.4x10^7$	$1.2x10^5$	$1.4x10^4$	$2.8x10^2$	0	0
NEE-0419-01	$9.1x10^3$	$1.2x10^3$	$1.3x10^2$	0	0	0
NEE-0419-02	$2.7x10^4$	$8.6x10^3$	$1.2x10^3$	0	$3.6x10^1$	0
NEE-0419-03	$7.7x10^3$	$3.6x10^3$	0	0	0	0

3.4.3 SPEV 008 cells

Initially, virus isolation in this cell line was performed using 0.2 ml (0.22 µm filtered) inoculum consisting of heart and spleen supernatant, previously used to attempt virus isolation on BT cells, and an additional serum sample from the same APPV positive animal (E10/18-2). Each passage was monitored over two time points and the 5 DPI collection was used as the starting inoculum for each subsequent passage. As detailed in Table 3-18, the isolation attempts using 0.2 ml heart, spleen or serum supernatant were unsuccessful. As an inoculum volume of 0.2 ml did not allow APPV isolation from any of the samples, further attempts to isolate the virus were performed using 0.5 ml of inoculum (see below). Large variability among different tissues (including serum) was detected in all cultures, using 0.2 ml of inoculum. More specifically between 3 and 5 DPI of each passage; moreover, the viral load of all cultures was undetectable by passage 4 and remained undetectable at passage 5. An

example of this can be seen at passage 1 and 2 of the heart replicates, where the viral load increased for one between day zero and three and for the other one between three and five, however this growth was not sustained. The viral load for spleen and serum followed a similar trend although at different time points. No virus was detected in either of the controls throughout the isolation attempt.

Table 3-18: Virus isolation attempt on SPEV 0008 cells using 0.2 ml inoculum volume. The average viral load (copies/µl, technical replicates=2) of the culture inoculated with 0.2 ml of heart and spleen supernatant and 10 DPI Serum from an APPV positive piglet (E10/18-2) collected as part of the postnatal APPV infection study (E10/18) is shown over 5 passages. Each passage was monitored at two-time points: day three and five post-inoculation by APPV RT-qPCR.

Sample	Tube	Passage														
		1			2			3			4			5		
		Days post-inoculation														
		0	3	5	0	3	5	0	3	5	0	3	5	0	3	5
E10/18-2 Heart	1	$1.4x10^6$	$7.0x10^5$	$3.7x10^4$	$7.4x10^3$	$1.4x10^7$	$5.1x10^4$	$1.1x10^4$	0	0	0	0	0	0	0	0
	2		$9.7x10^5$	$1.1x10^7$	$2.2x10^6$	$3.2x10^4$	$1.4x10^4$	$2.8x10^3$	0	0	0	0	0	0	0	0
E10/18-2 Spleen	1	$3.5x10^7$	$2.6x10^7$	$7.5x10^6$	$1.5x10^6$	$9.3x10^6$	0	0	$2.2x10^4$	0	0	0	0	0	0	0
	2		$2.0x10^7$	$3.9x10^5$	$7.8x10^4$	$8.0x10^5$	$3.8x10^6$	$7.6x10^5$	$1.1x10^4$	0	0	0	0	0	0	0

Continuation of Table 3-18: Virus isolation attempt on SPEV 0008 cells using 0.2 ml inoculum volume. The average viral load (copies/µl, technical replicates=2) of the culture inoculated with 0.2 ml of heart and spleen supernatant and 10 DPI Serum from an APPV positive piglet (E10/18-2) collected as part of the APPV infection study (E10/18) is shown over 5 passages. Each passage was monitored at two-time points: day three and five post-inoculation by APPV RT-qPCR.

Sample	Tube	Passage														
		1			2			3			4			5		
		Days post-inoculation														
		0	3	5	0	3	5	0	3	5	0	3	5	0	3	5
E10/18-2 Serum	1	$1.8x10^8$	$3.4x10^7$	$5.8x10^7$	$1.2x10^7$	$2.7x10^5$	$1.3x10^4$	$2.6x10^3$	$8.4x10^4$	$3.5x10^3$	0	0	0	0	0	0
	2		$4.5x10^7$	$3.8x10^7$	$7.6x10^6$	$4.2x10^4$	$3.5x10^3$	$7.0x10^2$	$1.2x10^5$	$4.4x10^4$	0	0	0	0	0	0
Negative control	1	0	0	0	0	0	0	0	0	0	0	0	0	0	0	0
Cell control	1	0	0	0	0	0	0	0	0	0	0	0	0	0	0	0

A further attempt to isolate APPV using an inoculum volume of 0.5 ml on SPEV 0008 cells was made by culturing serum from the three APPV positive piglets from the subclinical APPV infection study (E10/18 1-3) and three positive serum samples from the Suffolk January-18 field outbreak (SUF-0118 Chapter 6, Table 6-1), supplied by APHA. In all cultures, the viral load of the culture reduced over the five passages indicating that virus isolation was unsuccessful (as outlined in Table 3-19). No virus was detected in either the negative sham-inoculated culture or cell control in any passage through the isolation attempt. Again, variability of viral load between passages was observed in the first biological replicate of the SUF-0118-01 and SUF-0118-02 serum culture; this may be due to analytical sensitivity limitations in detection at very low concentrations as previously discussed.

Due to time, resources and the start of the SARS-CoV-2 pandemic, no further virus isolation attempts were made. Additional work is required to determine the permissiveness of other cell lines (both immortalised and primary) to APPV.

Table 3-19: APPV isolation attempt on SPEV 0008 cells using 0.5 ml inoculum volume. The average viral load (copies/µl, technical replicates=2) of the culture inoculated with 0.5 ml of serum collected at 10 DPI APPV positive piglets as part of the subclinical APPV infection study (E10/18 1-3) and serum from the Suffolk January-18 field case (SUF-0118-01-03) is shown over five passages. Each passage was monitored at 3 DPI by APPV RT-qPCR.

Sample	Tube	Passage									
		1		2		3		4		5	
		Days post-inoculation									
		0	3	0	3	0	3	0	3	0	3
E10/18-1 Serum	1	$2.0x10^7$	$2.7x10^5$	$1.4x10^5$	$3.5x10^4$	$1.8x10^4$	$8.9x10^3$	$4.5x10^3$	$6.4x10^1$	$3.2x10^1$	0
	2		$3.8x10^5$	$1.9x10^5$	$3.6x10^4$	$1.8x10^4$	$1.5x10^4$	$7.5x10^3$	$5.4x10^1$	$2.7x10^1$	0
E10/18-2 Serum	1	$3.7x10^7$	$2.7x10^5$	1.4x105	$3.5x10^4$	$1.8x10^4$	$8.9x10^3$	$4.5x10^3$	$1.4x10^2$	$7.0x10^1$	1.2
	2		$3.8x10^5$	1.9x105	$3.6x10^4$	$1.8x10^4$	$1.5x10^4$	$7.5x10^3$	$1.3x10^2$	$6.5x10^1$	$2.1x10^1$
E10/18-3 Serum	1	$2.4x10^7$	$1.4x10^6$	$7.0x10^5$	$2.6x10^5$	$1.3x10^5$	$4.7x10^4$	$2.4x10^4$	$2.6x10^3$	$1.3x10^3$	$2.1x10^2$
	2		$1.7x10^6$	$8.5x10^5$	$2.8x10^5$	$1.4x10^5$	$6.8x10^4$	$3.4x10^4$	$2.8x10^3$	$1.4x10^3$	$9.3x10^2$

Continuation of Table 3-19: APPV isolation attempt using 0.5 ml inoculum volume. The average viral load (copies/µl, technical replicates=2) of the culture inoculated with 0.5 ml of serum collected at 10 DPI APPV positive piglets as part of the subclinical APPV infection study (E10/18 1-3) and serum from the Suffolk January-18 field case (SUF-0118-01-03) is shown over five passages. Each passage was monitored at 3 days post-inoculation (DPI) by APPV RT-qPCR.

Sample	Tube	Passage									
		1		2		3		4		5	
		Days post-inoculation									
		0	3	0	3	0	3	0	3	0	3
SUF-0118-01	1	$8.1x10^5$	$1.6x10^4$	$8.0x10^3$	$3.1x10^3$	$1.6x10^3$	$9.1x10^3$	$4.6x10^3$	0	0	0
	2		0	$5.0x10^{-2}$	0	0	$3.1x10^2$	$1.6x10^2$	0	0	$1.0x10^1$
SUF-0118-02	1	$4.0x10^4$	$1.8x10^4$	$9.0x10^3$	$3.6x10^3$	$1.8x10^4$	$4.2x10^2$	$2.1x10^2$	0	0	0
	2		$7.0x10^2$	$3.5x10^2$	$4.8x10^1$	$2.4x10^1$	$7.4x10^2$	$3.7x10^2$	0	0	0
SUF-0118-03	1	$1.6x10^5$	$2.3x10^4$	$1.2x10^4$	$1.8x10^3$	$9.0x10^2$	$9.9x10^2$	$5.0x10^2$	9.6	$4.8x10^2$	0
	2		$3.1x10^4$	$1.6x10^4$	$6.1x10^3$	$3.1x10^3$	$1.2x10^3$	$6.0x10^2$	4.5	$2.3x10^2$	0

Continuation of Table 3-19: APPV isolation attempt using 0.5 ml inoculum volume. The average viral load (copies/µl, technical replicates=2) of the culture inoculated with 0.5 ml of serum collected at 10 DPI APPV positive piglets as part of the subclinical APPV infection study (E10/18 1-3) and serum from the Suffolk January-18 field case (SUF-0118-01-03) is shown over five passages. Each passage was monitored at 3 DPI by APPV RT-qPCR.

Sample	Tube	Passage									
		1		2		3		4		5	
		Days post-inoculation									
		0	3	0	3	0	3	0	3	0	3
Negative control	1	0	0	0	0	0	0	0	0	0	0
Cell control	1	0	0	0	0	0	0	0	0	0	0

3.5 Postnatal APPV infection in colostrum-deprived piglets (E10/18)

3.5.1 Study design

Ethical approval was obtained for the APPV infection of colostrum deprived piglets from the MRI Animal Experiments Committee (E10/18). The study was conducted under the Home Office license PFA7E7AD6 in accordance with the Animal (Scientific Procedures) Act 1986 and Home Office guidelines.

Due to the limited availability of APPV clinical material available for diagnostic test development and virus isolation, it was initially necessary to amplify the existing infectious material in pigs. An APPV infection in one-week-old pigs was conducted for this purpose but also to determine the outcome of APPV infection in neonatal piglets mimicking a horizontal transmission scenario. Due to the lack of an available serological test to determine previous exposure to the virus at the time of the study, it was important to source animals from a high health status closed unit with no known history of CT A-II. From this, six crossbred piglets (Landrace x Duroc) were snatched farrowed (taken from the mother during labour on the Moredun farm, and transported directly to the housing without environmental contamination) to reduce potential exposure to pathogens.

For the first 48 hours, piglets were fed a solution containing equal volumes of bovine colostrum and 10% glucose as a sow colostrum substitute to prevent the transfer of maternally-derived antibodies. The piglets were then bottle-fed with a mixture of 50% evaporated milk and 50% sterile water, with water and wet mash given *ad libitum*. Oroject (Neomycin Sulphate) was also administered daily (1-10 DPI) on the advice of the duty veterinarian alongside commercial (Fage) natural yoghurt to develop and enhance the gut microbiota of the piglets. All diet substitutes had no detectable APPV RNA or other non-

APPV pestivirus RNA present as determined by the APPV quantitative reverse-transcriptase PCR (RT-qPCR) (Chapter 2, Section 2.2.3), and a pan-pesti RT-PCR performed by the viral surveillance unit (MRI) respectively.

The six piglets were group-housed in an isolator base in a clean environment not used for at least 5 years) for pig studies and acclimated for seven days before splitting the groups into separate isolator bases (three piglets each) within the same pathogen-free environment at the commencement of the study as shown in Figure 3-20 and Figure 3-21. The climate was controlled by heaters placed at the base of the incubators and a heat lamp suspended over the bedding area. Autoclaved towel bedding and plastic toys were provided for enrichment purposes and replaced daily as part of the husbandry routine to allow the piglets to exhibit natural rooting and nesting behaviours. Strict biosecurity including the use of separate personal protective equipment and instruments/ utensils was followed for each pig group. The negative control group was attended to prior to interaction with the APPV infected group to prevent transmission.

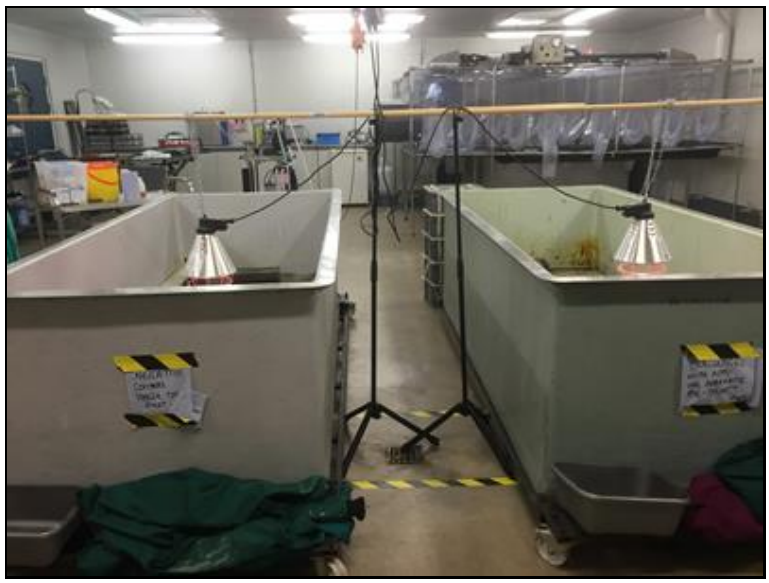

Figure 3-20: Housing of piglets within Moredun surgery unit.

Figure 3-21: Housing of piglets within the isolator base.

For the study, three piglets (E10/18, 1-3) were randomly assigned to the APPV infection group (Table 3-20). Each pig in this group was given a different inoculum consisting of tissue homogenates from one of three APPV cases (see, Chapter 6, Table 6-1 further details): NOR-0616-01 ($1.26x10^8$ copies/ml), NOR-0417-01 (1.1×10^9 copies/ml) and SUF-0617-01 ($3.13x10^8$ copies/ml). The three negative control animals (E10/18, 4-6) were given a sham inoculum consisting of the tissue from an APPV negative pig with no history of CT A-II. All inocula were prepared as follows: tissue homogenates were generated by homogenising brain, spinal cord, tonsil and spleen as detailed in 2.1.1, the tissue homogenate supernatants were pooled and passed through a 0.5 µM and a 0.45 µM filter. This was followed by adding gentamicin (1 mg/µl final), penicillin (100 units/ml final), streptomycin (100 µg/ml final) and Amphotericin B (0.25 µg/ml final). Each piglet was inoculated orally (2 ml), intranasally (1 ml per nostril) and through intramuscular injection (1 ml per hind leg).

Table 3-20: Summary of study groups

Infection group	Animal ID	Inoculum
APPV	E10/18 1	SUF-0617-01
	E10/18 2	NOR-0616-01
	E10/18 3	NOR-0417-01
Sham	E10/18 4	APPV Negative pig 334567
	E10/18 5	APPV Negative pig 334567
	E10/18 6	APPV Negative pig 334567

Serum and swab (oropharyngeal, nasal and rectal) samples were collected from all piglets at 0, 3, 5, 7, and 9 DPI. The serum and swab samples were processed according to 2.1.4 and 2.1.5 before extraction (2.2.1.1.2) and RT-qPCR (2.2.3), which was performed to determine peak viraemia and viral shedding. The serum samples were also used to test the optimised NS3 indirect ELISA according to 2.4.2, with samples diluted 1:200 to detect changes of IgG levels in response to APPV infection over time. The piglets were culled as soon as viraemia began to decline detected. In brief, the piglets were anesthetised in the surgery according to standard protocols, and a blood sample (to obtain serum) was collected by cardiac puncture. Once collected, the piglets were euthanised with an intravenous overdose of Pentobarbitone (Pentoject, Animalcare Ltd). Upon confirmation of death, the piglets were transported to the post mortem (PM) suite and an extensive necropsy was performed to collect tissues for assessing presence of APPV in tissues. Overall, 22 tissue types were sampled: brain and pituitary gland, cervical, thoracic and lumbar spinal cord, trigeminal nerve, submandibular, pre-scapular, tracheobronchial, retropharyngeal, mediastinal, superficial inguinal, mesenteric, and popliteal lymph nodes, palatine tonsil, thymus, spleen, heart, kidney, liver, lung and Peyer's patches collected from the ileocecal junction. Each tissue was collected individually using sterile trays, single-use forceps (Williams) and scalpels (number 10, Swann Morton) with sterilised bone cutters and PM knives (PM40, Barber medical) to avoid cross-contamination between tissues as shown in Figure 3-22. The area was also cleaned and disinfected between animals to avoid cross-contamination. Each

tissue sample was halved with a portion stored frozen at -80°C until homogenisation (2.1.1), extraction (2.2.1.1.1) and APPV RT-qPCR analysis. The other portion was immediately fixed by immersion in 10% buffered formalin (Cellstor pots, Cell path Ltd) for histopathological analysis (2.5.1).

Figure 3-22: Post mortem set-up for the collection of fresh and formalin-fixed tissue samples.

3.5.2 Assessment of colostrum-deprived model

The snatch-farrowed piglets all appeared healthy at birth with no clinical signs of CT A-II. All of the piglets survived the initial 24 hours, which is typically a critical period for snatch-farrowed piglets deprived of maternal colostrum. On 1 DPI both the APPV infected (E10/18 01-03) and sham-infected (E10/18 04-06) groups developed diarrhoea without pyrexia. After consultation with a veterinarian, it was attributed to increased stress as a result of the separation of piglets into groups for the inoculation coinciding with dietary changes,; as a result of this Oroject (Neomycin Sulphate) was given daily from 1-10 DPI alongside natural yoghurt to develop and enhance the piglet's gut microbiota as previously mentioned in 3.5.1

3.5.2.1 Assessment of viraemia in serum

Piglets E10/18-1 and E10/18-2 tested APPV positive from 3 DPI. Although APPV was detectable at 3 DPI, E10/18-3 was classified as equivocal until 5 DPI when it became positive. All of the APPV infected piglets remained APPV positive for the remainder of the study, as shown in Figure 3-23. The peak of viraemia was observed for E10/18-1 7 DPI ($1.4x10^{11}$ copies/ml) and at 9 DPI for E10/18-2 ($2.84x10^{11}$ copies/ml) and E10/18-3 ($1.64x10^{11}$ copies/ml). No virus was detected on any day post-inoculation for the sham-infected negative control piglets (E10/18-4, E10/18-5 and E10/18-6).

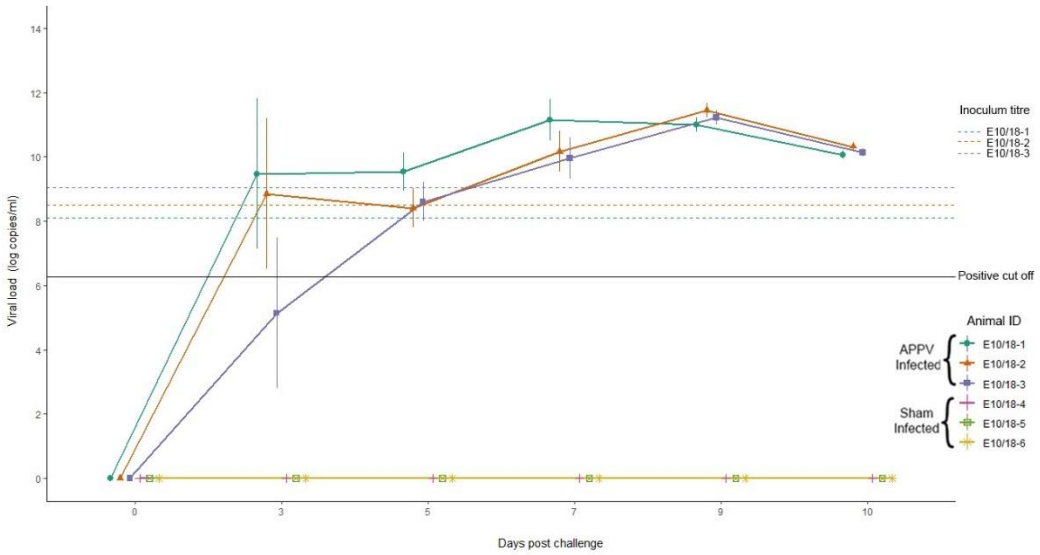

Figure 3-23: APPV viral load in serum. The average is based on two technical replicates and plotted as log_{10} copies/ml +/- Standard deviation for APPV infected (E10/18 1-3, n=3) and sham-infected piglets (E10/18 4-6, n=3) with respect to the limit of detection of the assay. The initial viral load for the inoculum for each of the APPV positively inoculated piglets is indicated by dashed lines.

3.5.2.2 Evaluation of viral shedding in swabs

Shedding of the virus orally, nasally and in faeces was determined through oropharyngeal, nasal and rectal swabbing (Figure 3-24, Figure 3-25 and Figure 3-26 respectively). No virus was detected in any swab type at any time point throughout the study for the three sham-infected piglets (E10/18-4, E10/18-5 and E10/18-6). As demonstrated in Figure 3-24, E10/18-1 had positive oral swabs on 7 and 9 DPI, E10/18-2 and E10/18-3 were positive on 9 DPI only. APPV positive nasal swabs were detected for E10/18-1 and E10/18-3 piglets on 9 DPI (Figure 3-25). No virus was detected in nasal swabs for E10/18-2 at any time point. Only piglet E10/18-1 7 DPI was APPV positive in rectal swabs (Figure 3-26). However, APPV was not detectable at any other time point. APPV was also undetectable in rectal swabs for E10/18-2 and E10/18-3 throughout the study.

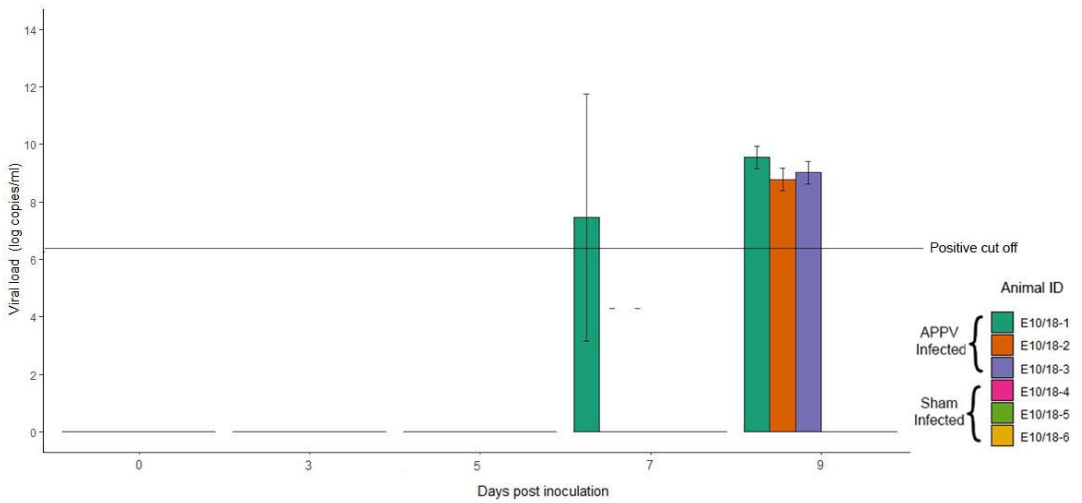

Figure 3-24: APPV viral load in oral swabs. The average is based on two technical replicates and plotted as log_{10} copies/ml +/- standard deviation for APPV infected (E10/18 1-3, n=3) and sham-infected piglets (E10/18 4-6, n=3) with respect to the limit of detection of the assay.

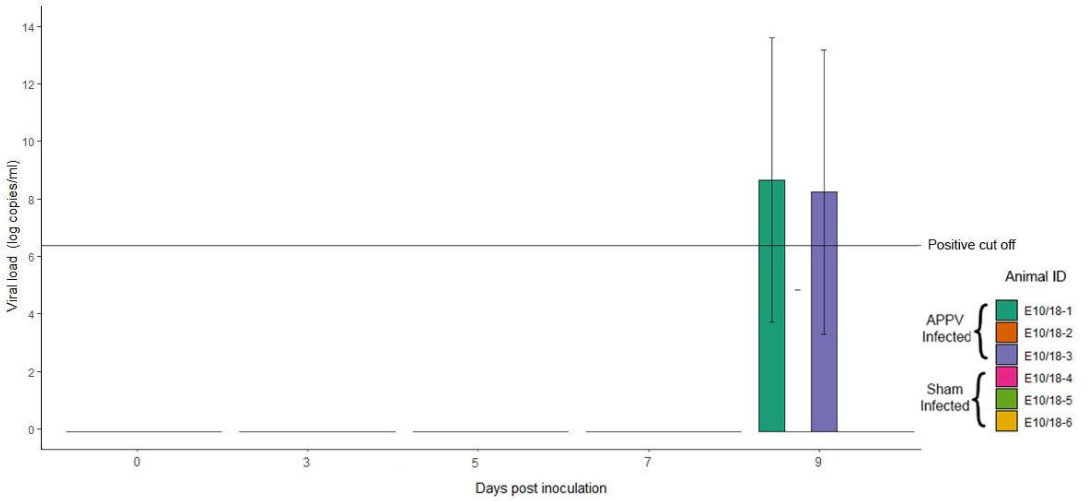

Figure 3-25: APPV viral load in nasal swabs. The average is based on two technical replicates and plotted as log_{10} copies/ml +/- standard deviation for APPV infected (E10/18 1-3, n=3) and sham-infected piglets (E10/18 4-6, n=3) with respect to the limit of detection of the assay.

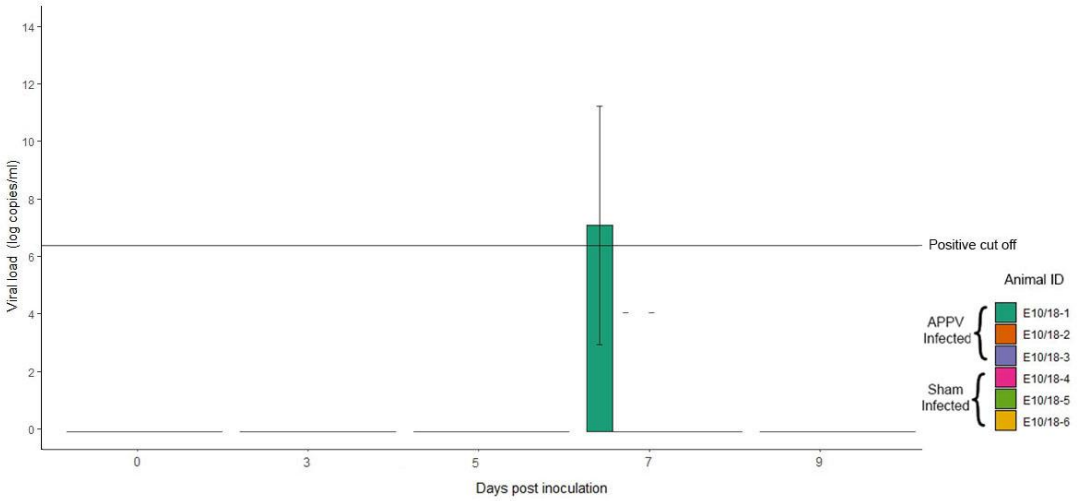

Figure 3-26: APPV viral load in rectal swabs. The average is based on two technical replicates and plotted as log_{10} copies/ml +/- standard deviation for APPV infected (E10/18 1-3, n=3) and sham-infected piglets (E10/18 4-6, n=3) with respect to the limit of detection of the assay**.**

3.5.2.3 Assessment of tissue tropism

Twenty tissue types collected during the post mortem examination were assessed for APPV RNA by RT-qPCR (Figure 3-27). No virus was detected in any tissue type from the three APPV negative sham-infected animals. All tissue types collected from E10/18-1 tested APPV positive; all tissue types with the exclusion of thymus (where no virus was detected) were positive for E10/18-2. For piglet E10/18-3, APPV was detected in all tissue types except for the lumbar spinal cord (which was classified as equivocal). On average, consistently high viral loads of the virus were detected in lymphoid tissues, with the greatest amount of virus found in the pre-scapular lymph node ($4.32x10^9$ copies/g), spleen ($1.55x10^9$ copies/g), and tonsil ($1.16x10^9$ copies/g) tissue. The tissues with the lowest APPV loads were in central nervous tissue (cervical [$4.77x10^7$ copies/g], thoracic [$3.09x10^7$ copies/g] and lumbar [$1x10^8$ copies/g] spinal cord sections), heart ($3.59x10^7$ copies/g), mesenteric lymph node ($1.25x10^7$ copies/g) and thymus ($3.33x10^6$ copies/g).

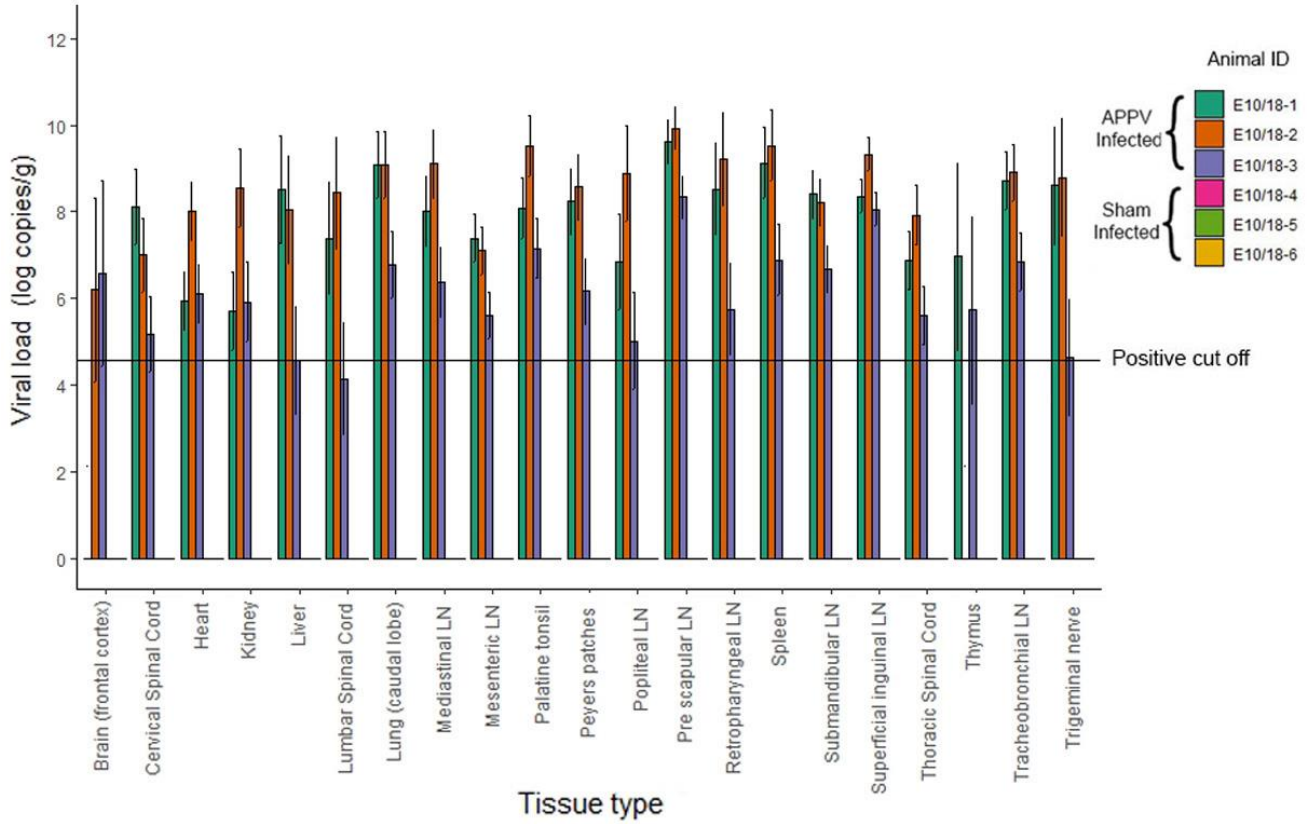

Figure 3-27: APPV viral load in tissues. The average is based on two technical replicates and plotted as log_{10} copies/ml +/- standard deviation collected at post mortem (10 DPI) from the APPV infected (E10/18 1-3, n=3) and sham-infected (E10/18 4-6, n=3) piglets with respect to the limit of detection of the assay.

3.5.2.4 Antibody response to APPV infection

Antibody response to the APPV infection for each animal was assessed by measurement of IgG levels using the NS3 indirect ELISA. The IgG levels for all animals remained consistently low (with normalised blank corrected OD values between 0.02 and -0.01) throughout the study.

3.6 Discussion

In order to characterise APPV infections by British strains, it was necessary to develop methods to identify and proliferate the virus, enabling further model development to investigate host—pathogen interactions. Due to the recent discovery of APPV at the commencement of the project, no diagnostic assays were commercially available, and only a small number of molecular and immunological tests were published with limited validation disclosed. Furthermore, these assays were limited in design: initial RT-qPCR development was impeded by the limited amount of published sequences available for primer and probe design making it difficult to account for the diversity of strains at target sites.

The initial limitations of designing an immunological assay were the lack of specific or cross-reactive available antibodies to APPV; moreover, antibodies that are reactive to APPV may not have the ability to be deployed in different techniques. For example, Schwarz *et al.* (2017) screened a panel of 120 monoclonal antibodies against structural and non-structural proteins of CSFV, BVDV and Bungowannah virus and found two APPV cross-reactive antibodies with only one suitable for the design of a serological test due to issues surrounding sensitivity. NS3-specific monoclonal antibodies generated by Schwarz *et al.* (2017) were unreactive in immunohistochemistry or immunofluorescence techniques. Although monospecific NS3 antibodies extracted from APPV positive sera were reactive in APPV cell culture, they

were unable to detect APPV infected tissue due to the high background levels of intrinsic porcine IgG present (Schwarz *et al.*, 2017). As a result of the limited amount of information on APPV available at the start of this work, the difficulties in culturing the virus, and the limited availability of reference samples of a known serological status it was difficult to accurately define the assays sensitivity and specificity.

The importance of performing validation on both diagnostic and research techniques should not be underestimated: it determines the limitations of the assay and increases confidence in the results reported. In this chapter, diagnostic methods for the detection and quantification of APPV were established. Although some of the techniques established were based on published methods, it should not be assumed that the assays would generate the same results under different experimental conditions. Differences in sample preparation, reagents, and instruments used all contribute to the overall effectiveness of the test (Bustin and Huggett, 2017). Therefore, additional modification, optimisation and validation steps were performed on all the techniques previously described.

A previously published APPV RT-qPCR by Arruda *et al.* (2016) was modified, optimised and validated to verify the suitability of the assay to detect genetic sequence variability, particularly of British field strains (unpublished). The importance of optimisation of the reaction chemistry and thermocycling profile in the improvement of sensitivity and specificity of the assay is well documented: poor design (mismatched annealing and melting temperatures) and lack of optimisation of primer and probe concentrations have been found to contribute to reduced product yield, produce non-specific amplification, primer-dimer formation and differences in calculated Ct values, resulting in reduced technical precision and false (positive or negative) amplification results (Rychlik, Spencer and Rhoads, 1990; Mikeska and Dobrovic, 2009; Bustin and Huggett, 2017). As well as determining the optimal parameters above, the probe was modified to reduce the difference in melting temperature

with the primers and the overall annealing temperature of the assay, and to alter the reporter and quencher dyes designed to improve future multiplexing possibilities based on the instrumentation capabilities. Multiplexing the test with the detection of a reference gene such as β-Actin as an internal positive control would improve the quality assurance of the assay by assessing the quality of the template and the success of the RNA extraction.

The use of a plasmid as a method of quantification is widely reported; however, the accuracy of quantification may be affected by the structure type (whether the plasmid deoxyribonucleic acid (DNA) is circular [supercoiled] or linearised). A study by Hou *et al.* (2010) found that there was a 2.65-4.38 overestimation in Ct values when using circular plasmid compared to using the linearised plasmid form. For this reason, absolute quantitation was performed using a linearised plasmid containing a clone of APPV to generate a standard curve for every run to account for inter-assay variations in amplification efficiency. However, to improve upon this and to consider not only the efficiency of amplification of template in the quantitative PCR stage of the assay but also the efficiency reverse transcription stage, an RNA standard should be synthesised. Efforts were made to generate RNA from the target in the plasmid: difficulties in separating the RNA from the plasmid were encountered, and further work would be needed to achieve this.

Meaningful and reliable data validation is of the utmost importance in understanding the limitations of the assay and to enable the correct classification of samples based on carefully considered cut-offs. Validation of the tests to ensure robustness was performed with consideration to the minimum information for publication of quantitative real-time experiments (MIQE) guidelines (Bustin *et al.*, 2009; Bustin, 2010). As a result of limited certified reference materials and no isolate of APPV available, validation of the analytical specificity and sensitivity of the assay was constrained. It is generally recommended to use the test to evaluate 20 closely related non-target samples in duplicate to ascertain specificity (Broeders *et al.*, 2014), However,

only five strains of pestiviruses were available for testing as well as seven other common porcine pathogens and the validation was performed on these.

The limit of detection was established for the initial RT-qPCR assay using a standard curve generated from a linearised plasmid containing the APPV target sequence. The test was found to be capable of the repeated detection of APPV (at a 95% probability) at a concentration of 3,190 copies. As determined by Poisson distribution, the lowest detection limit for a PCR is three copies, thus prompting further optimisation to improve analytical sensitivity (Bustin *et al.*, 2009; Kralik and Ricchi, 2017). As suggested by Bustin and Huggett (2017), assays may perform differently with different master mixes. Therefore, re-optimisation of the APPV RT-qPCR was performed using the qScript XLT One-Step RT-qPCR ToughMix, Low ROX kit (Quantabio). The limit of detection of the re-optimised assay was found to be 319 copies, and this threshold was used to define the classification of samples. Samples above this threshold were considered positive, whereas those that fell below could not automatically be classified as negative, as the probability of repeated detection was lower than 95%, therefore they were classified as equivocal. Only in samples where no RNA copy number was detected were samples classified as negative in accordance with the suggestion made by Kralik and Ricchi (2017). As no isolate of APPV was available for spiking experiments to determine the sensitivity of the assay to detect APPV in different matrices, clinical positives samples were used to evaluate the ability of the assay to detect APPV in those matrices. As more reference material or isolated strains become available, additional validation of the method should be performed.

As a measurement of reproducibility, the inter-assay variation was analysed using efficiency and linearity (R^2) as assessment criteria; assays were acceptable if the efficiency was within the optimal range 90 to 110% and the test had an R^2 value of 0.98 or higher, thus conforming to the recommendation of the MIQE guidelines and guidelines for validation of real-time PCR methods (Bustin *et al.*, 2009; Broeders *et al.*, 2014; Kralik and Ricchi, 2017).

One of the most common techniques for the detection and quantification of antibody/antigen levels is the ELISA. ELISAs were employed in this project to quantify antibody responses in a number of serological samples. Originally, a previously published (Schwarz *et al.*, 2017) NS3H blocking ELISA was kindly provided by Dr Benjamin Lamp at the University of Gießen. However, as a result of inconsistencies in assay performance, probably because of primary monoclonal mouse antibody instability during long-term storage, the NS3H antigen was employed to further develop an NS3 based indirect ELISA.

Both the sensitivity and specificity of an ELISA are affected by the quality of the interaction between the detection reagents and the analyte of interest; for this reason, the optimal concentration of the antigen was assessed and the recommended concentration of the commercial enzyme conjugated antibody used (Steinitz, 2000). This interaction may contribute to higher levels of background noise for the assay; other factors which may also alter the sensitivity but may increase background are sample volumes, buffer formulations and the temperature and length of incubation periods that were not however explored during the optimisation of this assay. A blocking step can be used to reduce non-specific binding and contribute to assay stability while producing minimal cross reactivity or enzymatic activity (Steinitz, 2000). To determine the optimal blocking reagent due to a lack of commercial porcine serum, pestivirus free FCS tested at 5% and 10%, and 1% fish gelatin were assessed for their effectiveness at blocking. Ideally, with more time and reagent availability, other reagents derived from species that are not susceptible to pestiviruses such as equine, poultry and other aquatic species should also have been tested. The comparison found that FCS was a more effective block agent, and these findings are consistent with a study by Mosadeghi and Heydari-Zarnagh (2018) which also found that 5% FCS is the optimal blocking agent defined by the highest ratio of positive to negative compared with 2.4% skimmed milk, 1% BSA and 1% gelatin. Another study by Martinez *et al.* (1993), testing six different blocking reagents in 0.5% Tween 20

including gelatin, bovine serum albumin, lactalbumin, non-fat dry cow milk, horse serum and FCS, found that full-fat dry cow's milk and FCS as the most efficient blocking agents defined by their ability to give a high positive to negative ratio with minimal background (<0.08) and an average absorbance of less than 0.2 for the negative control. In the current optimisation of the assay and the Martinez *et al.* (1993) study, the buffer used to dilute the protein contained Tween 20, which has been shown to be an appropriate blocking agent on its own and its inclusion in the buffer may have a synergistic effect on the proteins blocking ability of the ELISA reducing background further (Qu, Berghman and Vandesande, 1998; Steinitz, 2000).

Validation of the ELISA was hampered due to the unavailability of positive samples containing a known concentration of antibody needed for spiking experiments to determine definitive dilutional linearity of the assay. This is approached through the calculation of percentage recovery (or parallelism) between samples and a known concentration that can indicate differences in the immunoreactivity between the analytes possibly due to matrix effects. The lack of sample availability for validation in order to determine sensitivity and specificity is a commonly reported issue with APPV ELISA assay development (Hause *et al.*, 2015; Postel *et al.*, 2016; Cagatay *et al.*, 2019; Grahofer, Zeeh and Nathues, 2020). Reproducibility was determined using a Shewhart chart to assess inter-assay variability following controls and the coefficient of variability determined both within assay and between assays using a two-fold difference of the same sample to establish the upper and lower warning limit of variability (Reed, Lynn and Meade, 2002).

As only a limited number of APPV-specific immunological tests (such as IHC) have been currently established (Liu *et al.*, 2019), and variation is reported in both the observed pathology and severity after infection, additional work to develop assays that can identify APPV *in situ* to further characterise the pathological effects of the virus are needed. For example, the antibodies evaluated for APPV cross-reactivity (in this work) were expected to be non-

specific as they were raised against BDV and shown to be cross-reactive to BVDV (Dutia, Entrican and Nettleton, 1990), only VPM 25 and 26, showed some indication of APPV cross reactivity, which was however not deemed sufficient to continue with their use. Should they have given better results, they could have been used in combination with other techniques (clinical history of CT A-II presence, demyelination observed using luxol fast blue (LBF) staining of CNS tissue and positive RT-qPCR) as a useful confirmation assay and to better define virus tropism.

As the potential for the VPM antibodies to be used for APPV IHC was limited, an alternative technique, BaseScope ISH, was evaluated for the detection of APPV in tissue. Unlike IHC, which is not inherently quantitative, BaseScope is an RNA *in situ* hybridisation technique that can be used to identify and quantify APPV RNA within formalin-fixed tissue sections. This technique offers improved sensitivity and specificity due to the proprietary ZZ pair probe design which amplifies the target signal while suppressing background non-specific binding (Wang *et al.*, 2019). BaseScope, is chromogenic rather than immunofluorescent, employing an alkaline phosphatase horseradish peroxidase enzymatic reaction that allows visualisation by bright field microscopy (Wang *et al.*, 2019). The results from the APPV BaseScope ISH optimisation shows the capability of the assay to detect APPV *in situ* in different tissue types from both experimentally-infected and naturally-infected animals with different APPV strains circulating in Great Britain. As there is a compromise between optimising the assay for quality of RNA and the accessibility of the RNA in different tissues, a positive and negative control should always be included for each tissue type from each experiment. This will allow more accurate interpretation of the assay results while acknowledging the variability in tissue fixation due to different tissue types, formalin penetration and/or length of fixation. This work represents the first instance of the BaseScope ISH application designed to target the NS3 region of APPV to allow detection and quantification of the virus. Subsequent to the development of the assay described in this chapter, a sister technique, RNAScope has been

reported to successfully detect APPV in tissues of piglets experimentally infected *in utero* (Buckley *et al.*, 2021). In that study, the probe was designed to specifically detect the N^{pro} and E^{rns} of the inoculation strain. Due to the genetic variability of APPV strains, further investigation of the ability of the probe to detect other strains of APPV is needed. RNAScope has also been used to detect other pestiviruses such as in a previous study performed to identify the presence of a novel Phocoena (porpoise) pestivirus (PhoPeV) and investigate tissue tropism (Jo *et al.*, 2019). In both cases, the respective viruses were detected in brain, lung, spleen, and lymph nodes showing commonality amongst tissue types affected. Due to the nature of the chemistry of the assay, BaseScope ISH can be easily combined with other histological techniques such as counter staining with haematoxylin (as shown in this APPV study) or with additional IHC, increasing the flexibility of the assay. To further explore this potential the APPV BaseScope ISH specific assay could be used in conjunction with other histological stains labelling specific cells (e.g. leukocytes) to investigate cell tropism, with stains to visualize myelin in nerve tissue (such as LBF) and evaluate the level of damage or combined with oligodendrocytes-specific IHC to determine APPV presence and abundance in relation to pathological changes associated with CT A-II. Currently, this is the first deployment of this novel technique to identify and quantify APPV RNA within formalin-fixed tissue sections, however the successful development, optimisation and validation of the techniques discussed in this chapter can now be utilised to characterise the virus and host—pathogen interactions in further studies.

Virus isolation was attempted to enable completion of validation of diagnostic assays and further studies of the virus *in vivo*. However, all attempts to propagate the virus on porcine-derived and pestivirus-permissive cell lines (PK-15, SPEV 0008 and BT) were unsuccessful, using either serum from naturally-infected animals from field cases or serum and tissues from colostrum-deprived animals (devoid of maternal antibodies). These results confirm and further highlight the problematic nature of isolating and

propagating the virus as described by other authors (Hause *et al.*, 2015; Arruda *et al.*, 2016; De Groof *et al.*, 2016; Postel *et al.*, 2016; Yuan *et al.*, 2017).

To date, successful APPV isolation reports are limited (Beer *et al.*, 2017; Postel *et al.*, 2017b; Schwarz *et al.*, 2017; Cagatay *et al.*, 2019). Schwarz *et al.* (2017) published the detection of APPV antigen by immunofluorescence after five serial passages on PK-15 and SK6 cells (used for the isolation of CSFV) indicating propagation of the virus. However, viral infectivity in this case was found to be limited and inefficient (10^1—10^2 ffu/ml, fluorescent focus units), which further substantiates the validity of the PK-15 isolation outcome in this chapter. The remaining virus isolation attempts were performed using SPEV 008 cells according to the accredited protocol of the EU and OIE Reference Laboratory for classical swine fever (European Commision, 2002). Both Beer *et al.* (2017) and Postel *et al.* (2017b) experienced limited success with 1/10 (four tonsil and six sera) (Beer *et al.*, 2017), and 1/14 (seven cerebrospinal fluid and seven serum samples) (Postel *et al.*, 2017b) attempted and each requiring multiple passages. Subsequent to the current virus isolation attempts presented in this Chapter, Cagatay *et al.* (2019) isolation attempts also took several passages to produce low viral titres and the propagation of the APPV isolate Ger-NRW_L277 required more than 100 passes (APPV p100) and yielded only a titre of $8x10^4$ $TCID_{50}$/ml. This APPV p100 'cell-adapted' strain was sequenced in a later study of cell permissibility, three substitutions were found in the E^{rns} (H330Q) and E2 (N751K and D752N) regions of the polyprotein, which appeared after passage 45, and correlated to an increase in infected SPEV 0008 cell numbers (Cagatay *et al.*, 2021). Although SPEV 0008 cells were found to be the most efficient at propagating the virus, other common cell lines including SK6, PK15 and ST cells had limited viral replication and non-porcine cells (MDBK and Vero 76) showed no permissibility at all (Cagatay *et al.*, 2021).

Due to time constraints and limited availability of clinical samples, virus isolation attempts on SPEV 0008 cells using a protocol based on the EU and

OIE recommendations were carried out only for five passages for both clinical field samples and those from colostrum-deprived snatch-farrowed piglets. The unsuccessful propagation of APPV (using these samples and those) from colostrum-deprived snatch-farrowed piglets suggest that the presence of antibodies may not be a limiting factor in isolation of the virus. Future propagation of the virus using SPEV 0008 cells should be conducted with a range of sample types over a higher passage number. Further work is also needed to determine the permissiveness of other primary and immortalised porcine cell lines to the virus as more is understood about tissue tropism and specific target sites for replication become known.

To obviate the lack of *in vitro* grown virus, an *in vivo* expansion trial was conducted. Samples from this trial were also used for other aspects of this work, maximising use of the animals involved. In this study, a postnatal APPV infection, three one-week-old snatch-farrowed colostrum-deprived piglets were successfully inoculated inducing viraemia without clinical signs of CT A-II. The results of the study supply further evidence that the presence of clinical signs is due to pathological changes to the fetus as a result of viral infection *in utero* (Arruda *et al.*, 2016; De Groof *et al.*, 2016). This was similar to findings from a study of postnatal CSFV infection, which found piglets postnatally infected with the pestivirus exhibit no clinical signs of disease despite persistently high viral titres (Muñoz-González *et al.*, 2015).

The APPV viral titre in serum throughout the study followed a similar profile to that reported by De Groof *et al.* (2016) for a postnatal infection of six-week-old colostrum deprived piglets. However, the rate of increase in viral load for the current postnatal infection was marked, increasing on average by $7.16x10^{8}$ copies/ml by day three and a further $1.47x10^{10}$ copies/ml by day 10. This is therefore a more successful experimental infection than the one reported previously reported (De Groof *et al.*, 2016) in which the viral copy number/ml was found to be less than the detectable limit of the virus ($1x10^{3}$ copies/ml) on day three (lower than the inoculum; $3.9x10^{5}$—$8.6x10^{5}$ copies/ml) and up to a

maximum of $2.8x10^5$ copies/ml at day 10. Direct comparisons for subsequent time points could not be made as piglets in this study were culled on day 10 when the (average) peak of viraemia was detected. From data presented in the six-week-old postnatal infection study, the mean viral load continued to rise until day 14 ($2.7x10^6$ copies/ml) indicating a possible later peak.

Over the course of the study, APPV was detected in oropharyngeal nasal and rectal swabs suggesting potential routes of shedding and transmission of the virus. This finding was consistent with other studies of both experimentally-and naturally-infected piglets, able to detect APPV in nasal, saliva and faecal samples (Arruda *et al.*, 2016; De Groof *et al.*, 2016; Muñoz-González *et al.*, 2017; Schwarz *et al.*, 2017) with some studies describing prolonged periods of shedding from 12 weeks up to 8.5 months (De Groof *et al.*, 2016; Schwarz *et al.*, 2017). Due to the short nature of the postnatal infection study performed (10 days), persistent viral shedding could not be explored. However, the concept of persistent infection is investigated further in Chapter 4. The absence of APPV detection in nasal or rectal swabs in the piglets at specific time points may be due to the sampling methods reliability as the small size of the piglet (at one week old) may affect the ability to collect accurate swab samples.

Of the 20 tissue types analysed by RT-qPCR, all were positive, further adding evidence that the virus can infect and replicate systemically as postulated by Gatto, Sonálio and de Oliveira (2019). Consistently high viral loads were detected in lymphoid tissues, with the highest viral loads found in the pre-scapular lymph node, spleen and tonsil, this is similar to findings reported by other groups who found high titres in the tonsil (De Groof *et al.*, 2016; Postel *et al.*, 2016; Muñoz-González *et al.*, 2017) and spleen (Arruda *et al.*, 2016; Muñoz-González *et al.*, 2017). Other studies also observed high titres in other lymph nodes including the inguinal lymph node (Arruda *et al.*, 2016; De Groof *et al.*, 2016; Liu *et al.*, 2019) and submaxillary lymph node (Postel *et al.*, 2016; Yuan *et al.*, 2017; Liu *et al.*, 2019), both of which were also found to contain

high viral loads within the current study. Conversely, (Arruda *et al.*, 2016; Muñoz-González *et al.*, 2017) found high APPV titres in the mesenteric lymph node and thymus respectively, however, these tissue types had the lowest viral loads of the tissues investigated in the study described here, with almost a 1,000-fold reduction compared to the tissues with the highest viral load. Similarly, Gatto *et al.* (2018b) found high levels of APPV within the cerebellum and cervical spinal cord, an observation which was not replicated within the current study. Cervical, thoracic and lumbar spinal cord tested were all determined have a low viral load and only two of the three APPV positive animals had APPV detected within the brain (frontal cortex). However, samples from other areas such as the cerebellum (where APPV has been found in high abundance) may have yielded different results (Liu *et al.*, 2019). The difference in viral load between these studies may be due to sample type choice or sample pooling for testing (Gatto *et al.*, 2018b) pooled cerebellum and cervical spinal cord for testing, whereas (Liu *et al.*, 2019) found high viral titres in the cerebellum when tested separately suggesting this may be a confounding factor for the results presented in the Gatto *et al.* (2018b) study.

On an individual piglet level, detection of the virus in the thymus (two positive and one with no virus detected) and lumbar spinal cord (two positive and one equivocal) samples were inconsistent. This inconsistency may have been due to the collection of a small sample combined with reduced viral load and the limit of detection of the assay (as the study was performed before re-optimisation of the RT-qPCR test). As the inoculated group sizes were small (n=3), further research is needed to determine the tissue tropism of APPV and the overall value of specific tissue types as standard samples for diagnostic purposes (Chapter 4).

Chapter 4: A Scottish case study of atypical porcine pestivirus

4.1 Introduction

Most atypical porcine pestivirus (APPV) outbreaks occur in neonatal piglets born to young breeding females and present as upsurges of congenital tremors A-II (CT A-II) within several litters in the same herd. Occasionally, significant outbreaks can occur in naïve sows or gilt herds, affecting a high proportion of litters, with typically between 10 and 100% of the litter affected (Arruda *et al.*, 2016; De Groof *et al.*, 2016; Gatto *et al.*, 2018b). While no clinical signs are observed in the dam, clinical signs of the neonate are characterised by rhythmic tremors of the head, body and hind limbs, which usually resolve before weaning (De Groof *et al.*, 2016). In severe cases, tremors can cause ataxia, disrupting the ability of the piglets to stand and suckle, leading to starvation and death (Arruda *et al.*, 2016). Clinical signs may be exacerbated during periods of stress, such as exposure to cold temperature or handling, and reduced while the animal is at rest (Arruda *et al.*, 2016; De Groof *et al.*, 2016; Schwarz *et al.*, 2017). In less severe cases, tremors mostly resolve by the time piglets are weaned at 4 weeks of age; however, there have been reports of mild tremors that have persisted up to 14 weeks of age (Schwarz *et al.*, 2017).

Classically, transplacental transmission of established pestiviruses including bovine viral diarrhoea virus (BVDV), classical swine fever virus (CSFV) and border disease virus (BDV) has been found to cause different clinical outcomes and viral persistence depending on the timing of infection *in utero* (Sawyer, 1992; Peterhans, Jungi and Schweizer, 2003; Oğuzoğlu, 2012; Khodakaram-Tafti and Farjanikish, 2017; Ganges *et al.*, 2020; Barman *et al.*, 2021). Pestivirus infections in early gestation usually result in early embryonic death and commonly mummifications, stillbirths and abortions, although these

are not exclusive to this gestational stage (Sawyer, 1992; Grooms, 2004; Barman *et al.*, 2021).

Mid gestational pestivirus infections often result as either healthy animals that are persistently infected, if infection occurs before the establishment of immunocompetence (60—80 days *in utero* in sheep, 125—150 days in cattle and 70—80 days in pigs), or malformations due to a teratogenic effect of the viral infection during organogenesis (Brock, 2003; Grooms, 2004; Oğuzoğlu, 2012; Arruda *et al.*, 2016; Finlaison and Kirkland, 2020). Animals infected in late gestation can mount an immune response, clear the infection and only present with transient infection.

Like other pestiviruses, APPV infection can occur during pregnancy. APPV is transmitted vertically to the fetus *in utero*, leading to offspring affected by CT A-II. However, for APPV little is known about the relationship of infection, clinical outcome and possible induction of persistent infection through immune tolerance. A study by Schwarz *et al.* (2017), which monitored two congenital tremor (CT) piglets naturally infected with APPV over six months, detected the virus in both animals in saliva and in serum and raw (non-extended) semen collected from the boar at six months of age. However, no virus was detected from the sow serum at this time.

Another natural APPV infection resulting in congenital tremor (CT) piglets was described by Cagatay *et al.* (2019): 15 piglets (clinical and non-clinically affected littermates) from four CT A-II affected gilt litters (four of which were immediately cross fostered by a pluriparous sow post-partum) and five healthy piglets from a non-affected pluriparous sow litter were monitored by reverse transcriptase polymerase chain reaction (RT-PCR) for APPV viraemia and by enzyme-linked immunosorbent assay (ELISA) for APPV-specific antibodies at 6, 21 and 48 days of age (Cagatay *et al.*, 2019). Twelve of these animals (seven from affected litters and five from non-affected litters) were further monitored until slaughter (day 103, 127, and 161). The study found that six out

of seven piglets from CT affected litters were viraemic on day six, suggesting vertical transmission within the farrowing group. By day 21, all piglets from affected litters were positive, whereas no virus was detected in the piglets from the unaffected litter. By day 48, just after weaning and entering mixed housing, all five unaffected pigs had detectable levels of virus suggesting horizontal transmission of the virus (Cagatay *et al.*, 2019). Of the 12 animals with extended monitoring, four out of seven affected piglets remained APPV ribonucleic acid (RNA) positive in serum until slaughter. However, no virus was detected in any of the five unaffected piglets that had tested positive on day 48, indicating transient infection after horizontal transmission. Throughout the study, the level of APPV specific antibodies detected from the CT affected litters was variable. In contrast, the initially unaffected litter, where piglets were seemingly horizontally infected, all had detectable antibody titres starting from day 69 until study termination on day 161.

Buckley *et al.* (2021) were able to identify the presence and persistence of APPV within tissues in two pigs 11-month-old that had been experimentally infected with APPV *in utero* and had CT A-II at birth that later resolved. However, no information was provided on viraemia, viral shedding or antibody levels. Further clarification is needed to determine infection dynamics in naturally occurring APPV associated CT outbreaks at a farm level to facilitate a better understanding of infection outcomes both in terms of clinical status and viral persistence.

Cases of APPV induced CT A-II in commercial pig units have been investigated in several countries, including in North America, USA (Sutton *et al*. 2019) and Canada (Dessureault *et al.*, 2018), Brazil (Possatti *et al.*, 2018a; Gatto *et al.*, 2018b; Mósena *et al.*, 2018), China (Yuan *et al.*, 2017; Zhang *et al.*, 2017; Liu *et al.*, 2019) and in Europe including Germany (Cagatay *et al.*, 2019), Spain (Muñoz-González *et al.*, 2017) and Switzerland (Grahofer, Zeeh and Nathues, 2020). Although CT A-II has been identified to be present in Great Britain, and as part of a serum sample survey APPV was identified in

2/86 British serum samples by NS3 quantitative RT-PCR (RT-qPCR) (Postel *et al.*, 2017a), no investigations of CT cases have been reported as yet.

Most of the previously reported field studies have focused on identifying APPV in CT field cases by RT-qPCR in serum and tissue samples, and sequencing the virus to determine strain variation with limited investigations of associated pathology within the tissues (Yuan *et al.*, 2017; Dessureault *et al.*, 2018; Possatti *et al.*, 2018a; 2018b; Mósena *et al.*, 2018; Liu *et al.*, 2019; Kasahara-Kamiie *et al.*, 2021). In the first report of APPV associated CT A-II in Canada, two CT piglets were assessed for presence of APPV RNA in the thoracic spinal cord, brain, lung, heart, liver, kidney, spleen, intestines, tonsils and thymus (Dessureault *et al.*, 2018). Samples were collected for histological examination and stained with Haematoxylin phloxine saffron, with additional luxol fast blue (LBF) staining conducted on the spinal cord. Dessureault *et al.* (2018) found no macroscopic lesions in affected animals; however, they observed vacuolation of the lateral and ventral funiculi in the white matter of the spinal cord and hypomyelination was also apparent in the white matter of the spinal cord from affected animals. Tissues from both of the CT piglets tested positive for APPV by RT-PCR.

A study of three CT piglets in Brazil also detected the presence of APPV in the brain (cerebrum, cerebellum, and brainstem), tonsil, intestine and faecal samples in all animals by RT-PCR (Possatti *et al.*, 2018a). Additionally, tissues collected for histopathological examination (heart, intestine, lung, kidney, liver, mesenteric lymph node, spleen, tonsil, bladder, brain and spinal cord) were stained with haematoxylin and eosin (H&E) and brain and spinal cord also stained with LBF-cresyl violet to demonstrate the presence of myelination. The study found evidence of myelin vacuolisation of the white matter in the cerebellum, brainstem and spinal cord. In addition, there was evidence of marked demyelination of the grey and white matter of the brainstem and spinal cord. This study also found neuronal necrosis, neuronophagia and gliosis in the cerebral cortices and spinal cord sections (Possatti *et al.*, 2018a). In both

cases, although only a small number of animals were sampled, findings were reasonably consistent with other experimental studies (Postel *et al.*, 2016; Schwarz *et al.*, 2017).

Recently, an experimental infection of piglets *in utero* was conducted to model natural infection in order to investigate viral distribution within tissues of piglets born with CT A-II at six days old (Buckley *et al.*, 2021). Pregnant sows were inoculated using APPV positive serum at two different gestational time points (day 45 and 62), both intravenously and intranasally as well as in the fetal amniotic vesicles to ensure fetal infection. Distribution patterns of APPV in tissues of neonatal piglets were then compared to those collected from two 11-month-old boars born with APPV-associated CT that had resolved. For both age groups, the distribution of viral RNA in the tissues was consistent. Although younger animals displayed a greater viral load, the most marked presentation of APPV was found in the cerebrum and cerebellum of the brain. However, other tissues tested (lymph nodes, liver, kidney, heart, lung, tonsil thymus and colon) were also positive for viral RNA (Buckley *et al.*, 2021). This finding supports the systemic distribution of the virus in tissues reported in previous studies by RT-PCR (Gatto *et al.*, 2018b; Mósena *et al.*, 2018; Shen *et al.*, 2018; Liu *et al.*, 2019; Xie *et al.*, 2019; Guo *et al.*, 2020). Further investigation is nevertheless needed to understand cellular as well as tissue tropism of APPV in both clinical and non-clinical naturally infected piglets. To facilitate this, in this work, a BaseScope *in situ* hybridisation technique (ISH) was developed and optimised as described in 3.3.4). This chapter describes the incursion of natural APPV-associated CT A-II within the context of a small Scottish pig farm, characterising viral infection and immune status within the herd, and how these relate to clinical signs and live-weight gain in growing pigs.

4.2 Hypothesis, aims and objectives

This study aimed to identify the presence of APPV RNA and APPV-specific antibodies within a Scottish pig herd naturally infected with APPV to clarify the relationship of APPV with CT A-II. To investigate this, observational studies of two farrowing groups infected within an interval of three months were performed.

The exploratory study of the first farrowing group included clinical and non-clinical animals which were sampled twice, initially at two weeks and again at eight weeks of age to determine the relationship between clinical signs and viraemia at these time points. The hypothesis was that clinical signs would correlate with presence of APPV RNA in serum and tissues at both time points. Serum levels of anti-APPV antibodies were quantified to determine whether a piglet had acquired APPV-specific antibodies via maternal antibody transfer and to provide evidence of active seroconversion in response to APPV infection.

The second observational longitudinal study followed piglets from 2.5 weeks of age until slaughter to determine if presence of APPV RNA or clinical signs such as CT A-II affected growth as a production parameter, indicated by an increased time to slaughter. The study also aimed to identify factors (sex of the piglet, parity of the sow) possibly associated with clinical status and APPV positivity. APPV viral load and antibody levels were monitored throughout the study in serum samples collected at 2.5, 10, and post 20 weeks of age and in tissue samples collected at the time of slaughter, to validate observations from the exploratory study and determine infection dynamics, including the potential for viral persistence. Finally, the suitability of ear tissue sampling as a diagnostic sample for APPV RNA detection was determined by comparing viral load in paired ear notch and serum samples. The hypothesis was that viral load in ear tissue and serum are positively correlated, and both are associated with clinical signs.

4.3 Study design

A third-generation farrow-to-finish farm located in central Scotland, with a suspected CT A-II outbreak, was investigated for confirmation of APPV infection. As all pig sampling was carried out as part of a diagnostic workup in the field by the farm's veterinary practice, this study was not subject to ethical approval. Consent was given by the farmer for pictures to be taken and the sample analysis to be used as part of this research. Results from the APPV RT-qPCR were reported both to the farmer and their veterinary practice. The 300-sow unit had no previous history of CT prior to January 2019 and was considered a closed high health status unit. The breeding stock consisted of mixed breed sows (Large White x Duroc) with replacements bred on-farm. Gilts and sows were artificially inseminated with commercially available Duroc semen. The field case presented with observable tremors consistent with CT A-II in multiple piglets with affected litters present in each farrowing group. The disease presented in both consecutive and non-consecutive farrowing groups over six months. The housing conditions shown in Figure 4-1 (piglets from birth to four weeks) and Figure 4-2 (piglets eight week and older). Pre-weaning (at four weeks) the farrowing group which consisted of 12 individually sows and their litters were kept in the same room but separately crated with their litter until the piglets. Each crate had an individual feed trough and drinker plumbed into a communal water delivery system. Floors are part concrete with slatted areas on the back half of the pen to allow for waste removal. At four weeks old animals from the same farrowing group were combined and kept in larger pens to allow for appropriate stocking density for the animal size. Each room contained nipple drinkers and a feed hopper system.

Figure 4-1: Housing conditions of farrowing groups from birth to four weeks of age.

Figure 4-2: Housing conditions of farrowing groups post eight weeks.

The investigation started in March 2019 at which time CT had been observed in sporadic farrowing groups since late January 2019. Initially, a newly born farrowing group with visible CT (as shown in Figure 4-3) was studied. Two clinical and two non-clinical piglets from six litters were ear tagged using numbered coloured button tags to indicate their clinical status (white clinical and orange non-clinical) at two weeks of age (n=24). One clinical and one non-clinical tagged piglet from the selected litters was euthanised at two weeks of age with barbiturates by a veterinarian (n=12). At two weeks, environmental sampling was also performed by collecting used bedding (straw given to sow for enrichment) and swabs taken from pens, walkways and troughs (processed as described in 2.1.3). Due to logistical and ethical constraints of transporting very young live animals with neurological signs for long journeys, the piglets were euthanised on the farm. A blood sample was collected by cardiac puncture upon confirmation of death, and the carcasses were transported back to the post mortem (PM) suite at Moredun Research Institute (MRI) to perform the necropsy. Samples of the brain, cervical spinal cord, thoracic spinal cord, lumbar spinal cord, Peyer's patches, superficial inguinal lymph node, tonsil, thymus and spleen tissues were taken as previously described in 3.5 to determine APPV infection.

A serum sample was collected from each of the dams from the six litters at eight weeks post farrowing. Two piglets, one clinical and one non-clinical died after the initial bleed at two weeks on farm, and the remaining piglets (n=10) were transported to MRI when older than eight weeks. They were euthanased by barbiturate injection, then a serum sample was collected, and a PM was performed as detailed for the first set of piglets. The serum was tested for presence of APPV RNA using the previously established APPV RT-qPCR (2.2.3). Changes in antibody level in serum over the repeated sampling time points were evaluated using the APPV indirect ELISA with samples diluted at 1:200 (2.4.2). The non-fixed tissues collected at the PM were analysed for viral loads using the APPV RT-qPCR with polymerase chain reaction (PCR) products from four samples sent for confirmatory sequencing (as described in

2.2.6). The formalin-fixed tissues were trimmed, blocked, cut and mounted onto slides as described in 2.5.1 by the Histopathology Surveillance Unit at the, following standard operating procedures used for diagnostic submissions. Fixed paraffin-embedded brain and spinal cord sections were processed, mounted and stained with haematoxylin Z and eosin (H&E, Cellpath Ltd) following standard protocols. Histological examination of the brain and spinal cord of two clinical and two non-clinical eight-week-old piglets were then performed. No histology was performed on the two-week-old piglets as the nervous tissue was found to be autolytic due to the long (time) interval between pig euthanasia on farm and the PM at MRI. A blinded evaluation for morphological changes and APPV presence within the tissue was conducted in conjunction with Dr Jo Moore, the resident pathologist at MRI. Paired slides were also assessed for the presence of APPV RNA using BaseScope *in situ* hybridisation as described in 2.5.2. The results from group 1 were used to inform the study design for a second affected farrowing group which followed piglets from farrowing to slaughter.

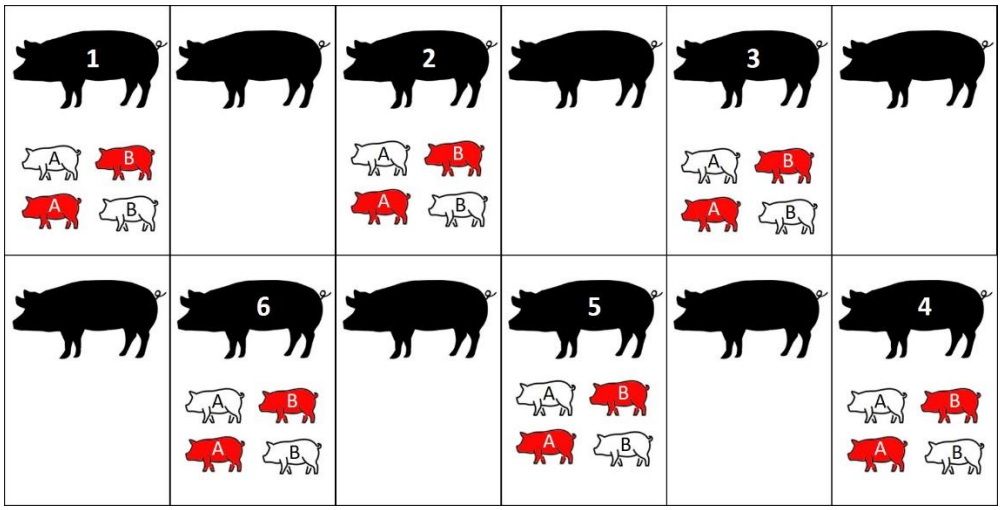

Figure 4-3: Experimental design for farrowing group 1. In each of six litters the two most clinically affected (red) piglets and two not clinically affected (white) piglets were selected for blood sampling and post mortem performed at two weeks (A) or eight weeks (B).

For the second farrowing group, 138 piglets from 12 litters were tagged based on the presence or absence of tremors at 2.5 weeks of age. A serum sample was collected from each piglet by the farm veterinarian alongside a paired ear notch. The ear notches were taken using a ¼ inch round ear punch, which was disinfected with 1% Virkon and 70% ethanol between animals and stored individually in Eppendorf tubes at -20°C until processed. Both samples were tested by RT-qPCR (2.2.3) to determine the presence and quantity of APPV RNA and to establish the utility of ear notch samples as a potential diagnostic sample. Following collection, the ear notch was processed as detailed in 2.1.2. Further serum samples were collected from the piglets at 10 weeks of age and at slaughter at approximately 22—28 weeks of age to monitor the infection using the RT-qPCR and APPV indirect ELISA as described in 2.4.2. At slaughter, spleen and retropharyngeal lymph node were also taken from all piglets with the testicles and epididymis collected from the male piglets. All samples were placed on ice packs and transported back to MRI. The serum samples were processed as described in 2.1.4. Semen was collected directly from the epididymis (2.1.6), and a testicle sample was collected. The tissue samples were prepared per 2.1.1 and all samples were extracted as outlined in 2.2.1.2 for APPV detection and quantification using the RT-qPCR described in 2.2.3. with polymerase chain reaction (PCR) products from three semen samples sent for confirmatory sequencing (as described in 2.2.6).

4.4 Statistical analysis

For statistical analysis in this chapter, due to the small group sample sizes, the classification of APPV RT-qPCR outcomes (as determined in 3.3.1.7) was redefined to be either virus detected (combining equivocal and positive outcomes) or no virus detected. Non-parametric statistical analysis was performed by Fisher's exact test on categorical variables with small sample sizes (such as clinical status, sex, litter and viral outcomes). When comparing more than one categorical variable (clinical status, viral outcome in serum and

ear tissue), a Cochran-Mantel-Haenszel chi-square test was used. The result was confirmed with a post hoc Woolf test for homogeneity. The Mann Whitney U test was applied to determine the relationship between categorical and continuous variables (antibody levels, viral load in serum or viral loads in ear tissue). For multiple comparison tests such as viral load in different tissue types, a Kruskal Wallis H test was performed with post hoc pairwise comparisons tested using Dunn's test with Bonferroni correction to correct for multiple simultaneous pairwise comparisons. Spearman's rank correlation was performed to ascertain the association between continuous variables. Repeated measures analysis was conducted for the viral load and antibody levels in serum over the three collections in the longitudinal study. The analysis of the study was performed using R version 3.6.1 (R Core Team 2019), and the repeated measures analysis implemented using the rptR package (Nakagawa and Schielzeth, 2013; Nakagawa, Johnson and Schielzeth, 2017).

4.5 Results

4.5.1 Exploratory study: first farrowing group

The purpose of the investigation of the CT affected first farrowing group was to explore the relationship between clinical signs and viraemia, to assess APPV-specific antibody levels (indicating an immune response to infection) and to provide further evidence for tissue/cell tropism.

Observationally, at two weeks of age, clinical signs associated with APPV infection were noted to varying degrees both within and between litters, ranging from animals appearing clinically normal or displaying mild ear, head or flank twitches to severe whole-body tremors with comorbidity of splay leg observed in some cases, causing piglets to struggle to stand. Conversely, at eight weeks of age, clinical signs within the group had appeared to largely resolve, with only a few animals showing signs of tremor under stress such as during transport and blood sampling. Further observation of tremors after eight weeks to determine when tremors completely resolved was then performed in the second farrowing group longitudinal study (4.5.2). No virus was detected in any of the environmental samples collected as part of this study.

4.5.1.1 Characterisation of APPV infection in the sows

Eight weeks postpartum, APPV RNA was not detected in any of the six dams that farrowed litters in which a portion of the piglets were affected by CT. However, four of the six sows were positive for anti APPV immunoglobulin G (IgG) antibodies at eight weeks postpartum using the NS3H blocking ELISA (Figure 4-4), suggesting previous exposure within the farrowing group to the virus. The farm reported that none of the sows from this farrowing group or any other farrowing group had shown clinical signs consistent with CT at any point before or during the CT outbreak.

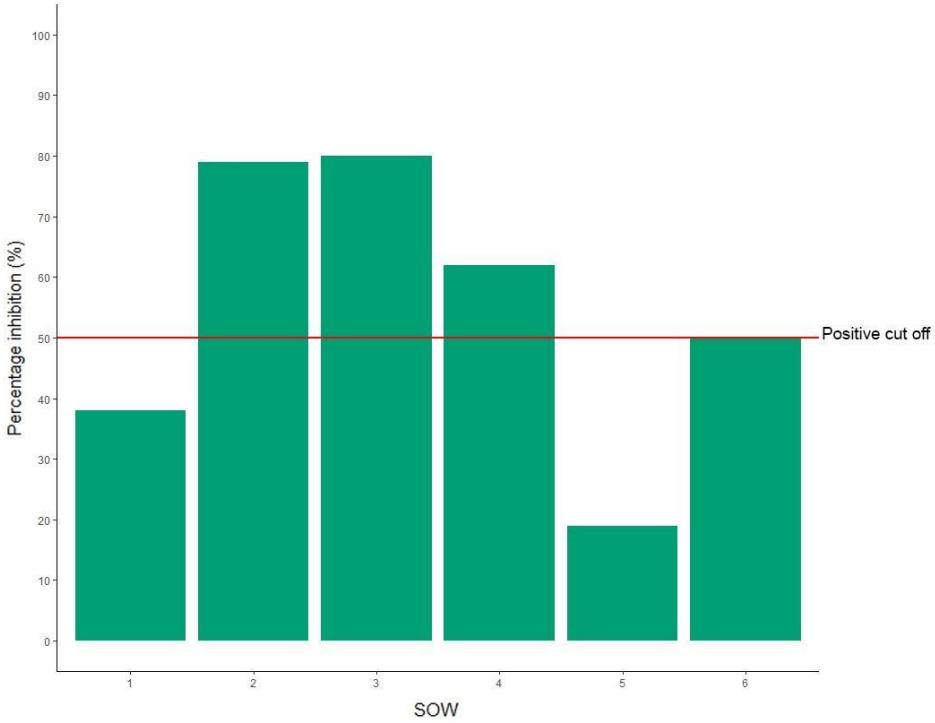

Figure 4-4: NS3H APPV blocking ELISA results for six sows corresponding to the six CT litters eight weeks postpartum. The red line indicates the positive cut-off for the assay: sows with an average percentage inhibition (technical replicates=2) greater than 50% were considered positive.

4.5.1.2 Viraemia in piglets

At 2 weeks of age, virus was detected in 9 of the11 clinical piglets and 6 of the 11 non-clinical piglets, with viral loads in positive piglets ranging from $6.63x10^3$ to $1.18x10^7$ copies/ml for clinical piglets and $1.55x10^4$ to $3.23x10^6$ copies/ml for non-clinical piglets. Viral load was not significantly different between clinical and non-clinical piglets (Figure 4-5) by Mann Whitney U test (W= 95.5, p-value= 0.18).

At eight weeks of age, all 10 remaining animals had low but still detectable levels of APPV RNA in serum regardless of their clinical status, with viral loads ranging from $5.81x10^3$ to $5.45x10^5$ copies/ml in clinical animals and $3.52x10^4$

to $2.12x10^5$ copies/ml in non-clinical animals (Figure 4-6). No significant difference between the amount of APPV in animals with and without clinical signs was found by the Mann Whitney U test (W= 15, p-value= 0.69) at this age. The relationship between APPV viral load in serum at both two and eight weeks of age was investigated as shown in Figure 4-7, with no association between the viral loads identified by Spearman's rank correlation in serum at the two time points (Rho= -0.04, p-value= 0.91).

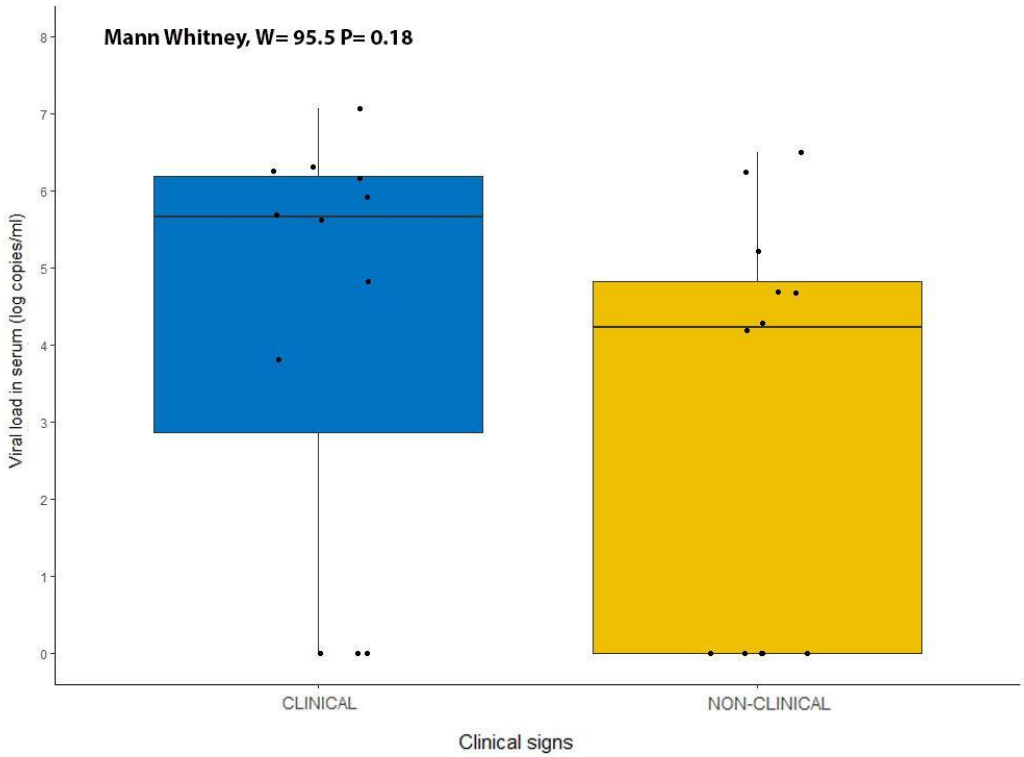

Figure 4-5: APPV viral load in serum of two-week-old pigs. The graph shows the average APPV viral load based on two technical replicates (log_{10} copies/ml) in clinical (n=12, blue) and non-clinical (n=12, yellow) piglets.

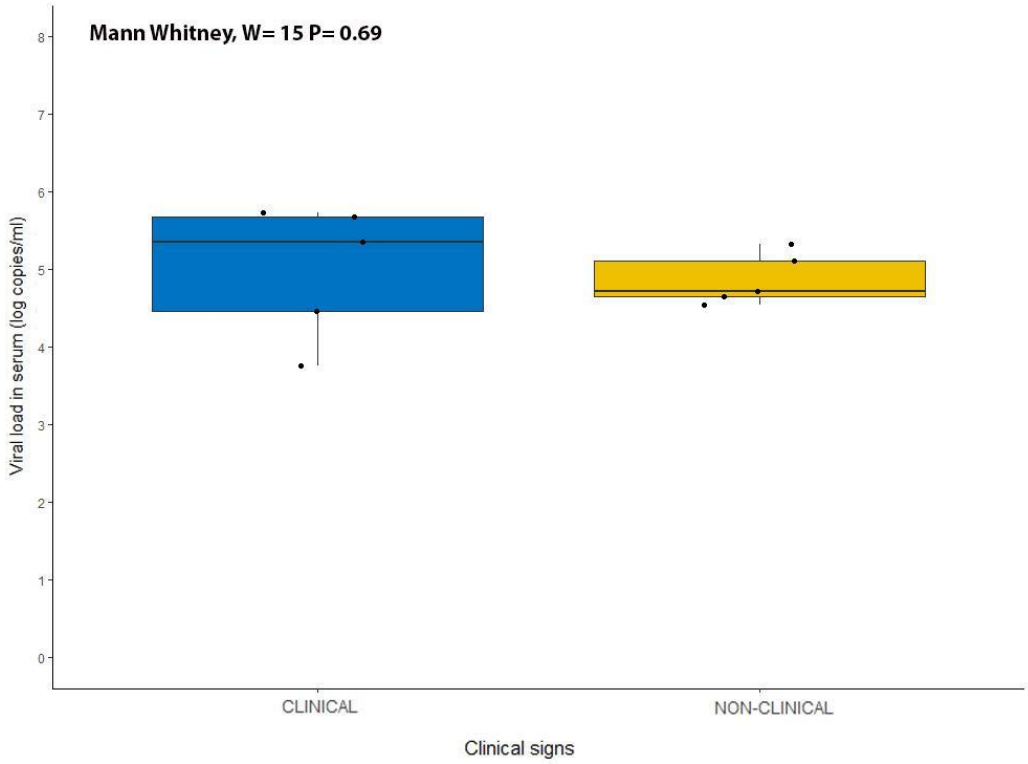

Figure 4-6: APPV viral load in serum of eight-week-old pigs. The graph shows the average APPV viral load based on two replicates (log_{10} copies/ml) in clinical (n=5, blue) and non-clinical (n=5, yellow) piglets.

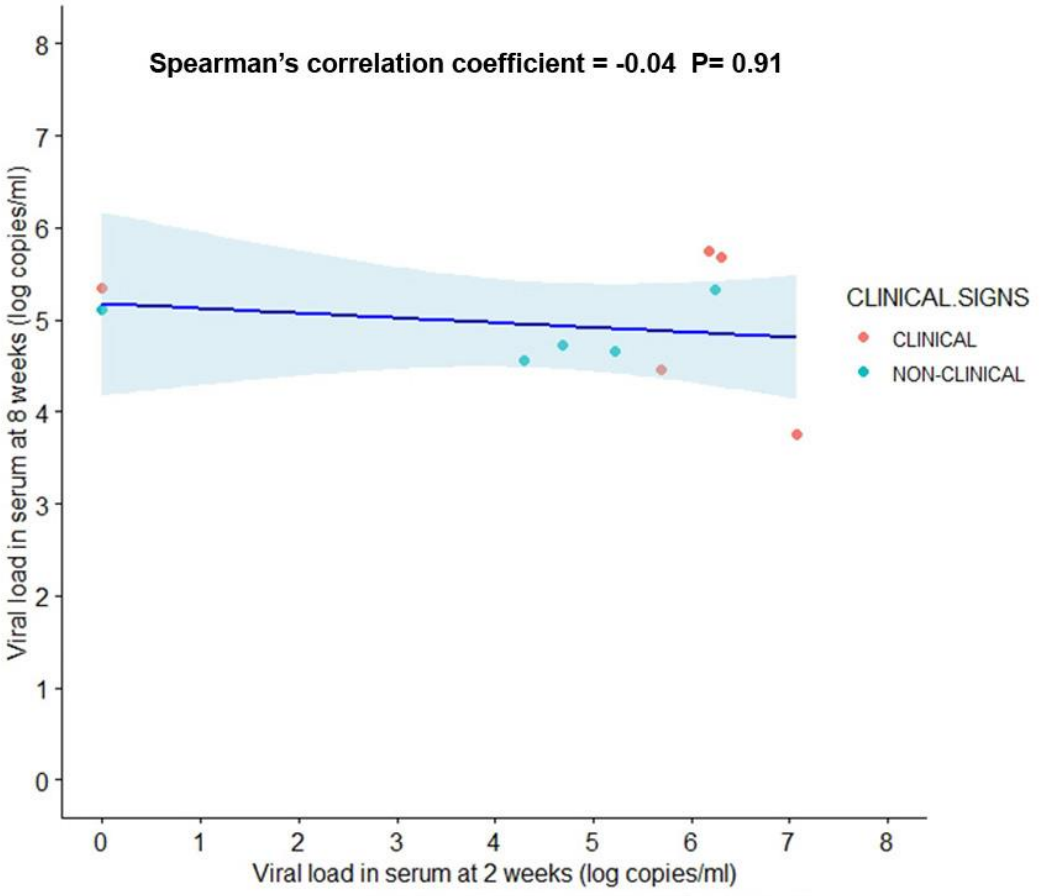

Figure 4-7: Relationship between APPV viral load in serum at two and eight weeks of age. The scatter graph shows the average viral loads (based on two technical replicates plotted as $\log_{10}$ copies/ml) for clinical (n=5, red) and non-clinical (n=5, blue) piglets. The blue line represents the line of best fit, and the shaded area in pale blue represents the 95% confidence interval.

4.5.1.3 Antibody response to APPV in piglets

The IgG antibody levels for clinical and non-clinical piglets were investigated at two and eight weeks of age using the indirect ELISA to determine the relationship between the antibody levels at each time point and how antibody levels associated with clinical signs (Figure 4-8). Only three animals had no detectable APPV-specific antibodies at two weeks of age (two clinical and one non-clinical; the clinical animals had a lower median antibody level (optical density [OD] of 0.43) than non-clinical animals (OD of 0.74). No significant relationship was found by the Mann Whitney U test between presence of

clinical signs and the antibody level at two weeks (W [sum of the ranks of the first sample] = 62.5, p-value= 0.60). All animals at eight weeks, regardless of clinical status, had OD values of < 0.01 with the exception of one clinical animal, which had an OD value of 0.26, indicating a reduction of APPV-specific antibodies between the two-week and the eight-week time-points (W= 81, p-value= 0.02). No significant relationship was found by the Mann Whitney U test between presence of clinical signs and the antibody level at eight weeks (W= 18, p-value= 0.23).

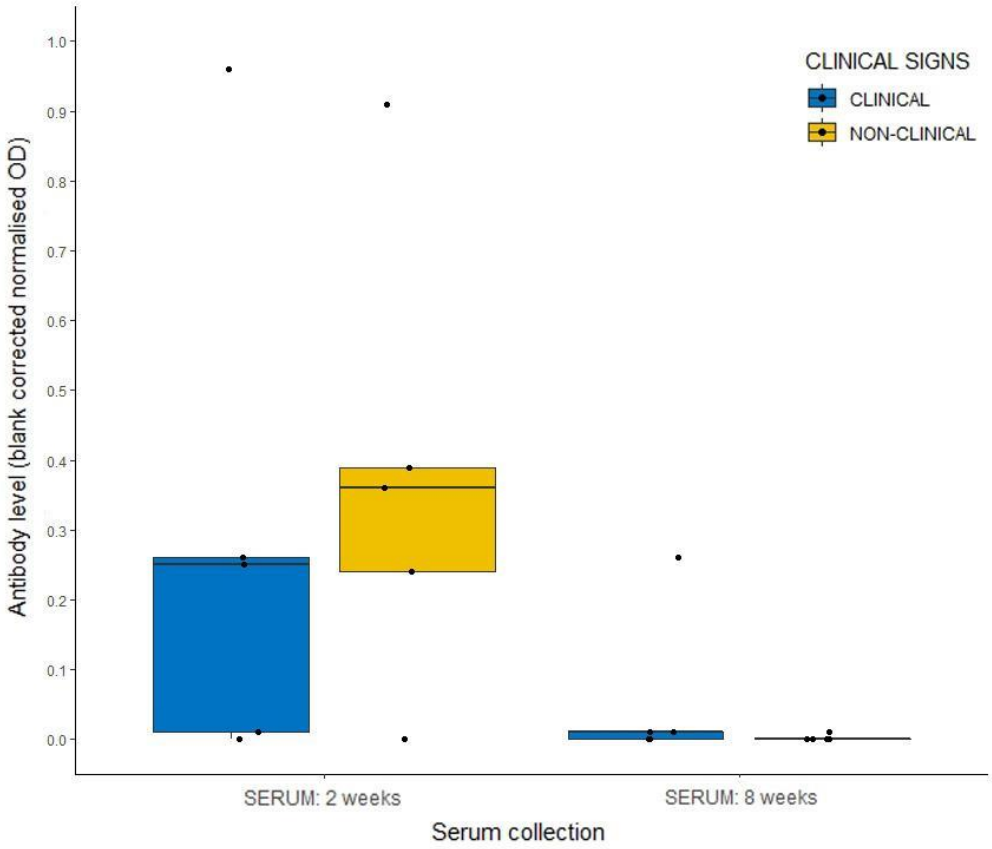

Figure 4-8: IgG antibody level (OD) in serum at two and eight weeks. The boxplot shows the average APPV antibody level (technical replicates =2) in clinical (n=5, blue) and non-clinical (n=5, yellow) piglets. The average of the blank wells (technical replicate=2) was subtracted from absorbance (OD) values to correct for background.

4.5.1.4 APPV viral load in tissues from piglets

APPV RNA was detected in all tissue types tested in both clinical and non-clinical animals, as shown in Figure 4-9. In one of the 11 animals with clinical signs, viral RNA was not detected in any of the tissues collected, while viral RNA was detected in all tissue types from four of the 11 non-clinical piglets. There was no significant difference in APPV viral loads of clinical and non-clinical animals for any of the tissue types tested as determined by Mann Whitney U tests presented in Table 4-1. The APPV viral loads between tissue types did vary significantly regardless of the clinical status, as identified by the Kruskal Wallis H test ($X^2(2) = 48.3$, p-value<0.0001, df= 8, eta2[H] (effect size) = 0.0.234). Pairwise comparisons using Dunn's test with Bonferroni correction showed that the APPV viral load in Peyer's patches was significantly lower than in lymph nodes (p-value= 0.016) and tonsil (p-value= 0.004). The APPV viral load in brain tissue was significantly different from that in the thymus (p-value<0.0001), lymph node (p-value<0.0001), and tonsil (p-value<0.0001). Sequence analysis results confirmed APPV presence in RT-qPCR positive tissue samples (alignment presented in Appendix A).

Table 4-1: Mann Whitney U test analysis for APPV viral loads between clinical and non-clinical animals in tissues.

Tissue Type	Wilcoxon value (W)*	Probability value (P)
Brain	55.5	0.750
Cervical spinal cord	35	0.76
Thoracic spinal cord	39	0.81
Lumbar spinal cord	29.5	0.83
Lymph node	74	0.40
Peyer's patches	69	0.60
Spleen	62	0.95
Thymus	84	0.13
Tonsil	58	0.90

* Wilcoxon value is the lowest sum of ranks in order to calculate the p-value where significance is assumed.

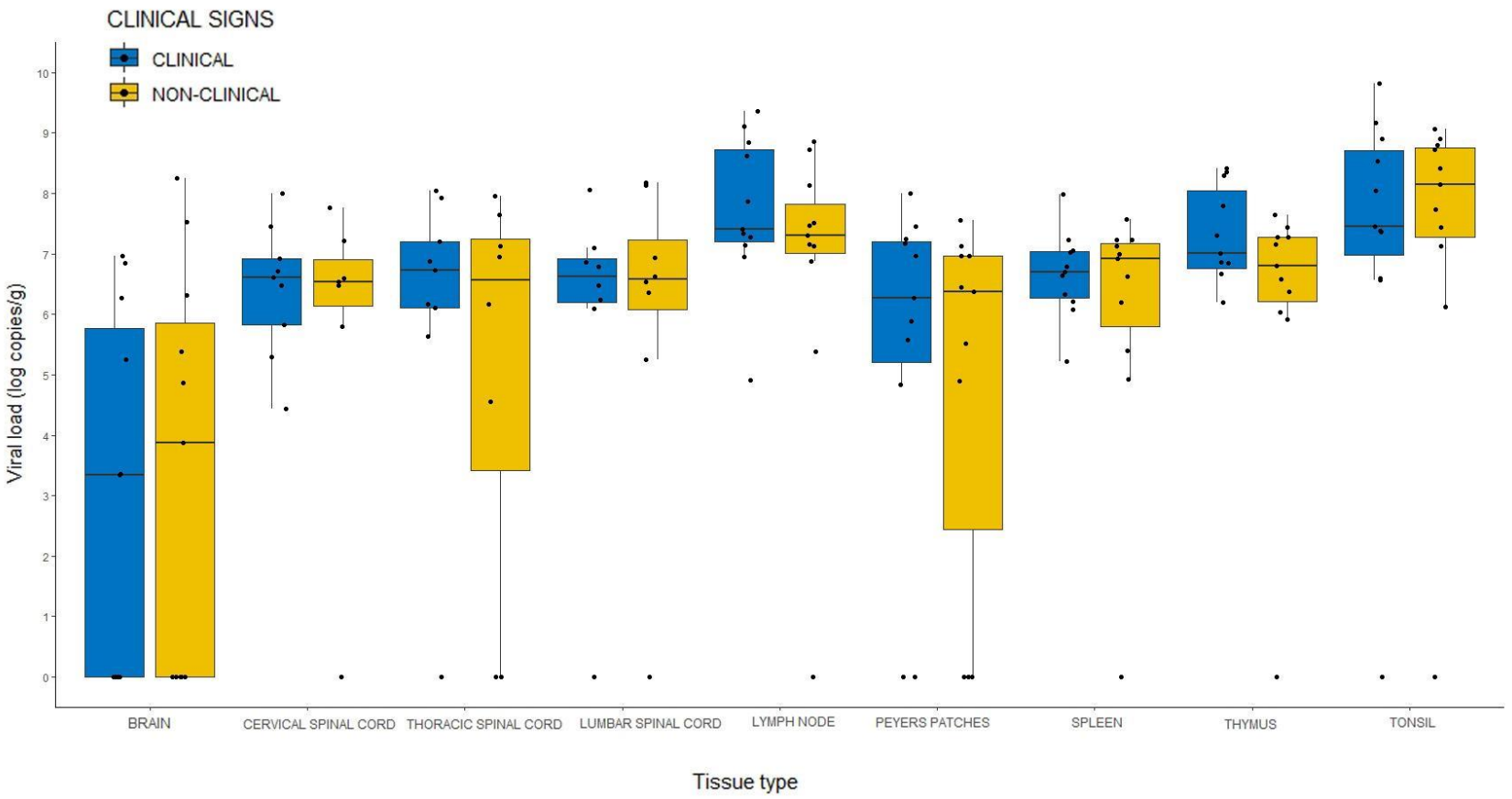

Figure 4-9: APPV viral load (log_{10} copies/g) in different tissue types from clinical and non-clinical piglets. Box plots show the average viral load in different tissues based on two technical (log_{10} copies/ml) for clinical (n=11, blue) and non-clinical (n=11, yellow) piglets.

4.5.1.5 Viral pathology

No gross pathological changes were observed in any of the organs collected from clinical and non-clinical piglets. Microscopically, H&E staining of the brain and spinal cord tissues collected from two clinical and two non-clinical piglets at eight weeks of age revealed no apparent changes in the tissue morphology. BaseScope ISH detected APPV RNA in the brain and spinal cord of all the animals tested. Notably, lower amounts of APPV RNA were detected in the brain of one of the clinical and of one of the non-clinical. Comparable amounts of APPV RNA were detected in the spinal cord of all four animals. In all cases, regardless of the amount of APPV RNA present, all piglets followed a similar pattern of APPV distribution and proportion of cells infected in the tissues when tested using BaseScope.

In the brain, APPV was detected in the frontal cortex, parietal cortex, thalamus, and occipital cortex, which were similar both in intensity and distribution. The virus was observed to be both non-cell-associated and associated with the endothelial cells in blood vessels in both the grey and white matter, but notably more present at the border between the two. A minority of glial cells (including microglia and oligodendrocytes) were also affected and, occasionally, APPV was found in neurons. In the hippocampus, APPV was primarily associated with the endothelial cells of blood vessels however, it was sometimes present in pyramidal neurons shown in Figure 4-10 (A) or non-cell-associated. APPV was also found in both the grey and white matter in the midbrain, with increased amounts of APPV at their border. Here the virus was equally distributed as non-cell-associated, in blood vessels, and cell-associated, primarily in glial cells and neurons with observable satellitosis shown in Figure 4-10 (B). The greatest concentration of APPV in the brain was detected in the cerebellum of all animals with a marked diffuse presentation in the granular and molecular layer and rarely in Purkinje cells of the grey matter as shown in Figure 4-10 (C), followed by a mild presentation in white matter, predominantly blood vessel associated. The presence of APPV in the medulla was similar to

what was observed in the neocortex, with a higher proportion of virus in the grey matter and most of it associated with blood vessels in endothelial cells or present as non-cell-associated.

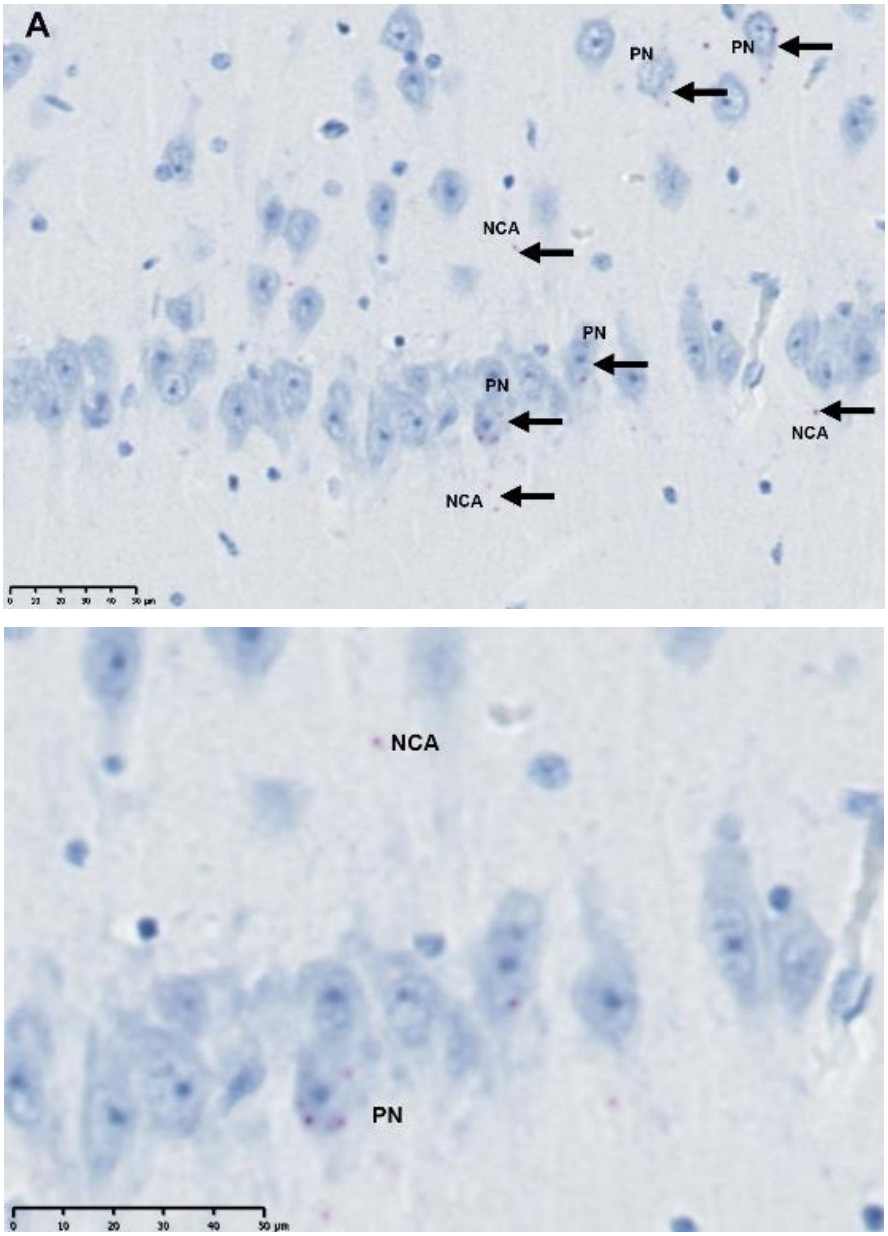

Figure 4-10: APPV detection in the brain of eight-week-old piglets by BaseScope. (A) APPV in the hippocampus of a non-clinical piglet with pyramidal neurons (denoted by PN) and non-cell-associated virus (labelled NCA) with higher magnification shown below. APPV signal is shown as red dots and indicated with a black arrow where appropriate.

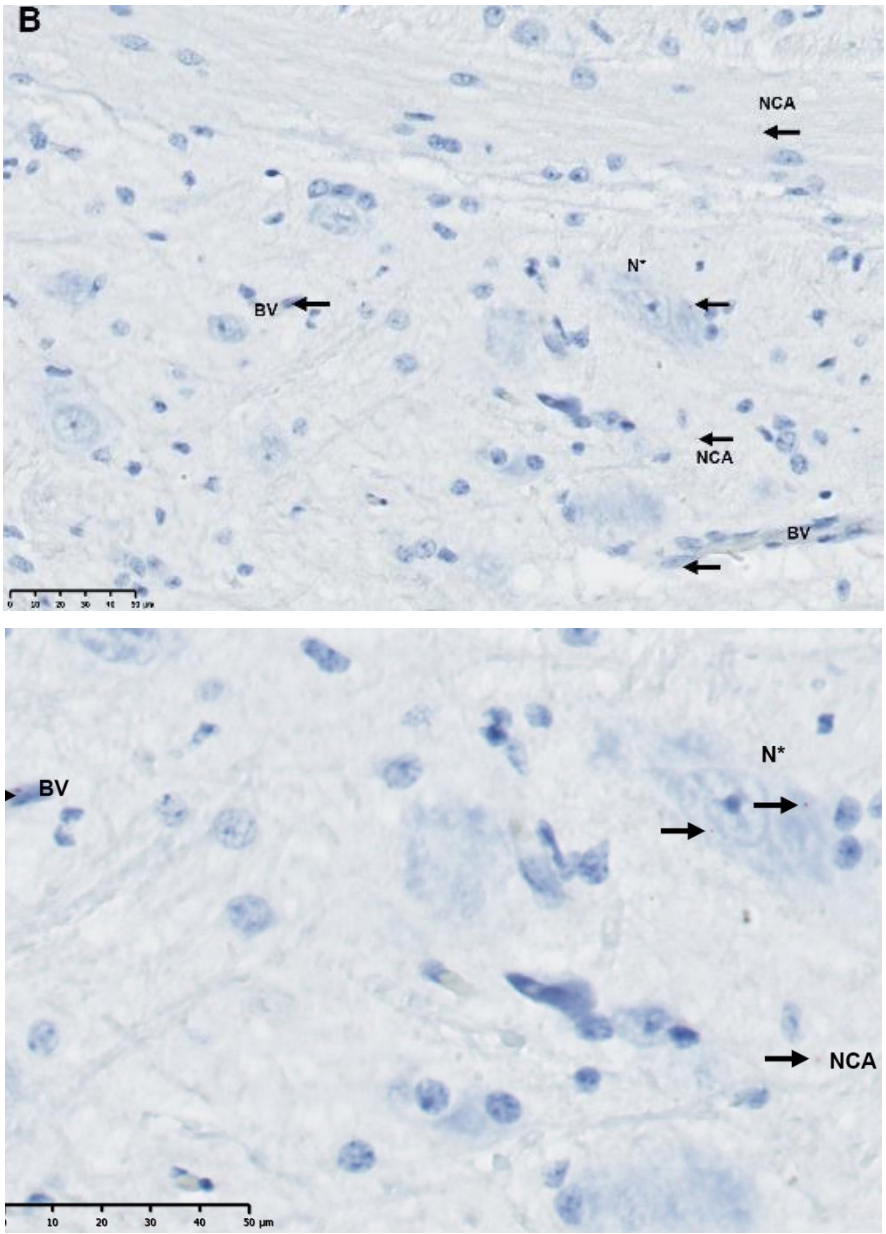

Continuation of Figure 4-10: APPV detection in the brain of eight-week-old piglets by BaseScope. (B) APPV in the midbrain of a clinical piglet with N* denoting a neuron displaying satellitosis, NCA denoting non-cell-associated virus and BV denoting blood vessels with higher magnification shown below. APPV signal is shown as red dots and indicated with a black arrow where appropriate.

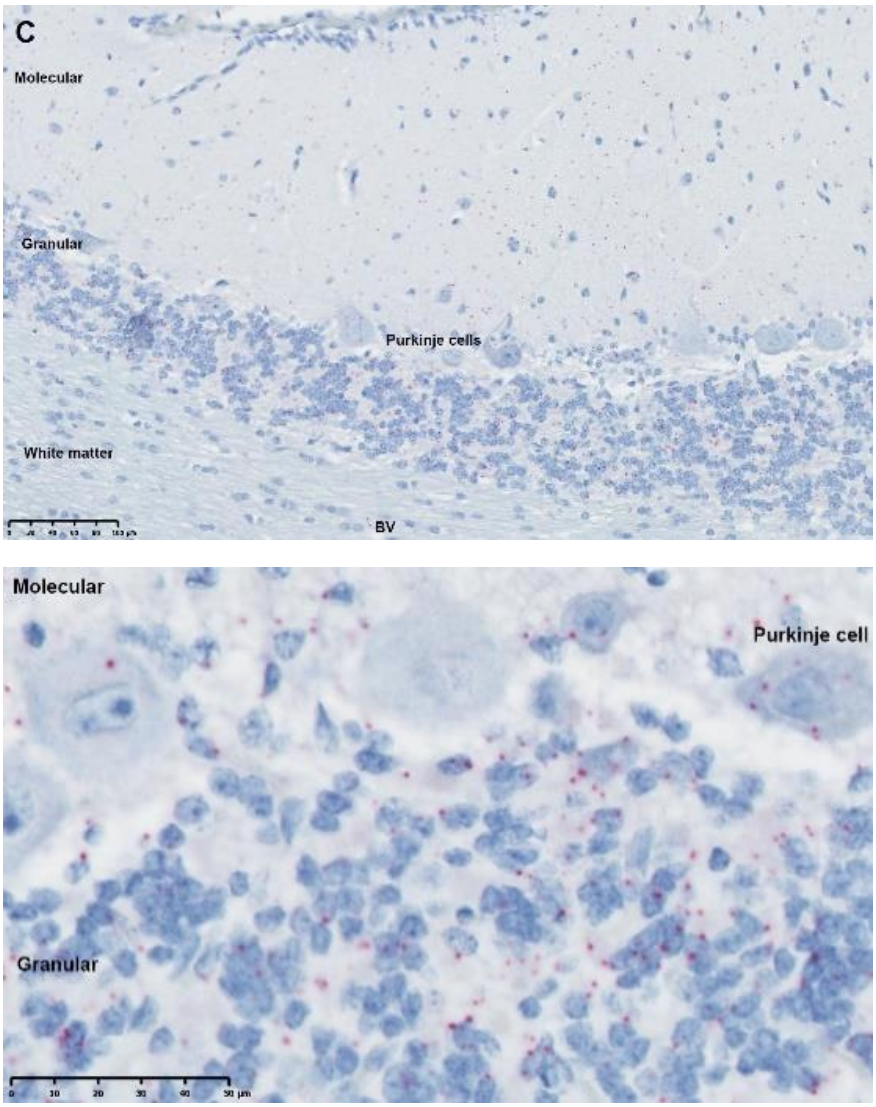

Continuation of Figure 4-10: (C) Cerebellum from a clinical piglet showing the diffuse presence of APPV in the molecular and granular layer of the grey matter with higher magnification shown below. APPV is also present in the Purkinje cells and with minimal occurrence in the white matter's blood vessels (BV). APPV signal is shown as red dots.

A similar distribution of APPV was found in the cervical, thoracic and lumbar spinal cord for clinical and non-clinical piglets. APPV was diffusely distributed in the grey matter, predominantly non-cell-associated or present in the endothelial cells of blood vessels; it could occasionally be found in glial cells and rarely in neurons with no particular group of neurons affected (Figure 4-11). In the white matter, the virus was associated mainly with the endothelial

cells of blood vessels. A moderate amount of virus was also observed in the meninges and spinal nerve root (Figure 4-12) of the spinal cord in myelin satellite cells and in swan cells.

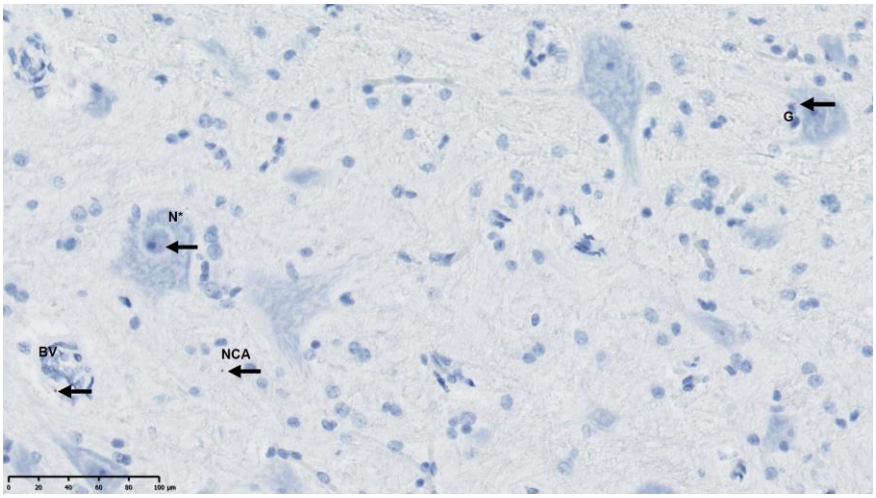

Figure 4-11: APPV distribution in the grey matter of cervical spinal cord for a clinical animal. BV denotes a blood vessel, NCA is non-cell-associated, G indicates a glial cell, and N* is a neuron with satellitosis. A positive APPV signal is shown as red dots and its presence indicated by black arrows.

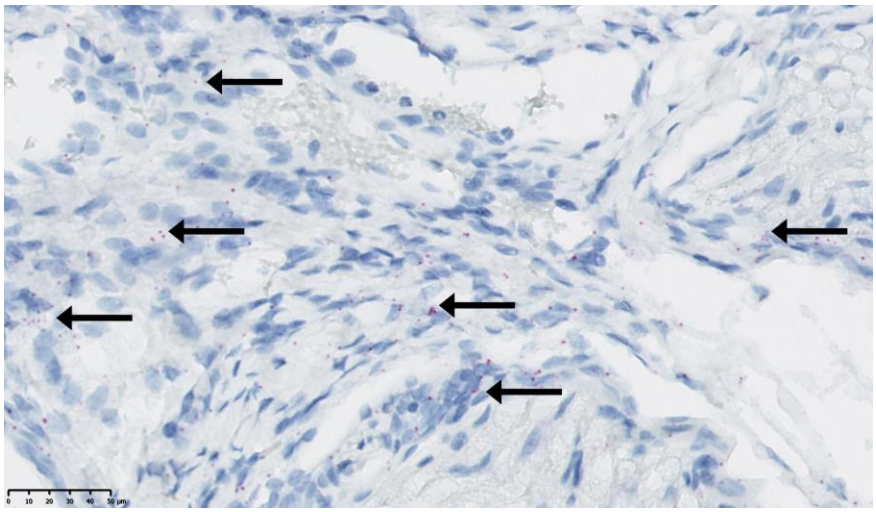

Figure 4-12: APPV distribution in the spinal root of the thoracic spinal cord from a non-clinical piglet at eight weeks old. APPV is shown as red dots and its presence indicated by black arrows.

4.5.2 Cohort study: second farrowing group

As part of the cohort study, ear tissue samples were evaluated for their potential as a standard diagnostic sample for APPV detection, to determine if virus levels in tissue had a better association with clinical signs than serum. The study also investigated the effects on the growth (production) of the piglets and additional factors associated with virus status and antibody response furthering understanding of the effects of APPV associated CT infection on the host and the viral persistence.

4.5.2.1 Ear tissue as a diagnostic sample

The association between APPV viral outcomes (virus detected/not detected) in ear tissue and serum samples was explored, accounting for clinical signs (Figure 4-13) in piglets at 2.5 weeks of age. The Cochran-Mantel-Haenszel chi-square test found a significant interaction between clinical status and the viral load outcomes in ear tissue and serum (OR= 2.67, $X^2(2) = 4.50$, df= 1, p-value= 0.03, 95% CI (1.17, 6.09)). Post hoc analysis of the homogeneity of the odds ratio by Woolf test found no significance ($X^2(2) = 0.41$, df= 1, p-value= 0.52), confirming the three-way interaction between clinical signs and viral result in serum or ear tissue. The median APPV viral load in serum at 2.5 weeks was $2.00x10^4$ copies/ml for clinical animals compared to the non-clinical group, which was $5.61x10^3$ copies/ml (Figure 4-14); although, no significant difference in viral load was found for clinical status by Mann Whitney U test (W= 1,654, p-value= 0.24). Moreover, the median viral load in ear tissue was higher in clinical piglets ($1.26x10^6$ copies/ml) compared to non-clinical piglets ($7.34x10^5$ copies/g) (Figure 4-15). This supports the significant association between clinical signs and viral load in ear tissue as shown by the Mann Whitney U test (W= 2,055.5, p-value= 0.0007). A weak positive correlation between viral load in ear tissue and serum at 2.5 weeks (shown in Figure 4-16) was identified by Spearman's rank correlation (Rho= 0.35, p-value= 0.0001).

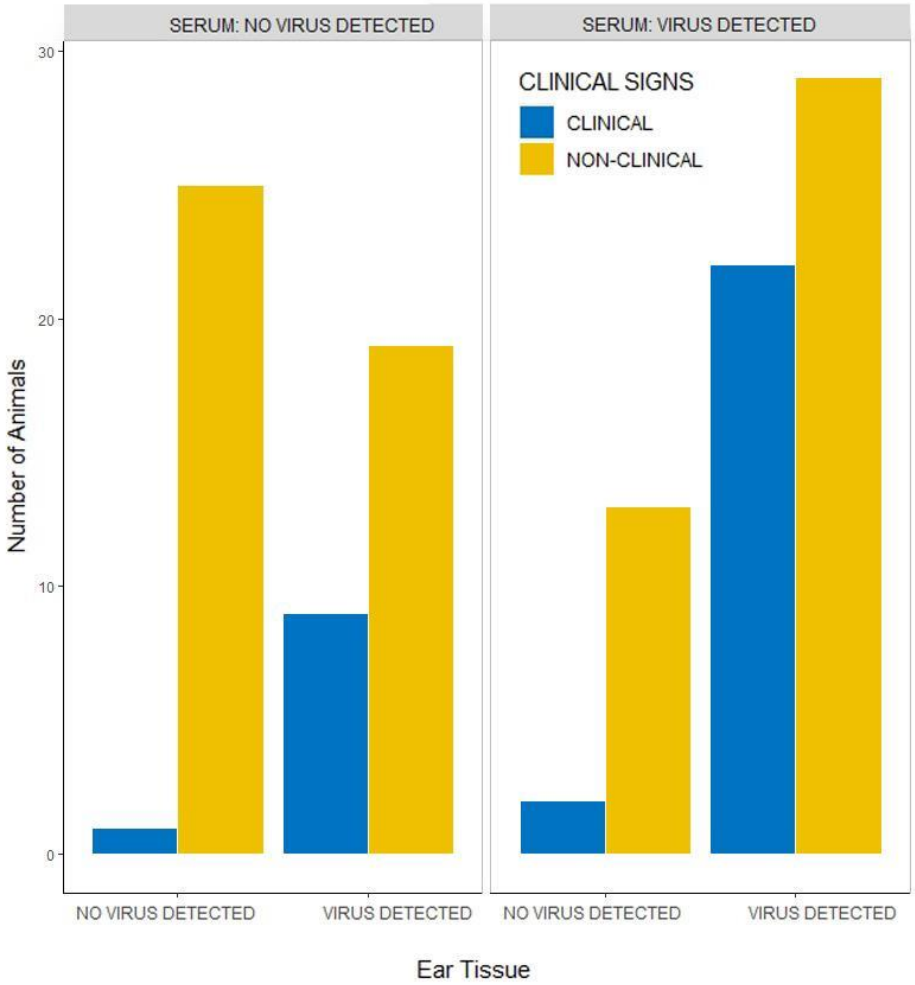

Figure 4-13: APPV viral outcomes in ear tissue and serum for clinical (n=34, blue) and non-clinical (n=86, yellow) piglets at 2.5 weeks of age.

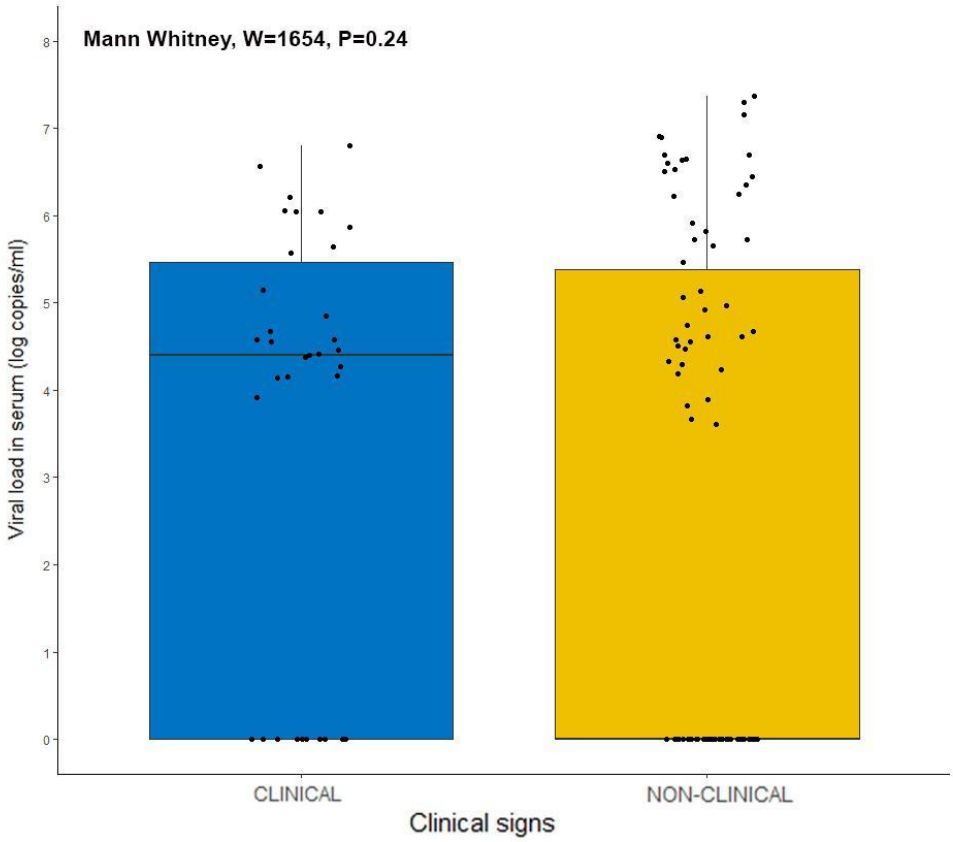

Figure 4-14: Average APPV viral load based on two technical replicates (log_{10} copies/ml) in serum at 2.5 weeks old for clinical (n=34, blue) and non-clinical (n=86, yellow) piglets from the 2nd farrowing group.

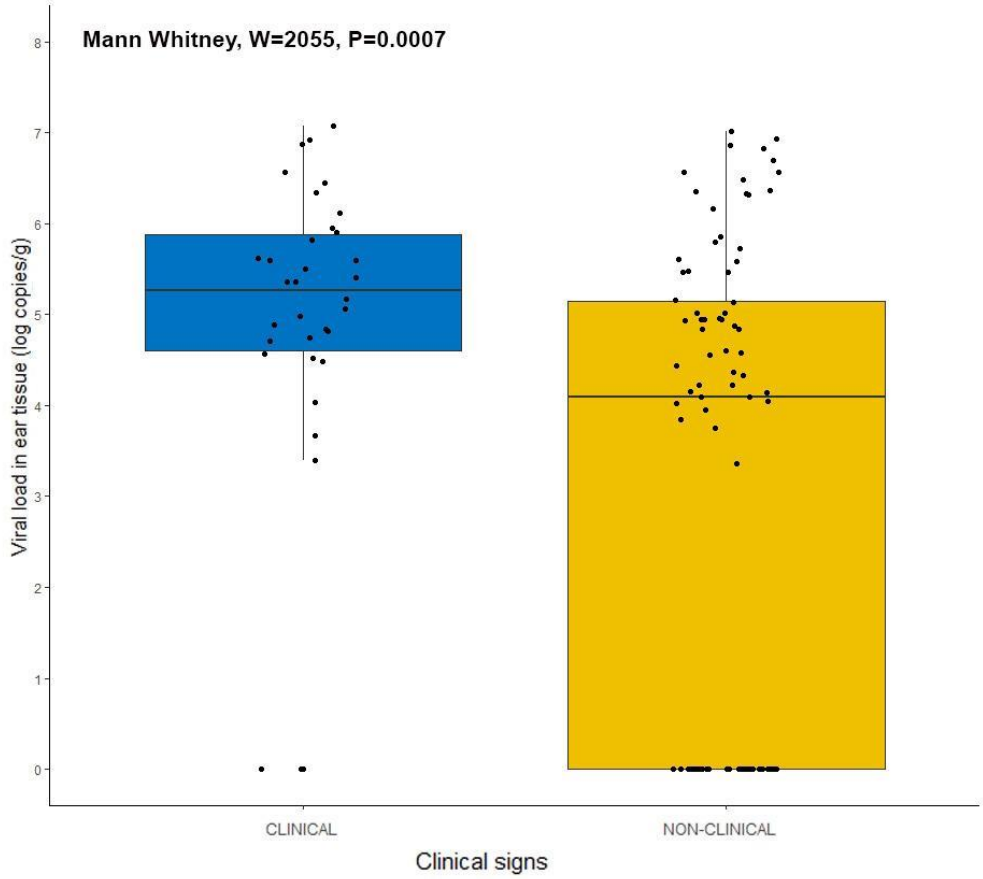

Figure 4-15: Average APPV viral load based on two technical replicates (log_{10} copies/ml) in ear tissue at 2.5 weeks old for clinical (n=34, blue) and non-clinical (n=86, yellow) piglets from the 2nd farrowing group.

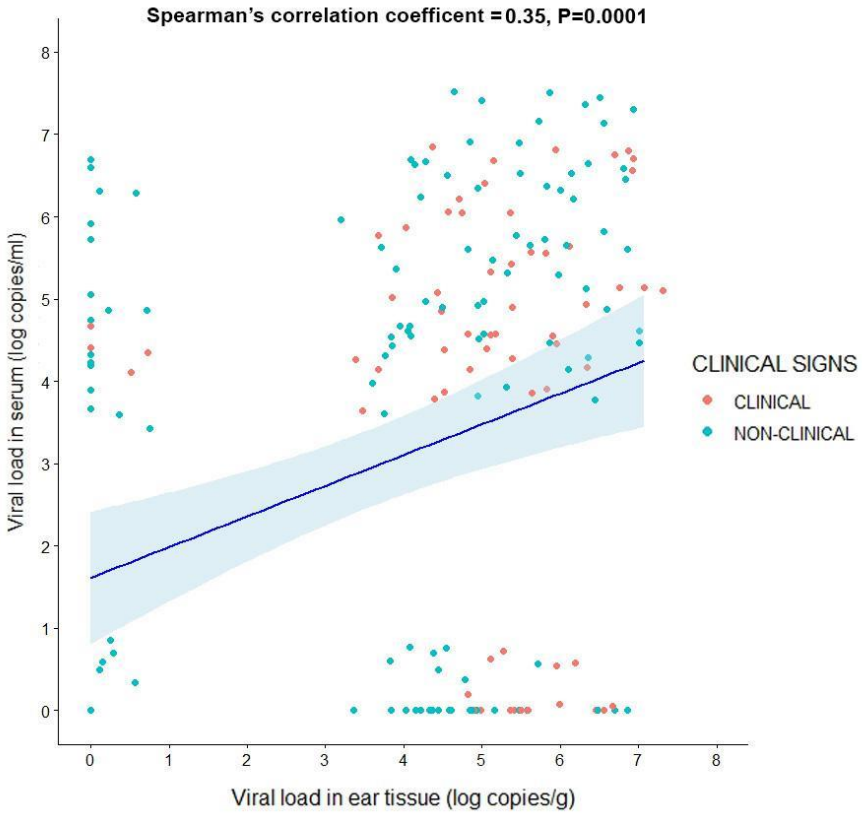

Figure 4-16: Relationship between APPV viral load in ear tissue (log_{10} copies/g) and viral load in serum (log_{10} copies/ml) at 2.5 weeks. The scatter graph shows the average viral loads (technical replicates=2) for clinical (n=34, red) and non-clinical piglets (n=86, blue). The blue line represents the line of best fit, and the shaded area in pale blue represents the 95% confidence interval.

4.5.2.2 Association between APPV status, clinical signs and production measurement (growth)

An investigation was carried out into whether growth as a production parameter, indicated by the length of time to finish, was impacted by the animal clinical status or by detecting APPV in ear tissue at 2.5 weeks or serum at any age. Similarly, to the first farrowing group, a range of clinical signs were observed within and between litters as discussed further in 4.5.2.3; moreover, the incidence of splay leg showed comorbidity with the most severely affected animals. Clinical signs were largely resolved within the farrowing group by 10

weeks: mild tremors were only observed after a period of stress (blood sampling), which were also observed in a minority of animals at slaughter. No significant differences were found in the length of time to finish between clinical and non-clinical piglets at 2.5 weeks old (Figure 4-17) by Mann Whitney U test (W= 589.5, p-value= 0.77). By Spearman's rank correlation no significant relationship was found between the detection of APPV in ear tissue at 2.5 weeks and time to finish, as shown in Figure 4-18 (Rho= 0.06, p-value= 0.62). There was also no significant association between APPV viral detection in serum at 2.5 weeks (Figure 4-19) (Rho= -0.07, p-value= 0.53), 10 weeks (Figure 4-20) (Rho= -0.09, p-value= 0.44) or at slaughter (Figure 4-21) (Rho= -0.09, p-value= 0.44) and time to finish as determined by Spearman's rank correlation.

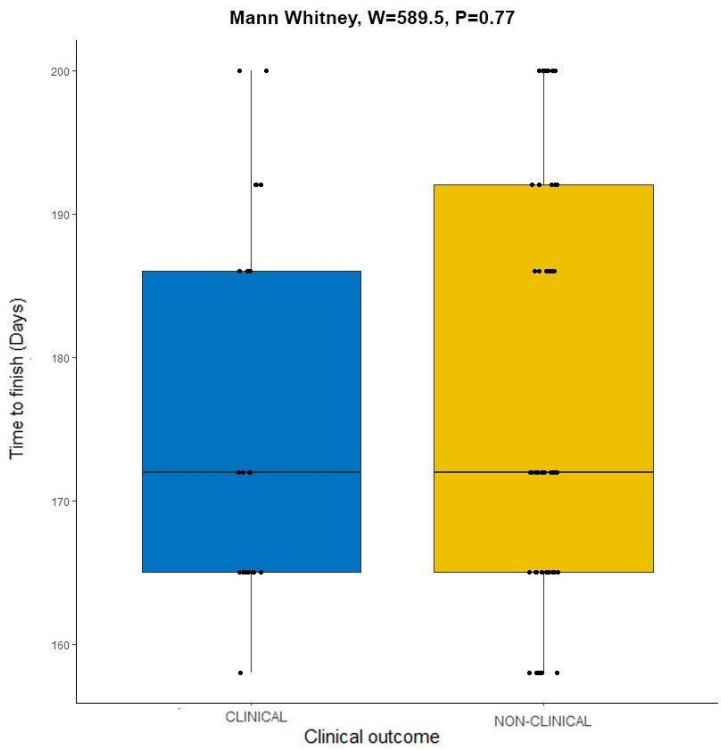

Figure 4-17: Time to finish as an indicator of production for clinical (n=22, blue) and non-clinical (n=56, yellow) piglets.

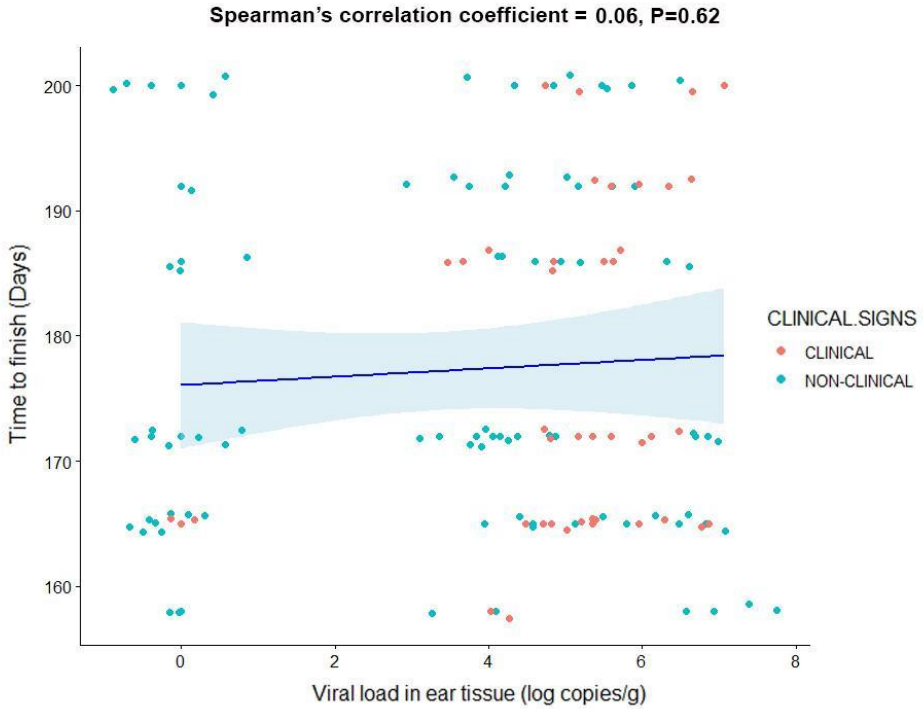

Figure 4-18: Relationship between time to finish (as an indicator of production) and APPV viral load in ear tissue at 2.5 weeks (log_{10} copies/g). The scatter graph shows the average viral loads (technical replicates=2) for clinical (n=22, red) and non-clinical piglets (n=56, blue). The blue line represents the line of best fit, and the shaded area in pale blue represents the 95% confidence interval.

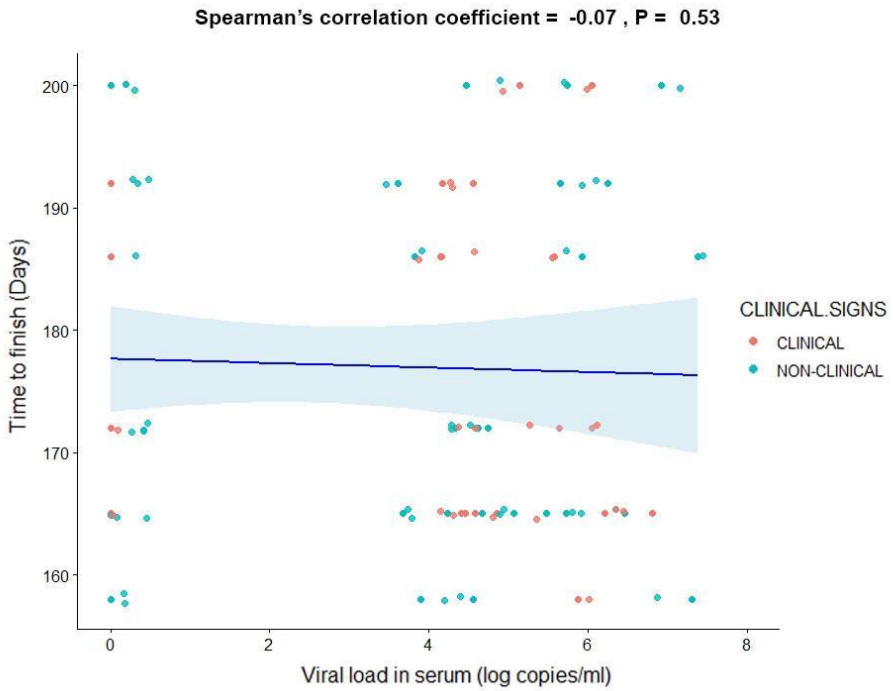

Figure 4-19: Relationship between time to finish (as an indicator of production) and APPV viral load in serum at 2.5 weeks (log_{10} copies/ml). The scatter graph shows the average viral loads (technical replicates=2) for clinical (n=22, red) and non-clinical piglets (n=56, blue). The blue line represents the line of best fit, and the shaded area in pale blue represents the 95% confidence interval.

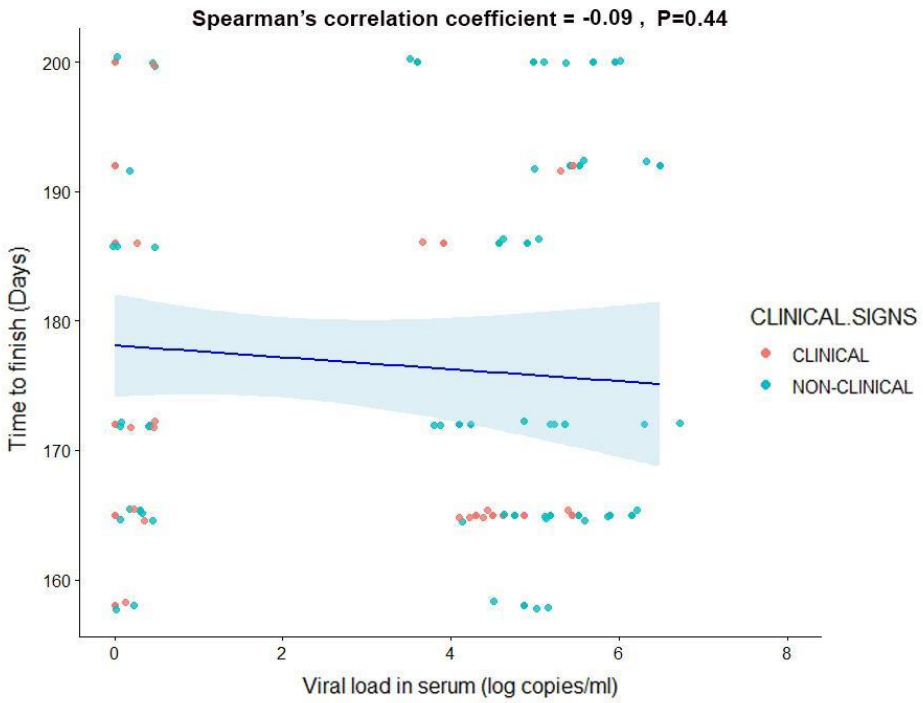

Figure 4-20: Relationship between time to finish (as an indicator of production) and APPV viral load in serum at 10 weeks (log_{10} copies/ml). The scatter graph shows the average viral loads (technical replicates=2) for clinical (n=32, red) and non-clinical piglets (n=86, blue). The blue line represents the line of best fit, and the shaded area in pale blue represents the 95% confidence interval.

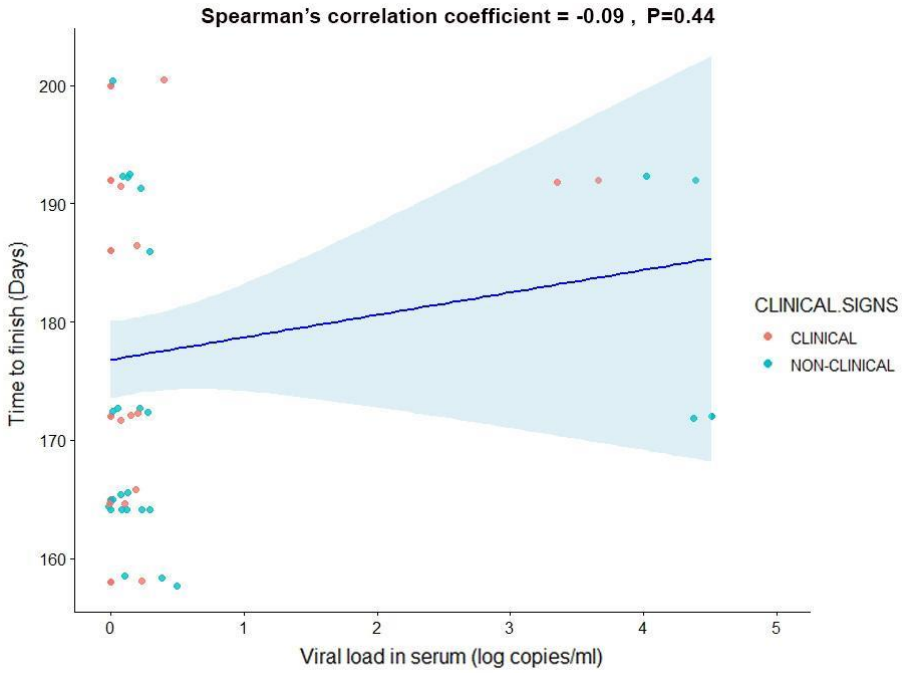

Figure 4-21: Relationship between time to finish (as an indicator of production) and APPV viral load in serum at slaughter (log_{10} copies/ml). The scatter graph shows the average viral loads (technical replicates=2) for clinical (n=20, red) and non-clinical piglets (n=55, blue). The blue line represents the line of best fit, and the shaded area in pale blue represents the 95% confidence interval.

4.5.2.3 Factors affecting the relationship between APPV status and clinical signs

As previously discussed in 4.5.2.1, no significant relationship was identified by the Mann Whitney U test between viral load in serum at 2.5 weeks and clinical status of the animal (Figure 4-14) (W= 1,654, p-value= 0.24). A significant relationship however existed between clinical signs and viral load in ear tissue (Figure 4-15) (W= 2,055.5, p-value= 0.0007). The sex of animals (Figure 4-22) (p-value= 0.62) or parity of the dam (Figure 4-23) (p-value= 0.27) had no significant association with the clinical status of the piglets, as determined by the Fisher's exact test. Both sexes had a higher proportion of non-clinical animals (29 male and 27 female non-clinical animals) compared to 11 males and eight females with clinical signs. Sows from every parity (1st to 6th)

produced clinical and non-clinical piglets; nine litters had piglets with clinical signs with the frequency of piglets with CT in the affected litters between 10% and 75%, with three litters clinically unaffected (Figure 4-24). A significant relationship was found by Fisher's exact test between the clinical status of the littermates and the clinical status of individual piglet (p-value=0.0005).

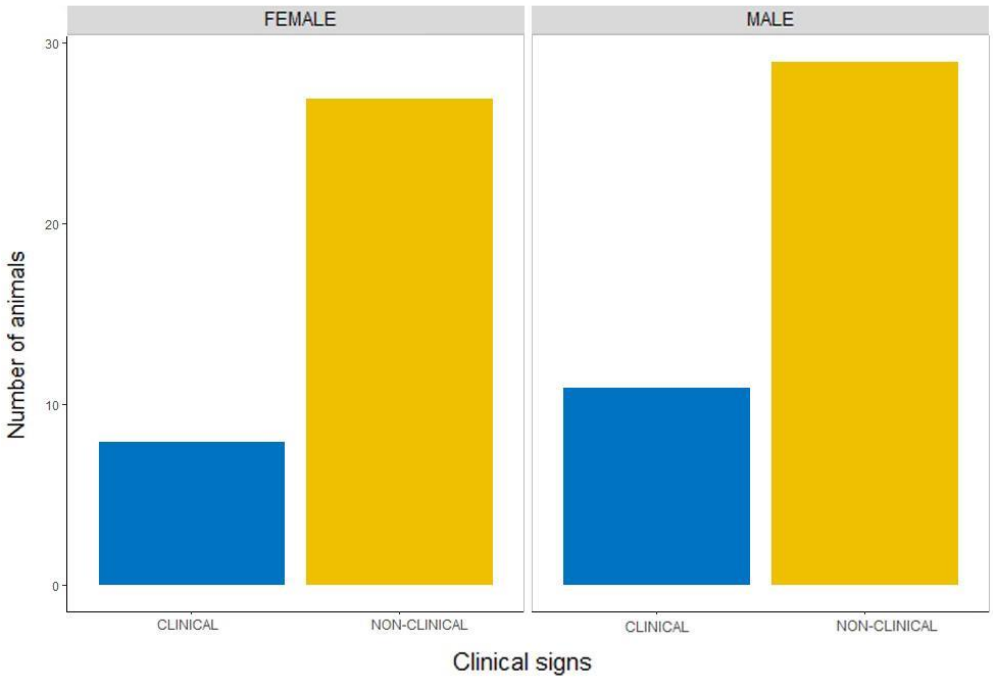

Figure 4-22: Frequency of clinical (n=11, blue) and non-clinical (n=56, yellow) animals separated by sex.

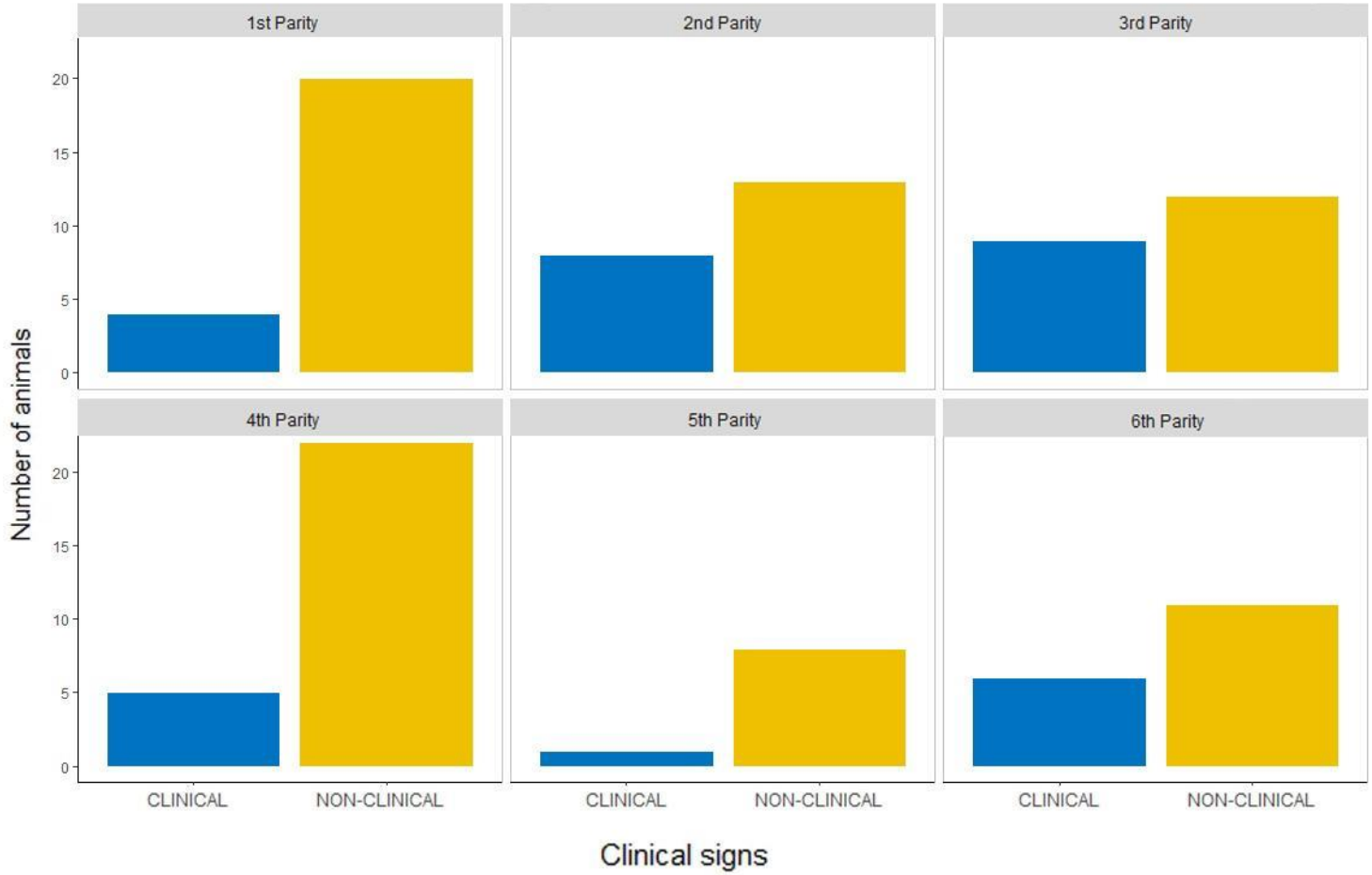

Figure 4-23: Frequency of clinical (n=34, blue) and non-clinical (n=86, yellow) animals separated by the parity of their dam.

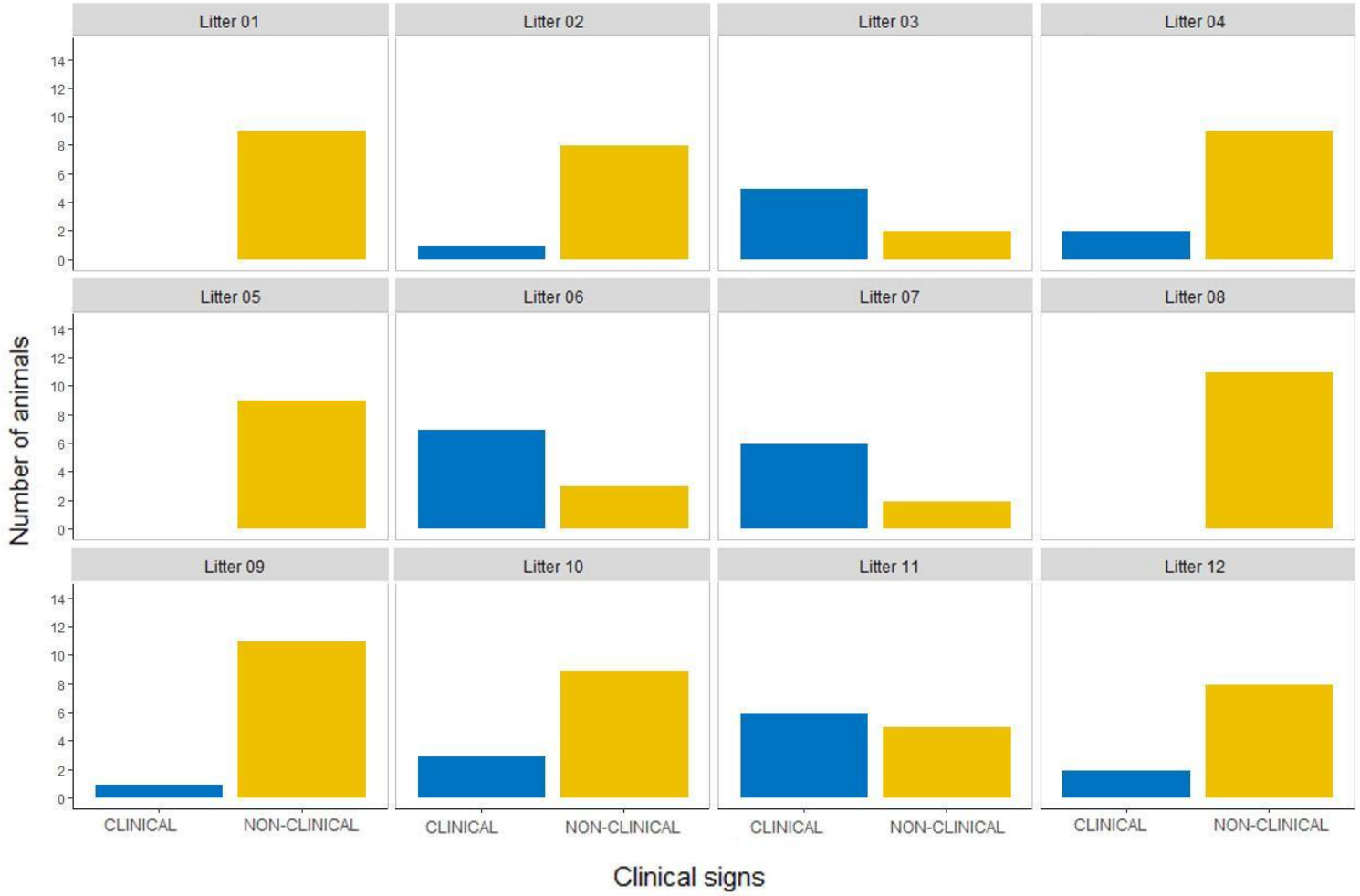

Figure 4-24: Frequency of clinical (n=34, blue) and non-clinical (n=86, yellow) animals separated by litter.

4.5.2.4 Factors affecting an APPV positive outcome in ear notch samples obtained at 2.5 weeks of age

Analysis was performed to determine if there was a relationship between having a detectable viral load in ear tissue at 2.5 weeks old and the sex of the animal (Figure 4-25), the parity of the piglet's dam (Figure 4-26) or the piglet's litter (Figure 4-27). Both sexes had a higher proportion of animals with APPV detected in ear tissue (two additional males and 14 females), although, no significant difference was found by Fisher's exact test between viral detection outcome and the sex of the animal (p-value= 0.48). Sows of every parity (first to sixth) produced piglets with detectable APPV in ear tissue, with the frequency of positive piglets per parity varying between 50 and 90%. Again, no significant difference was found by Fisher's exact test between viral detection outcomes and the parities of the piglet's dam (p-value= 0.12). There was, however, a significant relationship between the piglet's littermate's viral status and the individual piglet's status (p-value= 0.02). All litters had piglets with APPV positive ear tissue with the frequency of piglets in each litter with detectable viral load ranging between 27% and 100%.

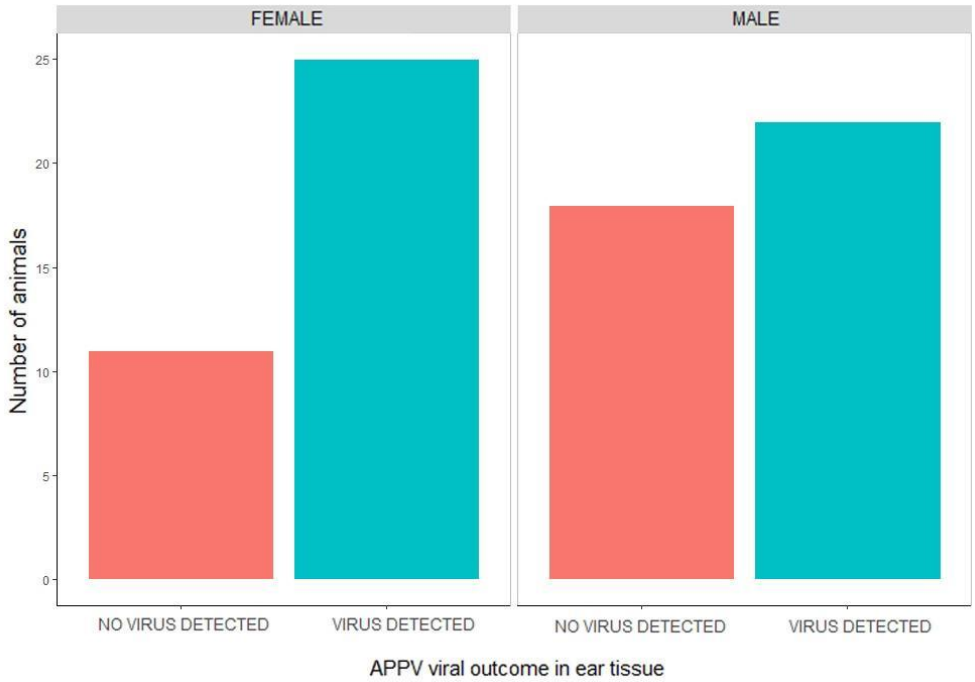

Figure 4-25: Frequency of APPV viral outcomes no virus detected (n=29, red) and virus detected (n=47, blue) in ear tissue at 2.5 weeks separated by sex of the animal.

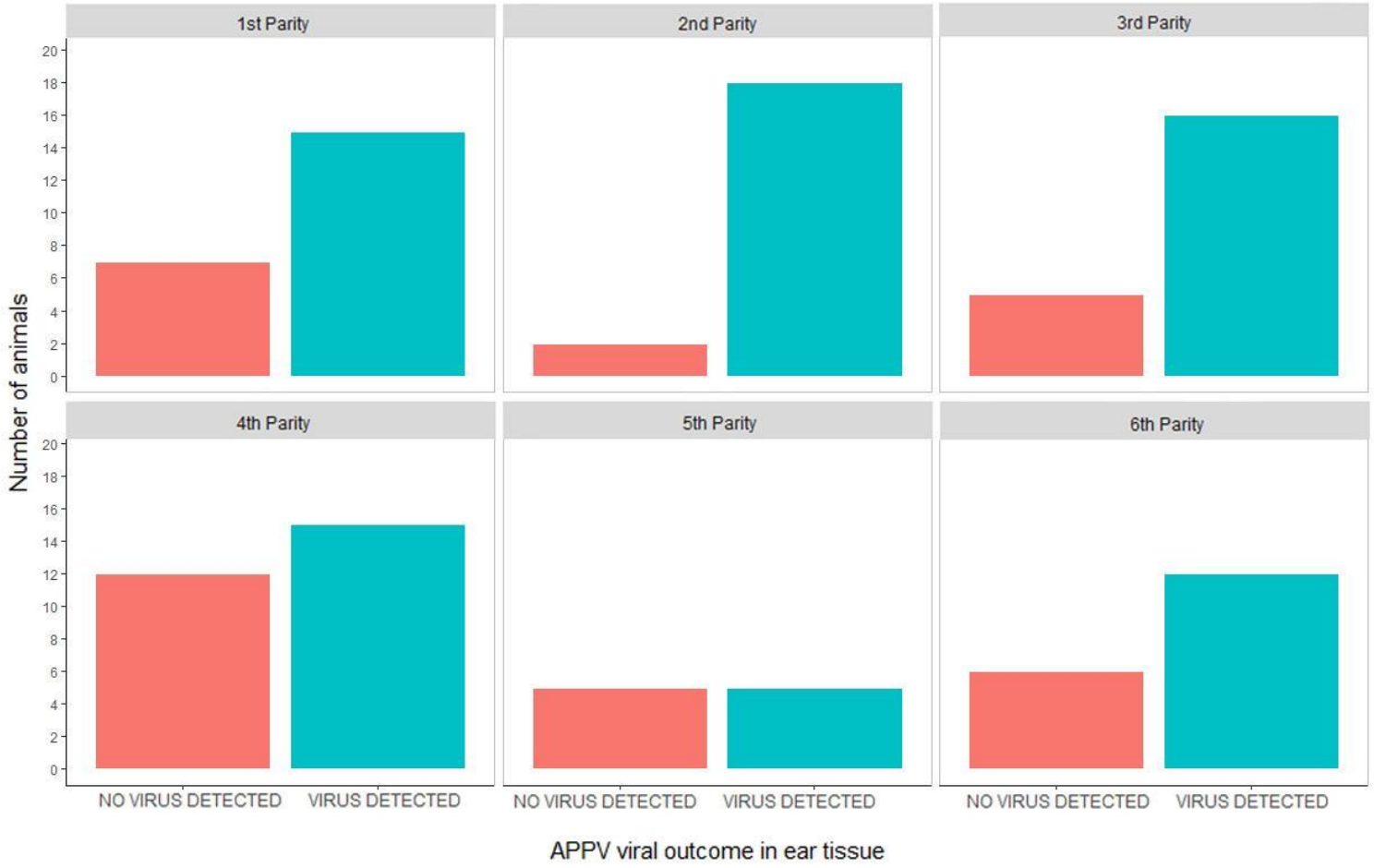

Figure 4-26: Frequency of APPV viral outcomes no virus detected (n=37, red) and virus detected (n=81, blue) in ear tissue at 2.5 weeks separated by the parity of the dam.

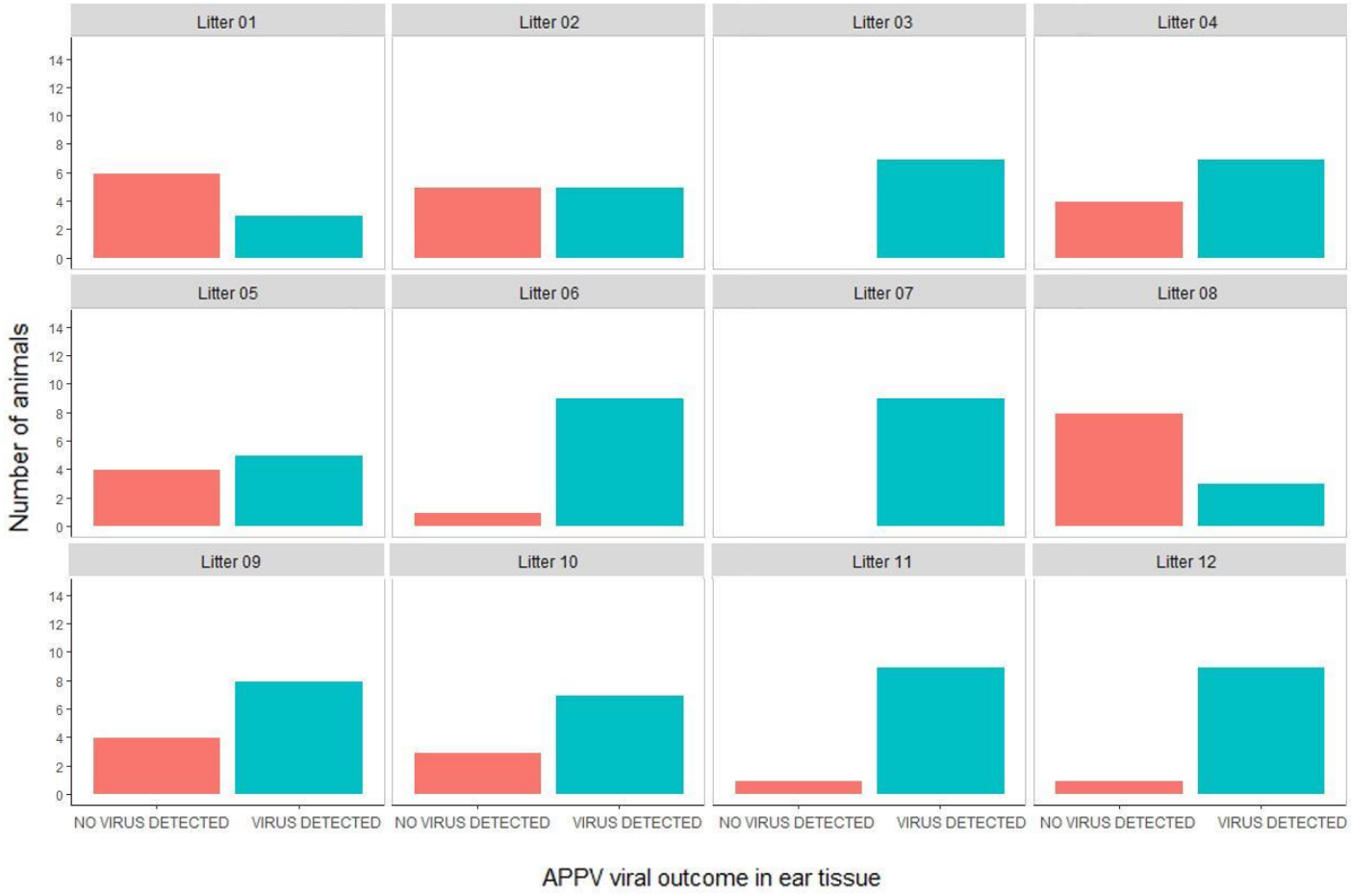

Figure 4-27: Frequency of APPV viral outcomes no virus detected (n=37, red) and virus detected (n=81, blue) in ear tissue at 2.5 weeks separated by the piglet's litter.

4.5.2.5 Factors affecting an APPV positive outcome in serum collected in piglets at 2.5 week of age

The analysis in 4.5.2.4 was repeated using the viral status (virus detected /no virus detected) of serum collected at 2.5 weeks old to determine if any relationship was present between this and the sex of the animal (Figure 4-28), the parity of the piglet's dam (Figure 4-29) or the specific litter (Figure 4-30). Males were found to have a greater proportion of positive viral outcomes compared to females, although Fisher's exact test found no statistical difference between sexes (p-value= 0.26). Both viral outcomes were present in all parities, with the frequency of piglets from each parity with a detectable viral load varying from 42% to 71%. No significant difference was found by Fisher's exact test (p-value= 0.15). All litters had piglets with APPV positive serum with the frequency of piglets in each litter having a detectable viral load ranging between 33% and 100%. No statistically significant relationship between the viral status of the littermates and the viral status of the individual piglet was determined by Fisher's exact test in serum at 2.5 weeks (p-value= 0.06).

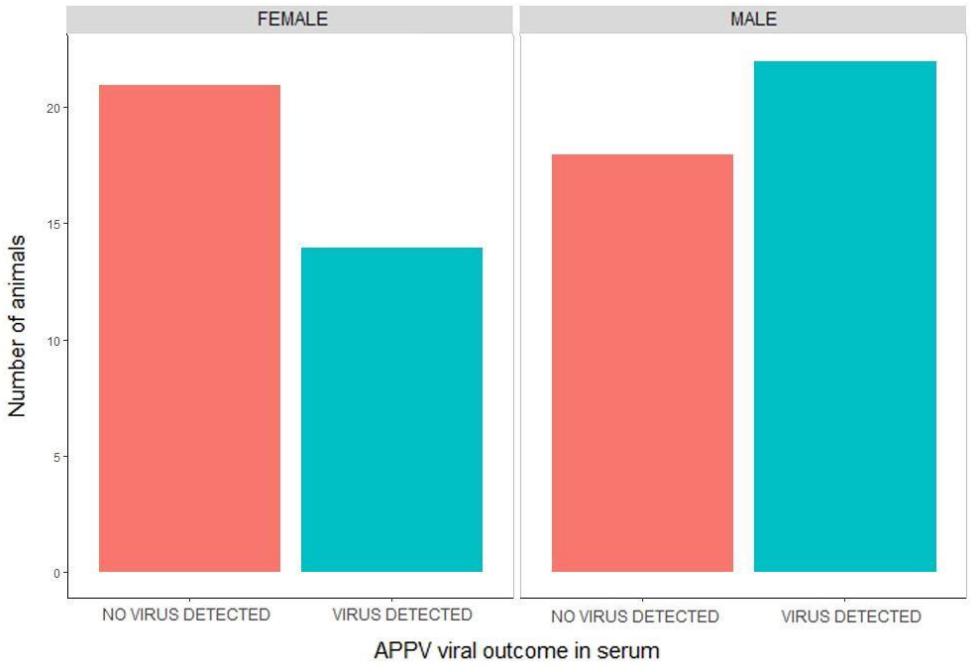

Figure 4-28: Frequency of APPV viral outcomes no virus detected (n=39, red) and virus detected (n=36, blue) in serum at 2.5 weeks separated by sex of the animal.

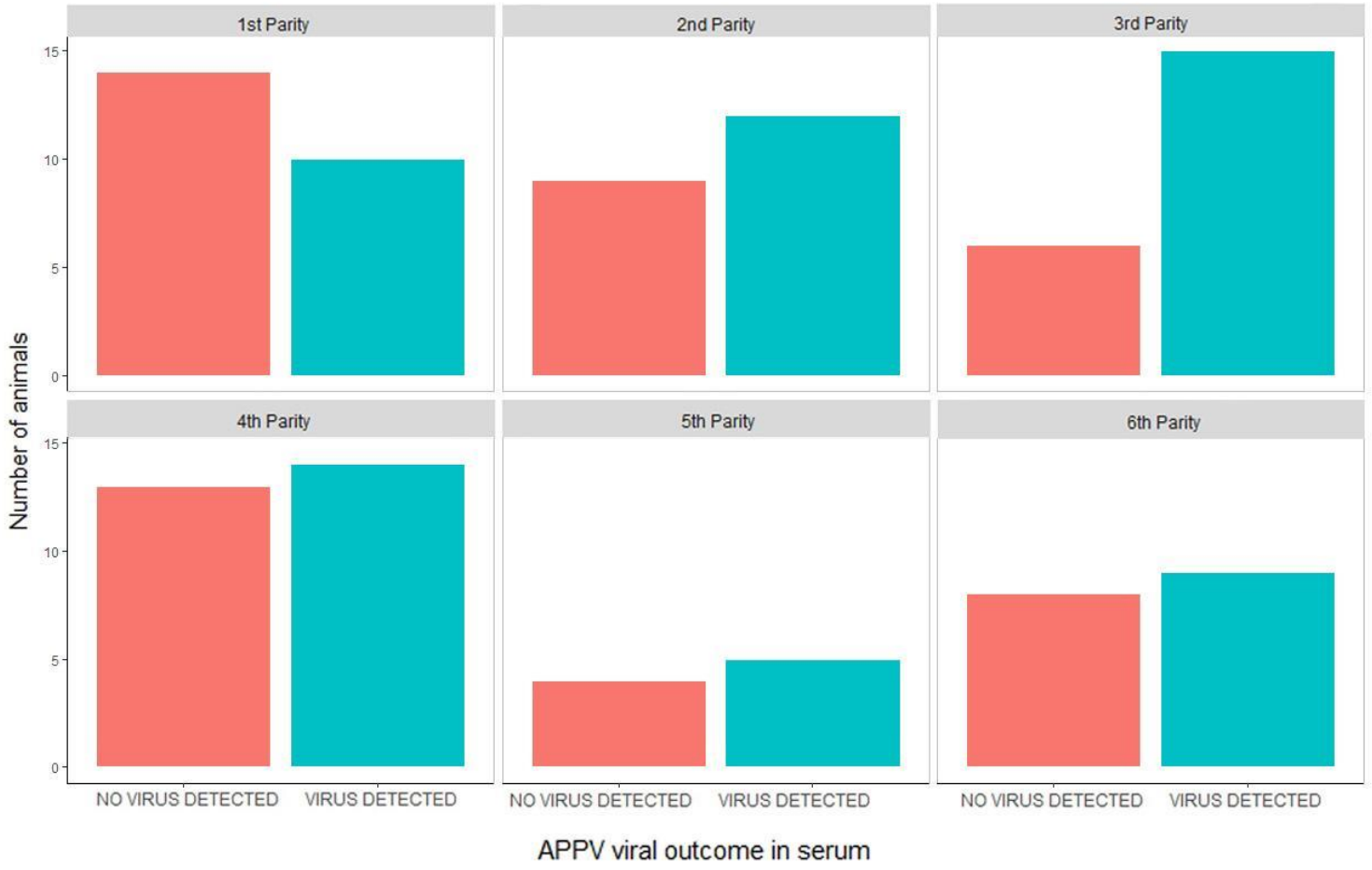

Figure 4-29: Frequency of APPV viral outcomes no virus detected (n=54, red) and virus detected (n=65, blue) in serum at 2.5 weeks separated by the parity of the dam.

Figure 4-30: Frequency of APPV viral outcomes no virus detected (n=54, red) and virus detected (n=65, blue) in serum at 2.5 weeks in relation to the piglet's litter.

4.5.2.6 Longitudinal analysis of APPV viraemia

The number of piglets with APPV present or not at the three serum collection points (2.5 weeks, 10 weeks and slaughter [22-28 weeks]), based on the initial clinical status is presented in Table 4-2. The most common outcome for non-clinical animals was to have no virus detected in any serum collection. In contrast, most clinical animals were APPV positive at 2.5 weeks, then generally had no virus detected at the following two time points. Only two animals (one clinical and one non-clinical) were found to have intermittent presence of APPV in serum, with virus detected at 2.5 weeks and slaughter, but not at 10 weeks. The serum viraemia status of individual animals throughout the study grouped by their clinical presentation at 2.5 weeks is presented in Figure 4-31. The average viral load in both the clinical and non-clinical groups reduced over the three collection points. Non-clinical animals had higher average viral load over time ($1.34x10^6$ copies/ml at 2.5 weeks, $1.81x10^6$ copies/ml at 10 weeks and $1.91x10^3$ copies/ml at slaughter) compared to clinical animals ($5x10^5$ copies/ml at 2.5 weeks, $3.54x10^4$ copies/ml at 10 weeks and $2.19x10^2$ copies/ml at slaughter). To investigate how viral outcomes for the individual animals changes over time repeatability analysis was performed (Figure 4-32) which found no significant repeatability (R= 0, Standard error= 0.034, 97.5% CI (0, 0.121) likelihood ratio of the test gives a test statistic= $4.04x10^{-11}$, df= 1, p-value= 1).

Table 4-2: APPV detection by RT-qPCR in serum at 2.5 weeks, 10 weeks and slaughter in clinical and non-clinical animals.

Clinical Status	2.5 weeks	10 weeks	Slaughter	Piglets
Clinical	Virus detected	Virus detected	Virus detected	0
Clinical	Virus detected	Virus detected	No virus detected	3
Clinical	**Virus detected**	**No virus detected**	**Virus detected**	**1**
Clinical	Virus detected	No virus detected	No virus detected	12
Clinical	No virus detected	Virus detected	Virus detected	0
Clinical	No virus detected	Virus detected	No Virus detected	3
Clinical	No virus detected	No virus detected	virus detected	0
Clinical	No virus detected	No virus detected	No Virus detected	1
Non-clinical	Virus detected	Virus detected	Virus detected	0
Non-clinical	Virus detected	Virus detected	No Virus detected	8
Non-clinical	**Virus detected**	**No virus detected**	**Virus detected**	**1**
Non-clinical	Virus detected	No virus detected	No virus detected	12
Non-clinical	No virus detected	Virus detected	Virus detected	1
Non-clinical	No virus detected	Virus detected	No virus detected	15
Non-clinical	No virus detected	No virus detected	Virus detected	1
Non-clinical	No virus detected	No virus detected	No virus detected	17

The two animals with intermittent viraemia are shown in **bold**

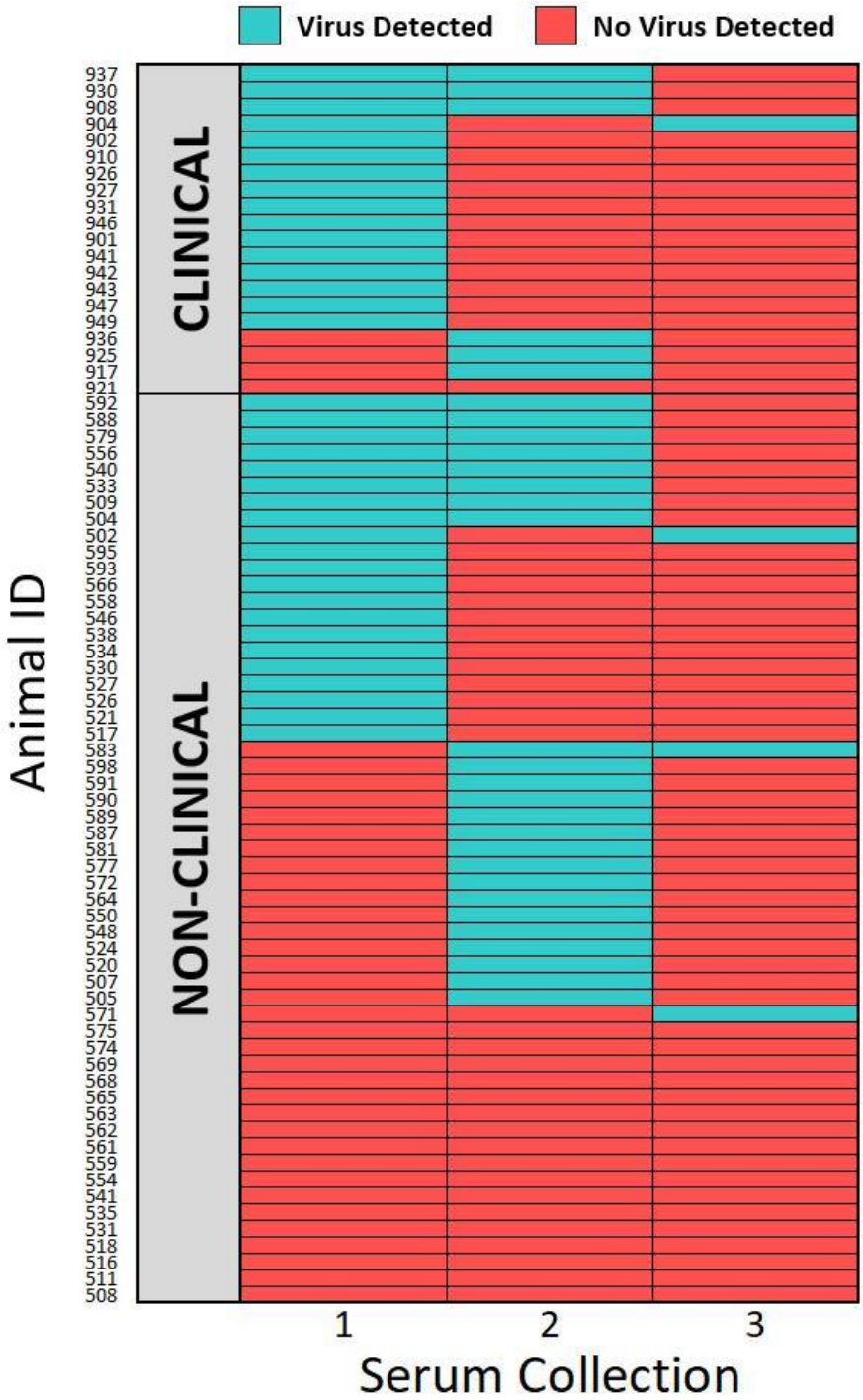

Figure 4-31: APPV detection in serum over time. The heat map shows the viral outcome (virus detected in blue and no virus detected in red) for each animal separated by clinical status (assigned at 2.5 weeks) at the three serum collection points; 2.5 weeks (1), 10 weeks (2) and at slaughter (3).

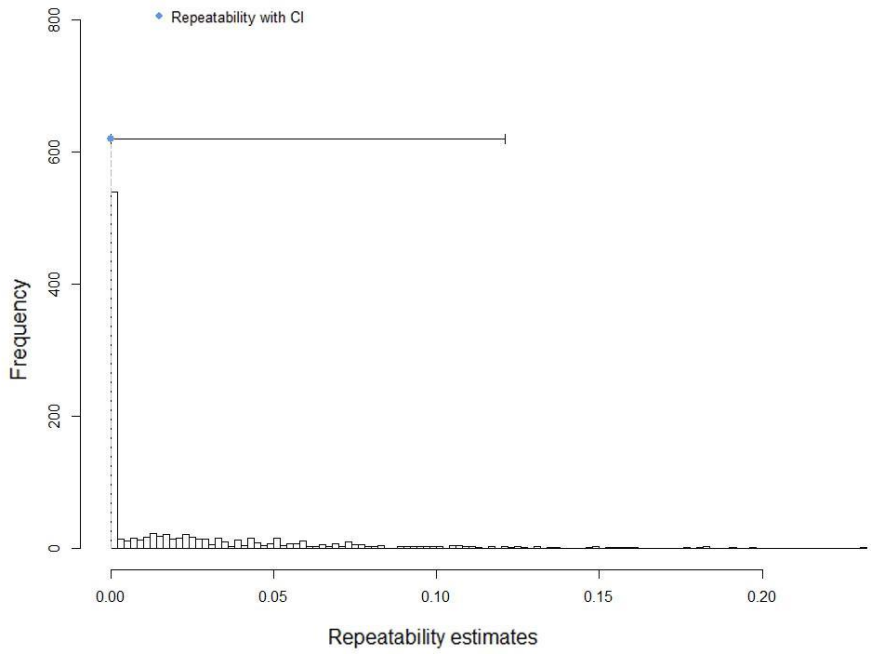

Figure 4-32: Repeatability analysis for the viral outcomes in serum over time (2.5 weeks, 10 weeks and at slaughter) bootstrapped to 1000 estimates. The blue point shows the overall estimate, and the line indicates the confidence interval.

4.5.2.7 Longitudinal analysis of APPV IgG antibody response

The IgG antibody levels over the three serum collections (2.5 weeks, 10 weeks and at slaughter) for each animal, as measured by indirect ELISA, are shown in Figure 4-33. Non-clinical animals had higher average antibody levels over time (normalised OD value of 0.52 at 2.5 weeks, 0.23 at 10 weeks and 1.14 at slaughter) than clinical animals (OD value of 0.48 at 2.5 weeks, 0.14 at 10 weeks and 0.83 at slaughter). In both clinical and non-clinical animals, the antibody levels decreased by 10 weeks of age compared to at 2.5 weeks of age but increased again by the time of slaughter. To further investigate changes of antibody levels in individual animals over time a repeatability analysis was performed (Figure 4-34) which found no significance in repeatability (R= 0.009, Standard error= 0.041, 97.5% CI (0, 0.134) likelihood ratio of the test gives a test statistic= 0.024, df= 1, p-value= 0.44).

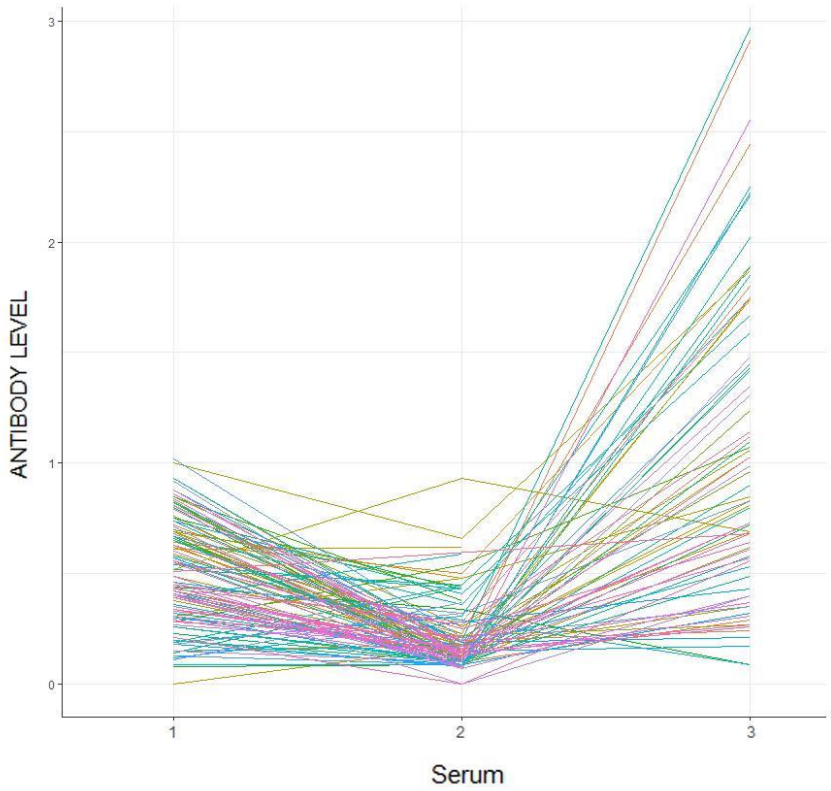

Figure 4-33: Average antibody level in serum based on two technical replicates (blank corrected, normalised OD) over time. The individual lines show the anti-APPV IgG level for each animal at the three serum collection points: 2.5 weeks (1), 10 weeks (2) and at slaughter (3).

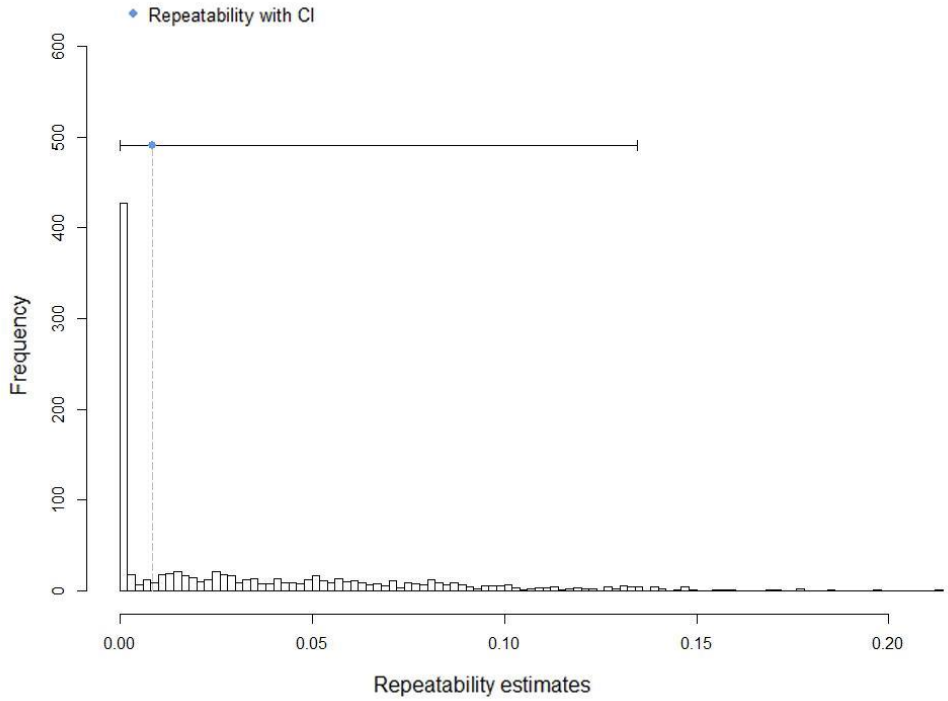

Figure 4-34: Repeatability analysis for the IgG levels in serum over time (2.5 weeks, 10 weeks and at slaughter) bootstrapped to 1000 estimates. The blue point shows the overall estimate, and the line indicates the confidence interval.

4.5.2.8 APPV Viral load in tissues collected at slaughter

APPV was detected in all tissue types collected at slaughter apart from the testicles as shown in Figure 4-35 with average viral loads of between $5.08x10^4$ copies/g and $3.08x10^7$ copies/g present in retropharyngeal lymph node and notably,$1.12x10^9$ copies/ml and $1.38x10^9$ copies/ml in non-extended semen (in clinical and non-clinical animals respectively). Additionally, virus RNA was detected in both clinical (average viral load of $7.86x10^4$ copies/g) and non-clinical (an average of $3.78x10^3$ copies/g) animals in the spleen. This data supports the observation that there was no significant difference (as determined by Fisher's exact test) for APPV viral loads between clinical and non-clinical animals for retropharyngeal lymph node (p-value=0.78), spleen (p-value=0.34), and non-extended semen (p-value=0.70), whereas a difference was detected in testicles (p-value=0.02). The APPV viral load between tissue

types did vary significantly regardless of the clinical status identified by the Kruskal Wallis H test ($X^2(2) = 23.72$, p-value=2.85×10^{-5}, df=3, eta2[H]= 0.0874). Pairwise comparisons using Dunn's test with Bonferroni correction showed that the APPV viral load was significantly higher in the retropharyngeal lymph node than in the spleen (p-value= 2.94×10^{-3}) and testicles (p-value= 5.79×10^{-4}). The APPV viral load was also significantly higher in non-extended semen than in the spleen (p-value= 3.16×10^{-2}) and testicle (p-value= 5.58×10^{-3}) tissues. Sequence analysis results confirmed APPV presence in RT-qPCR positive non-extended semen samples (alignment presented in Appendix A).

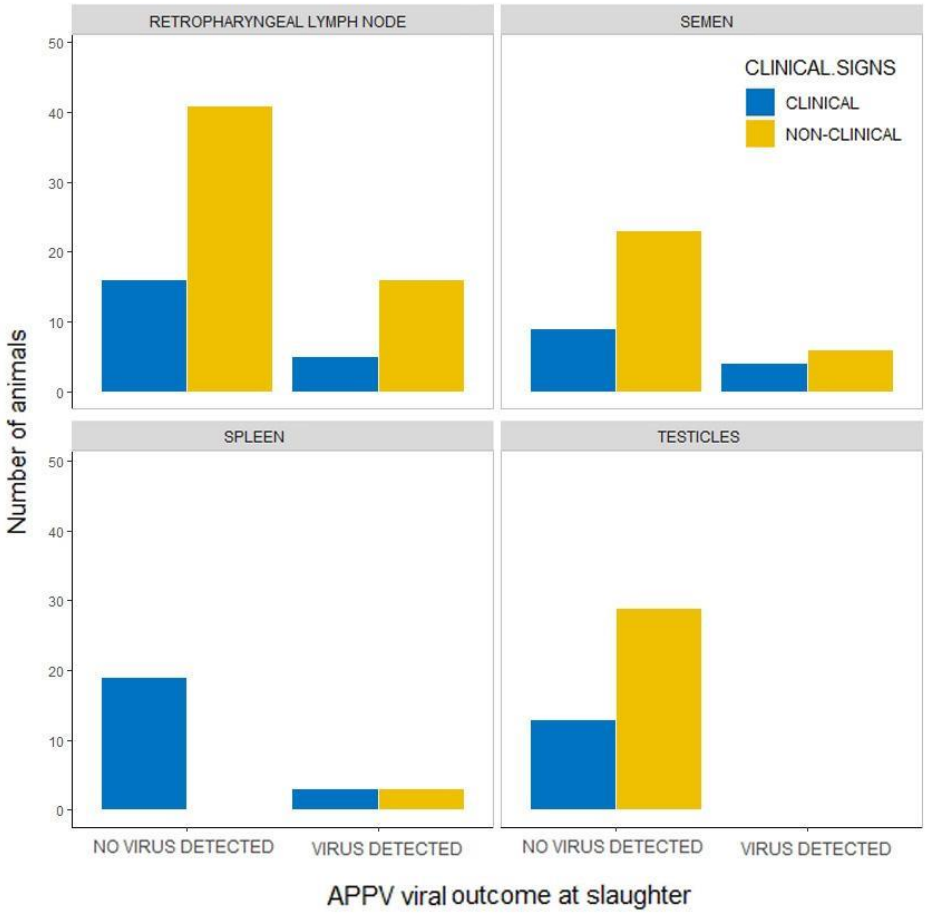

Figure 4-35: Frequency of APPV detection in different tissue types by clinical status. Viral outcomes in retropharyngeal lymph node (n=78, top left), spleen (n=79, bottom left), non-extended semen (n=42, top right) and testicles (n=42, bottom right) from clinical (blue) and non-clinical (yellow) animals.

4.6 Discussion

This chapter presents the investigation of a CT A-II outbreak on a Scottish farm, initially diagnosed by the farm's attending veterinarian; other types of CT were ruled out based on clinical signs and farm history. CT A-I caused by CSFV was excluded as the virus is exotic to the UK, with the last incursion occurring in 2000 (Animal and Plant Health Agency, 2018), CT A-III and A-VI, which are genetic defects of Landrace and Saddleback pigs, were excluded as pigs affected on this farm were of Large White and Duroc descent. A small number of piglets were also tested for other pathogens, including BVDV, BDV, PRRSV and porcine circovirus type 2 (PCV2) with negative results. APPV was widely detected in piglets from CT-affected farrowing groups' on-farm by RT-qPCR and confirmed to be APPV by Sanger sequence analysis, supporting the vet's initial diagnosis. Although no formal scoring was conducted for splay leg in association with CT, co-morbidity was observed in some animals, which is a consistent finding with other studies (Arruda *et al.*, 2016; De Groof *et al.*, 2016; Possatti *et al.*, 2018b; Gatto, Sonálio and de Oliveira, 2019; Sutton *et al.*, 2019; Guo *et al.*, 2020).

A strong association between APPV and clinical CT has been reported in a number of studies (De Groof *et al.*, 2016; Postel *et al.*, 2016; Muñoz-González *et al.*, 2017; Schwarz *et al.*, 2017; Zhou *et al.*, 2019). In the current CT outbreak, APPV was detected in both clinical and non-clinical littermates within serum and tissues, with no overall association observed between the clinical and viral status of the piglets (except for ear notches) in either of the two farrowing groups investigated. Industry-wide, the current lack of detection of APPV in animals without clinical signs presents a problem for the identification of infected animals by farmers and vets, hampering control strategies for managing outbreaks such as the removal of infected animals from breeding programmes and highlights the importance of diagnostic testing. Similarly, APPV has been detected from apparently healthy CT littermates in both natural and experimental infection studies. Catatay and colleagues identified

APPV in the serum of 14 out of 15 piglets from CT affected litters, regardless of the clinical status of the individual at six days post farrowing (Cagatay *et al.*, 2019). Gatto and colleagues also detected the presence of APPV within the cerebellum of an unaffected littermate while investigating the presence of APPV in CT outbreaks on four Brazilian farms (Gatto *et al.*, 2018b). In litters experimentally infected during gestation, Arruda *et al.* (2016) detected APPV in all piglets with clinical signs of CT and in 10 of 11 piglets without CT. De Groof *et al.* (2016) also identified APPV in the serum of two apparently healthy piglets from CT affected litters. As variation in the severity of clinical signs both between and within litters was observed in both farrowing groups, and tremors themselves are known to present differently during periods of stress and rest, this may have contributed to individuals with extremely mild or inapparent tremors being identified as unaffected during the clinical observational period affecting the association between clinical and viral status of this study. To better understand the relationship between APPV and clinical signs at a farm level, following litters from CT unaffected farrowing groups may have provided further clarification; however, it was not logistically possible during this study.

In other pestiviruse infections, infection at different gestational stages in relation to the development of the immune system and organ systems may lead to not only different viral outcomes such as transient or persistent infection but also different clinical outcomes for the fetus, including abortion and malformation (Peterhans, Jungi and Schweizer, 2003; Oğuzoğlu, 2012; Khodakaram-Tafti and Farjanikish, 2017; Ganges *et al.*, 2020; Barman *et al.*, 2021). The current understanding of the effects of APPV infection *in utero* at different gestational time points on clinical outcomes is limited. Sows conventionally do not show clinical signs of infection; in natural occurrences of disease, the first indication of the condition is the birth of CTaffected piglets, making it impossible to determine with any certainty when in pregnancy the sow was infected. Even in experimental infection studies, where the timing of infection during gestation is controlled, e.g. 32 days (De Groof *et al.*, 2016), 45 and 62 days (Arruda *et al.*, 2016; Buckley *et al.*, 2021), variability of the severity

of clinical signs was observed both between and within affected litters. Future investigation should focus on how APPV interacts with the developing fetus to elicit variation in clinical outcome.

Associations between clinical status, viral status and characteristics of the piglets (sex of the animal, parity of the dam and piglet's litter) were explored. The piglet's sex and sow parity did not affect either clinical or viral status; however, the individual's litter impacted the viral and clinical status. This may be due to the unique circumstances surrounding infection of the sow during pregnancy, for example, the strength and timing of viral challenge, differences in the immune system of the sow, fetal development including immunocompetence, and further research is needed to elucidate this. Usually, outbreaks of CT are primarily observed in gilt litters with occasional higher parity sows affected (De Groof *et al.*, 2016; Gatto *et al.*, 2018b; Pedersen *et al.*, 2021). A seven-year study of a closed herd with CT by Folgueiras-González *et al.* (2020) described the prevalence of clinical piglets in litters from first and second parity sows to be significantly higher (55%) than forth parity sows (5%), suggesting that the sows gain immunity after infection, therefore reducing the number of naive sows at each incursion, which is probably why repeated litters with CT from the same sow have not been reported. A study by Guo *et al.* (2020), which described a recent outbreak of CT in a large closed herd farrow to weaning unit in China, found a higher proportion of CT litters born to second (40%), and third parity (32%) litters compared to first (16%), and fourth (12%) parity with no CT litters born to sows of fifth parity or higher. In similarity to the current investigation, litters with the highest prevalence of CT piglets were born to second and third parity sows. However, affected animals could be found in litters belonging to all parities. As the farm in the current study was a closed high health status unit with no history of CT, this was likely to be the first incursion of APPV in a naive herd explaining indiscriminate infection of sows

The pattern of APPV detection in serum differed not only between farrowing groups, but also within individuals over time: in the first farrowing group, 75% of clinical and 58% of non-clinical animals were positive at two weeks old and by eight weeks old all animals, irrespective of clinical status, had detectable levels of APPV RNA. In the second farrowing group 80% of clinical animals and only 38% of non-clinical animals initially had detectable APPV RNA at 2.5 weeks, out of those initially infected only 15% and 14.5% respectively still had detectable levels of APPV by 10 weeks, with all but two (that had an intermittently detectable levels of APPV) of those that had APPV detected initially, regardless of clinical status, having no detectable APPV at slaughter. This suggests that piglets in this group, unlike in previously reported studies, were not persistently infected (as indicated by persistent viraemia) and only exhibited prolonged transient infection. Additionally, 24% of all animals with detectable APPV at 10 weeks did not have previous APPV detected at 2.5 weeks suggesting newly acquired APPV infections indicating horizontal transmission occurred within the group. Although animals with APPV and clinical signs at 2.5 weeks are likely to be the product of vertical transmission as initial sampling of the farrowing group occurred at 2.5 weeks, it was not possible to definitely differentiate between instances of vertical transmission and early horizontal transmission. This is especially true for APPV positive non-clinical animals which may either be a product of late gestational infection after the development of the piglet's nervous system or the product of postnatal horizontal transmission where infected piglets do not present with clinical signs (as shown in 3.5).

As part of an investigation of a naturally occurring APPV associated CT outbreak in the Netherlands, Schwarz *et al.* (2017) monitored 29 piglets from three affected litters over 4.5 months to determine the viral persistence in serum. Like the first farrowing group in the Scottish farm investigation where all animals remained positive until eight weeks of age, all of the animals tested remained positive with high titres up to nine weeks of age. However, by 4.5 months, both the APPV titre in serum and the number of positive animals had

reduced, with a minority (7 out of 20) of the initially positive piglets remaining APPV positive. The resolution of viraemia in the majority of animals supports the findings of a transient infection as observed in the second farrowing group. Nevertheless, some of the animals in the Dutch study were positive at 4.5 months, suggesting that the animals could be in a state of prolonged viral infection, which will eventually resolve over time or could also be persistent infection, which could only have been confirmed if monitoring had been carried out for more than 4.5 months.

Interestingly, Schwarz *et al.* (2017) also monitored viral shedding in five piglets with paired serum and stool sampling between 6 and 8.5 months. Three animals consistently shed virus in the faecal matter, two of which had undetectable titres at 7.5 months; however, one of these was positive again at 8 months. Whereas in serum, no virus was detected in the animals that had previously all been positive at earlier sampling points (nine weeks) from six months till 8.5 months, except for one boar with a detectable titre at 7.5 months, suggesting only transient viraemia. This study also was able to consistently detect the presence of APPV in the saliva of two animals at 6 months, one of which also had the virus present in serum. The discordance between serum results and other sample matrices may suggest that serum may not be the most precise indicator of viral persistence. Other sample types, especially less invasive, should be considered as valuable indicators of infection and viral persistence, and investigated further.

Contrary to what was observed in the second farrowing group of the described Scottish investigation, Cagatay *et al.* (2019) also found, that a proportion (four out of seven) of CT affected piglets initially positive for APPV at six days, old remained APPV positive at slaughter (161 Days), indicating that animals can become either transiently or persistently viraemic. The study also identified horizontal transmission of APPV in five virus negative piglets from a non-affected litter which became APPV positive on day 48, after weaning and mixing with infected animals. It should be noted that the animals were able to

eliminate the virus, only becoming transiently infected. These findings support observations within the second farrowing group of the current study, which found that 25% of animals with detectable APPV at 10 weeks old had not previously tested PCR positive at 2.5 weeks. Only one of these animals had a detectable viral load at slaughter. As other animals in this study had viraemia spanning two collections (10 weeks), it was assumed that had the animal not been slaughtered and further collections made, the viraemia would not have persisted. However, the possibility cannot be discounted as other pestiviruses such as CSFV, have been reported to cause persistent infection in postnatally infected animals, both in newborns and weaned six-week-old piglets (Baker and Sheffy, 1960; Vannier, Plateau and Tillon, 1981). Identification of horizontal transmission, which farmers and clinicians would otherwise miss as the animals do not develop clinical signs, may reduce the effectiveness of eradication and control strategies by allowing the virus to circulate on the farm subclinically.

Cagatay *et al.* (2019) also monitored the antibody levels of the piglets throughout their study: variable amounts of APPV-specific antibodies were detected in individuals born to CT affected litters (likely products of vertical transmission). Generally, antibody levels were high at 6 days then declined slowly over time to reach negligible levels at 21—48 days. This antibody kinetic likely indicates passively transferred antibodies from maternal colostrum. Then at later time points, varying antibody levels were detected, whereas horizontally infected piglets showed consistently high levels of antibodies from day 69. In the current study, differences in antibody levels were not specifically studied in terms of transmission routes; nevertheless, the majority of animals, regardless of clinical status, were found to have moderate antibody levels at 2.5 weeks which then reduced to minimal levels at 10 weeks, with the highest levels reported at slaughter, suggesting that the animals in most cases were able to mount an immune response against the virus which is further evidence of a transient, non-persistent infection. As the final collection of serum was at slaughter (between 22 and 28 weeks), no comments can be made on the

timing of the increase in antibody levels and whether they would have been maintained. Future studies should increase the number of collections by including a 15-week serum sample or extending the collection period where applicable.

Initially, moderate levels of antibodies were present at 2.5 weeks, followed by a reduction in titre by 10 weeks in the second farrowing group; this was also observed within the first farrowing group where piglets had moderate antibody levels regardless of clinical status at two weeks which then reduced to minimal levels to below detection by eight weeks of age. As the piglets remained with the dam until weaning, it is likely the moderate levels of antibodies in both groups were maternally derived from colostrum, since the pig epitheliochorial placenta does not allow antibody transfer; moreover, even after eight weeks when the sows were tested for the presence of antibodies, four out of six were positive. As the half-life of maternally derived IgG is 12—14 days, the reduction in antibody titre between the 2/2.5-week and 8/10-week samples is consistent with this (Curtis and Bourne, 1971; Bourne, 1973). For logistical reasons, in this study it was not possible to collect serum from the sows from the first farrowing group earlier than eight weeks. Ideally, a sample would have been taken at two weeks when the piglets were initially sampled as well as eight weeks to determine how antibody levels persisted within the sow and its relationship to viral and clinical outcomes. Incidentally, as with the Cagatay *et al.* (2019) study, which also reported horizontal transmission, the maternally derived antibodies did not confer protection to initially unaffected piglets. However, their presence may have reduced the amount of APPV in serum detected, unfortunately, the neutralising capacity of the antibodies present was not investigated due to the unavailability of a serum neutralisation assay at the time of the study, therefore additional research into this should be performed.

The distribution of APPV within tissues in the second farrowing group supports the findings of a postnatal infection in addition to the congenital one in different animals of this group. As described in Chapter 3, APPV RNA was detected in

all tissue types tested from the first farrowing group and the retropharyngeal lymph node and spleen from the second farrowing group. Similar to the experimental postnatal infection (3.5.2.3), where consistently high levels of APPV were observed in lymphoid tissues (lymph nodes, spleen and tonsil), the analysis of the second farrowing group also showed a significantly higher amount of APPV RNA in the tonsil, lymph node and thymus compared to the brain. Moreover, although APPV RNA was found in the brain of postnatally infected animals in the experimentally infected group, it was also of a lower frequency. Unlike the current study, the thymus was found to have one of the lowest viral loads for the postnatally infected piglets (3.5.2.3). These findings confirm the other studies which found systemic distribution of the virus within tissues (Arruda *et al.*, 2016; De Groof *et al.*, 2016; Postel *et al.*, 2016; Muñoz-González *et al.*, 2017; Yuan *et al.*, 2017; Liu *et al.*, 2019). As tissue samples were collected at slaughter in the second farrowing group, between 22 and 28 weeks, the detection of a viral load in the majority of animals indicates that the virus persists in tissues after viraemia has resolved, which should be taken into consideration when determining if animals remain persistently infected.

The virus was not detected in any of the testicular parenchyma collected from adolescent boars at slaughter. Paradoxically, a high viral load of APPV were detected in the non-extended semen collected from the epididymis of the same testis by RT-qPCR. Schwarz and colleagues also found APPV in the non-extended semen of a 6-month-old CT affected boar (Schwarz *et al.*, 2017), while (Gatto *et al.*, 2018a) detected an APPV prevalence of 34% in semen during a molecular survey of commercial stud units in the US, although neither study investigated the APPV load in the testicles. Other pestiviruses such as BVDV are known to replicate within the epididymis, which may explain why semen samples collected from this area were positive, further investigation into the detection of APPV from the epididymis tissue itself is necessary to elucidate these findings (Kirkland *et al.*, 1991). Conversely, another study found moderate APPV RNA signals in the tunica albuginea and the lumen of seminiferous tubules when evaluating testicular tissue via RNAScope *in situ*

hybridisation (Buckley *et al.*, 2021). The presence of APPV RNA in semen highlights the potential for venereal transmission. Further research is needed to determine the actual infectivity of APPV in semen and the importance of this transmission route in the circulation of the virus within Great Britain by investigating the prevalence of APPV in commercial semen used for AI (explored in Chapter 6) through the introduction of active surveillance programmes. In absence of an *in vitro* titration system, and to establish infectivity, naive seronegative sows should be inseminated with APPV positive semen and the fate of the litter followed. Future studies should also aim to characterize tissue, and cell tropism of the reproductive tract and associated bodily fluids of CT affected animals of both sexes to determine the relationship between APPV infection and reproductive outcomes.

Interestingly, in the current study, the APPV viral RNA load in the brain was found to be lower by RT-qPCR than in previous published studies. For example, Gatto *et al.* (2018b) and Liu *et al.* (2019) found high levels of APPV within the cerebellum. However, it should be noted that in the studies reported here RT-qPCR was only performed on a section of the frontal cortex, prior to the exploration of viral tropism within the brain with BaseScope ISH, which revealed the highest concentration of APPV to be located in the cerebellum of both CT affected and non-affected animals. Frozen sections of cerebellum were unfortunately not available for all the animals investigated. APPV was found to present with a marked diffuse distribution within the molecular and granular layers of the cerebellum, with BaseScope signal observed sporadically in the Purkinje cell layer and with minimal occurrence in the white matter associated primarily with blood vessels. This is consistent with a study of the cerebellum of CT affected piglets at 6 days and 11 months (Buckley *et al.*, 2021), and IHC results from a study by Liu *et al.* (2019), which noted moderate positive staining in the matrix of the molecular layer and axons of granular cells. However, unlike the current study, Liu *et al.* (2019) found no evidence of APPV in the Purkinje cell layer. Retrospective analysis of brain tissue collected from piglets with CT using *in situ* hybridisation also showed

strong positive APPV signals in the inner granular layer of the cerebellum (Postel *et al.*, 2016). Both the Buckley *et al.* (2021) and Liu *et al.* (2019) studies also detected APPV in lesser amounts in the cerebrum with multifocal distribution in the internal granular layers and mild occurrence in the external granular layer. Liu *et al.* (2019) were also able to detect APPV by IHC in low amounts in the brainstem, although neither study characterised cell association within these areas.

In studies identifying BVD in the brain and spinal cord by found the virus to be primarily associated with neurons in the spinal cord and brain, with the greatest infiltration of BVD in the cerebral cortex and hippocampus (Fernandez *et al.*, 1989; Hewicker *et al.*, 1990), although no morphological evidence of cellular alteration was observed. In contrast, APPV was found to be both non-cell-associated in the matrix and cell-associated within neurons, glial cells and endothelial cells within blood vessels in the cerebral cortex, and observed in pyramidal neurons within the hippocampus, although similarly to the BVD studies, no morphological changes were observed within the tissues. The lack of pathological changes in the current study in comparison to other APPV-associated CT investigations could be explained by the age of the piglets analysed, as typically histopathological changes (hypomyelination or the presence of vacuolation) are observed in neonatal piglets (Postel *et al.*, 2016; Schwarz *et al.*, 2017; Dessureault *et al.*, 2018; Mósena *et al.*, 2018; Sutton *et al.*, 2019). Due to logistical constraints, histopathological investigations could only be performed on eight-week-old piglets; as clinical signs are self-resolving, subtle changes in morphology within these tissues may also resolve during this time, causing associations to be missed. In the future, where possible, neonatal piglets should be assessed for APPV RNA via BaseScope ISH in conjunction with specific cell markers or in combination with specialised staining to clarify further cell tropism and the relationship between morphological changes and APPV presence in these areas.

On the farm investigated as part of the Scottish field study, neither the viral load in serum or ear tissue or clinical signs affected production, as evaluated by the length of time the piglets took to achieve slaughter weight (approximately 110kg). Ideally, other predictors of growth would also have been investigated, such as birth weights, live weight gain or feed consumption however, for logistical reasons, this was not practical within the current study setting. A study by Sutton *et al.* (2019) showed a strong relationship between CT and birth weight both between and within litters whereby piglets from non-affected litters had heavier birth weights than piglets from affected litters regardless of the individual's clinical status. Curiously, within CT-affected litters, clinical piglets were heavier at birth than their non-clinical counterparts although the reason for this and the long-term effect of this with regards to growth needs further investigation. The study of Sutton and colleagues also found higher pre-weaning mortality rates in CT-affected piglets (46.4%) as opposed to unaffected ones (15.3%) regardless of the overall litter status, with the majority of deaths occurring within the first five days (76%). Other studies have reported similar findings with increased mortality: De Groof *et al.* (2016) found a pre-weaning mortality rate of 26% in affected litters compared to 11% in unaffected litters with 60% of death within affected litters attributable to CT. Schwarz *et al.* (2017) observed mortality rates up to 25% on two CT-affected Austrian farms in 2015 and 30% in 2016. As well as postnatal mortality, Sutton *et al.* (2019) also investigated death during gestation, however no association was found between the incidence of stillborn or mummified fetuses and the presence of CT within the litters. Both stillborn and mummified fetuses can also be characteristic of other pestivirus infections, including CSFV, with incidence linked to strain virulence (Bohórquez *et al.*, 2020). Further investigations into the impact CT has on production are needed to ascertain the economic and welfare impact of the virus both within Great Britain and globally.

Other pestiviruses such as CSFV or BDV are considered as having high welfare and economic importance. BVDV is estimated to cost the UK cattle industry £39.6 million per year (Hardstaff *et al.*, 2020). Unlike classical swine

fever (CSFV), which is exotic, BVD is endemic, with great efforts undertaken to eradicate the virus from the UK herd through government accredited health assurance schemes. These programmes use molecular and serological diagnostics in combination with multiple sample types, including milk, serum and ear tissue, to identify BVD exposure of herds, informing prevention, control and eradication strategies (Scottish Government, 2019). As established in the current study and the Scottish sero-survey presented in Chapter 6, APPV appears to be endemic within the British pig population; although the impact of this is still under investigation, it is clear that the establishment of diagnostics as part of routine surveillance and the implementation of management strategies to control APPV is needed. The current study determined a positive correlation between APPV viral load in ear and serum samples and found a significant relationship between the viral load in ear tissue and the CT status of the piglets, which was not observed in serum. These findings highlight the potential of ear tissue as a diagnostic sample. While the application of milk sampling in pig production is not practical, ear tissue sampling can be performed as part of routine husbandry procedures using identification tags that simultaneously collect an ear punch. This procedure is less invasive than blood sampling, causing minimal stress to the animals and can be done without the aid of a veterinarian, making it a less expensive alternative to blood collection. Unlike serum samples, ear tissue samples are not affected by maternally derived antibodies that may interfere with serological outcomes in pre-weaning piglets, further demonstrating the sample type's versatility for diagnostic testing. However, serological examination of ear tissue samples for the detection of APPV specific antibodies and their comparability to APPV specific antibodies in serum samples were not investigated during this study and should be investigated in future work.

Chapter 5: Investigation of atypical porcine pestivirus as an immunosuppressive agent.

5.1 Introduction

A characteristic of many pestivirus infections such as classical swine fever virus (CSFV), bovine viral diarrhoea virus (BVDV), and border disease virus (BDV) is the ability to induce immunosuppression in the host species (Baker, 1995; O'Neill, O'Connor and O'Reilly, 2004; Lanyon and Reichel, 2013; Tarradas *et al.*, 2014). Suppression of the immune system in affected animals can lead to enhanced disease by affecting the severity and duration of the infections, increasing the susceptibility to other pathogens, or causing illness through the overgrowth of commensal or opportunistic pathogens (Baker, 1995).

Previous studies of congenital tremors (CT) have reported natural, simultaneous infections of atypical porcine pestivirus (APPV) with other pathogens. Chen and colleagues found a low level of concurrent infection of APPV and porcine pegivirus (PPgV) in serum from five out of 67 diagnostic cases from the USA detected by duplex reverse transcriptase polymerase chain reaction (RT-PCR) (Chen *et al.*, 2019). Interestingly, like APPV, PPgV is also a novel member of the *Flaviviridae* family as it was discovered in 2016 during a sequencing study of asymptomatic porcine serum however, unlike APPV, it has not been associated with clinical disease (Baechlein *et al.*, 2016; Yang *et al.*, 2018; Kennedy *et al.*, 2019).

A study by Liu *et al.* (2020) employed a multiplex RT-PCR assay for simultaneous detection of African swine fever virus (ASFV), CSFV and APPV within 384 clinical tissue samples. In this study, five samples were positive for

both APPV and CSFV and seven were positive for both APPV and ASFV. Recently, a retrospective study of APPV within USA swine herds was able to detect APPV coinfecting with eight other viruses: porcine respiratory and reproductive syndrome virus (PRRSV) (33/339), porcine circovirus type 2 (PCV2) (23/339), swine influenza A virus (SIV) (16/339), porcine epidemic diarrhoea virus (13/339), porcine rotavirus A, B, C (4/339) and porcine delta coronavirus (2/339), Seneca valley virus 1 (3/339), porcine parainfluenza virus (2/339) (Yuan *et al.*, 2021). Although co-infection was established in these studies, no investigation was conducted into the infection dynamics of each of the viruses.

A pathological and molecular examination of co-infection of APPV and porcine teschovirus (PTV) in three-day-old piglets with clinical signs of CT from a high mortality farm found both pathology consistent with APPV associated CT (marked by demyelination in the brain and spinal cord) and that of PTV linked encephalomyelitis (neuronal necrosis, colonic oedema and atrophic enteritis) (Possatti *et al.*, 2018a). The increased severity of the observed pathology and the high mortality rate of the farms with CT outbreaks was attributed to the synergistic effect of PTV. Conversely, the role of APPV as an immunosuppressive agent was not explored. Further research is needed to characterise the role of APPV in co-infections and define the potential immunosuppressive effect on the host.

Porcine reproductive and respiratory syndrome (PRRS) is one of the most significant diseases affecting both the British and the global swine industry. The disease impacts not only the health and welfare of the animals but also has direct economic consequences due to variable to high mortality and indirectly through reduced daily weight gain, lower reproductive efficiencies and increased veterinary interventions. The severity of the clinical signs associated with PRRS varies depending on the age of the animal at infection: in animals of breeding age, clinical signs relate to the reproductive issues such as decrease in conception rate, infertility, increase in abortions, birth of

premature piglets and/or stillborn or mummified fetuses but also sudden death of sows (Done, Paton and White, 1996; Lunney *et al.*, 2016; Burkard *et al.*, 2017). Young pigs between the ages of 4 to 12 weeks most commonly develop clinical signs consistent with respiratory disease including pyrexia, depression, anorexia, respiratory distress and pneumonia, which contribute to increased post-weaning mortality (Keffaber *et al.*, 1992; Done, Paton and White, 1996; Li *et al.*, 2016; Haiwick *et al.*, 2018). As PRRSV can be found in piglets of a similar age as unresolved APPV infections, and often is present in co-infections with other porcine viruses such as PCV2, including APPV it is a suitable candidate for co-infection studies in 10-week-old piglets naturally infected with APPV (Keffaber *et al.*, 1992; Houben, van Reeth and Pensaert, 1995; Kritas *et al.*, 2007; Yuan *et al.*, 2021).

Like APPV, PRRSV is also a single-stranded positive-sense enveloped virus. The virus belongs to the *Arteriviridae* family and is classified into species 1 (European strains) and species 2 (North American strains). Both species emerged simultaneously from a distant common ancestor in early 1990 late 1980 respectively, with highly pathogenic strains of species two emerging in China in 2006 (Keffaber 1989; Dial *et al.*, 1990; Wensvoort *et al.*, 1991; Tian *et al.*, 2007; Lunney *et al.*, 2016). The European species can be further sub-categorised, dependent on geographical distribution and the sequence of the open reading frame seven with subtype 1 being pan-European whilst subtypes 2 and 3 having limited circulation in Eastern Europe (Stadejek *et al.*, 2008). Since its introduction in 1991, PRRSV species 1, subtype 1 has been the only one detected within the UK and is now considered endemic; the introduction of other more virulent subtypes such as PRRSV species 1 subtype 2 (PRRSV-1.2) from Europe is considered a risk to the UK pig industry (Frossard *et al.*, 2017; Williamson, Frossard and Thomson, 2018).

5.2 Hypothesis, aims and objectives

In this chapter, the main aim was to investigate the importance of APPV as an immunosuppressive agent and to understand the possible role of APPV in co-infections. The hypothesis is that a progressive APPV infection would alter the infection dynamics and/or the host's immune response to a secondary pathogen such as PRRSV, increasing the severity of the disease outcome. To test this hypothesis 10-week-old piglets from an APPV induced congenital tremor type A-II (CT A-II) field case (as described in Chapter 4) were co-infected with PRRSV-1.2 to study the interaction of APPV and this pathogen during concurrent infection and determine if APPV has the potential to affect the overall clinical disease outcome for the host.

5.3 Study design

An APPV/PRRSV-1.2 co-infection study was performed in collaboration with Moredun Scientific (MSL) using their pre-established PRRSV challenge strain and protocol under Home Office license PFA7E7AD6. Ethical approval was obtained from the Moredun Research Institute (MRI) Animal Experiments Committee (E29/19).

Sixteen mixed breed (Large White x Duroc) piglets (either $APPV^{+ve}$ or $APPV^{-ve}$ by polymerase chain reaction [PCR]) from the Scottish congenital tremor field case (described in Chapter 4) were selected to investigate the potential immunosuppressive effects of a previous natural APPV infection on PRRSV infection dynamics at 10 weeks of age. Group sizes were calculated based on viraemia data from previous PRRSV challenge studies at MRI (D. Reddick personal communication) by Biomathematics and Statistics Scotland (BioSS). BioSS estimated that seven animals per group were sufficient to detect a $1x10^2$ magnitude difference between the $APPV^{+ve}/PRRSV^{+ve}$ and $APPV^{-ve}/PRRSV^{+ve}$ groups with an 80% power. Piglets were divided into three groups (Table 5-1): a negative control group APPV negative and not

challenged with PRRSV “uninfected” containing two animals, a group negative for APPV and inoculated with PRRSV “APPV^{-ve}/PRRSV^{+ve}” (seven animals), and an APPV positive PRRSV inoculated group “APPV^{+ve}/PRRSV^{+ve}” (seven animals).

All piglets were selected from the same farrowing group within six litters of which three produced piglets without clinical signs of CT (four out of seven of the APPV^{-ve}/PRRSV^{+ve} and both the animal in the negative control group) and the remainder had a mix of CT affected and unaffected animals (one APPV^{-ve}/PRRSV^{+ve} and seven APPV^{+ve}/PRRSV^{+ve}); in addition, all litters had both APPV ribonucleic acid (RNA) positive and negative piglets. Animals were considered APPV negative if at 2.5 weeks of age there were no observable clinical signs, and quantitative RT-PCR (RT-qPCR) detected no APPV RNA in an ear notch and serum sample collected at the same time as the clinical observations. Conversely, APPV positive animals had visible tremors at 2.5 weeks of age, and APPV RNA was detected in the paired ear notch and serum sample. All piglets were negative for the presence of antibodies to PRRSV as determined by enzyme-linked immunosorbent assay ([ELISA], PRRS X3 Ab ELISA-IDEXX) as described in 5.4.3, and no PRRSV virus was detected by Virotype PRRSV RT-PCR (Indical biosciences) as described in 5.4.4 prior to inoculation.

Table 5-1: Summary of study groups based on selection criteria at 2.5 weeks of age.

Group	Clinical signs	APPV Serum Result	APPV Ear tissue result	PRRSV serum result	PRRSV Antibody result
Uninfected	No	No virus detected	No virus detected	No virus detected	Negative
$APPV^{-ve}$/ $PRRSV^{+ve}$	No	No virus detected	No virus detected	No virus detected	Negative
$APPV^{+ve}$/ $PRRSV^{+ve}$	Yes	Positive	Positive	No virus detected	Negative

The $APPV^{-ve}$/$PRRSV^{+ve}$ and $APPV^{+ve}$/$PRRSV^{+ve}$ piglets were housed in their groups within the specified pathogen free rooms in the High Security Unit (containment level 2) at Pentlands Science Park. Within each room animals had straw bedding and plastic balls for environmental enrichment to allow them to exhibit natural behaviour, there was also a built-in penning area to minimise stress associated with separating and moving animals into unfamiliar areas for sampling procedures. As the uninfected group were healthy animals that did not receive any PRRSV inoculum they were housed separately in a low containment unit. All animals were acclimated for seven days before the study's commencement, as shown in Figure 5-1 (from nine weeks of age). The $APPV^{-ve}$/ $PRRSV^{+ve}$ and $APPV^{+ve}$/$PRRSV^{+ve}$ groups were inoculated intranasally at 10 weeks of age with 10 ml (5 ml per nostril) of 1.12×10^6 $TCID_{50}$/ml (1.3×10^9 copies/ml) of PRRSV-1.2 (Genbank accession number: KC714015.1).

Figure 5-1: Housing within the High Security Unit at Pentlands Science Park.

Rectal temperatures were taken daily from day 1 to 13, however due to trained staff shortages rectal temperatures were not collected prior to inoculation on day 0 or from the uninfected group. Serum and nasal swabs samples were collected on day 0, 1, 3, 5, 7, 10 and 14 for APPV RT-qPCR (2.2.3) and PRRSV RT-qPCR (5.4.4). Serum samples were also collected to be tested by APPV ELISA (2.4.2) and a PRRSV antibody ELISA (PRRS X3 Ab ELISA, IDEXX).

On day 14, the piglets were euthanised using Pentobarbitone (Pentoject, Animal care Ltd) and a PM performed. The lungs were removed and each lobe scored for consolidation as described in 5.4.5. bronchoalveolar lavage was collected by lavaging the lung using 10 ml of sterile PBS instilled into the lung via a syringe. The lung was massaged before collection of the lavage fluid via the syringe and placing immediately into a sterile falcon tube. Tissue samples were collected following the same procedure described in 3.5, Figure 3-22. Except for the right caudal lung sample, taken for RT-qPCR analysis and histopathology, all other tissue samples including brain, cervical spinal cord and superficial inguinal lymph node were collected and immediately frozen at -80°C for RT-qPCR analysis. From each pig, the spleen was collected and splenocytes prepared as described in 5.4.1 for lymphocyte re-stimulation

assays (porcine IFN-γ ELISpot BASIC, Mabtech). The spleen was placed in transport and wash media (TWM) (Hank's buffered salt solution without calcium or magnesium plus 2% heat inactivated pestivirus free fetal bovine serum (FBS), 200 units/ml penicillin, 200 µg/ml streptomycin, and 200 µg/ml gentamycin) and transported from the PM suite to the laboratory on ice.

5.4 Techniques for the evaluation of PRRSV infection

5.4.1 Preparation of splenocytes

The spleens were washed twice in Hank's buffered salt solution without calcium or magnesium (HBSS) and cut into small pieces before transfer to a stomacher bag already containing 15 ml of TWM and stomached for 30 seconds. The supernatant was passed through a 70 µm sterile cell strainer, and the total volume was adjusted to 20 ml using TWM. This was underlaid with 10 ml of Ficoll paque (Sigma Aldrich) and centrifuged at 800 x *g* for 30 minutes at 4°C before decanting the interface into a 50 ml Falcon tube and washing with 25 ml of phosphate-buffered saline (PBS). After centrifuging at 330 x *g* for five minutes at room temperature the cell pellet was washed with 15 ml of PBS. The cells were re-suspended in 3 ml of cell culture media (Roswell Park Memorial Institute Medium (RPMI) with 10% heat inactivated pestivirus FBS, 100 units/ml Penicillin and 100 µg/ml streptomycin and counted using a haemocytometer. The cells were re-suspended at $2x10^5$ cells/ml for seeding the plates for porcine Interferon-gamma ELISpot assays (continued in 5.4.2).

5.4.2 Lymphocyte re-stimulation assays: ELISpot

Porcine IFN-γ ELISpot^{BASIC} (Mabtech) assays were performed to quantify the number of PRRSV-specific interferon-gamma (IFN-γ) producing cells within

the spleen using splenocytes prepared as described in 5.4.1. The day prior to the assay re-suspended splenocytes were split into three groups and combined with either RPMI media for negative/background control wells, ConA for positive control wells at a final concentration of 5 µg/ml, or PRRSV-1.2 isolate as discussed in 5.3 at a final concentration of $5.6x10^4$ $TCID_{50}$/well for test wells for cellular stimulation assays and incubated overnight. ELISpot plates were prepared the day before the assay by priming the membrane with 50 µl of 70% ethanol per well for two minutes. The plates were washed with 200 µl of sterile water five times before adding 100 µl per well of diluted anti-porcine IFN-γ antibody solution and incubated at 4°C overnight: the coating antibody pIFN-γ-I (supplied with the kit) was diluted to a final concentration of 10 µg/ml in sterile PBS.

After incubation, the excess antibody was removed, and the plate washed as previously described. Two hundred microlitres of RPMI cell culture medium containing 10% heat inactivated pestivirus free FBS was added to each well and incubated for 30 minutes at room temperature. The media was then removed and replaced with 50 µl of the stimulated cells and incubated at 37°C in a humidified incubator with 5% CO_2 for 48 hours. Once the incubation step was complete, the cells were removed by emptying the plate, and the plate washed five times with 200 µl of PBS followed by incubation with 100 µl of the diluted detection antibody P2C11-biotin (supplied with the kit) at a final concentration of 0.5 µg/ml with PBS containing 0.5% heat inactivated pestivirus-free FBS at room temperature for two hours. The plate was washed as previously described, and 100 µl of diluted streptavidin conjugated with horseradish peroxidase (1:5,000 in PBS containing 0.5% heat inactivated pestivirus-free FBS, concentration not provided by the manufacturer) added to each well and incubated for an hour at room temperature. Finally, the plate was washed as previously detailed before adding 100 µl of tetramethylbenzidine (TMB) substrate and incubating until the spots visualised. The plate was then rinsed to stop overdevelopment in sterile water then air-dried before reading in the ELISpot reader (AID iSpot, AID) to inspect

and count spot numbers (AID ELISpot 7.0 Software). The data was expressed as number of spot forming units (SFU) per 10^6 cells. ConA and PRRSV-specific responses were reported as the fold-change in SFU/10^6 cells relative to the media-only control.

5.4.3 PRRSV ELISA

Serum samples were tested for presence of PRRSV antibodies using a commercial PRRSV ELISA kit (PRRS X3 Ab ELISA kit; IDEXX) as per the manufacturer's protocol. Briefly, 100 µl of neat positive and negative controls or 100 µl of the prediluted serum sample (diluted 1:40 in diluent buffer) were added to the appropriate pre-coated wells on the ELISA plate. The plate was sealed and incubated for 30 minutes before washing five times with 300 µl of wash buffer. One hundred microlitres of the anti-porcine IgG horseradish peroxidase conjugate were added to the plate and incubated for 30 minutes. The wash step was repeated then 100 µl of TMB substrate added to each well before a final incubation of 15 minutes. One hundred microlitres of the stop solution were dispensed into each well. All controls and samples were tested in duplicate, and the assay was performed at room temperature. The plate was read at an absorbance of 650 nm. The average value of the positive and negative controls was calculated. The test was considered valid if the average negative control was equal to or below an optical density (OD) of 0.15, and the difference between the average positive and negative control was above 0.15. The sample to positive ratio (S/P ratio) was calculated by dividing the difference between the samples value and the negative control by the difference between the positive and negative control averages. S/P ratios of less than 0.4 were considered negative and those equal to or greater than 0.4 as positive.

5.4.4 PRRSV RT-qPCR

The PRRSV RT-qPCR was performed using the Virotype PRRSV RT-PCR kit (Indical Biosciences). The commercial kit contained an all-in-one master mix formulated to provide all the necessary reverse transcription and PCR reagents including primers and probes for the detection of the North American (Texas red reporter), European (FAM reported) and high pathogenic (CY5 reporter) PRRSV species as well as an internal control (JOE reporter). The RT-qPCR was performed as per the manufacturer's instructions: 20 µl of the PRRSV master mix and 5 µl of the sample were added to the appropriate well of a 96-well 0.2 ml PCR plate (MicroAMP optical 96-well reaction plate, Applied Biosystems). Positive, negative extraction and no template controls and standards were included in each PCR test. The assay was performed on an ABI Prism 7500 instrument (Applied Biosystems) under the following thermocycling conditions: the reverse transcription step of one cycle consisting of 45°C for 10 minutes, followed by denaturation (95°C for 10 minutes) then by the PCR stage consisting of 40 cycles of denaturation at 95°C for fifteen seconds, annealing at 56°C for 30 seconds and extension at 72°C for 30 seconds.

The assay quantification was performed initially using an isolate of PRRSV (the same used for the inoculation of the piglets) of known concentration (1.12 $x10^6$ median tissue culture infectious dose 50 [$TCID_{50}$]/ml). The isolate was extracted using the MagMax automated extraction system (2.2.1.2) and a 10-fold serial dilution was used to produce a standard curve. Subsequently, plasmid standard was produced as follows: the PCR product (from the above PRRSV isolate) was visualised on a 2% agarose gel (2.2.2), and a number of bands excised, cleaned up using the QIAquick gel extraction kit (2.2.4) and sent for Sanger sequencing (Eurofins Genomics) to confirm identity. The confirmed European strain band’s purified product was cloned using the pGEM-T easy vector system, as outlined in 2.3. The plasmid containing the PRRSV European species sequence was then quantified (2.2.5), and a 10-fold

serial dilution of this was used for the creation of a standard curve; a copy number for this was determined using the same method as outlined in 2.3.8. The plasmid standards with a known copy number were used to determine the copy number of the extracted isolate standards. The initial assays quantification results were then adjusted accordingly to reflect the change from semi quantification ($TCID_{50}$/ml) to absolute (copies/ml). Results were classified, according to manufacturer's instructions: the assay was valid if the positive control yielded a signal in all channels and the negative control had signal in the internal positive control channel only (Joe). Samples were considered positive for a species if a positive signal was observed in the respective channel North American (Texas red reporter), European (FAM reported) and high pathogenic (CY5 reporter) and the sample also had a signal in the internal positive control channel (Joe). Samples were therefore considered negative if no signal was observed in the respective channel for the species, but a positive signal was still observed in the internal positive control channel.

5.4.5 PRRSV pathology and immunohistochemistry

A blinded gross pathological examination of the lung was conducted at PM. Each lung lobe (shown in Figure 5-2) was scored for consolidation using a modified scoring system (Jericho and Langford, 1982). This score was then converted into a score relative to the lung lobe's surface area, and each lobe's relative size: apical and cardiac lobes were scored out of 10, the diaphragmatic lobes scored out of 27.5 and the intermediate lobe out of five. The weighted scores were then used to calculate a total affected lung score out of 100 (adapted from Halbur *et al.* (1995)). As per Moredun Scientific standardised protocol samples from the right caudal lung were collected for histology and fixed in 60 ml Cellstor pots prefilled with 10% neutral buffered formalin (CellPath Ltd)

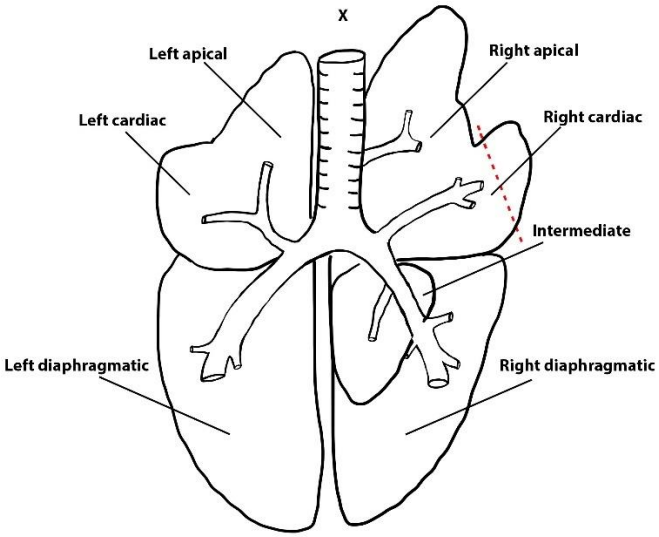

Figure 5-2: Porcine lung anatomy. The diagram shows the position of each lung lobe and its respective bronchus. X shows the point of entry for the PRRSV intranasal inoculation into the lung. The red dash line represents the section of the right cardiac lung collected for histology. Image prepared by John Lawlor.

The formalin-fixed right cardiac lung tissue samples (Figure 5-2) were trimmed, blocked, cut and mounted onto slides as outlined (2.5.1) by the Histopathology Surveillance Unit at the MRI following standard operating protocols used for diagnostic submissions. Mounted tissue sections were stained with Haematoxylin Z and Eosin (H&E,Cellpath Ltd) and a blinded evaluation for the presence of morphological changes and interstitial pneumonia (IP) conducted; this information was used to produce an IP score using the (Halbur *et al.*, 1995) scoring system which bases the score by presence and severity of PRRSV lesions as shown in Table 5-2. Paired slides were also sent to the veterinary diagnostic laboratory at Iowa State University for PRRSV immunohistochemistry (IHC) (evaluation criteria detailed in Table 5-2) which utilises an antibody that detects a nucleocapsid protein of PRRSV (Halbur *et al.*, 1994). Paired slides were also evaluated using BaseScope *in situ* hybridisation (ISH) to detect APPV as described in 2.5.2.

Table 5-2: Score criteria for interstitial pneumonia and PRRSV immunohistochemistry evaluation.

Interstitial Pneumonia		PRRSV Immunohistochemistry	
Score	Interpretation	Score	Interpretation
0	Negative	0	Negative
1	Mild focal	1	Positive - few positive cells
2	Mild multifocal	2	Positive - moderate numbers of positive cells
3	Moderate focal	3	Positive - large numbers of positive cells
4	Moderate multifocal		
5	Severe focal		
6	Severe multifocal		

5.5 Statistical analysis

Generalised Additive Mixed-effects Models (GAMMs) were used to investigate the effect of an existing APPV infection on PRRSV infection dynamics using viral loads in serum (RT-qPCR), PRRSV-specific antibody responses in serum, and rectal temperatures over time. GAMMs fit non-parametric smoothing functions relating a trait of interest to a covariate (in this case, time) and allow comparison of trajectories among groups of variables without the need to assume that traits all follow the same functional form of trajectory (e.g. linear, quadratic). The models shown in Table 5-3 compare the potential responses measured by changes in the variable of the APPV negative and

positive PRRSV inoculated groups ($APPV^{-ve}/PRRSV^{+ve}$ and $APPV^{+ve}/PRRSV^{+ve}$) throughout the study. The model with the lowest Akaike's Information Criteria (AIC) value (an estimator of the fit of the model to the data) was considered the most appropriate model to describe the relationship between groups for each variable (Table 5-4). Non-parametric Kruskal-Wallis H tests were used to determine differences in tissue viral loads, lung pathology and PRRSV-specific cellular immune responses (using ELISpot) in $APPV^{-ve}$ and $APPV^{+ve}$ groups at post-mortem. The study's analysis was performed using R version 3.6.1 (R Core Team, 2019), and Generalised Additive Mixed-effects Models implemented using the gamm4 package (Wood and Scheipl, 2017).

Table 5-3: Generalised additive mixed-effects models

Model number	Purpose of the model	Expected model outcome
0	Null model no differences observed between groups or response over time	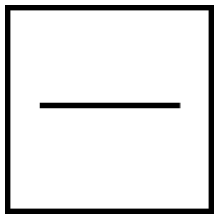
1	A difference observed between the groups but no change in the response over time	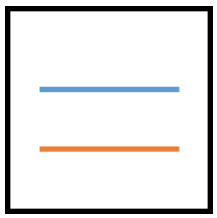
2	No difference observed between groups, but a change in the response observed over time	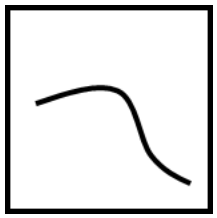
3	A difference between the group's intercept and a change in the response over time	
4	No difference in the intercept between groups but a change in the response observed over time	
5	A difference in the intercept and the response observed over time in both groups	

The intercept is the value of Y when X is equal 0.

Table 5-4: Assessment of model fit for the viral loads in serum, antibody response in serum and rectal temperature (temp). The most appropriate model with the lowest AIC value is highlighted in red.

Model	Degrees of Freedom	AIC* PRRSV viral load in serum	AIC* PRRSV antibody response	AIC* APPV antibody response	AIC* rectal temp
0	3	427.3	152.7	-196.5	340.1
1	4	428.3	157.4	-194.2	332.2
2	5	280.5	-57.0	-193.5	270.0
3	6	283.3	-50.4	-191.2	262.1
4	7	295.4	-35.2	-181.2	267.3
5	8	298.2	-28.7	-178.9	259.4

*AIC (Akaike's Information Criteria) value is the estimator of the quality of the model

5.6 Results

The pigs included in the APPV^{-ve}/PRRSV^{+ve} group were selected initially based on absence of clinical signs and APPV RNA in either the ear notch or serum sample taken at 2.5 weeks of age. However, even though the animals met these criteria, it was subsequently determined after PM that two pigs in this group had APPV RNA in tissues, suggesting the animals had become APPV infected post selection before the commencement of the study at 10 weeks of age therefore the two animals were excluded from the APPV negative PRRSV inoculated group on this basis. On commencement of the study, three of the seven piglets in the APPV^{+ve}/PRRSV^{+ve} group were still displaying mild clinical signs of congenital tremors exacerbated under stress. Although no formal clinical observations or weighing of the animals were conducted as part of the trial, observations during welfare checks post-inoculation showed that animals in the APPV^{+ve}/PRRSV^{+ve} group appeared more lethargic, accompanied by appetite suppression and breathing difficulties from 5—8 days post-inoculation (DPI) compared to the APPV negative group, with one animal (935) showing noticeable signs of weight loss.

5.6.1 Assessment of clinical outcome: rectal temperatures

A GAMM was performed to investigate the differences in temperatures between the APPV^{-ve}/PRRSV^{+ve} and APPV^{+ve}/ PRRSV^{+ve} groups throughout the study. As shown in Figure 5-3, the APPV^{+ve}/PRRSV^{+ve} group after 2 DPI had higher temperatures than that of the APPV^{-ve}/PRRSV^{+ve} negative group by an average of 0.58°C over the course of the study. In addition, the APPV^{+ve}/PRRSV^{+ve} group had a more extended pyrogenic response where average temperatures remained greater than or equal to 39.8°C for six days (4—9 DPI, peaking on 7 DPI at an average of 40.4°C) compared to the APPV^{-ve}/PRRSV^{+ve} group which only had average temperatures greater than or equal

to 39.8°C on two days (7-8 DPI with the average on both days reaching 39.8°C).

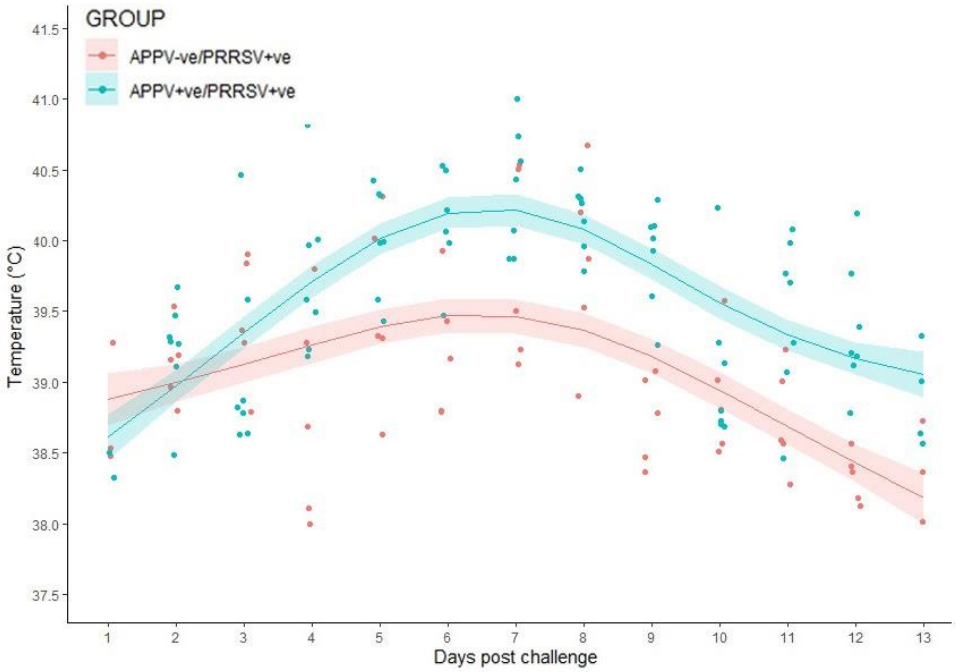

Figure 5-3: Generalised additive mixed effect model for rectal temperatures over time. The model shows the rectal temperature for APPV^{-ve}/PRRSV^{+ve} (n=5, red) and the APPV^{+ve}/PRRSV^{+ve} (n=7, blue) piglets. The line of best fit with standard error (shaded area) is presented for each treatment group.

5.6.2 Viraemia

The APPV^{+ve} and APPV^{-ve} PRRSV^{+ve} groups were PRRSV positive by RT-qPCR from 1 DPI and remained positive throughout the study. Peak PRRSVviraemia was observed on 5 DPI with an average viral load of 6.25x10^{8} copies/ml for the APPV^{-ve} and 4.69x10^{8} copies/ml for the APPV^{+ve} group. PRRSV was not detected in the serum of the uninfected negative control group. Generalised additive mixed effect model analysis (as shown in Figure 5-4) performed to determine the difference in PRRSV viral load between the

APPV^{+ve} and APPV^{-ve} groups throughout the study showed no significant differences between them.

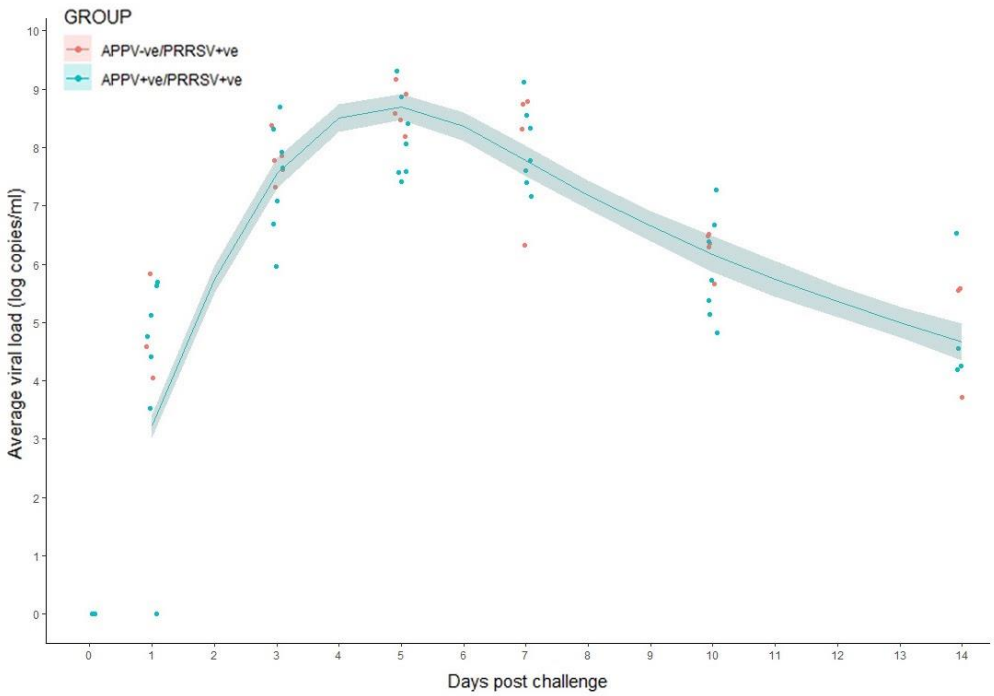

Figure 5-4: Generalised additive mixed effect model for PRRSV viral load over time. The model shows the average viral load based on two technical replicates for piglets in the APPV^{-ve}/PRRSV^{+ve} (n=5, red) and the APPV^{+ve}/PRRSV^{+ve} (n=7, blue) groups with the line of best fit presented and standard error indicated by the shaded area.

APPV was undetectable by RT-qPCR both in the APPV^{-ve} and uninfected groups. The average APPV viral load in serum in the APPV^{+ve} group, as shown in Figure 5-5, remained consistently high (1.94—3.12x10^5 copies/ml) until 3 DPI. It then decreased to undetectable levels at 7 DPI before increasing to a mean viral load of 3.59x10^5 copies/ml at 14 DPI.

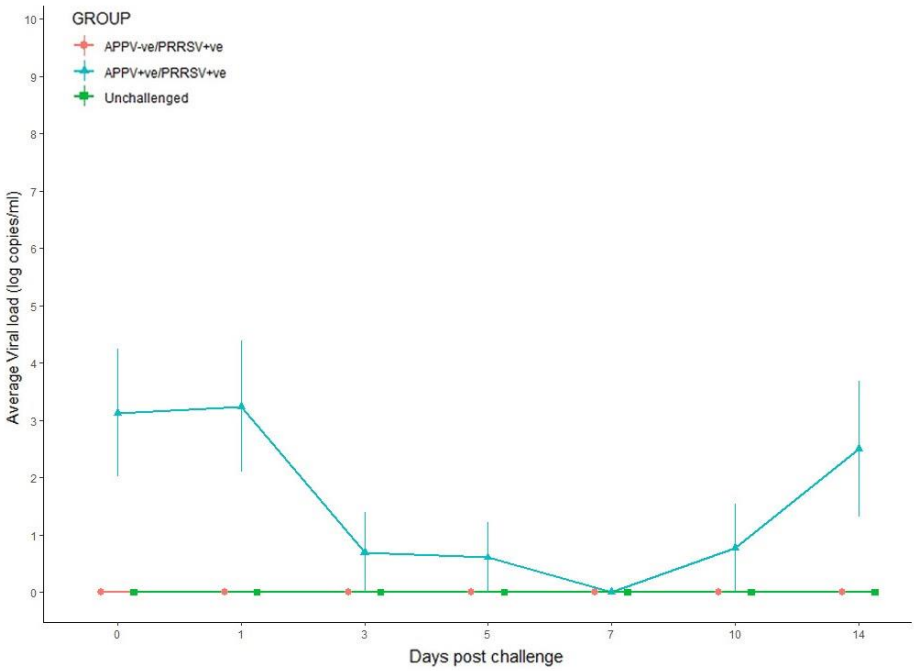

Figure 5-5: Average APPV viral load in serum (log_{10} copies/ml +/- SEM) over time for the $APPV^{-ve}/PRRSV^{+ve}$ (n=5, red), the $APPV^{+ve}/PRRSV^{+ve}$ (n=7, blue) and the uninfected group (n=2, green).

5.6.3 Presence of APPV and PRRSV in nasal secretions

One piglet from the $APPV^{-ve}$ group returned a PRRSV-positive nasal swab ($6.04x10^3$ copies/ml) on 5 DPI and one piglet from the $APPV^{+ve}$ group had a PRRSV-positive nasal swab ($4.9x10^4$ copies/ml) on 7 DPI as shown in Figure 5-6. Due to the low number of PRRSV-positive nasal swabs found in this study, no statistical analysis was performed on this data.

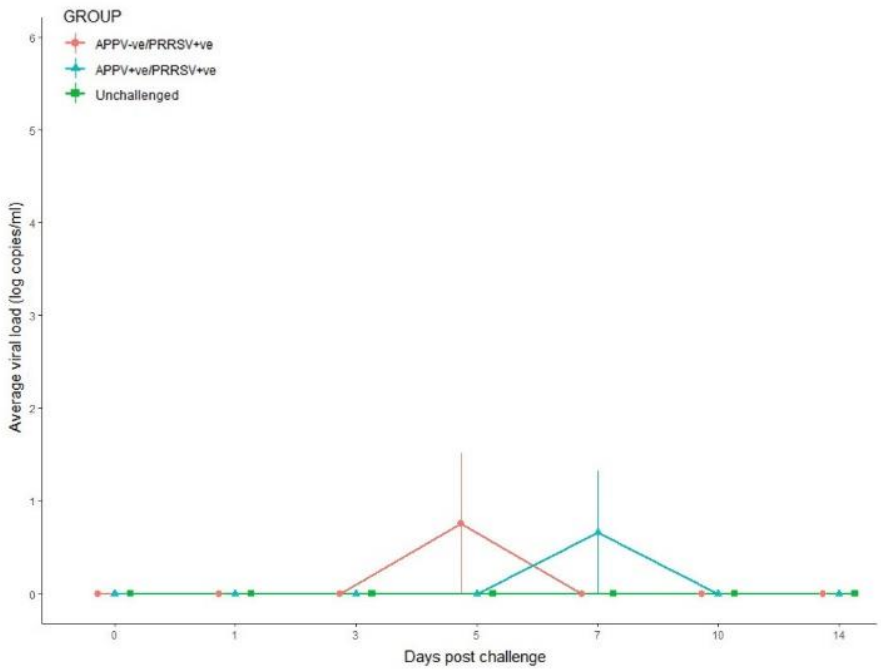

Figure 5-6: Average PRRSV viral load based on two technical replicates (log_{10} copies/ml +/- SEM) in nasal swabs over time for the $APPV^{-ve}/PRRSV^{+ve}$ (n=5, red), the $APPV^{+ve}/PRRSV^{+ve}$ (n=7, blue) and the uninfected (n=2, green) groups.

The $APPV^{+ve}$ group showed consistent shedding of APPV (measured as PCR positivity) nasally throughout the study except for 3 DPI, where no APPV was detected in the swabs for any piglet within the group (Figure 5-7). No APPV was detected in any of the other treatment groups ($APPV^{-ve}/PRRSV^{+ve}$ group and uninfected group) at any time-point.

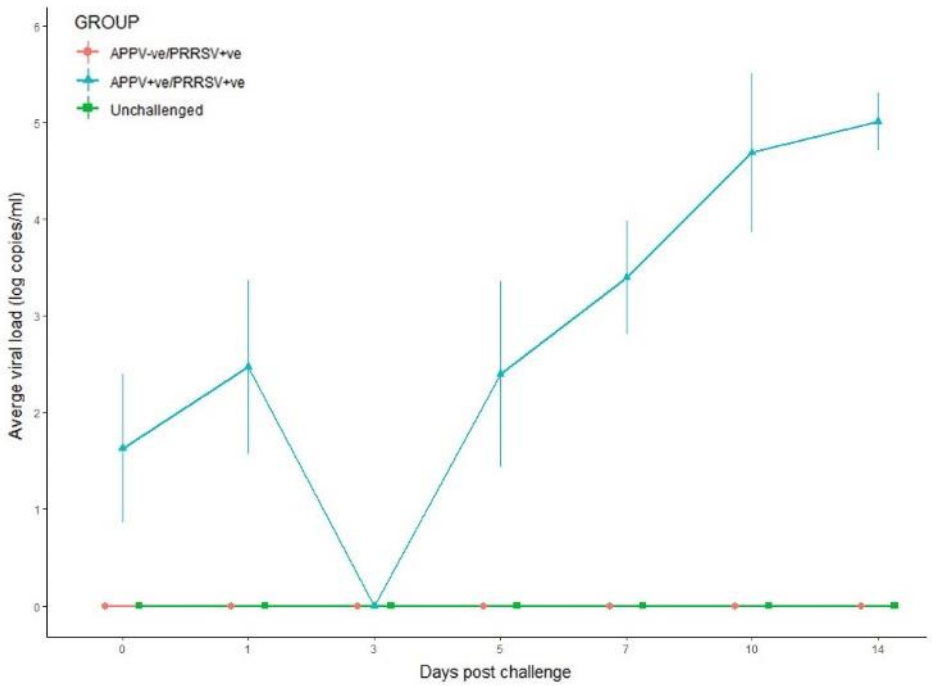

Figure 5-7: Average APPV viral load based on two technical replicates (log_{10} copies/ml +/- SEM) in nasal swabs over time for the $APPV^{-ve}/PRRSV^{+ve}$ (n=5, red), the $APPV^{+ve}/PRRSV^{+ve}$ (n=7, blue) and the uninfectd (n=2, green) groups.

5.6.4 Assessment of virus-specific immune responses

5.6.4.1 Humoral response

All animals in both the $APPV^{-ve}/PRRSV^{+ve}$ and $APPV^{+ve}/PRRSV^{+ve}$ groups were PRRSV seronegative until 10 DPI at which point all PRRSV inoculated animals became seropositive for PRRSV IgG antibodies. The uninfected group remained seronegative for PRRSV through the course of the study. A GAMM was performed to investigate the antibody titre differences between the $APPV^{-ve}/PRRSV^{+ve}$ and $APPV^{+ve}/PRRSV^{+ve}$ groups. As shown in Figure 5-8, both the APPV positive and negative groups show large data variability and overlapping profiles indicating no differences in antibody levels between the groups. The piglets were also tested for APPV antibody levels (IgG). No difference was

observed in these APPV antibody levels for either the APPV^{-ve}/PRRSV^{+ve} or APPV^{+ve}/PRRSV^{+ve} groups throughout the study, as shown in Figure 5-9.

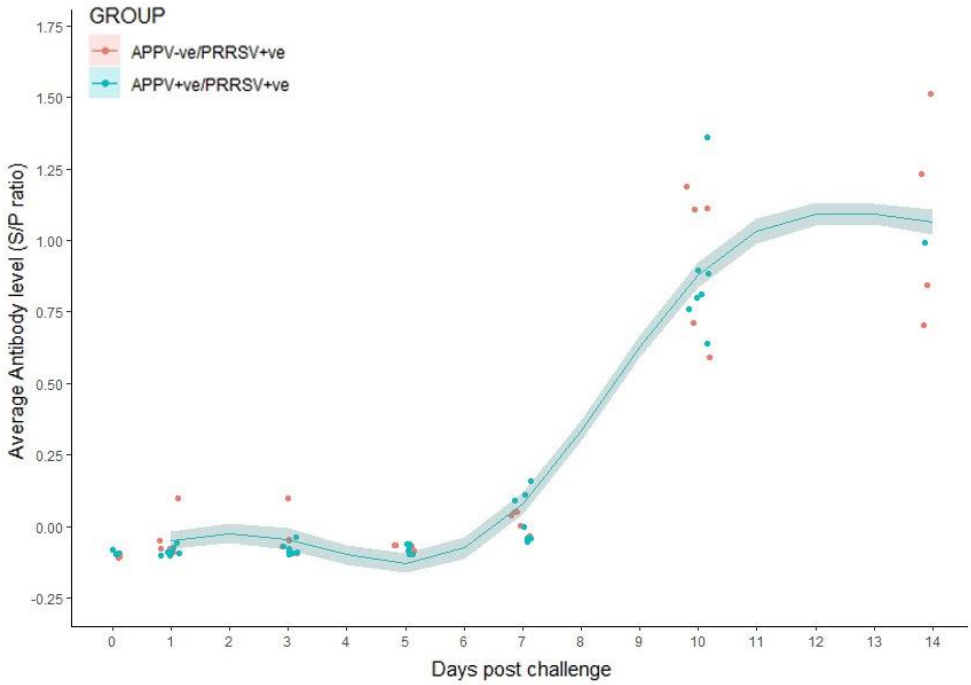

Figure 5-8: Generalised additive mixed effect model for PRRSV antibody level over time (S/P ratio). The model shows the average antibody level based on two technical replicates for piglets in the APPV^{-ve}/PRRSV^{+ve} (n=5, red) and the APPV^{+ve}/PRRSV^{+ve} (n=7, blue) groups with the line of best fit presented and standard error indicated by the shaded area.

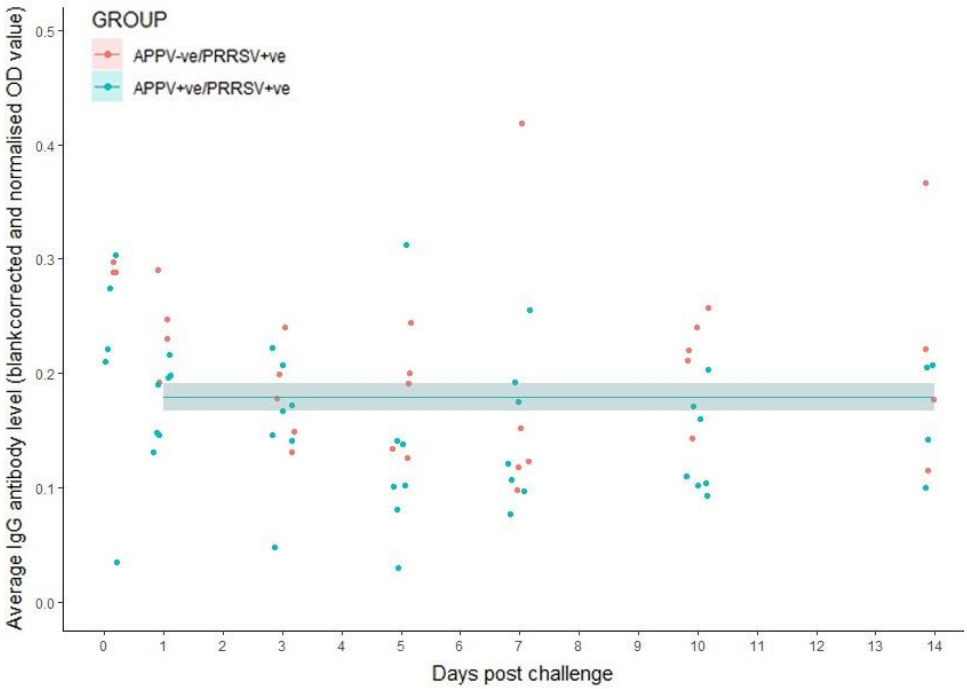

Figure 5-9: Generalised additive mixed effect model for APPV antibody level over time (blank corrected normalised). The model shows the average antibody level based on two technical replicates for piglets in the APPV^{-ve}/PRRSV^{+ve} (n=5, red) and the APPV^{+ve}/PRRSV^{+ve} (n=7, blue) groups with the line of best fit presented and standard error indicated by the shaded area.

5.6.4.2 PRRSV specific cellular immune responses

ELISpot was used to determine numbers of IFN-γ producing cells within the spleen following stimulation with either the T cell mitogen ConA or PRRSV antigen, with the aim to capture both polyclonal and PRRSV-specific T cell responses. The results are shown in Figure 5-10. Data was analysed using a Kruskal-Wallis H test, which showed no significant difference in fold-change of IFN-γ producing splenocytes for the APPV^{-ve}/PRRSV^{+ve} and APPV^{+ve}/PRRSV^{+ve} groups for stimulation by either ConA ($X^2(2)$= 1.4835, p=0.2232, df=1, eta2[H]= 0.0484) or PRRSV Isolate ($X^2(2)$=3.0857, p=0.07898, df=1, eta2[H]=0.209).

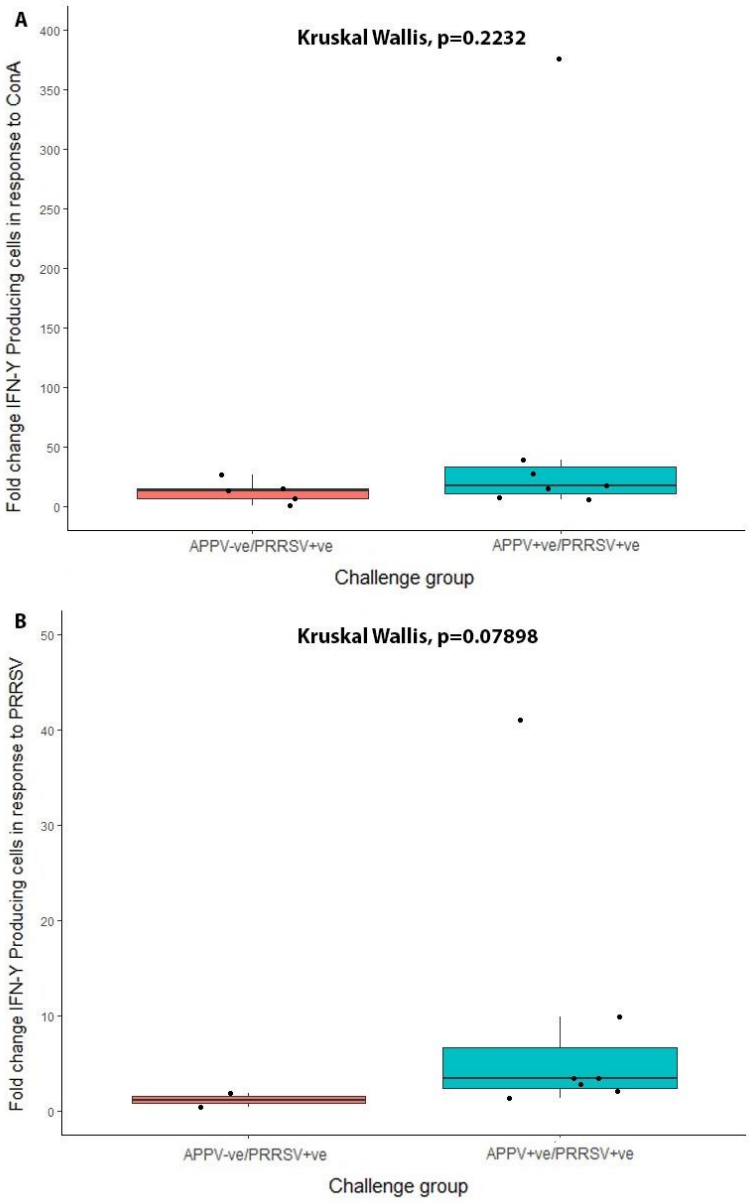

Figure 5-10: IFN-γ ELISpot of splenocytes at post-mortem. (A) The fold change in the number of IFN-γ producing splenocytes collected from the APPV-ve/PRRSV+ve (n=5, red) and the APPV+ve/PRRSV+ve (n=7, blue) groups stimulated with ConA. (B) The fold change in the number of IFN-γ producing splenocytes collected from the APPV-ve/PRRSV+ve (red) and the APPV+ve/PRRSV+ve (blue) groups stimulated with PRRSV.

5.6.5 Viral load in tissues

Tissues collected at PM compared for PRRSV viral load in $APPV^{-ve}$ and $APPV^{+ve}$ PRRSV inoculated groups to ascertain if APPV affected PRRSV viral load. As shown in Figure 5-11, PRRSV was detected in in superficial inguinal lymph node tissue of both the $APPV^{-ve}$ and $APPV^{+ve}$ groups (1.04×10^6—9.45×10^7 copies/g), as well as in the right cardiac lung tissue (9×10^4 - 5.66×10^8 copies/g) and bronchoalveolar lavage (3.50×10^4—1.33×10^7 copies/ml). Although no PRRSV titres were detected in any of the tissues tested for one of the $APPV^{-ve}/PRRSV^{+ve}$ animals (503), nor for one of the $APPV^{+ve}/PRRSV^{+ve}$ animals (939) both showed similar PRRSV titres in the right cardiac lung tissue and bronchoalveolar lavage. As determined by Kruskal-Wallis H test, no significant differences were found between the PRRSV viral load in the $APPV^{-ve}/PRRSV^{+ve}$ and $APPV^{+ve}/PRRSV^{+ve}$ groups in the following tissues: superficial inguinal lymph node ($X^2(2)= 1.9055$, $p=0.1675$, $df=1$, $eta2[H]= 0.0905$), right cardiac lung tissue ($X^2(2)= 1.9055$, $p=0.1675$, $df=1$, $eta2[H]= 0.0905$), or bronchoalveolar lavage ($X^2(2)= 1.4835$, $p=0.2232$, $df=1$, $eta2[H]= 0.0484$). Neither APPV nor PRRSV were detected in any of the tissues from the uninfected group. PPRSV was also not detected in both the $APPV^{-ve}/PRRSV^{+ve}$ or $APPV^{+ve}/PRRSV^{+ve}$ groups in the brain and spinal cord samples collected at PM; however, APPV was present in all tissue types at similar titres (brain: 2.33×10^5—9.72×10^7 copies/g, spinal cord: 6.9×10^4—5.21×10^6 copies/g, superficial inguinal lymph node: 1.89×10^5—2.77×10^7 copies/g, and bronchoalveolar lavage: 1.56×10^4—9.37×10^5 copies/ml) for the $APPV^{+ve}/PRRSV^{+ve}$, as shown in Figure 5-12.

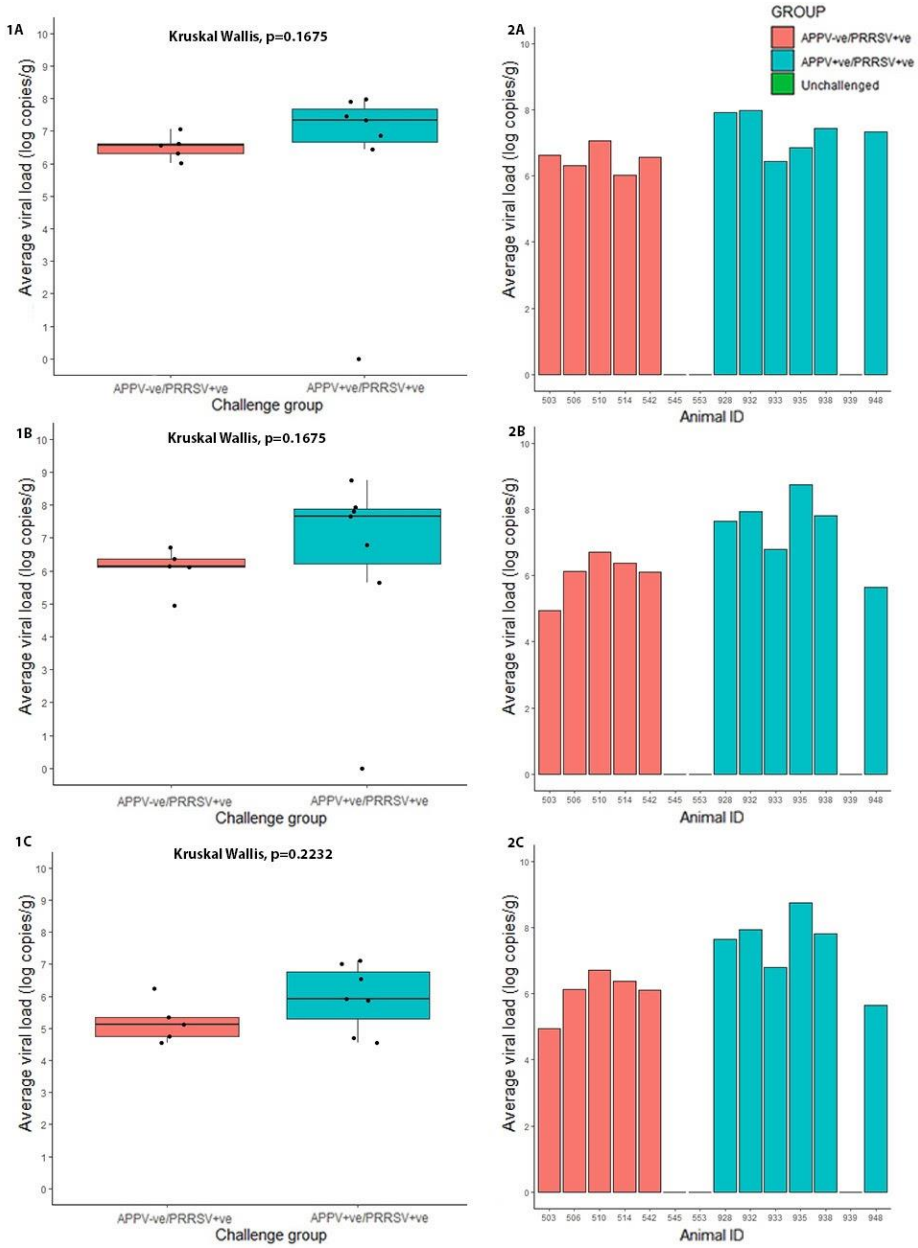

Figure 5-11: Comparison of PRRSV viral load in tissues. 1) Mean PRRSV viral load in tissues (log_{10} copies/g) in the different treatment groups: $APPV^{-ve}/PRRSV^{+ve}$ (n=5, red), $APPV^{+ve}/PRRSV^{+ve}$ (n=7, blue) and uninfected (n=2, green). 2) Average PRRSV viral load (technical replicates=2) in tissues per animal for each treatment group (log_{10} copies/g) as previously defined. (A) Superficial inguinal lymph node, (B) Right cardiac lung and (C) Bronchoalveolar Lavage.

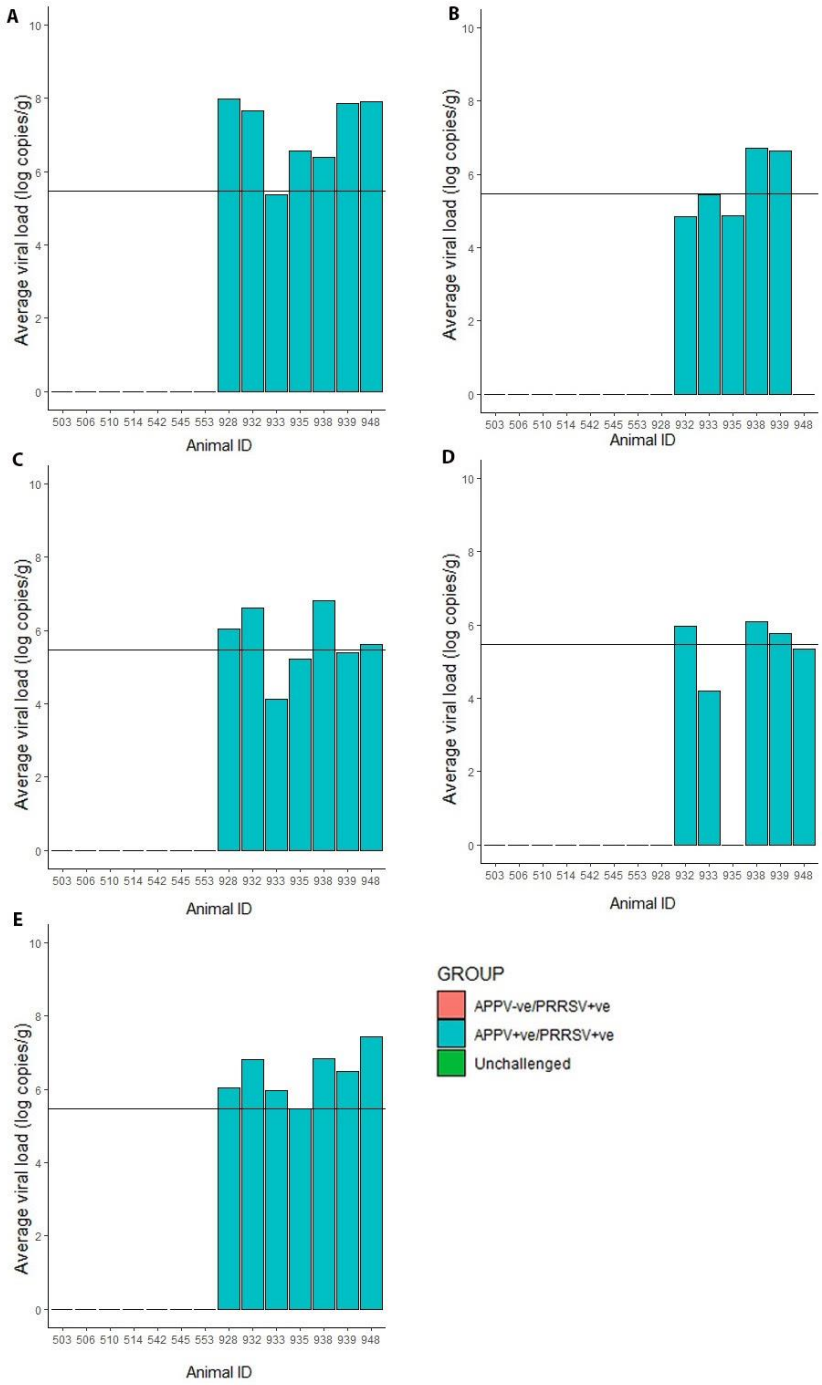

Figure 5-12: Average APPV viral load based on two technical replicates (log_{10} copies/g) in tissues in the $APPV^{-ve}/PRRSV^{+ve}$ (n=5, red), the $APPV^{+ve}/PRRSV^{+ve}$ (n=7, blue) and the uninfected (n=2, green) groups. (A) Brain, (B) Spinal cord, (C) Right cardiac lung, (D) Bronchoalveolar lavage, and (E) Superficial inguinal lymph node. The horizontal line indicates the positive cut-off for the samples.

5.6.6 Lung pathology of APPV and PRRSV

5.6.6.1 Gross lung pathology

Presence of lung pathology was assessed to determine if APPV affected the severity of disease caused by PRRSV infection. At PM, no discrete gross lesions were observed on any of the lungs from animals in either the APPV^{-ve}/PRRSV^{+ve} or APPV^{+ve}/PRRSV^{+ve} groups, but lung consolidation was variably present across the lobes. The comparisons of the lung consolidation scores for each of the two groups in each lung lobe are presented in Figure 5-13. The weighted consolidation lung scores for the individual animals in the APPV^{-ve}/PRRSV^{+ve} and APPV^{+ve}/PRRSV^{+ve} groups (Table 5-5) show that more APPV^{+ve} animals have on average higher scores than the APPV^{-ve} group in all lung areas (average total lung consolidation was 9.8/100 in the APPV^{-ve}/PRRSV^{+ve} group compared to 35.4/100 in the APPV^{+ve}/PRRSV^{+ve} group).

No significant difference as determined by a Kruskal-Wallis H test was found for the left and right cardiac lobe, the left and right diaphragmatic lobe and the total lung scores (Table 5-6) although there was a trend for increased scores in the APPV^{+ve}/PRRSV^{+ve} group. The APPV^{+ve}/PRRSV^{+ve} group however, had a statistically significant higher consolidation pathology score ($X^2(2) = 5.2381$, $p=0.0221$, $df=1$, eta2[H]= 0.4240) than the APPV^{-ve}/PRRSV^{+ve} group in both the left and right apical lobes and the intermediate lobe (Table 5-6). This trend suggests APPV may play a role in contributing to the increased amount of consolidation caused by the PRRSV infection. No consolidation was detected in the negative control group.

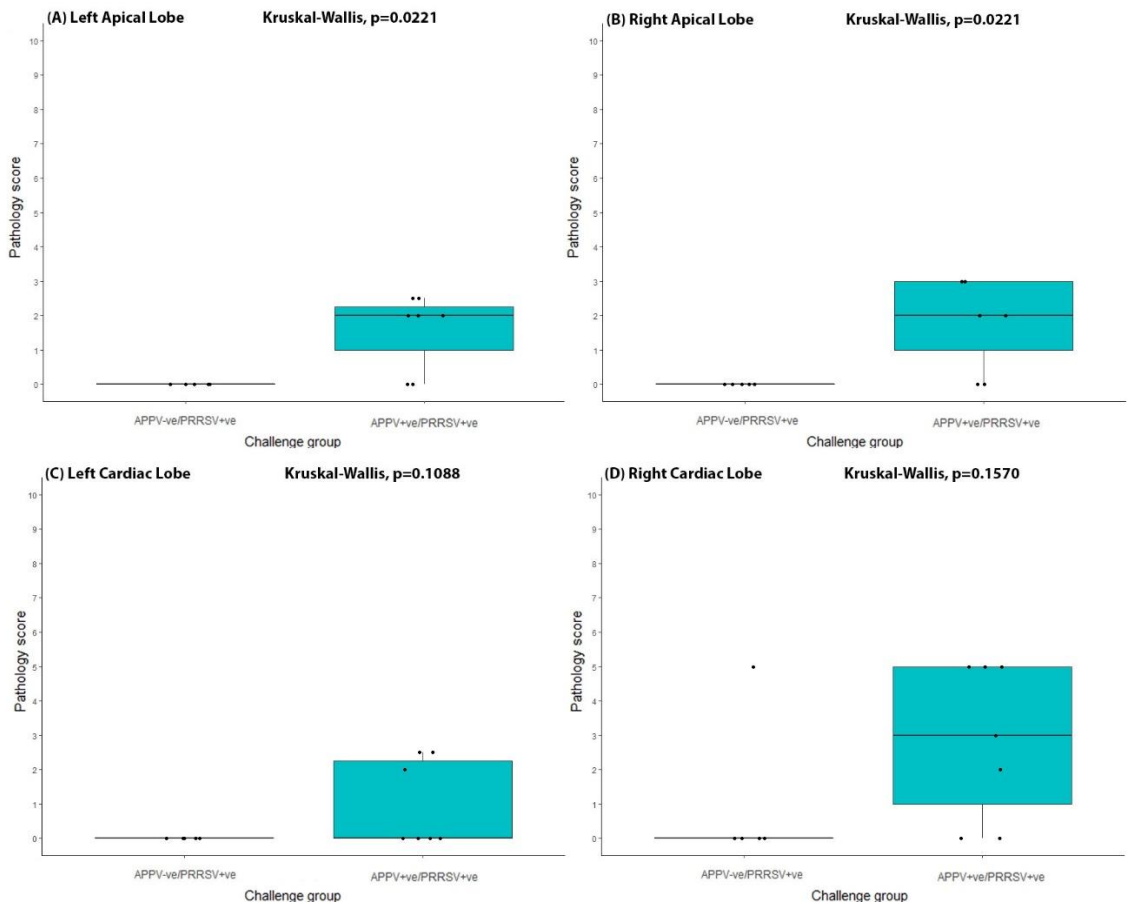

Figure 5-13: Comparison of consolidation pathology score for each lung lobe from the APPV^{-ve}/PRRSV^{+ve} (n=5, red) and the APPV^{+ve}/PRRSV^{+ve} (n=7, blue) groups. (A) left apical, (B) right apical, (C) left cardiac and (D) right cardiac score.

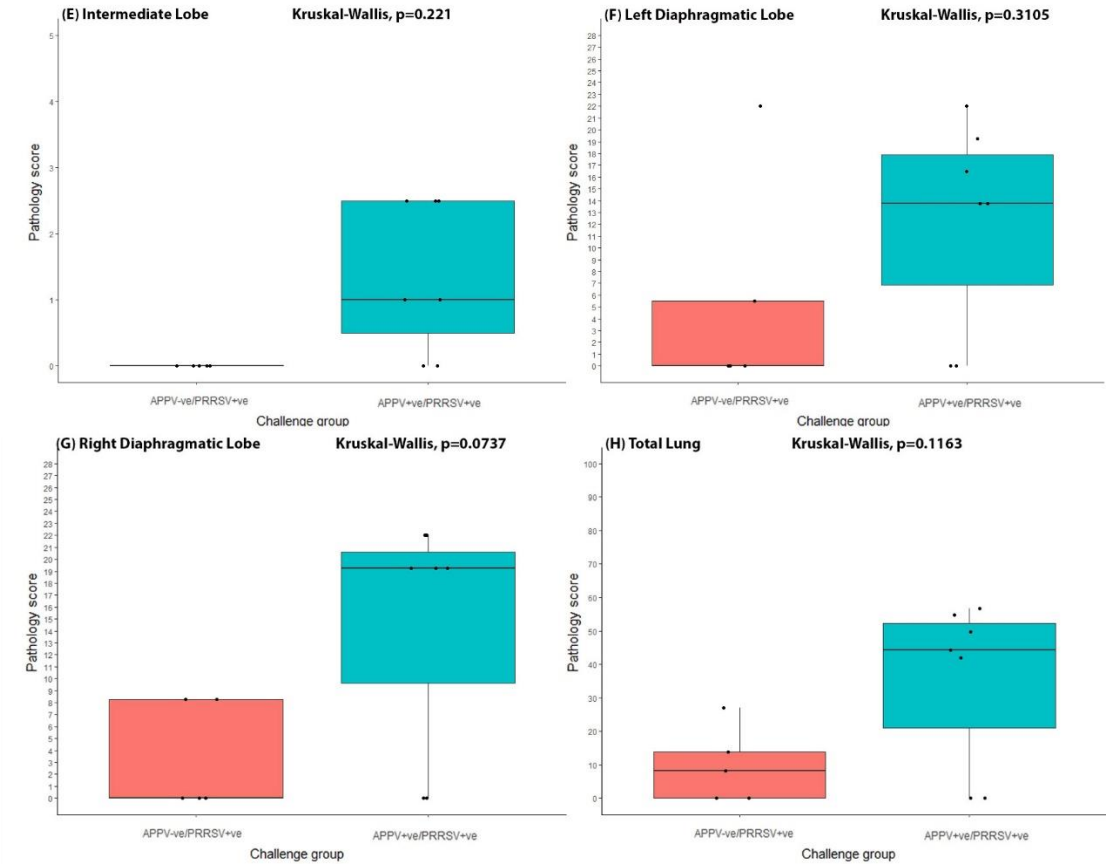

Continuation of Figure 5-13: Comparison of consolidation pathology score for each lung lobe from the APPV^{-ve}/PRRSV^{+ve} (n=5, red) and the APPV^{+ve}/PRRSV^{+ve} (n=7, blue) groups. (E) intermediate, (F) left diaphragmatic, (G) right diaphragmatic and (H) total lung score.

Table 5-5: Individual lung consolidation scores for the APPV^{-ve}/PRRSV^{+ve} (n=5) and the APPV^{+ve}/ PRRSV^{+ve} (n=7) groups.

APPV Group	ID	Left apical	Right apical	Left cardiac	Right cardiac	Left diaphragm	Right diaphragm	Intermediate	Total lung score
Negative	510	0/10	0/10	0/10	0/10	0/27.5	8.3/27.5	0/5	8.3/100
Negative	514	0/10	0/10	0/10	0/10	0/27.5	0/27.5	0/5	0/100
Negative	503	0/10	0/10	0/10	0/10	0/27.5	0/27.5	0/5	0/100
Negative	506	0/10	0/10	0/10	0/10	5.5/27.5	8.3/27.5	0/5	13.8/100
Negative	542	0/10	0/10	0/10	5/10	22/27.5	0/27.5	0/5	27/100
Average		**0/10**	**0/10**	**0/10**	**1/10**	**5.5/27.5**	**3.3/27.5**	**0/5**	**9.8/100**

Continuation of Table 5-5: Individual lung consolidation scores for the APPV^{-ve}/PRRSV^{+ve} (n=5) and the APPV^{+ve}/ PRRSV^{+ve} (n=7) groups.

APPV Group	ID	Left apical	Right apical	Left cardiac	Right cardiac	Left diaphragm	Right diaphragm	Intermediate	Total lung score
Positive	935	2/10	2/10	0/10	2/10	13.8/27.5	22/27.5	2.5/5	44.3/100
Positive	939	0/10	0/10	0/10	0/10	0/27.5	0/27.5	0/5	0/100
Positive	933	2/10	2/10	2/10	5/10	22/27.5	19.3/27.5	2.5/5	54.8/100
Positive	938	0/10	0/10	0/10	0/10	0/27.5	0/27.5	0/5	0/100
Positive	928	2.5/10	3/10	2.5/10	5/10	19.3/27.5	22/27.5	2.5/5	56.8/100
Positive	932	2.5/10	3/10	2.5/10	5/10	16.5/27.5	19.3/27.5	1/5	49.8/100
Positive	948	2/10	3/10	0/10	3/10	13.8/27.5	19.3/27.5	1/5	42/100
Average		**1.6/10**	**1.9/10**	**1/10**	**2.9/10**	**12.2/27.5**	**14.6/27.5**	**1.4/5**	**35.4/100**

Table 5-6: Kruskal-Wallis H test statistical analysis of consolidation pathology score for each area of the lung from the APPV^{-ve}/PRRSV^{+ve} (n=5) and the APPV^{+ve}/ PRRSV^{+ve} (n=7) groups.

Lung Area	Chi-Squared	P-Value	Degrees of Freedom	Effect Size
Left apical	5.2381	0.0221*	1	0.4240†
Right apical	5.2381	0.0221*	1	0.4240†
Left cardiac	2.5140	0.1088	1	0.1570†
Right cardiac	2.0031	0.1570	1	0.1000
Intermediate	5.2381	0.0221*	1	0.4240†
Left diaphragmatic	1.0286	0.3105	1	0.0029
Right diaphragmatic	3.1985	0.0737	1	0.2200†
Total lung	**2.4665**	**0.1163**	**1**	**0.1470†**

* Statistical significance: P<0.05

† Effect size: Large >0.14, Moderate 0.06<0.14, Small 0.01<0.06

5.6.6.2 Detection of APPV in the lung

APPV specific staining was detected in the right cardiac lung sections of both the APPV^{-ve}/PRRSV^{+ve} and APPV^{+ve}/PRRSV^{+ve} groups by BaseScope ISH. BaseScope ISH APPV specific probe staining was observed to be heterogeneous with the largest proportion of staining localised within the smooth muscle layer of bronchioles and endothelial cells in blood vessels. Figure 5-14 shows the difference between APPV BaseScope ISH staining *in situ* for both animals from the APPV^{-ve}/PRRSV^{+ve} (A) and APPV^{+ve}/PRRSV^{+ve} (B) groups. As expected, significantly higher APPV probe counts were found in the APPV^{+ve}/PRRSV^{+ve} group as shown in Figure 5-15 (Kruskal Wallis H test: $X^2(2)= 8.0769$, p=0.004483, df=1, eta2[H]= 0.708).

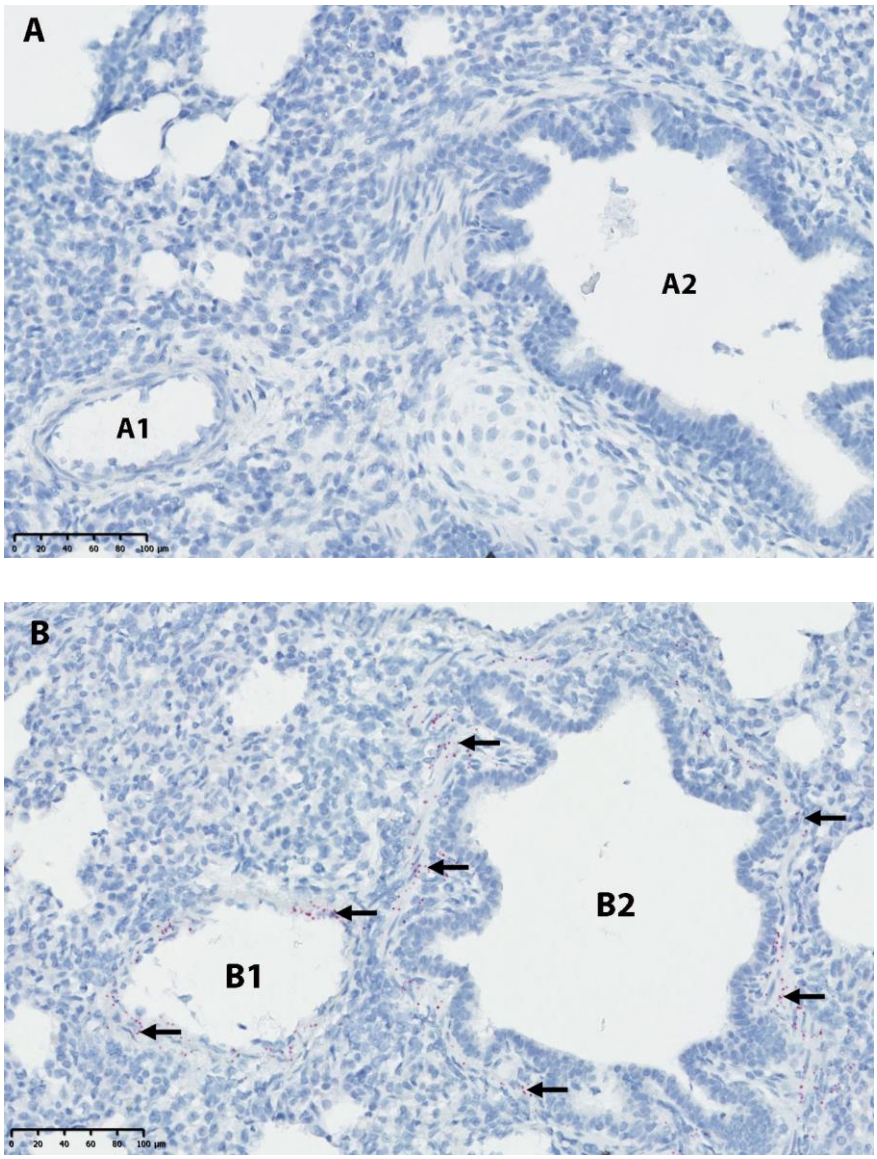

Figure 5-14: Detection of APPV within right cardiac lung tissue by BaseScope ISH RNA *in situ* hybridisation. (A) APPV negative blood vessel (lumen indicated by A1) and bronchiole (Lumen indicated by A2) from an APPV^{-ve}/PRRSV^{+ve} pig at 200x magnification. (B) APPV positive blood vessel (lumen indicated by B1) and bronchiole (lumen indicated by B2) from an APPV^{+ve}/PRRSV^{+ve} pig at 200x magnification. APPV positive probe is observed as red dots (indicated by the arrows).

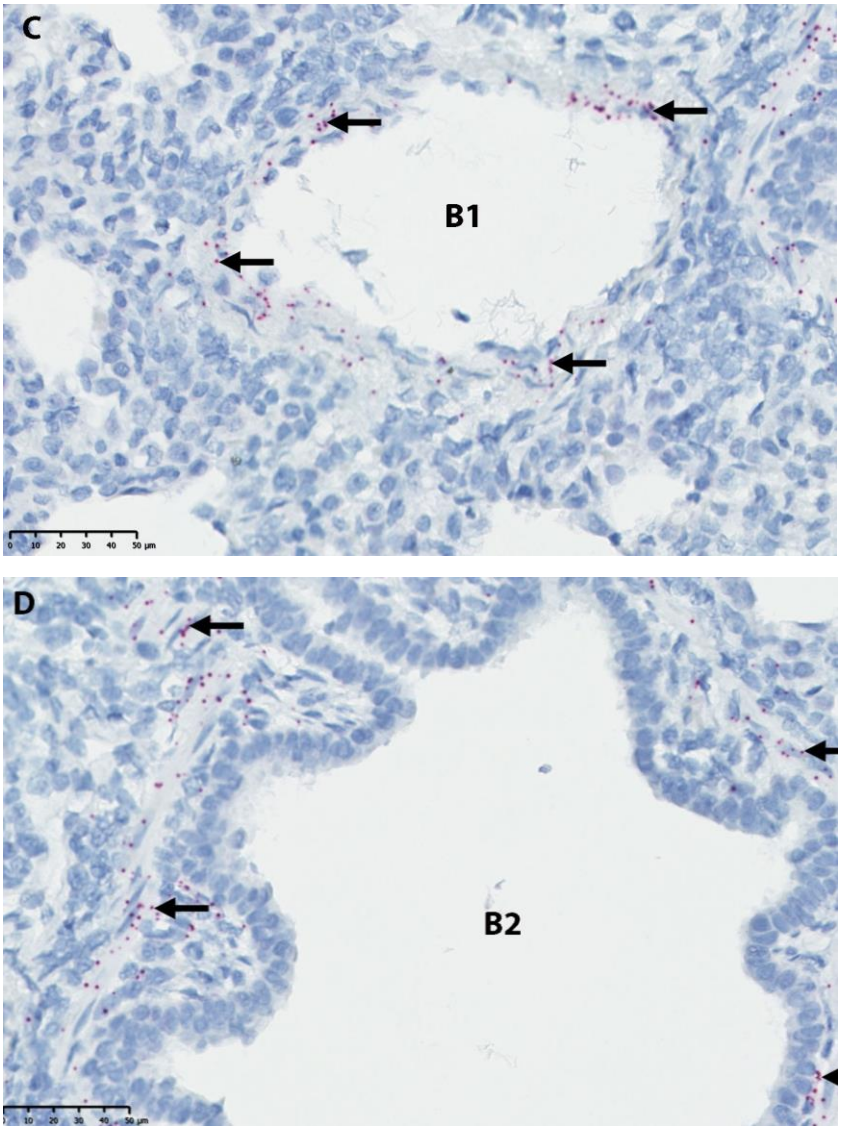

Continuation of Figure 5-14: Detection of APPV within right cardiac lung tissue by BaseScope ISH RNA *in situ* hybridisation. (C) APPV positive blood vessel (B: B1) and (D) APPV positive bronchiole (B: B2) are at a 400x magnification. APPV positive probe is observed as red dots (indicated by the arrows) concentrated in the bronchiole and blood vessels smooth muscle and endothelial cells respectively.

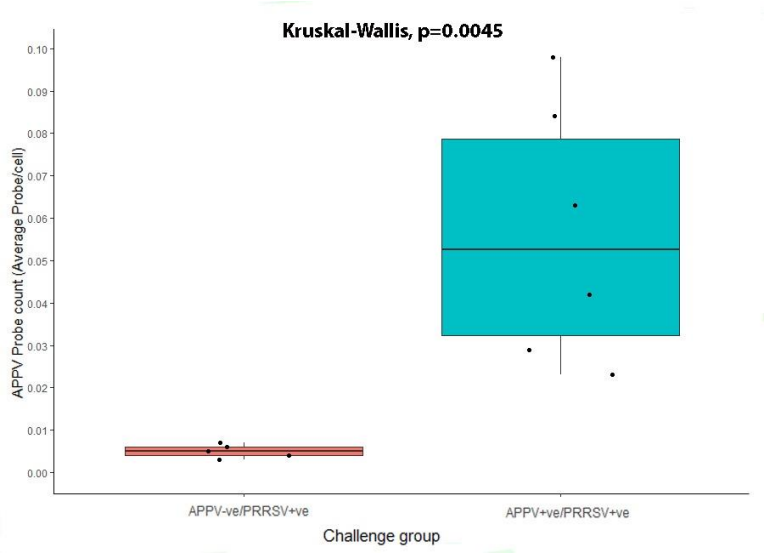

Figure 5-15: A comparison of APPV probe counts in the right cardiac lung tissue for the APPV^{-ve}/PRRSV^{+ve} (n=5, red) and the APPV^{+ve}/PRRSV^{+ve} (n=7, blue) groups.

5.6.6.3 Detection of PRRSV induced pathology in the lung

Analysis of the H&E stained right cardiac tissue shows evidence of IP with thickening of the alveolar septa due to an increased presence of pneumocytes type II cells (notable by their rounded appearance) and inflammatory cells such as macrophages (Figure 5-16 A and B). Individual interstitial pneumonia scores showed animals from both groups had evidence of interstitial pneumonia (Table 5-7): the APPV^{+ve}/PRRSV^{+ve} group had a greater frequency of higher IP scores than the APPV^{-ve}/PRRSV^{+ve} group indicating an increased severity of pathological changes in the lung of APPV positive animals, although this increase was not statistically significant ($X^2(2) = 2.2629$, p=0.1325, df=1, eta2[H]= 0.126) (Figure 5-17).

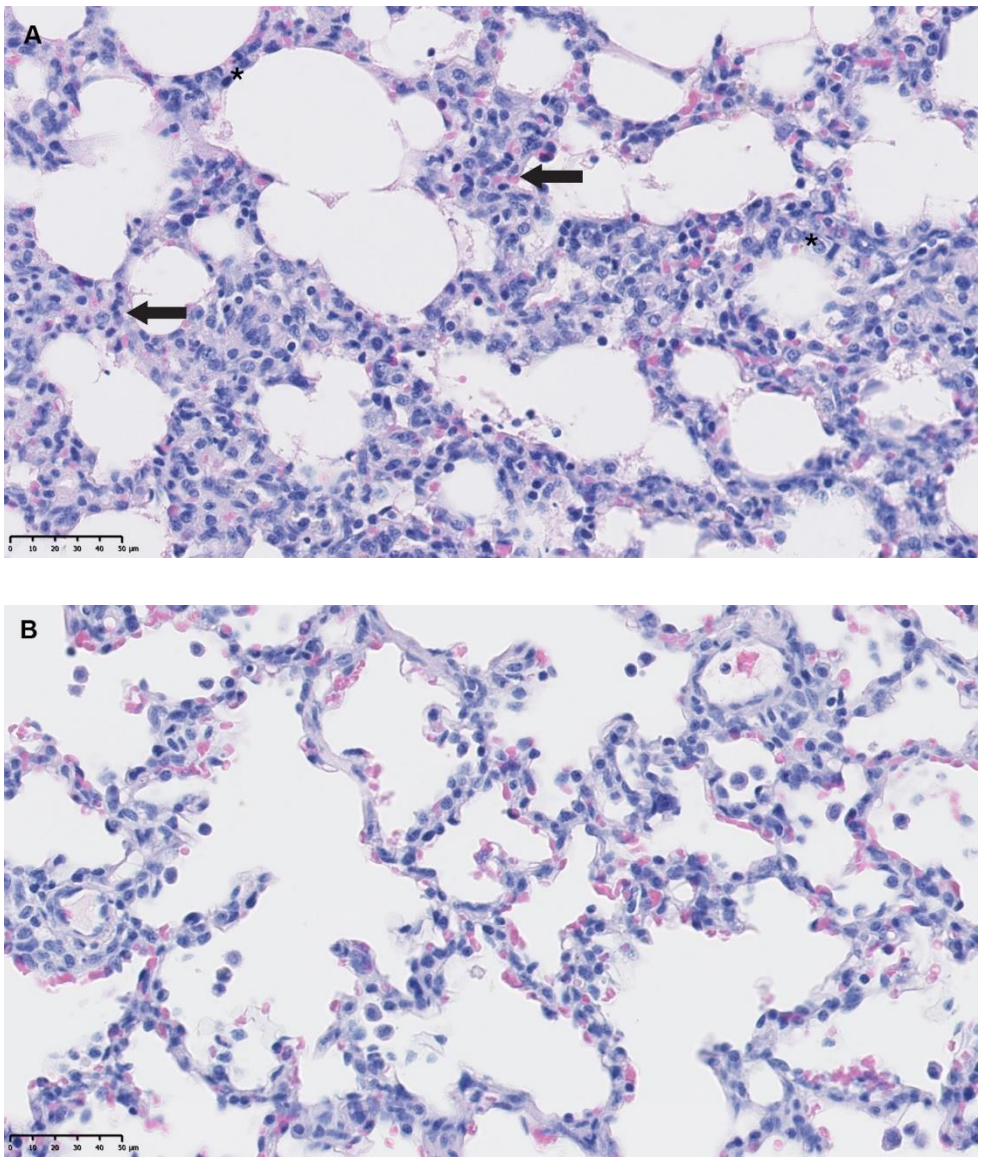

Figure 5-16: Detection of PRRSV induced pathology in right cardiac lung tissue. A Comparison of haematoxylin and eosin staining for an APPV^{-ve}/PRRSV^{+ve} animal (A, top) and a PRRSV^{-ve} uninfected animal (B, bottom). Thickening of the alveoli septa is indicated by the arrows and increased presence of pneumocytes type II by *.

Table 5-7: Individual interstitial pneumonia scores for right cardiac lung tissue of APPV^{-ve}/PRRSV^{+ve} (n=5) and APPV^{+ve}/PRRSV^{+ve} (n=7) groups.

Group	ID	Interstitial pneumonia score
APPV^{-ve}/PRRSV^{+ve}	510	3
APPV^{-ve}/PRRSV^{+ve}	514	5
APPV^{-ve}/PRRSV^{+ve}	503	4
APPV^{-ve}/PRRSV^{+ve}	506	4
APPV^{-ve}/PRRSV^{+ve}	542	2
APPV^{+ve}/PRRSV^{+ve}	935	6
APPV^{+ve}/PRRSV^{+ve}	939	3
APPV^{+ve}/PRRSV^{+ve}	933	5
APPV^{+ve}/PRRSV^{+ve}	938	5
APPV^{+ve}/PRRSV^{+ve}	928	4
APPV^{+ve}/PRRSV^{+ve}	932	4
APPV^{+ve}/PRRSV^{+ve}	948	6

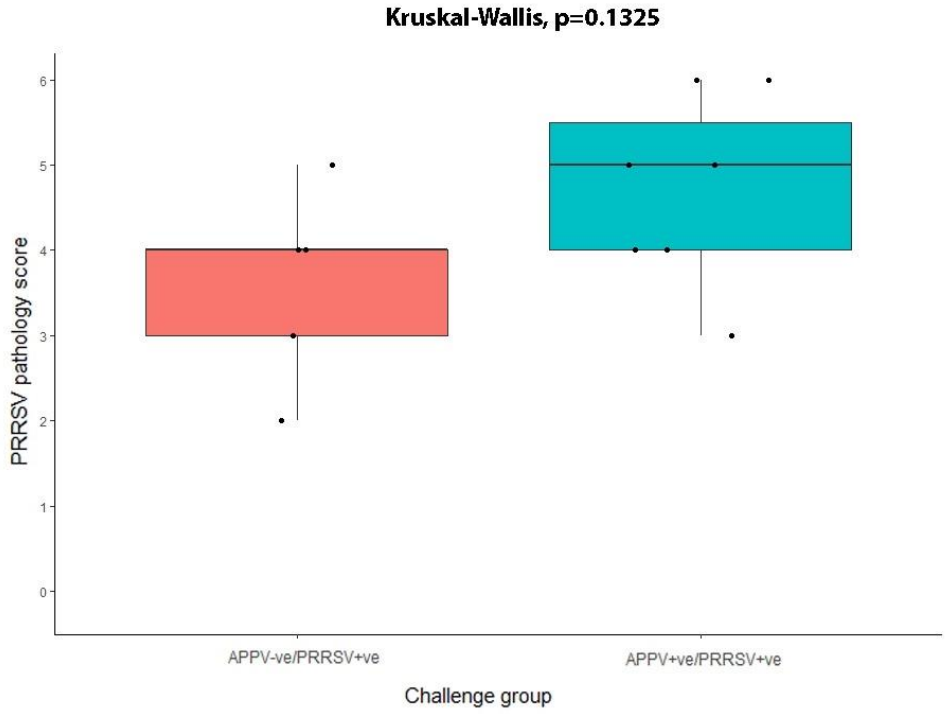

Figure 5-17: Comparison of PRRSV associated interstitial pneumonia score in right cardiac lung tissue from the APPV^{-ve}/PRRSV^{+ve} (n=5, red) and the APPV^{+ve}/PRRSV^{+ve} (n=7, blue) groups.

5.6.6.4 Detection of PRRSV in the lung

PRRSV specific staining was detected in the right cardiac lung tissue of both the APPV^{-ve}/PRRSV^{+ve} and APPV^{+ve}/PRRSV^{+ve} groups by IHC analysis. The PRRSV specific IHC signal was localised macrophage-like cells within alveoli and interstitial space, as presented in Figure 5-18. The individual IHC scores for each group (Table 5-8) indicate that a greater frequency of animals in the APPV^{+ve}/PRRSV^{+ve} group had a higher IHC score with a greater number of PRRSV positive cells than the APPV^{-ve}/PRRSV^{+ve} group, although this difference was not statistically significant by Kruskal-Wallis H test ($X^2(2)$= 1.1038, p=0.2934, df=1, eta2[H]= 0.0104) as shown in Figure 5-19.

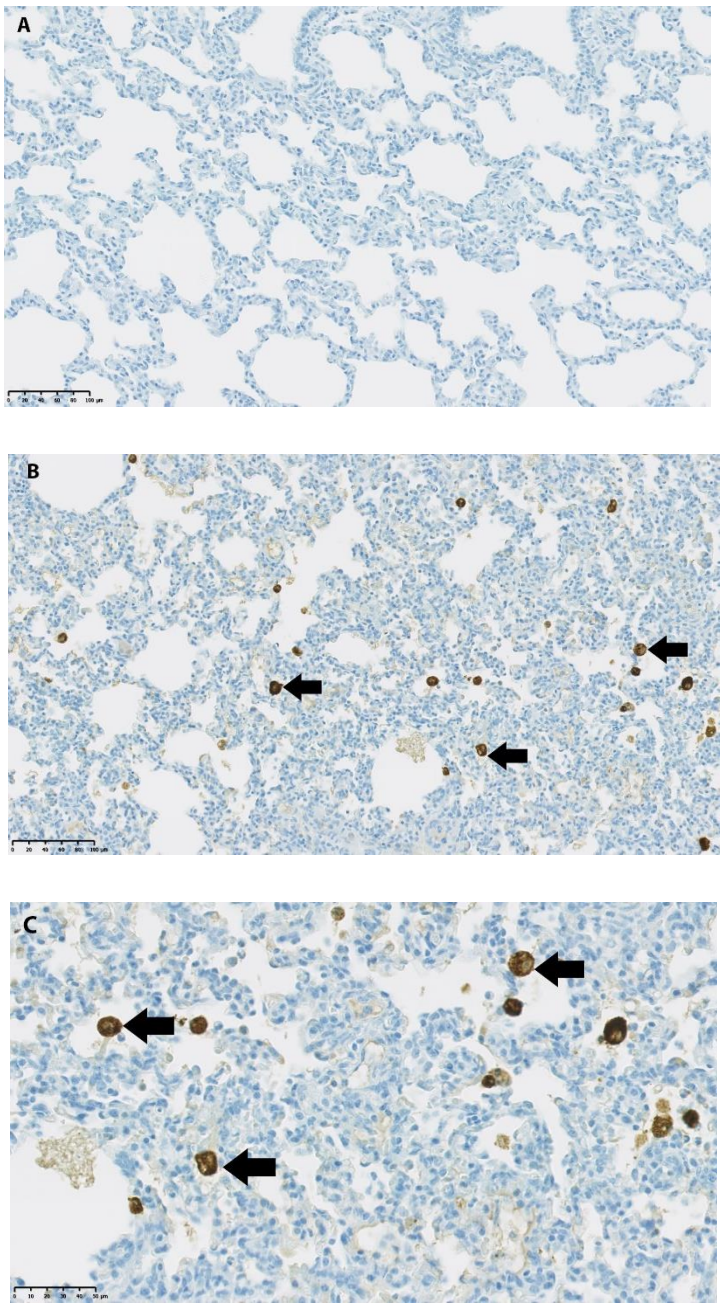

Figure 5-18: Detection of PRRSV within macrophage-like cells in right cardiac lung tissue by IHC. A Comparison of PRRSV specific immunohistochemistry staining for PRRSV^{-ve} uninfected animal (A) and APPV^{-ve}/PRRSV^{+ve} animal (B) at a 200x magnification. C shows an increased magnification (400x) of the APPV^{-ve}/PRRSV^{+ve} animal. The brown PRRSV specific signal is indicated by the arrows.

Table 5-8: Individual immunohistochemistry (IHC) scores for right cardiac lung tissue of APPV^{-ve}/PRRSV^{+ve} (n=5) and APPV^{+ve}/PRRSV^{+ve} (n=7) groups.

Group	ID	IHC
APPV^{-ve}/PRRSV^{+ve}	510	0
APPV^{-ve}/PRRSV^{+ve}	514	1
APPV^{-ve}/PRRSV^{+ve}	503	0
APPV^{-ve}/PRRSV^{+ve}	506	1
APPV^{-ve}/PRRSV^{+ve}	542	0
APPV^{+ve}/PRRSV^{+ve}	935	0
APPV^{+ve}/PRRSV^{+ve}	939	0
APPV^{+ve}/PRRSV^{+ve}	933	0
APPV^{+ve}/PRRSV^{+ve}	938	3
APPV^{+ve}/PRRSV^{+ve}	928	2
APPV^{+ve}/PRRSV^{+ve}	932	1
APPV^{+ve}/PRRSV^{+ve}	948	2

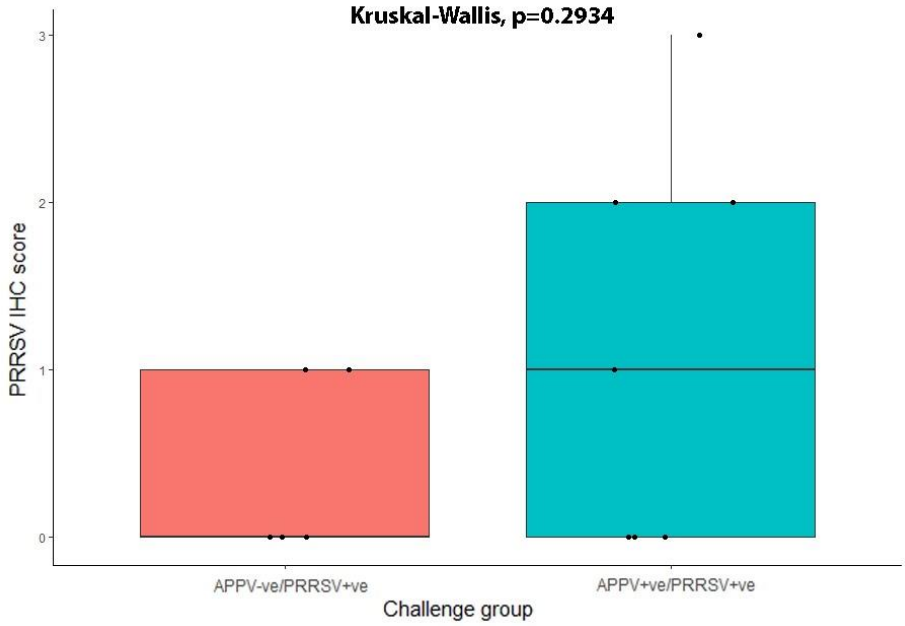

Figure 5-19: Comparison of PRRSV Immunohistochemistry score in right cardiac lung tissue from the APPV^{-ve}/PRRSV^{+ve} (n=5, red) and the APPV^{+ve}/PRRSV^{+ve} (n=7, blue) groups.

5.7 Discussion

Naturally occurring co-infections are well documented within pig farms and can have severe implications for health and production (Krakowka *et al.*, 2000; Opriessnig, Giménez-Lirola and Halbur, 2011; Ouyang *et al.*, 2019; Wang *et al.*, 2020). In this chapter, we established a co-infection model to assess the effect of a natural APPV infection on a concurrent infection with a secondary pathogen (PRRSV) to investigate the role of APPV as potential immunosuppressive agent similarly to what has been previously established for other pestiviruses such as bovine viral diarrhoea virus (BVDV) (Potgieter, 1997).

Only one clinical outcome, temperature, was assessed during the current study, although, routine health and welfare observations of the animals gave anecdotal evidence of breathing difficulty, lethargy, inappetence and weight loss which have been observed in other PRRSV infection studies (Rossow *et al.*, 1994; Doeschl-Wilson *et al.*, 2009; Díaz *et al.*, 2012; Morgan *et al.*, 2016; Stadejek *et al.*, 2017). A significant difference in rectal temperatures was found between the APPV negative and positive PRRSV inoculated groups. The APPV positive group had an increased average daily rectal temperature (equal to or greater than 39.8°C) for six consecutive days, compared to the APPV negative group, which only had two consecutive days of elevated temperature. The APPV positive group also displayed an average increase of 0.58°C temperature throughout the study. A study investigating PRRSV and swine influenza A virus (swIAV) co-infection also found that 71.5% of the swIAV co-infected group had higher rectal temperatures of between 40-41.4°C for longer (up to 10 DPI) compared to the PRRSV only group, which had increased temperature in 21.5% of the group and for less than 3 days (Pomorska-Mól *et al.*, 2020). These findings suggest that even if APPV has a limited effect on the PRRSV viral replication or the cellular immune response to the virus, it can still worsen the clinical outcome of the PRRSV infection.

The febrile response observed in this study is not only a clinical outcome, but also a feature of an inflammatory response that is driven by the production of pyrogenic cytokines such as IL-1 and IL-6 as a response to viral infection, and promotes both innate and adaptive immunity (Netea, Kullberg and Van der Meer, 2000; Evans, Repasky and Fisher, 2015). Increases of body temperature in mammals by 1°C require a rise in metabolic rate by 10—12.5% which may explain the decreases in weight observed within this study and found experimentally in other studies (Evans, Repasky and Fisher, 2015). Future studies should aim to further characterise the role of APPV in the inflammatory response by investigating its effect on the production of these cytokines in relation to weight loss and other clinical outcomes such as behavioural markers and breathing frequency.

The pattern of PRRSV viraemia observed in this study agreed with other reported PRRSV infections (Wesley, Lager and Kehrli, 2006; Lunney *et al.*, 2016; Stadejek *et al.*, 2017; Pomorska-Mól *et al.*, 2020). During co-infection of PRRSV with swIAV, PRRSV was detectable in serum from 1 DPI until the end of the study (21 DPI), co-infection with swIAV did not have an effect on PRRSV viraemia as there was no difference between the single (PRRSV only) and co-infected groups (Pomorska-Mól *et al.*, 2020). However, the peak of viraemia was observed on day 10 for the swIAV positive PRRSV inoculated group, but was delayed (14 DPI) for the swIAV negative PRRSV inoculated group. In the current study, peak viraemia (serum) was observed on 5 DPI for both the APPV negative and positive groups. An earlier study also found virus titres in serum to peak on day 7 although this was only a single infection (Duan, Nauwynck and Pensaert, 1997). In both cases, the animals infected were younger (6—7 weeks of age) than the one used in the current study (10 weeks of age), of a different breed (Landrace instead of Large White x Duroc) and also inoculated with a different subtype of PRRSV-1 (Duan, Nauwynck and Pensaert, 1997; Pomorska-Mól *et al.*, 2020). All of these factors have been reported to affect peak viraemia timing (Petry *et al.*, 2005; Doeschl-Wilson *et al.*, 2009; Klinge *et al.*, 2009; Stadejek *et al.*, 2017).

No significant differences in the pattern of PRRSV viraemia or overall virus titres within the serum were detected between groups over the course of the study, suggesting that co-infection with APPV may not enhance or prolong PRRSV infection. However, the kinetics of APPV viraemia inversely followed the PRRSV viraemia pattern over the study: PRRSV was at the highest level between day 3 and 7 when the APPV titre was at its lowest; APPV then became undetectable on day seven which coincided with the start of the progressive reduction in the PRRSV titre (7 DPI until study termination). Simultaneously, the APPV titre began to increase again for the remainder of the study, suggesting a viral interference between PRRSV and APPV. The viral shedding of APPV (nasal swabs) further supports this conclusion as it followed the same pattern as the APPV in sera. A study by Kitikoon *et al.* (2009) to assess the effect of co-infections of PRRSV on the efficacy of an inactivated swine influenza virus (SIV) vaccine found that piglets from the non-vaccinated group challenged with virulent H1N1 SIV strain had significantly higher SIV titres on 2 and 5 DPI compared to the piglets from non-vaccinated group with concurrent SIV and PRRSV infections, suggesting that PRRSV did not enhance or prolong viral shedding in nasal swabs. Further investigation is needed to understand the mechanisms of the interaction between APPV and PRRSV.

Due to the sample size and limited detection of PRRSV in nasal swabs (out of the nasal swabs collected on day 0, 1, 3, 5, 7, 10 and 14 only one animal per group had a positive swab at one time point only), no inferences can be made regarding the impact of APPV on PRRSV shedding from the respiratory tract. Other studies monitoring nasal shedding have also reported inconsistent results when quantifying PRRSV viral load in nasal secretions (Yoon *et al.*, 1993; Rossow *et al.*, 1994). Duan, Nauwynck and Pensaert (1997) were only able to detect PRRSV-1 in four out of eight pigs on 3 DPI and only in one of the eight animals on 7 DPI, whereas Charpin *et al.* (2012) found that PRRSV-1 could be detected in nasal swabs from 2—48 DPI with peak viral

loads on day two (Charpin *et al.*, 2012). The variability in detection may be due in part to virus species and subtype differences in their ability to replicate in the nasal mucosa (Frydas *et al.*, 2013; Frydas and Nauwynck, 2016), which may affect shedding in nasal secretions. As well as increasing the sample size in future investigations, the collection of additional sample types to assess shedding should be considered. A study which compared diagnostic specimens for the detection of acute PRRSV in boars found that oral fluid samples gave comparable results to serum for PRRSV detection for both viral detection by RT-qPCR and PRRSV antibody detection via ELISA (Pepin *et al.*, 2015). This type of sampling may also be advantageous in co-infections because one sample could be used for the dual detection of APPV and PRRSV, as oropharyngeal swabs have been successful in detecting APPV shedding (3.5.2.2).

The humoral immune response to PRRSV appeared to be unaffected by the APPV animal status, as no difference was found between the PRRSV infected groups. All animals inoculated with PRRSV seroconverted on 10 DPI and remained positive until the end of the study at day 14. Pomorska-Mól *et al.* (2020) also found that all the PRRSV infected animals regardless of swIAV status seroconverted on 10 DPI, and Duan, Nauwynck and Pensaert (1997) found all PRRSV inoculated animals had seroconverted by 10 DPI. However, other studies found that animals inoculated with PRRSV alone seroconverted earlier, from 8—9 DPI (Labarque *et al.*, 2000; Klinge *et al.*, 2009). As serum sampling was carried out on days 7 and 10 post-inoculation in the current study, seroconversion between these time points and differences between the two groups could have been missed. Additional sample collections should be incorporated into future studies to confirm the results presented here. Variation in individual APPV antibody levels over time were detected in both PRRSV inoculated groups for the study duration, although the levels detected were very low; this is not wholly unexpected due to the prolonged nature of the APPV infection observed in the littermates of animals under experiment (as discussed in Chapter 4). Since the animals used for the co-infection study

came from the same farm, they could have been exposed to the virus for at least 10 weeks before the study commenced (with some potentially exposed *in utero*). Antibody levels would therefore appear to have stabilised, which may explain the apparent lack of interaction between the viruses. However, the interpretation of this result in relation to the viraemia data requires caution as the presence of antibodies in APPV^{-ve} animals could indicated either prior exposure or infection, and absence in APPV^{+ve} animals could be result of prenatal immune tolerance, as observed in other pestivirus infections (Palfi, Houe and Philipsen, 1993). Moreover, maternal antibodies acquired through colostrum can also interfere with result interpretation.

The cellular immune response to PRRSV was assessed by quantifying PRRSV-specific IFN-γ responses from spleen cells, using ELISpot; the spleen is a known target tissue for both PRRSV and APPV (Pileri and Mateu, 2016; Postel *et al.*, 2016). While the results were not statistically significant, higher mean PRRSV-specific IFN-γ responses were observed in the APPV positive group, suggesting that co-infection with APPV may enhance the cellular immune response to PRRSV and requires further investigation with a larger sample size.

PRRSV was detected, at similar titres, in the bronchoalveolar lavage, right cardiac lung lobe and superficial inguinal lymph node of animals in both the APPV positive and negative groups, suggesting that APPV infection does not interfere with PRRSV viral replication. Only tissue from the right cardiac lung lobe was tested for PRRSV viral load and may not represent viral load within the lung as a whole. However, Labarque *et al.* (2000) found that PRRSV viral titres were similar in the apical, cardiac and diaphragmatic lung lobes and bronchoalveolar lavage fluid. The detection of high PRRSV titres within the lung and lymphoid tissues are well documented (Sur *et al.*, 1996; Lamontagne *et al.*, 2003; Morgan *et al.*, 2016; Nazki *et al.*, 2020). Higher viral titres may have been observed if the PM had been conducted closer to the peak of viraemia instead of on day 14 as indicated by the work of Nazki *et al.* (2020)

which showed the highest viral titres in lung tissue between 3 and10 DPI. Labarque and colleagues also detected peak viral load in bronchoalveolar lavage fluid at 7 DPI and in lung at 9 DPI (Labarque *et al.*, 2000). Future investigations should consider serial culls to determine if a difference in viral load occurs between APPV positive and negative PRRSV inoculated groups at an earlier time point that may have resolved by PM at day 14. The presence of APPV in all tissues and in the bronchoalveolar lavage in the APPV positive group only indicates active APPV infection and further supports findings on tissue tropism in 3.5.2.3.

In a PRRSV infection, the degree of gross pathology observed in the lung can vary from no observed lesions to gross lesions and notable signs of consolidation dependant on the strain of PRRSV, breed and age of the animal and additional environmental stress factors (Rossow, 1998; Brockmeier and Lager, 2002; Salguero *et al.*, 2015). In this study, no discrete gross lesions, apart from consolidation, were detected in either of the APPV positive and negative and positive PRRSV inoculated groups. Consolidation scoring between groups however showed significant differences between APPV negative and positive groups for the apical and intermediate lobes. Although significant differences were not established between groups for the overall lung and cardiac or diaphragmatic lobes, there was a trend that more of the APPV positive animals had higher consolidation scores compared to the APPV negative group in all areas of the lung, suggesting that APPV does have an impact on PRRSV lung pathology. This increase in pathology resulting from the destruction of alveolar macrophage-like cells and the infiltration of inflammatory and immune cells caused the accumulation of intra-alveolar exudate, which may indicate why the affected animals displayed signs of respiratory distress including coughing and dyspnoea. Future studies investigating lung pathology should also monitor breathing and behaviour markers indicating distress as previously discussed to determine the level of association between the pathology observed and the clinical signs present.

Both APPV negative and APPV positive PRRSV inoculated groups displayed signs of PRRSV infection with mild to moderate interstitial pneumonia and positive IHC staining. No significant difference in the interstitial pneumonia or IHC scores were detected between the APPV negative and positive PRRSV inoculated groups. However, this may be a result of conducting the scoring on the cardiac lung lobe tissue, which had already shown no significant differences in consolidation between groups. Differences in the level of pathology observed between lobes following PRRSV infection were reported by Beyer *et al.* (2000), who found that diaphragmatic lobes had a greater number of focal subpleural changes than apical, middle and accessory lobes in pigs inoculated oronasally with PRRSV. In contrast, Morgan *et al.* (2016) found a greater incidence of changes associated with interstitial pneumonia in the apical lung lobes of pigs which like the current study were intranasally inoculated with PRRSV. The different distributions of lung pathology between these two studies may have been the result of differing routes of inoculation (oronasally vs intranasally). The full inoculation dose given intranasally may not have been distributed through the lung equally. A study by Hemmink *et al.* (2016) showed variation between the distribution of Evan's blue dye in the respiratory tract following aerosol and intranasal delivery. Intranasal inoculation delivered dye mainly to the upper respiratory tract and alimentary canal whereas the dye distribution after aerosol inoculation included both the upper and lower respiratory tract and encompassed the entire bronchial tree (Hemmink *et al.*, 2016). This may explain the lack of significant distal lobe pathology reported in both the current study and by Morgan *et al.* (2016), although further investigation is needed to determine the repercussions of this. The results of this work indicate that intranasal inoculation deposits the viral inoculum predominantly in the proximal lung lobes indicating that future studies delivering this type of viral challenge should also include pathological assessment of those areas. Future investigations should also consider using an inoculation route known to evenly distribute the virus throughout the lung and conduct the pathological assessment on all areas of the lung, or at least, if using an intranasal route, perform the analysis of the lung areas identified

with significant differences in consolidation (apical and intermediate lobes), accounting for differences in presentation between the lobes, which could cause subtle interactions between APPV and PRRSV to be missed.

Both the APPV^{-ve}/PRRSV^{+ve} and APPV^{+ve}/PRRSV^{+ve} groups had signs of macroscopic lesions with signs of interstitial pneumonia characterised by thickening of alveolar septa, the proliferation of pneumocytes type II and inflammatory cells. This presentation is commonly reported as PRRSV associate lung pathology in species 1 infections (Salguero *et al.*, 2015; Morgan *et al.*, 2016; Stadejek *et al.*, 2017; Nazki *et al.*, 2020). One study found that interstitial pneumonia was greater at the peak of viraemia at ten days post-infection and began to decline at later time points, suggesting that a PM performed before day 14 may have shown more significant pathology (Nazki *et al.*, 2020).

This study is the first detailed report of APPV detection via BaseScope *in situ* hybridisation in lung tissue although an experimental APPV inoculation study of sows investigating viral distribution of tissues of the piglets displaying congenital tremors employed a similar ISH technique (RNAScope) using a probe designed specifically to detect the N^{pro} and E^{rns} portion of the inoculation strain (Buckley *et al.*, 2021). The study found APPV present in lung tissue commonly observed in endothelial cells of blood vessels. The findings presented in this chapter are in agreement with the detection of APPV by Buckley *et al.* (2021) and other pestiviruses such as BVDV in lung tissue by IHC (Nelson *et al.*, 2008; Liu *et al.*, 2019). Unlike the study by Liu *et al.* (2019), which found strong APPV positive IHC signal in ciliated cells of the bronchioles and moderate to weak signal in the epithelial cells of the pulmonary alveoli, APPV signal in the current study was detected predominantly in the smooth muscle of bronchioles and within the epithelial and smooth muscles of blood vessels within all APPV positive animals. APPV was sporadically found in low levels within the alveoli. However, APPV signal was not found to be co-localised with PRRSV in macrophage-like cells. A study of a novel

Phocoena pestivirus (PhoPeV) also found presence of the pestivirus by RNAScope *in situ* hybridisation in bronchiolar smooth muscle cells, alveolar wall and interstitial cells within lung tissue as well as smooth muscle cells in arteries suggesting a specific cell tropism (Jo *et al.*, 2019).

Although APPV was not detected by RT-qPCR in the right cardiac lung tissue or bronchoalveolar lavage in animal 933 and 935 from the APPV positive inoculated group, APPV was detected by BaseScope ISH suggesting that the virus was present, but in limited amount and able to be detected by this possibly more sensitive technique. Additional studies, outside the aim of this project should compare and cross-validate these techniques and characterise APPV cell tropism within the lung and other tissues and determine infection mechanisms and replication sites, especially in relation to co-infections.

Overall, even though some of the variables measured did not show statistical significance (apart from the clinical outcome and lung pathology), which may have been a result of insufficient numbers of animals per group, there were subtle but observable differences between groups that may hold biological relevance or indicate interactions between the viruses. As experimental APPV co-infection studies have previously not been reported, estimations were made to determine the appropriate group size to detect a difference based on previous PRRSV co-infection studies; the results of this study will be useful in informing follow up studies to ensure sufficient animal numbers to detect the observed effect size will be selected.

The limited statistical significance of results collected as a result of PM (viral load in tissues, lung lesions and PRRSV-specific IFN-γ responses from spleen cells) may also be due in part to the timing of the PM examination. Both the peak of viraemia in serum (day five) and the peak in rectal temperatures indicating a pyrogenic and inflammatory response on day seven were much earlier than the PM conducted on 14 DPI, by which time both parameters had reduced suggesting that the infection was beginning to resolve and that

differences between the group may have been missed. For this reason, future studies should carry out a serial cull so that PMs are staggered throughout the experiment.

It should also be considered that the limited impact of APPV on PRRSV reported here may be due not only to the sample size, but also to the time elapsed between infection, the initial dose of the virus in the inocula and the different routes of transmission which have all been shown to influence viral interactions and co-infection outcomes (Brockmeier and Lager, 2002; Opriessnig, Giménez-Lirola and Halbur, 2011; Kumar *et al.*, 2018). In this study, APPV was a naturally acquired infection contracted *in utero* transmitted vertically via the placenta and detected at low titres, whereas the animals were infected experimentally with a high dose of PRRSV intranasally 10 weeks later. Natural infections in a co-infection setting may introduce increased variability in results: the naturally infected APPV piglets may have been at different stages of their infection when inoculated with PRRSV or infected to different extents. Future studies should consider controlled infections using isolates of both viruses where the strength of the challenge, timing of the challenges in relation to each other and the route of infection can all be strictly controlled. Furthermore, as viruses that benefit from advantageous interactions with other pathogens are more likely to be observed in co-infection, it would be prudent to perform additional epidemiological investigations of naturally occurring APPV co-infections in the field.

Chapter 6: Atypical porcine pestivirus epidemiology in Great Britain

6.1 Introduction

Since its discovery in the USA in 2015 (Hause *et al.*, 2015), atypical porcine pestivirus (APPV) has been found in association with congenital tremor type A-II (CT A-II) infections in North and South America (Arruda *et al.*, 2016; Dessureault *et al.*, 2018; Gatto *et al.*, 2018a; 2018b;), Asia (Kim *et al.*, 2017; Yan *et al.*, 2019; Yin *et al.*, 2019; Liu *et al.*, 2020), and Europe (Blomström *et al.*, 2016; Williamson, 2017; Grahofer, Zeeh and Nathues, 2020) as shown in Figure 6-1 and is now considered to have a global distribution.

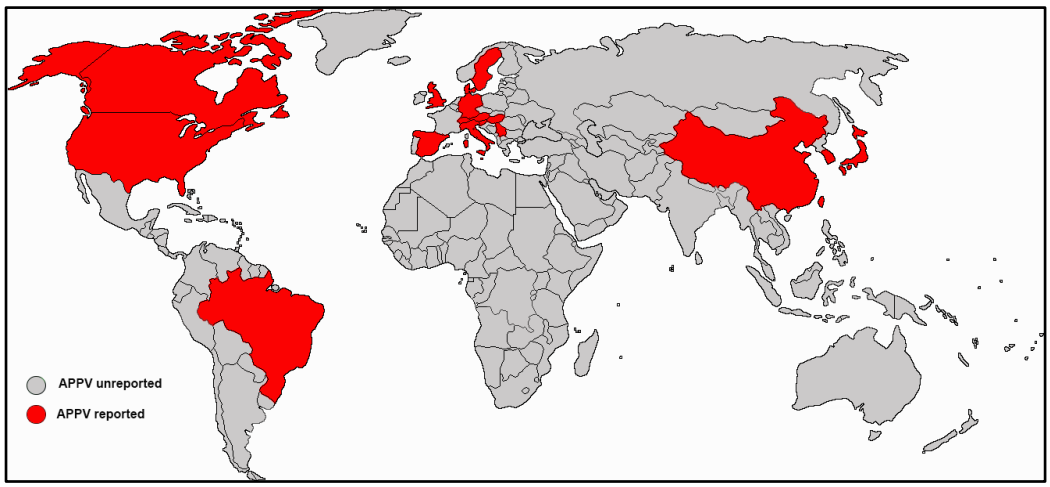

Figure 6-1: Global documented distribution of APPV. Countries with reports of APPV are marked in red: Canada, USA, Brazil, Spain, Great Britain, Germany, Switzerland, Italy, Serbia, Hungary, The Netherlands, Denmark, Sweden, China, South Korea, Japan and Taiwan.

The prevalence of APPV within these countries has been investigated and has identified differences in levels of circulating APPV depending on the region sampled, number of samples, sample type and the assay used to detect the virus. Postel *et al.* (2017a) employed a non-structural (NS) 3 reverse

transcriptase quantitative polymerase chain reaction (RT-qPCR) and an enzyme-linked immunosorbent assay (ELISA) for detection of the envelope protein E^{rns} to screen 1,460 serum samples from healthy pigs collected from seven countries (five European and two from Asia). In Asia, the survey found that the APPV detection rate using the molecular assay was 5% in China and 11% in Taiwan, whereas seroprevalence was 58.6% in China and 86% in Taiwan. The APPV detection rate in these countries was much higher than reported by Kasahara-Kamiie *et al.* (2021) in a Japanese molecular survey of 399 samples obtained from healthy pigs between 2005 and 2020, which used the same RT-PCR as Postel and colleagues, found only three positive samples (0.8%), one 3-week-old piglet kept in Kyushu in 2007, one 10-weekold piglet from the main island in 2018 and one 12-week-old pig from Kyushu in 2018.

The Postel *et al.* (2017a) survey showed that in Europe, Great Britain (GB) had the lowest prevalence when measured by the molecular assay (2.3%) compared to other countries including Germany (6.2%), Serbia (12.3%), Switzerland (13.3%), and Italy (17.5%) which had the greatest detection rate. In contrast, seroprevalence (based on moderate to high levels of antibody detection) was lowest in Germany (47.1%) compared to other European countries: Switzerland (58.3%), Serbia (64.3%), Great Britain (66.3%) and Italy (70.5%). A serological survey (Michelitsch *et al.*, 2019) of German pig farms using indirect immunofluorescence test (IFI) found a much lower seroprevalence in 2018 (17.5% from 37.1% of farms tested) compared to that reported by Postel *et al.* (2017a), which represented an increase of 2.2% on a 2009/10 survey (seroprevalence 15.3% from 46.7% of farms tested) as reported in the same study. Although (Beer *et al.*, 2017), using a molecular assay, detected variability in APPV amounts from two neighbouring northern states: 9% of tonsils collected from a rendering plant in Mecklenburg-Western Pomerania and 22% of sera collected from Schleswig-Holstein herds were positive, which is higher than what was reported by Postel *et al.* (2017a) in the same year. In Italy, a NS5B RT-qPCR molecular survey of 360 fetuses collected between 2016 and 2018 detected APPV in 0.6% of samples (Sozzi

et al., 2019), again, with a much lower detection rate than previously reported (Postel *et al.* 2017a). The detection rate of APPV found by Postel *et al.* (2017a) in Switzerland (13.3%) was in agreement with a retrospective analysis of 1,080 serum samples collected between 1986 and 2018 and tested by APPV 5′ untranslated region RT-qPCR, which showed an average detection rate of 13% (Kaufmann *et al.*, 2019). Detection rates in the study performed by Kaufmann *et al.* (2019)varied depending on the collection year, with the lowest detection rate of 7% in 1986, the earliest reported detection of APPV to date, and the highest in 2006 at 18%.

In addition to the detection of APPV from sera and tissues from healthy pigs, a molecular survey was conducted in the USA to identify the presence and distribution of APPV in commercial boar units from three different states (Gatto *et al.*, 2018a). The authors detected APPV in 12.9% of semen, 22.8% of preputial fluid and 23.8% of preputial swabs tested, with variation between states ranging from 10% to 23% regardless of sample type. Currently, no evaluation of British commercial semen samples has been reported.

As well as reports of APPV detection in commercial units, studies carried out by molecular surveys of sera have also found the virus circulating in wild boar populations in Spain (1/437) (Colom-Cadena *et al.*, 2018), Germany (87/456) (Cagatay *et al.*, 2018), Italy (3/430) (Sozzi *et al.*, 2019), Sweden (73/595) (Stenberg, Jacobson and Malmberg, 2020), and South Korea (18/2,297) (Choe *et al.*, 2020). Although none of the 15 Serbian serum samples tested had detectable APPV by RT-qPCR, 10 of these samples were seropositive by the E^{rns} ELISA, indicating previous exposure of the animal and by extension APPV circulation within the wild boar population (Cagatay *et al.*, 2018). Even though wild boar became extinct in Great Britain in the 13th century, wild boar populations have been locally introduced back into parts of England (Kent/East Sussex border, Dorset, Devon and Gloucestershire) and Wales (Monmouthshire) with a total population of less than 500 (Battersby, 2005).

In Great Britain, congenital tremors A-II (CT A-II) have been reported consistently at low levels (no greater than five cases annually), with a total of 41 outbreaks reported between 2000 and 2020 (Animal and Plant Health Agency, 2008, 2015, 2021). However, the number of cases reported to the Veterinary Investigation Diagnosis Analysis database (VIDA) may be underestimated as it only represents diagnostic submissions for investigation to the Animal and Plant Health Agency (APHA) Veterinary Investigation Centres, APHA post mortem partner providers and Scotland's Rural College (SRUC) Disease Surveillance Centres. As CT A-II outbreaks are not notifiable and are perceived as self-limiting, samples may not be submitted for extensive veterinary investigations or outbreaks recorded (Williamson, 2017). This assumption supports the finding reported in a 2016 survey conducted by the Pig Veterinary Society, which showed that 65% of respondents had either seen first-hand or been made aware of at least one herd affected by CT A-II within the previous 12 months. Cases of CT A-II were reported to be UK wide; however, there was an increased number of cases found in areas with high pig populations such as East Anglia and the North East of England (NEE), with no reports of CT A-II from Wales or either the North West or South East of England (Animal and Plant Health Agency, 2016).

The study by Postel *et al.* (2017a) is the only epidemiological survey to include GB samples. However, the study only tested 86 samples, and unfortunately, no information regarding the age, breed or geographic distribution (either on a country or county level) was disclosed. In 2020, there were four million pigs in England and 338,000 pigs registered in Scotland (Scottish Government, 2020; Department for Enviroment, Food and Rural Affairs, 2021). Given the small sample size in the Postel *et al.* (2017a) study and the variation reported by other studies within the same country arising from differences in assays, sampling sizes and regions tested, further investigation into the serological and molecular prevalence of APPV within Scotland is needed.

6.2 Hypothesis, aims and objectives

The primary aim of this chapter was to determine the circulation of APPV in Scotland to provide insights into the epidemiology of the virus. To investigate this, a serological and molecular survey for the detection of APPV RNA and APPV-specific IgG antibodies in 1,177 serum samples collected from healthy five-month-old pigs in 2018 from 108 arbitrarily selected Scottish pig units was undertaken. The hypothesis was that although molecular detection of APPV rates would be low, seroprevalence would be moderate to high based on previous findings (Postel *et al.*, 2017a). Additionally, molecular detection of APPV from 475 normal commercial semen samples from 41 healthy boar studs was performed to determine the presence of the virus in commercial semen in Scotland.

As well as identifying APPV circulating in healthy pigs in Scotland, detection of the virus in suspected CT A-II outbreaks from England and Scotland submitted for veterinary investigation to APHA and SRUC was performed to confirm viral association with disease and to allow genetic characterisation of British based strains through the sequencing of a subset of samples from each of the outbreaks.

6.3 Materials and methods

6.3.1 Scottish serological and molecular serum survey

A total of 1,077 serum samples from the 2018 biobank collection were evaluated for APPV-specific IgG antibodies using the APPV NS3 indirect ELISA as detailed in 2.4.2. Serum samples were collected from five-month-old mixed breed pigs at slaughter. Ten samples were analysed per farm (apart from one farm where only seven samples were available) from all 108 pig units

geographically distributed throughout Scotland. The number of samples to be tested from the biobank collection was calculated by Biomathematics and Statistics Scotland (BioSS) based on previously reported British genomic detection rate of 2.25% (Postel *et al.*, 2017a) with a 1% margin of error at a 95% confidence interval. For the ELISA, the serum samples and no serum controls were diluted at 1:50, and the positive and negative controls were diluted in wash buffer at a high concentration of 1:50 and a low concentration of 1:200, as previously detailed in 3.3.2. The positive cut-off threshold was determined to be an optical density (OD) value of 0.77 after blank correction and normalisation was performed as described in 2.4.2 In order to establish the positive cut-off threshold Bayesian latent class modelling and ROC analysis was performed by BioSS shown in Appendix B. For the detection of APPV RNA, serum samples were extracted according to the procedure described in 2.2.1.2 and tested using the APPV NS3 RT-qPCR developed in 3.3.1 following the protocol outlined in 2.2.3 to determine the prevalence and viral load of the virus.

6.3.2 Scottish semen evaluation

Raw (non-extended) fresh semen samples (475) from 41 commercial boar units were submitted to SRUC between September and November 2019 for routine testing to confirm freedom from porcine respiratory and reproductive syndrome virus (PRRSV). Samples were pooled in groups of five by farm submission on receipt and then extracted by SRUC following the standard protocol for semen extraction using the Magmax Core Kit in conjunction with the automated MagMax Express 96 extraction robot (outlined in 2.2.1.2). The total nucleic acid extract was stored at -20°C for less than three months prior to the commencement of testing by RT-qPCR as part of this investigation as described in 2.2.3.

6.3.3 Suspected CT A-II case submissions from Great Britain

Cases of CT A-II (Table 6-1) were initially diagnosed by attending veterinary practitioners based on clinical signs and farm history followed by submission to the Animal and Plant Health Agency (APHA) laboratory and SRUC for diagnostic confirmation. After positive confirmation, samples (serum and/or tissues) were transferred and further tested using an APPV RT-qPCR (2.2.3). Confirmatory sequencing was performed where possible on at least one sample per case using purified polymerase chain reaction (PCR) product as described in 2.2.4. Multiple sequence alignments and phylogenetic analysis were performed as described in 2.2.6.

6.3.4 Statistical analyses

Statistical analysis to determine the sample size required for the study and the indirect ELISA positive cut-off was performed by BioSS as outlined in 6.3.1 and Appendix B respectively. To determine the relationship between viral load and the APPV-specific antibody level detected in serum using the Spearman's Rank Correlation Coefficient. A Cochran-Mantel-Haenszel Chi-square test was employed (Figure 6-2) to determine if a three-way interaction existed between RNA detection outcome (positive, equivocal or no virus RNA detected), antibody outcome (Anti-APPV IgG detected or no anti-APPV IgG detected) and the farm the sample originated from.

Table 6-1: Submissions of suspected CT A-II field cases from Great Britain

ID	Unit type	Location	Date of collection	Number of pigs	Sample type
NOR-0616-01	Outdoor	Norfolk	Jun-16	1	Brain, Spinal cord, Tonsil, Spleen
NOR-0417-01	Outdoor	Norfolk	Apr-17	1	Brain, Tonsil, Spleen
SUF-0617-01	Outdoor	Suffolk	Jun-17	1	Brain, Tonsil, Spleen
SUF-0118-01-03	Commercial	Suffolk	Jan-18	3	Serum
ABE-0818-01-05	Commercial indoor breeding	Aberdeenshire	Aug-18	5	Serum, Brain, Spinal cord, Tonsil, Thymus, Superficial inguinal lymph node, Retropharyngeal lymph node, other lymph nodes
SWE-1018-01-02	Commercial closed	South West England	Oct-18	2	Serum
NEE-0419-01-03	Commercial	North East England	Apr-19	3	Serum
NEE-1119-01-02	Commercial	North East England	Nov-19	2	Serum
NEE-0120-01-03	Commercial	North East England	Jan-20	3	Serum

6.4 Results

6.4.1 Scottish serological and molecular serum survey

Due to the volume of serum available, one of the 1,077 samples could not be tested for the presence of APPV by RT-qPCR only for APPV-specific antibodies by indirect ELISA. Out of a total of 1,076 serum samples tested by RT-qPCR for APPV RNA, 4.7% (50/1,076) were positive, with APPV titres ranging from $3.87x10^5$ to $1.45x10^8$ copies/ml and 1.6% (17/1,076) equivocal, with titres between $5.35x10^3$ and $1.32x10^5$ copies/ml, below the sensitivity of the assay ($1.44x10^5$ copies/ml). The remaining 93.8% (1009/1076) samples had no virus detected. Twenty five percent of the farms sampled (27/108) had one or more positive piglets (10 to 100% positive samples per farm). Overall, 5.6% (6/108) of the farms sampled had no positive animals but had one or more equivocal piglets (20% or less equivocal samples per farm), with no virus detected in any of the animals from the remaining 75 farms.

APPV-specific IgG antibodies were detected in 48.8% (525/1,077) of serum samples with 86.1% (93/108) of herds with one or more seropositive animals (10 to 100% positive samples per farm). There was no significant relationship between the viral load and the APPV-specific antibody level detected in serum (shown in Figure 6-2) (Spearman's rank correlation Rho= -0.01, p-value= 0.64). There was also no association between the RNA detection outcome (positive, equivocal or no virus RNA detected), antibody outcome (anti-APPV IgG detected or no anti-APPV IgG detected) and the farm the sample originated from, as determined by the Cochran-Mantel-Haenszel Chi-square test ($X^2(2)= 4.61$, df= 2, p-value= 0.10).

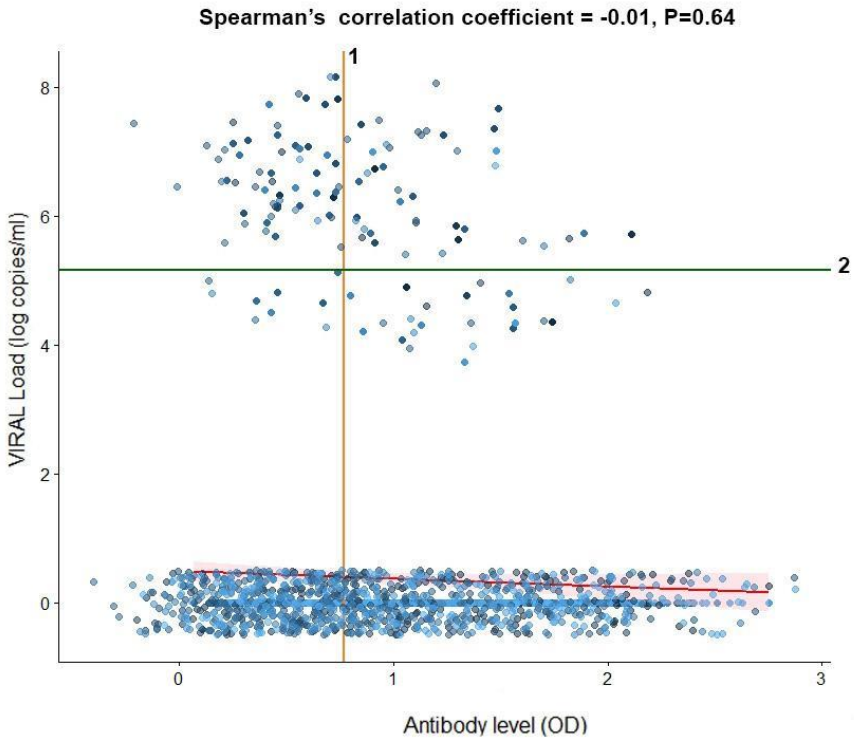

Figure 6-2: Relationship between average APPV viral load (log_{10} copies/ml) and average APPV-specific IgG antibody levels (OD). The scatter graph shows the viral load and antibody level (n=1,077, technical replicate=2) coloured by the farm collection. The red line represents the line of best fit, and the shaded area in pink represents the 95% confidence interval. The positive threshold for the ELISA (1) is shown in yellow, and the RT-qPCR threshold is shown in green (2).

6.4.2 Scottish semen evaluation

No virus was detected in the pooled semen from any of the boar stud submissions, as shown in Table 6-2. Semen samples were pooled in groups of five on receipt by SRUC prior to the extraction. As individual boars could not be tested in this study, it is unknown whether the sensitivity of the assay is sufficient to detect APPV at a 1 in 5 pooling ratio.

Table 6-2: Evaluation of boar studs by RT-qPCR. Semen was pooled in groups of five within the same farm for testing.

Boar stud	Number of boars tested	Viral outcome
1	15	No virus detected
2	15	No virus detected
3	5	No virus detected
4	10	No virus detected
5	30	No virus detected
6	5	No virus detected
7	15	No virus detected
8	15	No virus detected
9	5	No virus detected
10	15	No virus detected
11	5	No virus detected
12	15	No virus detected
13	5	No virus detected
14	5	No virus detected
15	5	No virus detected
16	15	No virus detected
17	15	No virus detected
18	15	No virus detected
19	5	No virus detected
20	5	No virus detected
21	30	No virus detected
22	15	No virus detected
23	5	No virus detected
24	15	No virus detected
25	15	No virus detected

Continuation of Table 6-2: Evaluation of boar studs by RT-qPCR. Semen was pooled in groups of five within the same farm for testing.

Boar stud	Number of boars tested	Viral outcome
26	5	No virus detected
27	10	No virus detected
28	15	No virus detected
29	15	No virus detected
30	5	No virus detected
31	5	No virus detected
32	5	No virus detected
33	15	No virus detected
34	15	No virus detected
35	5	No virus detected
36	15	No virus detected
37	15	No virus detected
38	15	No virus detected
39	15	No virus detected
40	10	No virus detected
41	10	No virus detected

6.4.3 Suspected CT A-II case submissions from Great Britain

All animals were APPV positive by RT-qPCR with viral loads ranging from $1.86x10^6$ to $5.56x10^9$ copies/ml (Figure 6-3 and Figure 6-4), except for one piglet (ABE-0818-02) from the Aberdeen August 18 suspected CT outbreak. Although ABE-0818-02 had no detectable APPV in serum, APPV was detected in all other tissues tested (Figure 6-5).

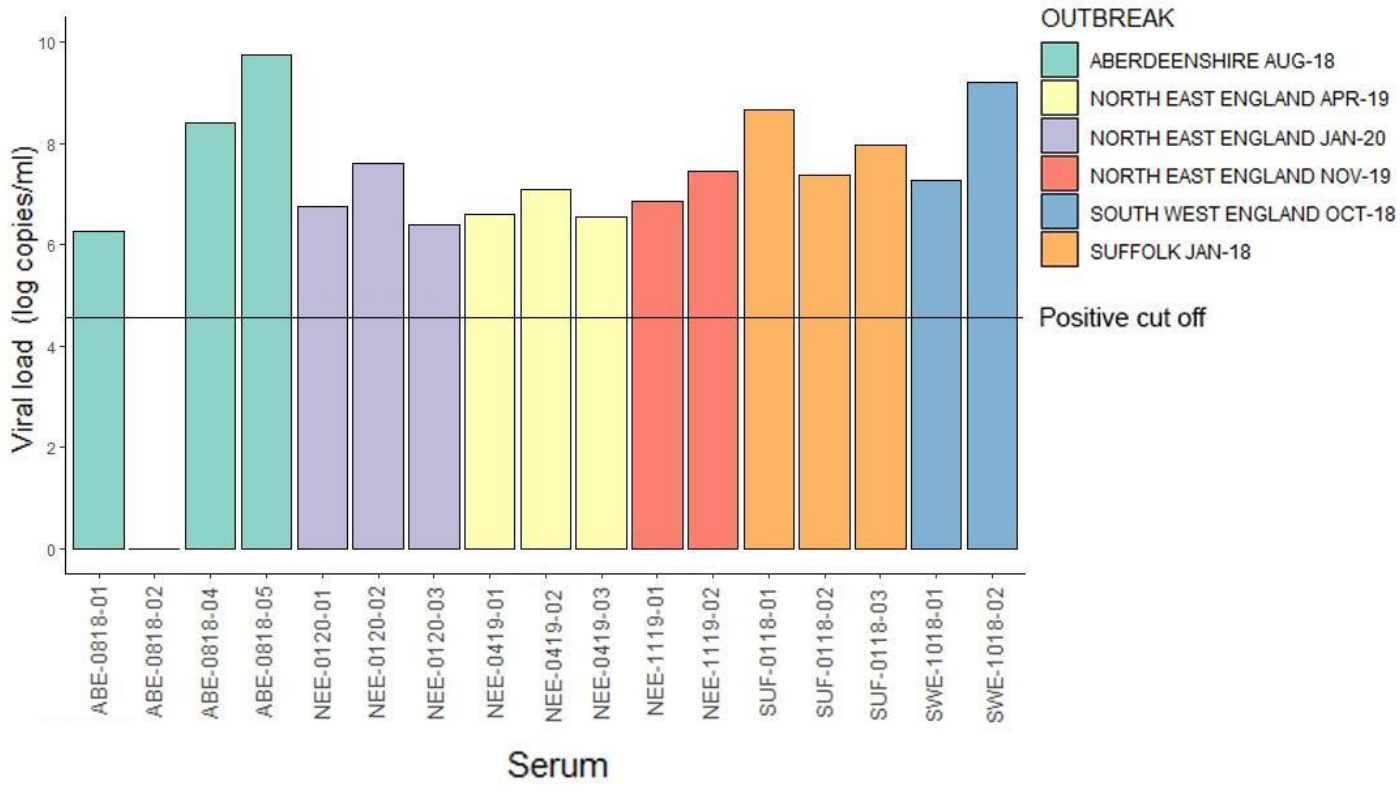

Figure 6-3: Average APPV viral load based on two technical replicates (log_{10} copies/ml) in serum collected from suspected British CT cases. The graph colours identify suspected outbreaks from Aberdeenshire (ABE), North East England (NEE), South West England (SWE), and Suffolk (SUF). The horizontal line indicates the positive cut-off of the RT-qPCR.

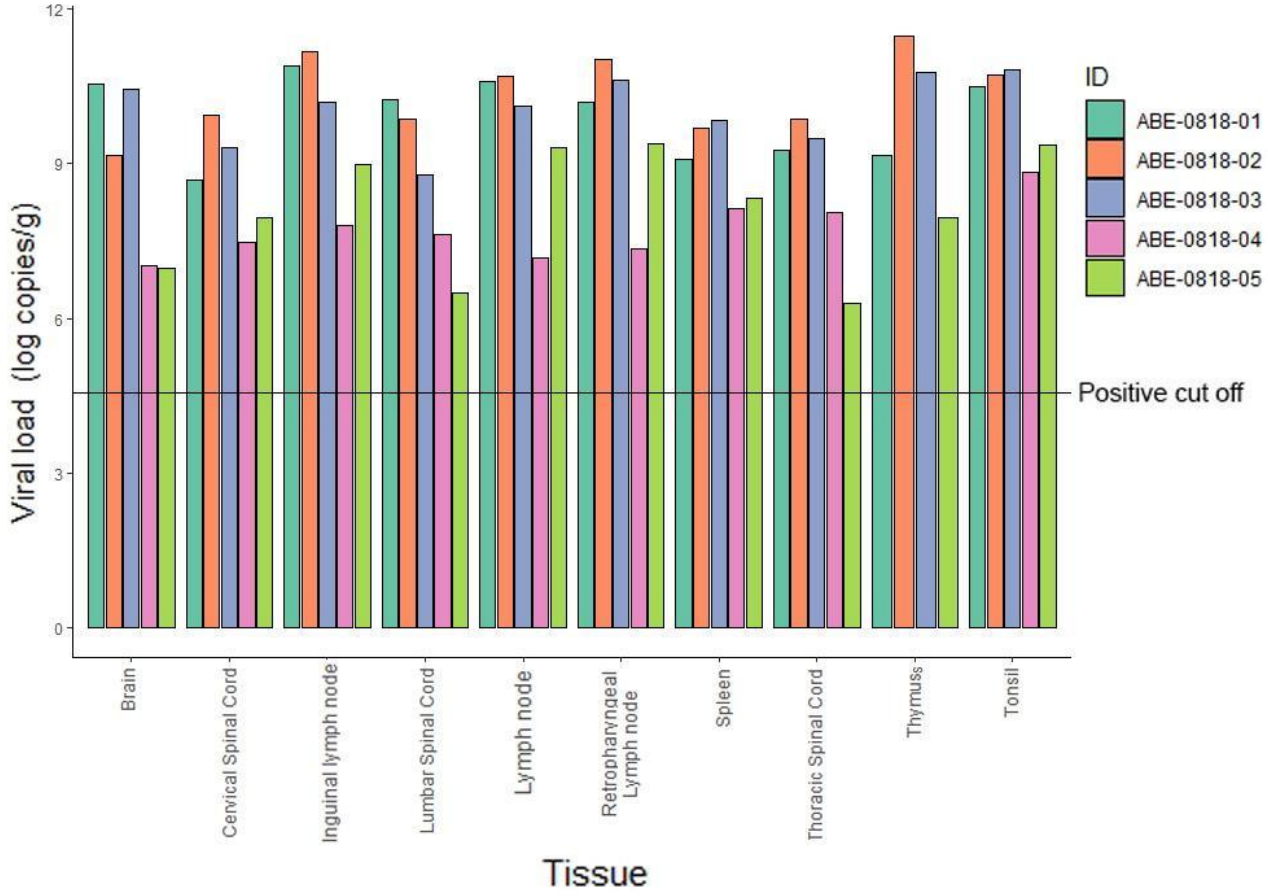

Figure 6-4: Average APPV viral load based on two technical replicates (log_{10} copies/g) in tissues collected from a Scottish suspected CT outbreak. Each individual animal is represented by a different colour, and the horizontal line indicates the positive cut-off of the RT-qPCR.

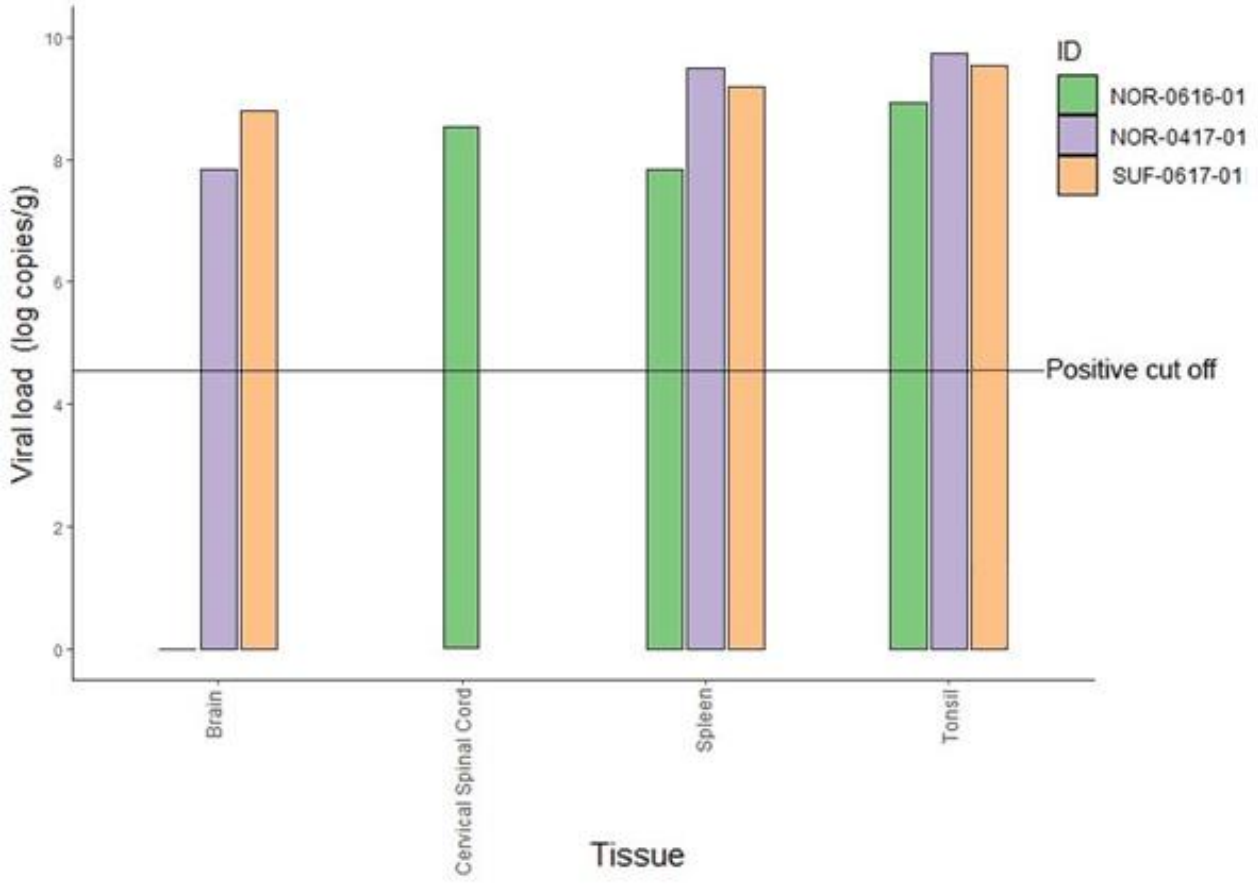

Figure 6-5: Average APPV viral load based on two technical replicates (log_{10} copies/g) in tissues collected from English suspected CT outbreaks. The graph shows the viral load in the brain, cervical spinal cord, tonsil and spleen, with the individual animal case ID identified by a different colour. The horizontal line indicates the positive cut-off of the RT-qPCR.

Sequence analysis of suspected CT cases confirmed all of them to have APPV present, as shown in Appendix A The phylogenetic relationship based on partial NS3 gene sequences is shown as a maximum likelihood tree in Figure 6-6. Samples from each of the following cases: NOR-0616 (100%), ABE-0818 (100%), SUF-0118 (98.86%) and NEE-0120 (98.86%) had the greatest nucleotide identity similarity with a 2015 German strain from Lower Saxony (Genbank accession: KU041637.1). Other cases shared the greatest nucleotide percentage identity with sequences from the USA; SWE-1018 (94.32%) with a sequence collected in 2012 (Genbank accession: KU194231.1) and NOR-0417 (98.85%), SUF-0617 (97.70%), and NEE-1119 (94.38-96.55%) with a sequence collected in 2013 (Genbank accession: NC_038964.1). Another case, NEE-0419, was most closely related to a sequence from China collected in 2018 (Genbank accession: MH499643.1) with a percentage identity of 96.59%. Samples from the Scottish CT field case described in Chapter 4 (CSCOT-FG1 and CSCOT-FG2) were also sequenced to confirm APPV positivity in all samples, and were most closely related to a Hungarian sequence collected in 2017 (Genbank accession: MH049532.1).

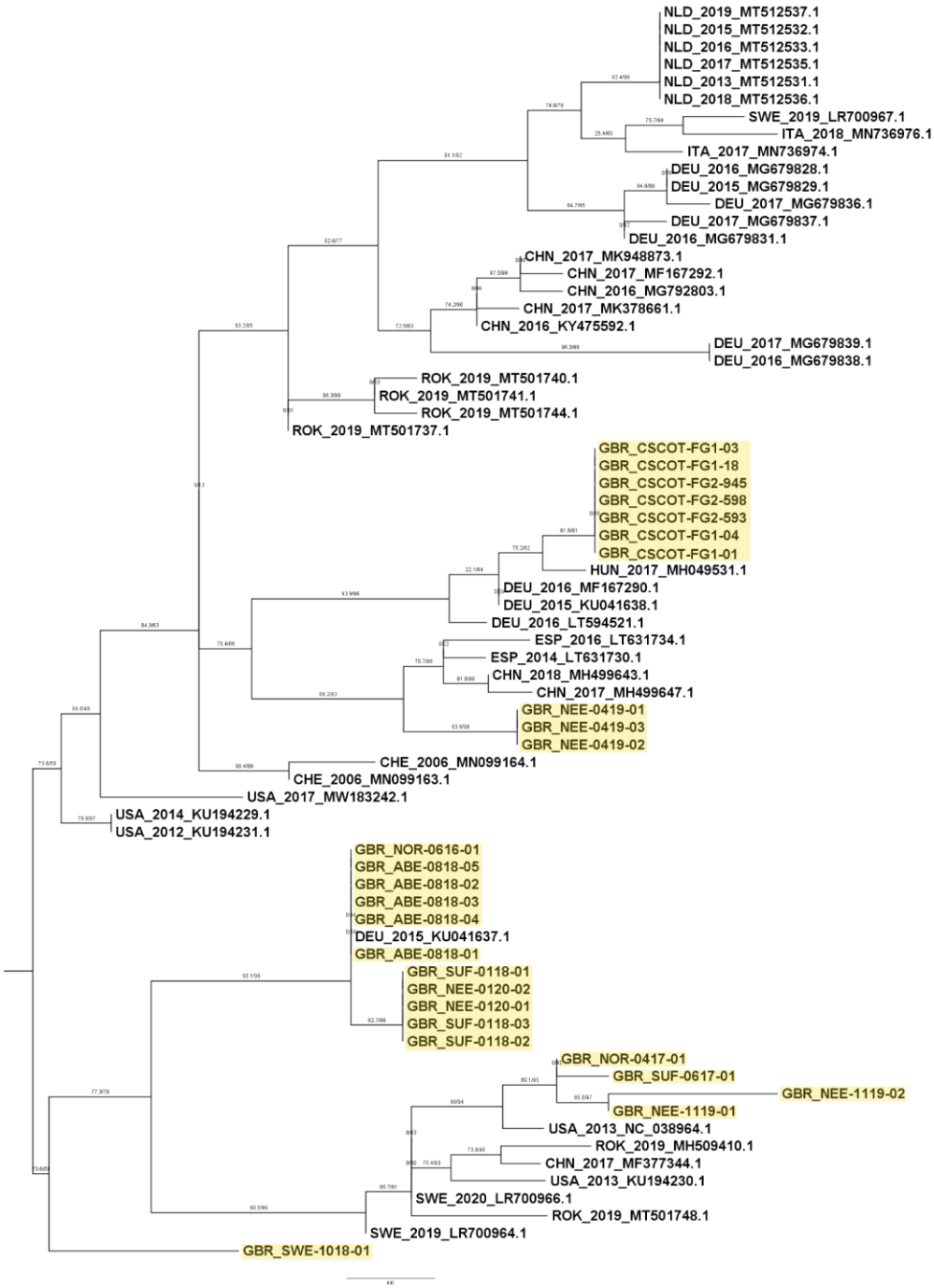

Figure 6-6: Phylogenetic tree of the partial NS3 gene (5546-5636) sequence of APPV. The maximum likelihood tree was calculated using a K2P +G4 model in IQ-TREE in combination with 1,000 bootstrap replicates (shown on arms). British sequences collected from suspect CT outbreaks are indicated in yellow. Published sequences that share more than 80% nucleotide identity to the British samples are also included. Published sequences are named based on their country of origin, collection date and GenBank accession number.

6.5 Discussion

The serological and molecular survey of healthy five-month-old pig sera presented in this chapter was the first epidemiological investigation of APPV within the Scottish pig industry. The APPV molecular detection rate in this survey (4.65%) was found to be double that previously reported for Great Britain (2.3%) by Postel *et al.* (2017a). This may be due to the increased sample size with 1,076 serum samples from 108 farms tested as opposed to only 86 samples from an unknown number of farms analysed by Postel *et al.* (2017a). Therefore, this study gives a more robust indication of circulating APPV levels in Scotland. It should also be noted that there were no overlapping samples tested between the current study and the one by Postel *et al.* (2017a) for which British samples were sourced from APHA in or before 2017, whereas the current study used previously untested Scottish samples only, collected in 2018. Conversely, the study by Postel *et al.* (2017a) used 369 previously screened German serum samples and Swiss serum samples sourced from the same repository (Swiss Federal Food Safety and Veterinary Office) as the retrospective study (Kaufmann *et al.*, 2019) which may have resulted in overlapping use of samples and explain the similar prevalence rates. No comparison between the current study and the one carried out by Postel *et al.* (2017a) can be made regarding the breed, or the age of the animals sampled, as no indication was given to the background history of the samples used in the initial study.

Another possible reason for the difference in detection rate between surveys may be the RT-qPCR used for APPV detection. The assay used by Postel *et al.* (2017a) was evaluated in this work for the detection of APPV in British samples (Chapter 3) and found to be slightly less sensitive than the assay subsequently adopted (Arruda *et al.*, 2016) after modification and optimisation to be used in this work. For this reason, it is possible that some of the more variable British APPV strains may have gone undetected by the Postel *et al.* (2017a) study. Unfortunately, variation in British APPV sequences presented

in this chapter could not be compared to that of the published sequence as the portions of NS3 gene targeted in these two studies did not overlap (Postel *et al.*, 2017a). As samples from both studies were collected from healthy animals, this suggests that APPV is in circulation subclinically both within Scotland and the rest of Great Britain.

The molecular detection rate presented in the current study (4.7%) is closest to that reported for China and is lower than reported for most other European countries (Beer *et al.*, 2017; Postel *et al.*, 2017a; Kaufmann *et al.*, 2019). A study by Sozzi *et al.* (2019) found only 0.6% of 360 domestic pig fetuses tissue samples (brain, lung, liver, kidney and spleen) collected between 2016 and 2018 to be APPV positive. However, this is in contradiction with the study that found a genome detection rate in serum of 17.5%, suggesting a higher level of APPV circulation within Italy (Postel *et al.*, 2017a). These discrepancies could be explained by differences in the number of animals and the sample types tested. A Danish study investigated healthy pig serum from five 'control herds' without incidence of congenital tremor (CT) from different geographic areas and detected APPV from 1/25 piglets (4%), similar to the detection rate identified in this study in Scotland. However, due to the small number of herds tested in comparison to the Scottish survey, levels of circulating APPV in Denmark cannot be robustly determined (Pedersen *et al.*, 2021).

As expected, the seroprevalence of APPV in the Scottish survey was found to be high, with 86.1% (93/108) of herds having one or more seropositive pig. The overall Scottish sample seroprevalence of 48.8% (525/1,077) instead was lower than previously reported by Postel *et al.* (2017a) (66.3%), which could be due to differences in sample size, collection date and location but also to differences between serological assays. As discussed in Chapter 3, limited assay validation was undertaken for both the assays used in this study and the one used by Postel *et al.* (2017a). Although the Scottish prevalence reported here is similar to that reported for Germany (47.1%) by Postel *et al.* (2017a), it

is lower than that in most other European countries, which showed higher seroprevalence in the same study.

The British suspected CT cases provided further evidence of APPV circulating within Great Britain, with APPV detected in all cases. Four of the ten cases submitted were closely related to sequence from Germany in 2015 (KU041637.1), one case to the 2017 Hungarian (MH049532.1) strain, four cases related to sequences from the USA (one case most closely related to KU194231.1 from 2012 and three cases related to NC_038964.1 from 2013), and one case to a 2018 Chinese (MH499643.1) sequence. The diversity in strains detected suggests that not only is APPV circulating within the UK, but that multiple incursions of APPV into Great Britain might have occurred from Europe, USA and Asia, which may be due to the import of live pigs, germplasm (semen/embryos), or animal by-products such as raw meat.

In 2016, 360 live pigs were imported from Canada, and 151 from the USA, in addition to a total of 472,769 live pigs imported from Europe, with all of the pigs originating from five member states: Ireland (471,081), Denmark (1,442), Netherlands (133), Germany (101) and Sweden (12) (Animal and Plant health Agency, 2020). The number of germplasm (individual embryos or insemination doses of semen) imported into the UK in the same year from Europe was 82,678 (Animal and Plant health Agency, 2020). Although the potential risk of APPV transmission through semen was discussed in Chapter 4, currently no studies have been conducted to determine the risk of APPV transmission from imported raw/processed pig meat products. The transmission of other viruses that affect pigs such as ASFV and other pestiviruses including classical swine fever virus (CSFV) constitute a significant concern for both the European and British pig industries, and raw meat should be explored further as a potential route of APPV transmission (Farez and Morley, 1997; Bronsvoort, Alban and Greiner, 2008; Olesen *et al.*, 2020). Although, since 1996 it has been illegal to feed animal by-products in the form of catering scraps or domestic food waste to pigs in the UK (Animal and Plant Health Agency, 2017).

Interestingly, no viral RNA was detected in the non-extended fresh semen from any of the farms tested. A study by Rovira *et al.* (2007) found that pooling in groups of either three or five when testing non-extended semen for PRRSV by RT-qPCR reduced detection of positive samples at every time point tested, which may explain the lack of APPV detection in the non-extended semen samples (pooled in groups of five) in the current study. Unfortunately, due to the lack of available non-extracted semen samples at the time of the survey, it was not possible to perform individual testing versus spiked pool testing to determine the effect of pooling on the sensitivity of the APPV RT-qPCR assay. Previously, APPV RNA had been detected individually at high titres in non-extended semen from CT affected boars, as discussed in Chapter 4. This result contradicts the findings by Gatto and colleagues who detected APPV in 12.9% of semen samples (59/457) tested individually by RT-qPCR from commercial US boar units (Gatto *et al.*, 2018a).

Other pestiviruses such as bovine viral diarrhoea virus (BVDV) are known to not only replicate in the genital tract of bulls and can be easily detected in semen, but are also transmitted to inseminated animals, especially when bulls have acute, persistent or persistent testicular infections (Kirkland *et al.*, 1991; Givens, 2018). A study demonstrated the transmissibility of border disease virus (BDV) by infecting five pestivirus naive cows (as determined by pestivirus specific ELISA) via artificial insemination of cryopreserved semen from a BDV persistently infected bull; all cows had seroconverted (determined by serum neutralisation test and ELISA) by day 28 post insemination (Braun *et al.*, 2015). Further analysis of British semen samples from boar is required to determine the prevalence of APPV and the potential risk of venereal transmission of the virus. Active surveillance programmes through the continuation of APPV epidemiological surveys such as the ones presented here provide valuable information on the level of circulation of the virus and its distribution within Great Britain to aid in the improvement of prevention and control strategies necessary to eradicate APPV associated CT A-II from the British herd.

Chapter 7: General Discussion and conclusions

The understanding of atypical porcine pestivirus (APPV) pathogenesis and immunogenicity is currently limited due to the novelty of the virus, its association with congenital tremors A-II (CT A-II) which is not common and often difficult to investigate, and its apparent genetic diversity both within atypical porcine pestivirus (APPV) itself and from other members of the *Pestivirus* genus. The impact of APPV and CT A-II on the British pig industry has been the subject of limited investigations, with minimal studies carried out into the effect on production, the strains present in the British pig population and the extent of circulation of these within the national herd. Prior to this PhD study, only one epidemiological study had been conducted in Great Britain (GB) using a small sample size (86 serum samples collected from healthy pigs), which determined a genomic prevalence of 2.3% (2/86) and seroprevalence of 66.3% (57/86) (Postel *et al.*, 2017a). From this study, only one partial APPV NS3 sequence was recovered.

A lack of commercially available diagnostic tests to aid in the detection and characterisation of the virus in CT A-II infections, and a concomitant lack of known positive clinical material hampers the development of highly validated diagnostic assays. Therefore, the main aim of this work was to characterise British field strains of APPV and to investigate the clinical, virological, pathological, and immunological outcomes associated with APPV induced CT A-II infections, including the potential role of APPV in immunosuppression. Central to this aim was the establishment of robust diagnostic assays capable of detecting and quantifying GB field strains.

7.1 General findings and limitations

The establishment and improvement of diagnostics was an ongoing part of the project. This involved the initial optimisation and re-optimisation of the APPV non-structural (NS)3 reverse transcriptase quantitative polymerase chain reaction (RT-qPCR) to detect, quantify and characterise APPV ribonucleic acid (RNA) of GB field strains with an emphasis on investigating the most appropriate sample type for each assay (serum, oral, nasal and rectal swabs, tissues and semen) that could be applied in a UK routine diagnostic settings, epidemiological investigations and surveillance programmes. Subsequently, a BaseScope *in situ* hybridisation (ISH) assay was developed, based on the NS3 gene of sequenced GB strains, to visualise the location and quantity of APPV RNA in different cells and tissues, allowing for more in-depth investigations of cellular tropism and viral pathogenesis.

Ear tissue notches can be easily collected during piglet tagging, and are already employed as a powerful screening tool to aid bovine viral diarrhoea virus (BVDV) eradication programmes in cattle. Ear notches were therefore evaluated as a standard diagnostic sample, found to be a more suitable sample than serum, as APPV RNA titres in ear tissue had a higher degree of correlation with clinical signs in the Scottish APPV outbreak investigated. Furthermore, the preparation methodology was successfully modified to allow performing RT-qPCR on ear notch samples without the need to undergo conventional nucleic acid extraction. This represents a significant technical advancement however, further work is needed to determine the suitability of ear notch samples for detection of APPV antigen by ELISA assays, as currently in use for BVDV.

APPV-specific immunoglobulin G (IgG) antibody detection and quantification were achieved by developing and validating an indirect NS3 enzyme-linked immunosorbent assay (ELISA), using the recombinant antigen produced for the NS3H blocking ELISA by Schwarz *et al.* (2017); this ELISA was also used

to investigate the potential immunosuppressive properties of APPV on the antibody response. As more isolates of the virus, including pure cultures, become accessible, efforts should be made not only in the development of new serological and molecular based assays, but the continued improvement of the existing ones. This includes determining the most effective, least invasive sampling methods for APPV detection and the capability of current diagnostic tests to detect positives in pooled samples of different types (semen, oral fluids and serum) at different stages of infection (early and late). Established assays should also be compared to determine their sensitivity in the detection of different strains of APPV, due to the high genetic variability of the virus.

The development of validated sensitive and specific techniques capable of detecting APPV and associated immune responses to the virus is paramount in gaining an understanding not only the risk and impact of the virus within the national herd, but in the implementation of prevention and control strategies necessary to improve animal health and welfare as well as to minimise both the direct and indirect economic consequences of APPV infection across the industry. In order to transcend the application of these tests in a strictly research setting, these techniques need to become more widely available to farmers and vets through commercialisation to enable their routine use as a diagnostic test in holistic intervention strategies.

Unfortunately, virus isolation was not achieved during this work due to time constraints and the limited availability of clinical material. When isolation was attempted, only five passages were performed on SPEV 0008, porcine kidney-15 (PK-15) and bovine turbinate (BT) cell lines, lines known to be permissive to other pestiviruses. Successful isolation from serum was reported by Cagatay *et al.* (2021) using the SPEV 0008 cell line after 100 passages, with cell adaptation thought to have occurred between passage 45 and 100 as a result of substitutions in the E^{rns} (H330Q) and E2 (N751K and D752N) regions of the polyprotein. Although the permissibility varied significantly, this cell-adapted strain was observed to propagate on different porcine cell lines (PK-

15, swine kidney-6 [SK-6] and swine testis [ST]). While virus isolation was not successful in this work, further isolation attempts should be pursued using British strains to understand cell adaptation, the differences in the permissibility of porcine cell lines and fully characterise the cellular entry mechanism of APPV.

This project also required a substantial amount of material; therefore, an alternative approach was devised to obtain enough virus to carry out challenge infections and provide material for assay validation. Successful infection of snatch farrowed colostrum deprived piglets enabled the study of postnatal infection of the virus and the collection of known positive material from different sample types which, in addition to enabling virus isolation attempts, allowed further validation of the diagnostic tests, increasing their robustness (RT-qPCR and BaseScope ISH) and strengthening confidence in the results. The postnatal infection showed detectable virus from day three with a peak of viraemia on day seven to nine, detectable virus in oral and rectal swabs from day seven and nasal swabs from day nine, suggesting viral shedding in oronasal secretions and faecal matter poses a risk for viral transmission. These findings confirm those reported in other experimental infections (Arruda *et al.*, 2016; De Groof *et al.*, 2016). At post-mortem, APPV was detected by RT-qPCR in all major organs indicating a systemic viral distribution. Both the APPV challenged animals and control animals shared the same airspace and, as there was no evidence of viral transmission between the groups, it is unlikely that airborne transmission is an important route of viral dissemination in this infection. Further postnatal infections should be performed using different transmission routes and possibilities for direct and indirect contact to determine how the virus spreads within infected herds. Also, a more in-depth characterisation of the immune responses to the virus in early, mid and late-stage infections including antibodies (IgM antibody in early infections and IgG antibodies in mid-later infections once affinity maturation and class switching has occurred) and cell mediated kinetics is still required.

APPV was identified in a field case of CT A-II from Scotland, and with permission from the farm the outbreak was investigated to determine the outcome of infection of the offspring within two farrowing groups. Phylogenetic analysis based on the NS3 partial sequence indicated that the Scottish viral strain was most closely related to a Hungarian strain (MH049532.1) sequenced (Dénes *et al.*, 2018). Within both farrowing groups at two weeks of age, APPV RNA and APPV-specific antibodies were detected in serum at varying levels regardless of clinical signs of CT A-II, suggesting that the development of clinical signs may be critically dependent on the timing of infection *in utero*, and the degree of fetal immune and nervous system development. Investigation into the development of CT A-II in relation to infection *in utero* have been conducted. De Groof *et al.* (2016) inoculated three sows intramuscularly with APPV positive serum at 32 days of gestation produced two litters containing CT affected piglet (84-87% of the litter affected). Two other studies inoculated sows with APPV positive serum at 45 and 62 days of gestation; in both studies all litters had CT affected piglets with litter prevalence between 57and 100% (Arruda *et al.*, 2016; Buckley *et al.*, 2021). Additional controlled APPV experimental infections are required to confirm the importance of viral introduction in utero in relation to gestational developmental stage and to determine the impact of this on the severity of disease (described further in 7.2).

In the first farrowing group, at the final sample collection (eight weeks of age), APPV RNA was detected in all animals in concomitance with minimal levels of APPV-specific IgG. Moreover, in the second farrowing group at the second collection time point (10 weeks of age), APPV-specific antibody levels had waned. These results, in conjunction with the lack of APPV-specific IgG in APPV challenged colostrum deprived piglets at day 10 (E10/18), indicate that early antibody levels observed in the majority of piglets in both farrowing groups were most likely maternally derived rather than being generated by the piglets themselves. Examination of the second farrow group revealed multiple clinical outcomes for offspring, both within the farrowing group and within

individual litters, regardless of piglet sex or sow parity. Piglets exhibiting CT A-II clinical signs with detectable APPV RNA at two weeks of age were likely the result of vertical transmission. In contrast, piglets without clinical signs that were initially APPV RNA negative then developed APPV RNA positivity at a later stage (10 weeks or more), were most likely infected through direct contact with other positive animals present in the same farrowing group. A number of non-clinical piglets also had APPV RNA detected earlier, at two weeks old. This could have been a result of a vertical transmission in late gestation after the nervous system had developed to a point that APPV infection did not adversely affect myelination, or it may have been a result of early horizontal transmission. As no samples were collected from animals younger than two weeks old, it was not possible to determine exactly how these transmissions occurred. The number and timing of sample collections was restricted due to the nature of the study (a field case in a commercial unit outside of a controlled experimental environment), and the need for co-operation from the farm and the farm's veterinary team. Several piglets also had no detectable APPV RNA at two weeks old despite presenting with CT, this in combination with the detection of moderate APPV-specific antibodies levels suggests that piglets may have mounted an immune response to clear APPV infection prior to testing. These findings are noteworthy in understanding the transmission and subclinical circulation of APPV within Great Britain. Horizontal transmission of the virus without clinical signs may lead to viral dissemination without detection, not only within units but between units, and further epidemiological study is needed to determine the effect of this within the industry. To investigate this, ear notches testing to detect viral presence and active infection or bodily secretions to confirm viral shedding should be considered either prior to pig movement within farm production pyramids(nucleus, boar studs, multiplier herds, production fattening/finishing units) or at mixing locations (such as auction houses or show grounds).

Piglets were only observed to have transient APPV infections (viraemic for a maximum of 10 weeks) with no viral persistence in serum. This was supported

by the increased APPV-specific antibody response observed in the majority of animals by slaughter (22—28 weeks), indicating that an antibody response was mounted, with no evidence of tolerance or immune suppression within the group. The lack of viral persistence in serum contradicted reports from another study that identified the virus in serum until slaughter (23 weeks old) (Cagatay *et al.*, 2019). Unfortunately, no oral-nasal secretions or faecal material was collected during the study to determine levels of viral shedding in these piglets. This would have been useful as it would allow investigation of viral shedding, rather than viraemia, in relation to the antibody response and should be considered for future work.

While viral persistence in serum was not observed in the second farrowing group, APPV RNA persisted in tissues in both farrowing groups (at eight weeks in group 1 and at slaughter (22—28 weeks) in group 2) suggesting that APPV detection in serum is not necessarily an indication of viral clearance, but rather a quantitative measure of viral control. Future work should also consider using uncoagulated whole blood samples to determine APPV viraemia as it is possible that APPV may be cell associated (leukocytes) and only released by infected cells into serum. This could potentially result in lower viral titres in the serum, and thus warrants further studies to elucidate this.

High viral loads were detected in lymphoid tissue (tonsil, lymph node and thymus), similarly to what was observed in the postnatal APPV infection (E10/18) and other studies investigating tissue tropism (Arruda *et al.*, 2016; Muñoz-González *et al.*, 2017; Shen *et al.*, 2018; Liu *et al.*, 2019). APPV RNA was also found in high abundance in the cerebellum (in the granular and molecular layer), in the cerebrum and the spinal cord (both in the matrix and cell-associated) within glial cells, epithelial cells in blood vessels and neurons, with and without satellitosis. This agrees with other studies showing similar distribution (Possatti *et al.*, 2018b; Buckley *et al.*, 2021); however, samples for this investigation were only collected from eight-week-old piglets from the first farrowing group. Additional studies are needed to understand the

pathogenesis of the CT A-II in relation to cellular tropism, cellular damage and how this may change over time.

High titres of APPV RNA were also detected in semen at slaughter, at the point where APPV viraemia had resolved; this corroborates a previous report that found APPV present in a six-month-old CT affected boar (Schwarz *et al.*, 2017). These animals may have the potential to transmit APPV sexually, posing a risk to the British breeding system, impacting the health and welfare of animals directly through CT A-II outbreaks and indirectly through the potential effects on fertility and production, leading to additional financial repercussions. However further research is needed to establish if venereal transmission is present and the infectivity of APPV detected in semen. If demonstrated, the pig industry should consider self-regulation measures through the implementation of active surveillance and accreditation schemes to prove virus free status for boar studs, especially in commercially available semen for artificial insemination. As a result of these findings, a small Scottish molecular survey of raw unprocessed non-extended semen from 41 commercial boar studs in Scotland was performed (Chapter 6), using pooled semen from each stud. APPV was not identified within any of the boar units, which was inconsistent with the Perthshire outbreak findings where APPV was detected in semen at slaughter and also with reports of a high prevalence of APPV in commercial stud units in the USA (Gatto *et al.*, 2018a). However, the Scottish molecular survey was conducted on pooled semen samples from each stud, not single samples as with the field case study; therefore, the sensitivity of the RT-qPCR assay may have affected the assays capability of detecting infected individual boars within the pool as the positive serum would have been diluted 5-fold. This needs to be clarified by performing studies on pooled APPV spiked semen samples to determine the optimal pooling ratio for APPV detection, as discussed previously.

APPV viraemia, and clinical signs were not influenced by the sex of the piglet or parity of the sow and were not found to impact growth (as a parameter of

production) when measured by the length of time to finish. However, the litter the piglets were from did significantly affect APPV viraemia and clinical signs. Unfortunately, due to the limitations in farm records, no additional parameters of production could be analysed. In order to determine the true cost of the virus and its associated disease to the UK pig industry, other indicators of growth such as birth weights or daily live weight gain, and other production parameters such as fertility, litter size, pre- and post-weaning mortality and comorbidity with other diseases should be investigated more thoroughly. Additionally, an investigation into the attitudes, awareness, and level of education regarding APPV and CT A-II within the industry (producers, independent farmers, AI services and clinicians) surrounding current control and prevention strategies alongside an economic analysis of the direct and indirect cost should be conducted. This is likely to produce a comprehensive understanding of the true impact of outbreaks on the UK pig herd.

The effect of APPV as an immunosuppressive agent and its potential role in co-infections was explored in an experimental infection with PRRSV species 1 subtype 2. Although no severe immune suppression was observed in the study, there was a clear interaction between the two pathogens. All animals became PRRSV antibody positive by day 10 and no difference in polyclonal or PRRSV-specific T cell response (indicated by production of IFN-γ by splenocytes) was observed, which supports the findings of the CT A-II field case study. APPV infection however enhanced PRRSV clinical signs and inflammatory responses, as indicated by heightened and prolonged rectal temperatures in the APPV/PRRSV co-infected group. As interactions between pathogens are complex and depend on the timing of infection in relation to each other and the strength of viral challenge, the use of 10-week-old animals which acquired the APPV infection *in utero* (APPV positive with CT A-II clinical signs) may have resulted in additional subtle interactions between the viruses being missed in this study.

As well as differences in the febrile response, significant increase in the consolidation of the apical and intermediate lung lobes was present in the co-infected piglets, indicating increased inflammation and cellular infiltration in response to PRRSV. However, differences in the degree of consolidation between lobes was also observed and likely due to uneven distribution of the PRRSV inoculum. Additional studies should be pursued in an experimental setting in which the timing of infection, the strength of the challenge, the route of inoculation and the age of the animal can be controlled to provide further confirmation of the results presented in this work. Future studies should also investigate the virulence of different APPV strains and the impact of these strains on co-infections with other pathogens, given that APPV has been detected in natural co-infections such as porcine circovirus type 2, swine influenza virus or porcine epidemic diarrhoea virus (Yuan *et al.*, 2021)

Following the identification of APPV within Scotland in a CT A-II field outbreaks, further epidemiological investigations were undertaken to determine the prevalence of APPV currently circulating in the Scottish pig population and the extent of previous exposure within the national herd. In this work APPV was detected in one or more samples from healthy 5-month-old pigs from 33/108 farms sampled, with an overall molecular detection rate of 4.7% and a seroprevalence of 48.8% (93/108 farms affected). These results indicate that the level of APPV circulating in the British population previously reported may have been an underestimate (Postel *et al.*, 2017a). The evidence from the work presented here suggests that APPV was not only present in Scottish farms in 2018, but that the virus had been circulating sub-clinically, with the majority of farms being exposed as recently as within 5 months prior to the collection. Further work is needed to identify whether this is an endemic, emerging or re-emerging problem within the national pig herd by expanding the investigation to include other collection years to understand the significance of this finding to the UK pork industry. Additionally, analysis of self-reporting data (production data submitted to quality management scheme

from each of the herds sampled as part of the biobank collection) should also be performed.

Suspected CT outbreaks analysed in this thesis provided further evidence of APPV circulation within the British pig herd. Interestingly, sequencing of the virus isolated from different British cases were closely related to APPV strains from other countries of origin at different time points; USA 2012 (KU194231.1) and 2013 (NC_038964.1), Germany 2015 (KU041637.1), and China 2018 (MH499643.1). As only partial NS3 sequences of approximately 90 bp were used for phylogenetic analysis in this thesis, as with the CT A-II Scottish field case, the relatedness of strains may have been subject to change had a longer portion of the NS3 gene or multiple genes (Erns, NS5B) been sequenced. Whole-genome sequencing should be conducted to confirm the phylogenetic analysis results presented in this work. Additional large-scale epidemiological studies to understand the extent of genetic diversity of APPV circulating strains and their distribution within farm production pyramids (nucleus, boar studs, multiplier herds, production fattening/finishing units) in the UK and Ireland should also be undertaken.

This research provides a foundation step in the understanding of APPV associated CT A-II within the British pig industry. The insights into the pathogenesis and immunogenicity of the virus and its associated disease presented as a result of the validated diagnostic techniques developed specifically for British APPV strains are critical in expanding the understanding of the consequences of APPV infection. Moreover, the same techniques will be underpinning future surveillance programmes and epidemiological investigations needed to continue to inform prevention, control and eradication strategies for the UK.

7.2 Future work

In order to further expand on the findings of the research presented here and address some of the limitations, a longitudinal cohort study exploring how the timing of infection *in utero* in relation to fetal development affects the outcomes for the offspring should be undertaken. The study should aim to infect gilts with APPV at different time points in their gestation related to key time points in fetal development, such as the onset of innate and adaptive immunity (approximately 45 days) and immune competence (70—80 days), the primary brain growth phase (64—104 days) and the onset of myelination brain and spinal cord (70—80 days). This should be accompanied by serial culls of fetuses during pregnancy and postnatally (up to one year) to characterise viral and antibody profiles and collect nervous and lymphoid samples to identify pathological changes and cell tropism. This work would help to clarify the link between clinical signs, viraemia, humoral and cellular immune response, immunocompetence and possible induction of tolerance. A portion of sows should be inseminated with semen with detectable APPV RNA from infected boars to clarify venereal transmission and characterise infection at the point of conception.

The above vertical transmission study would also allow the analysis of infection on other production parameters pertaining to reproduction, including fertility, fetal abnormalities, stillbirths, litter sizes and birth weights and growth. It would also present an opportunity for the prolonged study of piglets in a controlled environment, including further research on shedding, immunosuppression and susceptibility to disease, viral persistence and the resolution of clinical signs in relation to pathology. In addition to this, APPV induced CT A-II positive pigs at sexual maturity could also be bred to establish the implications for their offspring.

As well as continuing to investigate naturally-occurring co-infections of APPV CT A-II and other pathogens in a field setting, further experimental

investigations of APPV co-infections should be considered. Piglets *in utero* and postnatally could be co-infected with other common porcine pathogens to determine the clinical, virological, immunological and pathological outcomes of concurrent infections in piglets at various developmental stages. This would allow a better understanding of the complex interactions between the host and APPV and between APPV and the different pathogens and present an opportunity to produce disease management strategies with immediate and direct application for the control of the disease in the field.

Appendix A: Sequencing

The sequences for APPV RT-qPCR positive samples collected in Chapter 4 from farrowing group 1 (tonsil collected from animal 18 and lymph node collected from animal 01, 03 and 04) and farrowing group 2 (semen collected from animal 945, 593 and 598) are shown in Figure A-1 and the British suspected CT cases for APPV confirmatory testing are shown in Figure A-2. The multiple sequence Cluster Omega analysis which combines NS3 sequences from both chapter 4 and 6 and published NS3 sequences which share more than an 80% nucleotide identity is presented in Figure A-3.

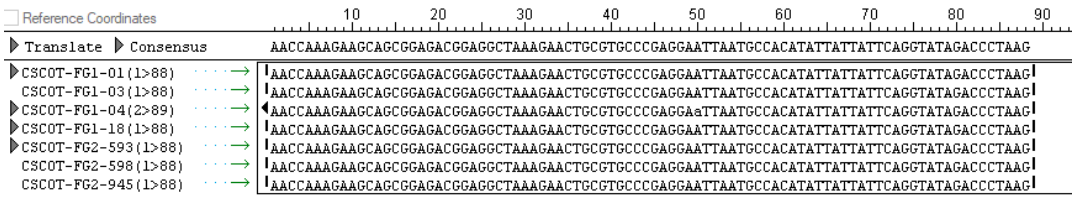

Figure A-1: Consensus sequence alignment for APPV RT-qPCR positive samples collected from animals in farrowing group 1 (tonsil collected from animal 18 and lymph node collected from animal 01, 03 and 04) and animals in farrowing group 2 (semen collected from animal 945, 593 and 598). The sequences for individual samples are shown in black and the consensus shown at the top.

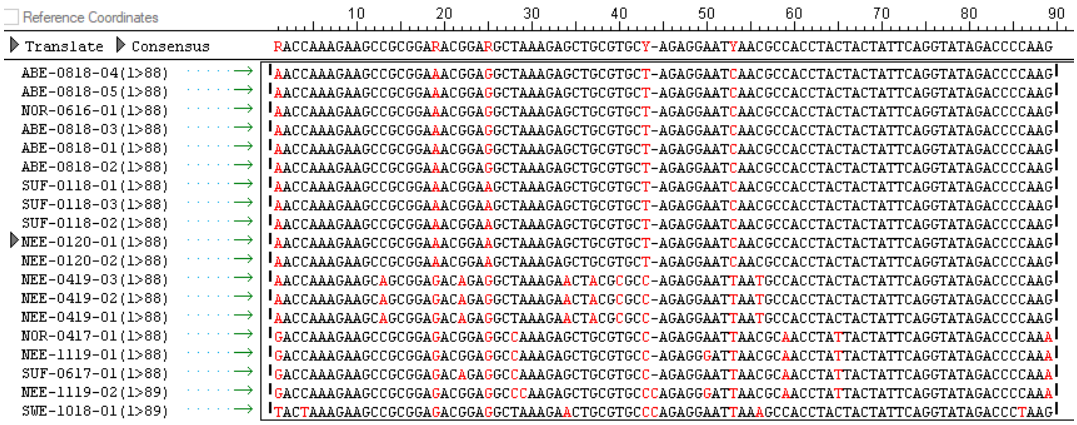

Figure A-2: Consensus sequence alignment for UK suspected CT cases submitted for confirmatory testing of APPV. The sequences for samples are shown in black with base disagreements in red and the consensus shown at the top

```
GBR_NEE-1119-02          ----------GACCAAAGAAGCCGCGGAGACGGAGGCCMAAGAGCTGCGTGCC43
GBR_NOR-0616-01          ----------AACCAAAGAAGCCGCGGAAACGGAGGCTAAAGAGCTGCGTG--41
GBR_ABE-0818-01          ----------AACCAAAGAAGCCGCGGAAACGGAGGCTAAAGAGCTGCGTG--41
GBR_ABE-0818-02          ----------AACCAAAGAAGCCGCGGAAACGGAGGCTAAAGAGCTGCGTG--41
GBR_ABE-0818-03          ----------AACCAAAGAAGCCGCGGAAACGGAGGCTAAAGAGCTGCGTG--41
GBR_ABE-0818-04          ----------AACCAAAGAAGCCGCGGAAACGGAGGCTAAAGAGCTGCGTG--41
GBR_ABE-0818-05          ----------AACCAAAGAAGCCGCGGAAACGGAGGCTAAAGAGCTGCGTG--41
DEU_2015_KU041637.1      -------TGTTCGTGGCAACCAAAGAAGCCGCGGAAACGGAGGCTAAAGAGCTGCGTG--51
GBR_SUF-0118-01          ----------AACCAAAGAAGCCGCGGAAACGGAAGCTAAAGAGCTGCGTG--41
GBR_SUF-0118-02          ----------AACCAAAGAAGCCGCGGAAACGGAAGCTAAAGAGCTGCGTG--41
GBR_SUF-0118-03          ----------AACCAAAGAAGCCGCGGAAACGGAAGCTAAAGAGCTGCGTG--41
GBR_NEE-0120-01          ----------AACCAAAGAAGCCGCGGAAACGGAAGCTAAAGAGCTGCGTG--41
GBR_NEE-0120-02          ----------AACCAAAGAAGCCGCGGAAACGGAAGCTAAAGAGCTGCGTG--41
USA_2013_NC_038964.1     ----TGGTATTCGTGGCAACCAAAGAAGCCGCGGAGACGGAGGCCAAAGAGCTGCGTG--54
GBR_NEE-1119-01          ----------GACCAAAGAAGCCGCGGAGACGGAGGSCAAAGAGCTGCGTG--41
GBR_NOR-0417-01          ----------GACCAAAGAAGCCGCGGAGACGGAGGCCAAAGAGCTGCGTG--41
GBR_SUF-0617-01          ----------GACCAAAGAAGCCGCGGAGACAGAGGCCAAAGAGCTGCGTG--41
ROK_2019_MH509410.1      TGTCTGGTTTTCGTGGCAACCAAAGAAGCCGCGGAGACGGAGGCCAAAGAGCTGCGTG--58
CHN_2017_MF377344.1      ----TGGTATTCGTGGCAACCAAAGAAGCCGCGGAGACGGAGGCCAAAGAGCTGCGTG--54
ROK_2019_MT501748.1      -------TATTCGTGGCAACCAAAGAGGCCGCGGAGATGGAGGCCAAAGAGCTGCGTG--51
USA_2013_KU194230.1      -------TATTCGTGGCAACCAAAGAAGCCGCGGAGACGGAGGCCAAAGAGCTGCGTG--51
SWE_2020_LR700966.1      ----TGGTATTCGTGGCAACCAAAGAAGCCGCGGAGACGGAGGCCAAAGAGCTGCGTG--54
SWE_2019_LR700964.1      -------TGTTCGTGGCAACCAAAGAAGCCGCGGAGACGGAGGCCAAAGAGCTGCGTG--51
GBR_SWE-1018-01          ----------TACTAAAGAAGCCGCGGAGACGGAGGCTAAAGAACTGCGTGC-42
DEU_2017_MG679837.1      -------TGTTCGTGGCAACCAAAGAAGCTGCGGAGACAGAGGCCAAAGAATTGCGT-A-51
DEU_2016_MG679831.1      -------TGTTCGTGGCAACCAAAGAAGCTGCGGAGACAGAGGCCAAAGAACTGCGT-A-51
DEU_2017_MG679836.1      -------TGTTCGTGGCAACCAAAGAAGCTGCGGAGACAGAGGCCAAAGAACTGCGT-A-51
DEU_2016_MG679828.1      -------TGTTCGTGGCAACCAAAGAAGCTGCGGAGACAGAGGCCAAAGAACTGCGT-A-51
DEU_2015_MG679829.1      -------TGTTCGTGGCAACCAAAGAAGCTGCGGAGACAGAGGCCAAAGAACTGCGT-A-51
SWE_2019_LR700967.1      -------TGTTCGTGGCAACCAAAGAGGCTGCGGAGACAGAGGCCAAAGAACTGCGC-A-51
ITA_2018_MN736976.1      -------TGTTCGTGGCAACCAAAGAGGCTGCGGAGACAGAGGCGAAAGAACTGCGG-A-51
NLD_2019_MT512537.1      -------TGTTCGTGGCAACCAAAGAGGCTGCGGAGACAGAGGCTAAAGAACTGCGC-A-51
NLD_2018_MT512536.1      -------TGTTCGTGGCAACCAAAGAGGCTGCGGAGACAGAGGCTAAAGAACTGCGC-A-51
NLD_2017_MT512535.1      -------TGTTCGTGGCAACCAAAGAGGCTGCGGAGACAGAGGCTAAAGAACTGCGC-A-51
NLD_2016_MT512533.1      -------TGTTCGTGGCAACCAAAGAGGCTGCGGAGACAGAGGCTAAAGAACTGCGC-A-51
NLD_2015_MT512532.1      -------TGTTCGTGGCAACCAAAGAGGCTGCGGAGACAGAGGCTAAAGAACTGCGC-A-51
NLD_2013_MT512531.1      -------TGTTCGTGGCAACCAAAGAGGCTGCGGAGACAGAGGCTAAAGAACTGCGC-A-51
ITA_2017_MN736974.1      -------TGTTCGTGGCAACTAAAGAGGCTGCGGAGACAGAGGCCAAAGAACTGCGT-A-51
GBR_NEE-0419-01          ----------AACCAAAGAAGCAGCGGAGACAGAGGCTAAAGAACTACGC-G-41
GBR_NEE-0419-02          ----------AACCAAAGAAGCAGCGGAGACAGAGGCTAAAGAACTACGC-G-41
GBR_NEE-0419-03          ----------AACCAAAGAAGCAGCGGAGACAGAGGCTAAAGAACTACGC-G-41
ESP_2016_LT631734.1      -------TGTTCGTGGCAACTAAAGAAGCAGCGGAGACGGAGGCTAAAGAACTACGC-G-51
ESP_2014_LT631730.1      -------TGTTCGTGGCAACCAAAGAAGCAGCGGAGACGGAGGCTAAAGAACTACGC-G-51
CHN_2018_MH499643.1      -------TGTTCGTAGCAACCAAAGAAGCAGCGGAGACGGAGGCTAAAGAACTACGC-G-51
CHN_2017_MH499647.1      ------TTGTTCGTAGCAACCAAAGAAGCAGCGGAGACGGAGGCTAAAGAACTACGC-G-52
USA_2017_MW183242.1      -------TGTTCGTGGCAACTAAAGAAGCCGCGGAGACGGAGGCTAAAGAACTGCGT-A-51
USA_2014_KU194229.1      -------TGTTCGTGGCAACCAAAGAAGCCGCGGAGACGGAGGCTAAAGAACTGCGC-A-51
USA_2012_KU194231.1      -------TGTTCGTGGCAACCAAAGAAGCCGCGGAGACGGAGGCTAAAGAACTGCGC-A-51
GBR_CSCOT-FG1-03         ----------AACCAAAGAAGCAGCGGAGACGGAGGCTAAAGAACTGCGT-G-41
GBR_CSCOT-FG1-04         ----------AACCAAAGAAGCAGCGGAGACGGAGGCTAAAGAACTGCGT-G-41
GBR_CSCOT-FG1-18         ----------AACCAAAGAAGCAGCGGAGACGGAGGCTAAAGAACTGCGT-G-41
GBR_ CSCOT-FG1-01                ----------CAACCAAAGAAGCAGCGGAGACGGAGGCTAAAGAACTGCGT-G-42
GBR_CSCOT-FG2-945        ----------AACCAAAGAAGCAGCGGAGACGGAGGCTAAAGAACTGCGT-G-41
GBR_CSCOT-FG2-593        ----------AACCAAAGAAGCAGCGGAGACGGAGGCTAAAGAACTGCGT-G-41
GBR_CSCOT-FG2-598        ----------AACCAAAGAAGCAGCGGAGACGGAGGCTAAAGAACTGCGT-G-41
DEU_2016_LT594521.1      -------TGTTCGTGGCAACCAAAGAAGCAGCAGAGACGGAGGCCAAAGAACTGCGT-G-51
HUN_2017_MH049531.1      -------TGTTCGTGGCAACCAAAGAAGCAGCGGAGACGGAGGCCAAAGAACTGCGT-G-51
DEU_2016_MF167290.1      -------TGTTCGTGGCAACCAAAGAAGCAGCAGAGACGGAGGCCAAAGAACTGCGT-G-51
DEU_2015_KU041638.1      -------TGTTCGTGGCAACCAAAGAAGCAGCAGAGACGGAGGCCAAAGAACTGCGT-G-51
DEU_2017_MG679839.1      -------TGTTCGTGGCAACCAAAGAGGCTGCGGAGACAGAGGCCAAAGAATTGCGC-A-51
DEU_2016_MG679838.1      -------TGTTCGTGGCAACCAAAGAGGCTGCGGAGACAGAGGCCAAAGAATTGCGC-A-51
CHN_2017_MK378661.1      -------TGTTCGTGGCAACCAAAGAAGCTGCGGAGACAGAGGCTAAAGAATTGCGT-A-51
CHN_2016_KY475592.1      -------TGTTCGTGGCAACCAAAGAAGCTGCGGAGACAGAGGCCAAAGAATTGCGT-A-51
CHN_2016_MG792803.1      -------TGTTCGTGGCAACAAAAGAAGCTGCGGAGACAGAGGCCAAAGAATTGCGT-A-51
CHN_2017_MK948873.1      -------TGTTCGTGGCAACAAAAGAAGCTGCGGAGACAGAGGCCAAAGAATTGCGT-A-51
CHN_2017_MF167292.1      -------TGTTCGTGGCAACAAAAGAAGCTGGGGAGACAGAGGCCAAAGAATTGCGT-A-51
CHE_2006_MN099164.1      -------TGTTCGTGGCAACCAAAGAAGCCGCGGAGACGGAGGCCAAAGAACTGCGT-G-51
CHE_2006_MN099163.1      -------TGTTCGTGGCAACCAAAGAAGCCGCGGAGACGGAGGCCAAAGAACTGCGT-G-51
ROK_2019_MT501737.1      -------TGTTCGTGGCAACCAAAGAAGCTGCGGAGACGGAGGCCAAAGAACTGCGT-G-51
ROK_2019_MT501740.1      -------TATTCGTGGCAACCAGAGAAGCTGCAGAGACGGAGGCCAAAGAACTGCGT-G-51
ROK_2019_MT501744.1      -------TATTCGTGGCGACCAAAGAAGCTGCAGAGACGGAGGCCAAAGAACTGCGT-G-51
ROK_2019_MT501741.1      -------TATTCGTGGCAACCAAAGAAGCTGCAGAGACGGAGGCCAAAGAACTGCGT-G-51
** * *** ** *  ** *  ** *   **** * **
```

Figure A-3: Cluster Omega multiple sequence analysis for NS3 region of UK based samples: samples collected from field case in Chapters 4, suspected CT cases from chapter 6 and published sequences with more than an 80% nucleotide identity. Published sequences are named based on their country-of-origin collection date and GenBank accession number.

```
GBR_NEE-1119-02          CAGAAGGGATTAACGCAACCTATTACTATTCAGGTATAGACCCCAAA-----------90
GBR_NOR-0616-01           CTAGAGGAATCAACGCCACCTACTACTATTCAGGTATAGACCCCAAG-----------88
GBR_ABE-0818-01          CTAGAGGAATCAACGCCACCTACTACTATTCAGGTATAGACCCCAAG-----------88
GBR_ABE-0818-02          CTAGAGGAATCAACGCCACCTACTACTATTCAGGTATAGACCCCAAG-----------88
GBR_ABE-0818-03          CTAGAGGAATCAACGCCACCTACTACTATTCAGGTATAGACCCCAAG-----------88
GBR_ABE-0818-04          CTAGAGGAATCAACGCCACCTACTACTATTCAGGTATAGACCCCAAG-----------88
GBR_ABE-0818-05          CTAGAGGAATCAACGCCACCTACTACTATTCAGGTATAGACCCCAAG-----------88
DEU_2015_KU041637.1      CTAGAGGAATCAACGCCACCTACTACTATTCAGGTATAGACCCCAAGACTTTGGAACAT110
GBR_SUF-0118-01          CTAGAGGAATCAACGCCACCTACTACTATTCAGGTATAGACCCCAAG-----------88
GBR_SUF-0118-02          CTAGAGGAATCAACGCCACCTACTACTATTCAGGTATAGACCCCAAG-----------88
GBR_SUF-0118-03          CTAGAGGAATCAACGCCACCTACTACTATTCAGGTATAGACCCCAAG-----------88
GBR_NEE-0120-01          CTAGAGGAATCAACGCCACCTACTACTATTCAGGTATAGACCCCAAG-----------88
GBR_NEE-0120-02          CTAGAGGAATCAACGCCACCTACTACTATTCAGGTATAGACCCCAAG-----------88
USA_2013_NC_038964.1     CCAGAGGAATCAACGCAACCTATTACTATTCAGGTATAGACCCCAAAACTCTGGAACAT113
GBR_NEE-1119-01          CCAGAGGGATTAACGCAACCTATTACTATTCAGGTATAGACCCCAAA-----------88
GBR_NOR-0417-01           CCAGAGGAATTAACGCAACCTATTACTATTCAGGTATAGACCCCAAA-----------88
GBR_SUF-0617-01          CCAGAGGAATTAACGCAACCTATTACTATTCAGGTATAGACCCCAAA-----------88
ROK_2019_MH509410.1      CTAGAGGAATTAACGCCACCTATTACTATTCAGGTATAGACCCAAAAACTCTGGAACAT117
CHN_2017_MF377344.1      CTAGAGGAATTAATGCCACTTATTACTATTCAGGTATAGACCCAAAAACTCTGGAACAT113
ROK_2019_MT501748.1      CCAGAGGAATTAACGCCACTTATTACTATTCAGGCATAGACCCCAAAACTCTGGAACAT110
USA_2013_KU194230.1      CTAGAGGGATTAACGCCACTTATTACTATTCAGGGATAGACCCCAAAACTCTGGAACAT110
SWE_2020_LR700966.1      CCAGAGGAATTAACGCCACTTATTACTATTCAGGTATAGACCCCAAAACTCTGGAACAT113
SWE_2019_LR700964.1      CCAGAGGAATTAACGCCACTTATTACTATTCAGGTATAGACCCCAAAACTCTGGAACAT110
GBR_SWE-1018-01          CCAGAGGAATTAAAGCCACCTACTACTATTCAGGTATAGACCCTAAG-----------89
DEU_2017_MG679837.1      CCAGAGGAGTCAATGCCACCTACTACTATTCAGGTATAGATCCTAAGACTTTGGAACAT110
DEU_2016_MG679831.1      CCAGAGGAGTCAATGCCACCTACTACTATTCAGGTATAGATCCTAAGACTTTGGAACAT110
DEU_2017_MG679836.1      CCAGAGGAGTAAATGCCACCTACTACTATTCAGGTATAGATCCCAAGACTTTGGAACAT110
DEU_2016_MG679828.1      CCAGAGGAGTCAATGCCACCTACTACTATTCAGGTATAGATCCCAAGACTTTGGAACAT110
DEU_2015_MG679829.1      CCAGAGGAGTCAATGCCACCTACTACTATTCAGGTATAGATCCCAAGACTTTGGAACAT110
SWE_2019_LR700967.1      CCAGAGGGATTAATGCCACCTACTACTATTCAGGTATAGATCCTAAGACTCTGGAATAT110
ITA_2018_MN736976.1      CCAGAGGGATTAATGCCACCTACTACTATTCAGGTATAGATCCTAAGACTCTGGAACAT110
NLD_2019_MT512537.1      CCAGAGGAATCAATGCCACCTACTACTATTCAGGTATAGATCCTAAGACTCTGGAACAT110
NLD_2018_MT512536.1      CCAGAGGAATCAATGCCACCTACTACTATTCAGGTATAGATCCTAAGACTCTGGAACAT110
NLD_2017_MT512535.1      CCAGAGGAATCAATGCCACCTACTACTATTCAGGTATAGATCCTAAGACTCTGGAACAT110
NLD_2016_MT512533.1      CCAGAGGAATCAATGCCACCTACTACTATTCAGGTATAGATCCTAAGACTCTGGAACAT110
NLD_2015_MT512532.1      CCAGAGGAATCAATGCCACCTACTACTATTCAGGTATAGATCCTAAGACTCTGGAACAT110
NLD_2013_MT512531.1      CCAGAGGAATCAATGCCACCTACTACTATTCAGGTATAGATCCTAAGACTCTGGAACAT110
ITA_2017_MN736974.1      CCAGAGGGATCAATGCCACCTACTACTATTCAGGTATAGATCCTAAGACTCTGGAACAT110
GBR_NEE-0419-01          CCAGAGGAATTAATGCCACCTACTACTATTCAGGTATAGACCCCAAG-----------88
GBR_NEE-0419-02          CCAGAGGAATTAATGCCACCTACTACTATTCAGGTATAGACCCCAAG-----------88
GBR_NEE-0419-03          CCAGAGGAATTAATGCCACCTACTACTATTCAGGTATAGACCCCAAG-----------88
ESP_2016_LT631734.1      CTAGGGGAATTAATGCCACCTACTACTATTCAGGTATAGACCCTAAGACTCTGGAACAT110
ESP_2014_LT631730.1      CTAGAGGAATTAATGCCACTTACTACTATTCAGGTATAGACCCTAAGACTCTGGAACAT110
CHN_2018_MH499643.1      CTAGAGGAATTAATGCCACCTACTACTATTCAGGTATAGACCCTAAGACTCTGGAACAT110
CHN_2017_MH499647.1      CTAGAGGAATTAATGCCACCTACTACTATTCGGGTATAGACCCTAAGACTCTGGAACAT111
USA_2017_MW183242.1      CCAGAGGAATTAATGCCACCTACTACTACTCAGGTATAGACCCCAAGACTCTGGAACAT110
USA_2014_KU194229.1      CCAGAGGAATTAACGCCACCTACTACTATTCAGGTATAGACCCTAAGACTCTGGAACAT110
USA_2012_KU194231.1      CCAGAGGAATTAACGCCACCTACTACTATTCAGGTATAGACCCTAAGACTCTGGAACAT110
GBR_CSCOT-FG1-03         CCCGAGGAATTAATGCCACATATTATTATTCAGGTATAGACCCTAAG-----------88
GBR_CSCOT-FG1-04         CCCGAGGAaTTAATGCCACATATTATTATTCAGGTATAGACCCTAAG-----------88
GBR_CSCOT-FG1-18         CCCGAGGAATTAATGCCACATATTATTATTCAGGTATAGACCCTAAG-----------88
GBR_CSCOT-FG1-01                 CCCGAGGAATTAATGCCACATATTATTATTCAGGTATAGACCCTAAG-----------89
GBR_CSCOT-FG2-945        CCCGAGGAATTAATGCCACATATTATTATTCAGGTATAGACCCTAAG-----------88
GBR_CSCOT-FG2-593        CCCGAGGAATTAATGCCACATATTATTATTCAGGTATAGACCCTAAG-----------88
GBR_CSCOT-FG2-598        CCCGAGGAATTAATGCCACATATTATTATTCAGGTATAGACCCTAAG-----------88
DEU_2016_LT594521.1      CCCGAGGAATTAATGCCACCTATTATTATTCAGGCATAGACCCTAAGACTCTGGAACAT110
HUN_2017_MH049531.1      CCCGAGGAATCAATGCCACATATTATTATTCAGGTATAGACCCTAAGACTCTGGAACAT110
DEU_2016_MF167290.1      CCCGAGGAATTAATGCCACATATTATTATTCAGGTATAGACCCTAAGACTCTGGAACAT110
DEU_2015_KU041638.1      CCCGAGGAATTAATGCCACATATTATTATTCAGGTATAGACCCTAAGACTCTGGAACAT110
DEU_2017_MG679839.1      CTAAAGGAATTAATGCTACCTACTACTATTCAGGTATAGACCCTAAGACCCTGGAGCAT110
DEU_2016_MG679838.1      CTAAAGGAATTAATGCTACCTACTACTATTCAGGTATAGACCCTAAGACCCTGGAGCAT110
CHN_2017_MK378661.1      CCAAAGGAATTAATGCCACCTACTACTATTCAGGTATAGACCCTAAGACACTGGAACAT110
CHN_2016_KY475592.1      CCAAAGGAATTAATGCCACCTACTACTATTCAGGTATAGACCCTAAGACACTGGAACAT110
CHN_2016_MG792803.1      CCAAAGGAATTAACGCCACCTACTACTATTCAGGTATAGACCCTAAGACACTGGAACAT110
CHN_2017_MK948873.1      CCAAAGGAATTAATGCCACCTACTACTATTCAGGTATAGACCCTAAGACACTGGAACAT110
CHN_2017_MF167292.1      CCAAAGGAATTAATGCCACCTACTACTATTCAGGTATAGACCCTAAGACACTGGAACAT110
CHE_2006_MN099164.1      CCAGAGGAATTAATGCCACTTACTATTATTCAGGTATAGACCCTAAAACTTTGGAACAT110
CHE_2006_MN099163.1      CCAGAGGAATTAATGCCACCTACTATTATTCAGGTATAGACCCTAAAACTCTGGAACAT110
ROK_2019_MT501737.1      CCAAAGGAATTAATGCCACCTACTACTATTCAGGTATAGACCCTAAGACTCTGGAACAT110
ROK_2019_MT501740.1      CCAAAGGAATTAATGCCACCTACTACTATTCAGGTATAGACCCTAAGACTCTGGAACAT110
ROK_2019_MT501744.1      CCAAAGGAATTAATGCCACCTACTACTATTCAGGTATAGACCCTAAGACTCTGGAACAT110
ROK_2019_MT501741.1      CCAAAGGAATTAATGCCACCTACTACTATTCAGGTATAGACCCTAAGACTCTGGAACAT110
*    **  * ** ** ** ** ** ** ** ** ***** ** **
```

Continuation of Figure A-1: Cluster Omega multiple sequence analysis for NS3 region of UK based samples: samples collected from field case in Chapters 4, suspected CT cases from chapter 6 and published sequences with more than an 80% nucleotide identity. Published sequences are named based on their country-of-origin collection date and GenBank accession number.

Appendix B: Interpretation of NS3 indirect ELISA results

The statistical analysis and modelling performed to determine the positive cut-off the threshold of the APPV Indirect ELISA developed in Chapter 3 and employed in the Chapter 6 sero-survey was carried out by Dr Giles Innocent on behalf of Biomathematics & Statistics Scotland (BioSS).

Data exploration

Initial data exploration was conducted as shown in Figure B-1 and B-2 to determine the distribution of the ELISA and RT-qPCR results.

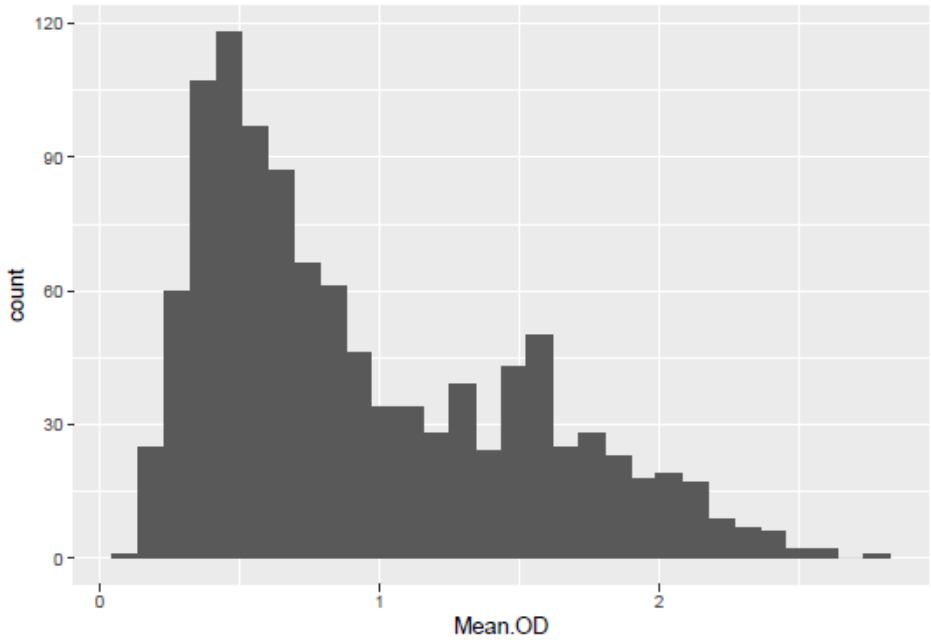

Figure B- 1: Frequency of APPV-specific IgG levels (OD) within sero-survey. The graph shows two overlapping distributions with means of approximately 0.5 and 1.5.

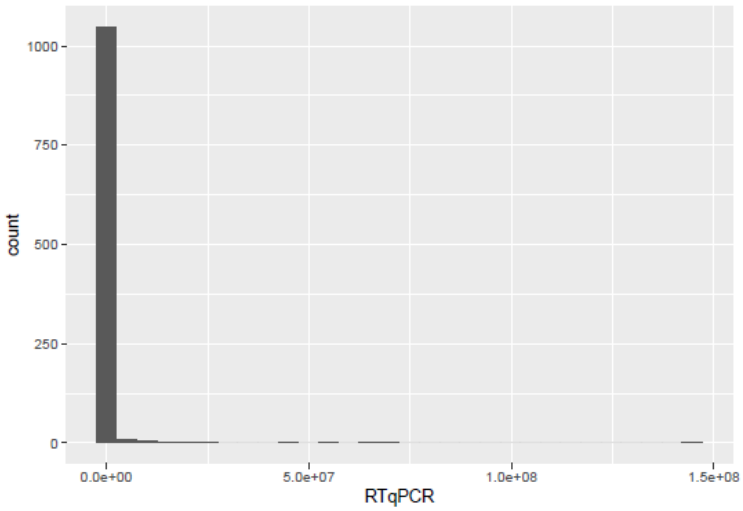

Figure B- 2: Frequency of APPV viral load in serum (copies/ml) within sero-survey.

A mixture of normal distributions

Initially, a Gamma distribution model was performed to identify the cut-off threshold for the APPV indirect ELISA however this failed to converge. For this reason, a model approach based on a mixture of normal (Gaussian) distributions (as shown in Figure B-3) was performed with the only stipulation in their formulation that the hte mena of the positive distribution was greater than the mean of the negative distribution. Although this model converges well to the parameters of the distributions, there is less convergence observed for individual latent classes. Due to this, the ROC analysis (Figure B-4) for the ELISA was performed twice with identical results confirming convergence. In both cases, the ROC analysis demonstrated the test to have good discriminating power between positives and negative samples and good precision (based on the size of the confidence envelope).

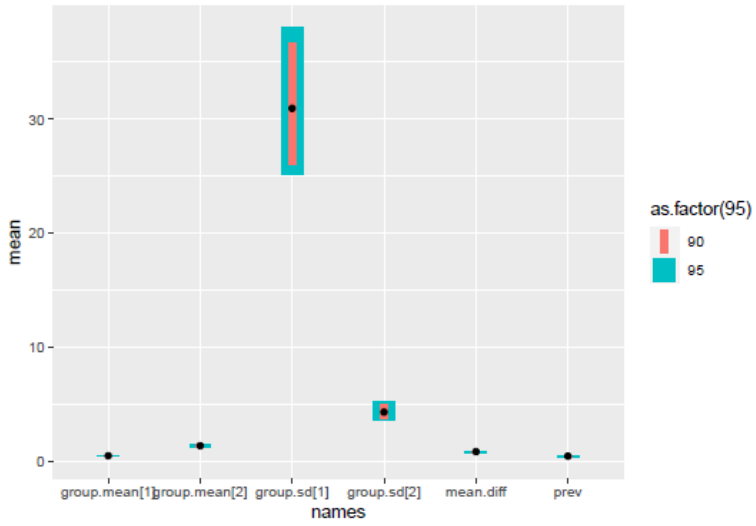

Figure B-3: Gamma distribution model for APPV-specific antibody results. From left to right the graph shows the mean OD of negative animals, the mean OD of positive animals, the standard deviation of OD of negative animals and the standard deviation of OD of positive animals, the standard deviation of OD of negative animals and the standard deviation of OD of positive animals, the difference in the means and the proportion of samples that the model predicts as being positive (about 50%). The black dot represents the median estimate, the red bar is the 90% CI and the blue bar the 95% CI.

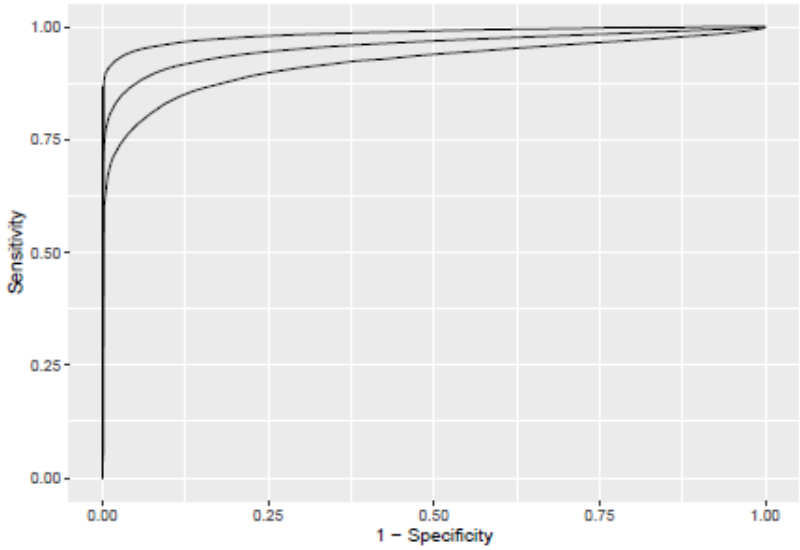

Figure B-4: ROC analysis for the APPV indirect ELISA. The middle line indicates the mean estimate, and the two lines surround it represents the 95% confidence envelope.

Mean estimated sensitivity and specificity at a number of cut-offs are presented in Table B-1. The cut-off threshold for positive/negative samples was determined by finding the highest value at which sensitivity and specificity values were equal. In this case, the most suitable cut-off value was 0.77 with a sensitivity and specificity equal to 90%.

Table B-2: The sensitivity and specificity for different ELISA cut-off values to determine the threshold for positive and negative sample populations.

Cut-off	Sensitivity	Specificity
0.066	1.000	0.000
0.094	1.000	0.001
0.121	1.000	0.001
0.148	1.000	0.003
0.175	0.999	0.006
0.202	0.998	0.018
0.229	0.996	0.041
0.256	0.995	0.056
0.283	0.993	0.083
0.310	0.991	0.126
0.337	0.988	0.170
0.365	0.985	0.231
0.392	0.982	0.280
0.419	0.979	0.329
0.446	0.976	0.394
0.473	0.972	0.458
0.500	0.968	0.509

Continuation of Table B-1: The sensitivity and specificity for different ELISA cut-off values to determine the threshold for positive and negative sample populations.

Cut-off	Sensitivity	Specificity
0.527	0.965	0.562
0.554	0.961	0.607
0.581	0.957	0.655
0.609	0.953	0.692
0.636	0.946	0.745
0.663	0.940	0.782
0.690	0.933	0.819
0.717	0.927	0.845
0.744	0.915	0.887
0.771	0.909	0.903
0.798	0.899	0.920
0.825	0.885	0.940
0.852	0.867	0.959
0.880	0.849	0.972
0.907	0.830	0.981
0.934	0.808	0.989
0.961	0.796	0.992
0.988	0.778	0.995
1.015	0.764	0.996
1.042	0.741	0.998
1.069	0.724	0.999
1.096	0.703	0.999

Continuation of Table B-1: The sensitivity and specificity for different ELISA cut-off values to determine the threshold for positive and negative sample populations.

Cut-off	Sensitivity	Specificity
1.123	0.684	1.000
1.150	0.661	1.000
1.178	0.638	1.000
1.205	0.628	1.000
1.232	0.619	1.000
1.259	0.601	1.000
1.286	0.586	1.000
1.313	0.566	1.000
1.340	0.533	1.000
1.367	0.514	1.000
1.394	0.506	1.000
1.422	0.491	1.000
1.449	0.473	1.000
1.476	0.464	1.000
1.503	0.423	1.000
1.530	0.400	1.000
1.557	0.361	1.000
1.584	0.332	1.000
1.611	0.324	1.000
1.638	0.295	1.000
1.665	0.277	1.000
1.693	0.264	1.000
1.720	0.248	1.000

Continuation of Table B-1: The sensitivity and specificity for different ELISA cut-off values to determine the threshold for positive and negative sample populations.

Cut-off	Sensitivity	Specificity
1.747	0.229	1.000
1.774	0.217	1.000
1.801	0.204	1.000
1.828	0.192	1.000
1.855	0.175	1.000
1.882	0.167	1.000
1.909	0.151	1.000
1.936	0.142	1.000
1.964	0.132	1.000
1.991	0.120	1.000
2.018	0.109	1.000
2.045	0.097	1.000
2.072	0.087	1.000
2.099	0.081	1.000
2.126	0.072	1.000
2.153	0.058	1.000
2.180	0.050	1.000
2.207	0.047	1.000
2.235	0.043	1.000
2.262	0.037	1.000
2.289	0.031	1.000
2.316	0.031	1.000
2.343	0.023	1.000

Continuation of Table B-1: The sensitivity and specificity for different ELISA cut-off values to determine the threshold for positive and negative sample populations.

Cut-off	Sensitivity	Specificity
2.370	0.021	1.000
2.397	0.012	1.000
2.424	0.012	1.000
2.451	0.010	1.000
2.478	0.008	1.000
2.506	0.008	1.000
2.533	0.006	1.000
2.560	0.006	1.000
2.587	0.004	1.000
2.614	0.004	1.000
2.641	0.002	1.000
2.668	0.002	1.000
2.695	0.002	1.000
2.722	0.002	1.000
2.749	0.000	1.000

References

Advanced Cell Diagnostics, Bio-Techne. (2018) *BaseScope Detection Reagent Kit v2 – RED User Manual*. Available at: https://acdbio.com/system/files_force/USM23900%20BaseScope%20Detection%20Reagent%20v2%20_ 06082018.pdf (Accessed: 17 February 2020)

Agri-Food and Biosciences institute (2015) *Final report of BVDV control in Europe*, *Agri-Food and Biosciences institute*. Available at: https://www.afbini.gov.uk/articles/final-report-bvdv-control-europe (Accessed: 13 August 2021).

Animal and Plant Health Agency (2008) *Defra, UK - Veterinary Investigation Surveillance Report (VIDA): 2000-2007*. Department for Environment, Food and Rural Affairs (Defra), Nobel House, 17 Smith Square, London SW1P 3JR helpline@defra.gsi.gov.uk.Available at: https://webarchive.nationalarchives.gov.uk/20140307032908/http://www.defra.gov.uk/ahvlaen/publication/vida07/ (Accessed: 3 June 2021).

Animal and Plant Health Agency (2015) *Veterinary Investigation Diagnosis Analysis (VIDA) report: 2007-2014*. GOV.UK. Available at: https://webarchive.nationalarchives.gov.uk/20200807145152/https://www.gov.uk/government/publications/veterinary-investigation-diagnosis-analysis-vida-report-2014 (Accessed: 3 June 2021).

Animal and Plant Health Agency (2016) *Pig: disease surveillance reports, 2016*. GOV.UK. Available at: https://webarchive.nationalarchives.gov.uk/20200804050505/https://www.gov.uk/government/publications/pig-disease-surveillance-reports-2016 (Accessed: 13 July 2021).

Animal and Plant Health Agency (2017) *Pig keepers warned not to feed kitchen scraps to pigs due to African swine fever risk*, *GOV.UK*. Available at: https://www.gov.uk/government/news/pig-keepers-warned-not-to-feed-kitchen-scraps-to-pigs-due-to-african-swine-fever-risk (Accessed: 13 August 2021).

Animal and Plant Health Agency (2018) *Classical swine fever: how to spot and report the disease*. Available at: https://www.gov.uk/guidance/classical-swine-fever (Accessed: 24 June 2021).

Animal and Plant health Agency (2020) *Livestock Demographic Data Group: Pig Enhanced Demographics – summary for external report 2018*. Available at: http://apha.defra.gov.uk/documents/surveillance/diseases/lddg-dem-report-pig2019.pdf (Accessed: 25 July 2021).

Animal and Plant Health Agency (2021) *Defra, UK - Veterinary Investigation Surveillance Report (VIDA): 2013-2020*. .GOV.UK. Available at: https://public.tableau.com/app/profile/siu.apha/viz/VIDAAnnualReport2020/VIDAAnnualReport2020 (Accessed: 3 June 2021).

Antonson, A.M., Balakrishnan, B., Radlowski, E.C., Petr, G. and Johnson, R.W. (2018) "Altered Hippocampal Gene Expression and Morphology in Fetal Piglets Following Maternal Respiratory Viral Infection." *Developmental Neuroscience* 40 (2): 104–19.

Arruda, B.L., Arruda, P.H., Magstadt, D.R., Schwartz, K.J., Dohlman, T., Schleining, J.A., Patterson, A.R., Visek, C.A. and Victoria, J.G. (2016) "Identification of a Divergent Lineage Porcine Pestivirus in Nursing Piglets with Congenital Tremors and Reproduction of Disease Following Experimental Inoculation." *PloS One* 11 (2): e0150104.

Baechlein, C., Grundhoff, A., Fischer, N., Alawi, M., Hoeltig, D., Waldmann,K-H. and Becher, P. (2016) "Pegivirus Infection in Domestic Pigs, Germany." *Emerging Infectious Diseases* 22 (7): 1312–14.

Baker, J.A. and Sheffy, B.E. (1960) "A Persistent Hog Cholera Viraemia in Young Pigs." *Proceedings of the Society for Experimental Biology and Medicine. Society for Experimental Biology and Medicine* 105 (December): 675–78.

Baker, J.C. (1995) "The Clinical Manifestations of Bovine Viral Diarrhoea Infection." *The Veterinary Clinics of North America. Food Animal Practice* 11 (3): 425–45.

Barman, N.N., Khatoon, E., Bora, M., Deori, L., Gogoi, S.M. and Kalita, D. (2021) "Investigation of Congenital Tremor Associated with Classical Swine Fever Virus Genotype 2.2 in an Organized Pig Farm in North-Eastern India." *Virus disease*, March, 1–10.

Battersby, J. (2005) *UK Mammals: Species Status and Population Trends*. Joint Nature Conservation Committee.

Beer, M., Reimann, I., Hoffmann, B. and Depner, K. (2007) "Novel Marker Vaccines against Classical Swine Fever." *Vaccine* 25 (30): 5665–70.

Beer, M., Wernike, K., Dräger, C., Höper, D., Pohlmann, A., Bergermann, C., Schröder, C., Klinkhammer, S., Blome, S. and Hoffmann, B. (2017) "High Prevalence of Highly Variable Atypical Porcine Pestiviruses Found in Germany." *Transboundary and Emerging Diseases* 64 (5): e22–26.

Beyer, J., Fichtner, D., Schirrmeir, H., Polster, U., Weiland, E. and Wege, H. (2000) “Porcine Reproductive and Respiratory Syndrome Virus (PRRSV): Kinetics of Infection in Lymphatic Organs and Lung.” *Journal of Veterinary Medicine Series B*. https://doi.org/10.1046/j.1439-0450.2000.00305.x.

Blome, S., Aebischer, A., Lange, E., Hofmann, M., Leifer, I., Loeffen, W., Koenen, F., and Beer, M. (2012) “Comparative Evaluation of Live Marker Vaccine Candidates ‘CP7_E2alf’ and ‘Flc11’ along with C-Strain ‘Riems’ after Oral Vaccination.” *Veterinary Microbiology* 158 (1–2): 42–59.

Blome, S., Meindl-Böhmer, A., Loeffen, W., Thuer, B., and Moennig, V. (2006) “Assessment of Classical Swine Fever Diagnostics and Vaccine Performance.” *Revue Scientifique et Technique (International Office of Epizootics)* 25 (3): 1025–38.

Blome, S., Moß, C., Reimann, I., König, P., and Beer, M. (2017a) “Classical Swine Fever Vaccines-State-of-the-Art.” *Veterinary Microbiology* 206 (July): 10–20.

Blome, S, Staubach, C., Henke, J., Carlson, J. and Beer, M. (2017b) “Classical Swine Fever-An Updated Review.” *Viruses* 9 (4).

Blome, S., Wernike, K., Reimann, I., König, P., Moß, C., and Beer, M. (2017c) “A Decade of Research into Classical Swine Fever Marker Vaccine CP7_E2alf (Suvaxyn® CSF Marker): A Review of Vaccine Properties.” *Veterinary Research* 48 (1).

Blomström, A-L., Fossum, C., Wallgren P., and Berg, M. (2016) “Viral Metagenomic Analysis Displays the Co-Infection Situation in Healthy and PMWS Affected Pigs.” *PLOS ONE*.

Blomström, A-L., Ley, C. and Jacobson, M. (2014) “Astrovirus as a Possible Cause of Congenital Tremor Type AII in Piglets?” *Acta Veterinaria Scandinavica* 56 (1): 82.

Bohórquez, J.A., Muñoz-González, S., Pérez-Simó, M., Muñoz, I., Rosell, R., Coronado, L., Domingo, M. and Ganges, L. (2020) “Foetal Immune Response Activation and High Replication Rate during Generation of Classical Swine Fever Congenital Infection.” *Pathogens* 9 (4).

Bourne, F. J. (1973) “The Immunoglobulin System of the Suckling Pig.” *The Proceedings of the Nutrition Society* 32 (3): 205–15.

Bradley, R., Done, J.T., Hebert, C.N., Overby, E., Askaa, J., Basse, A. and Bloch, B. (1983) “Congenital Tremor Type AI: Light and Electron Microscopical Observations on the Spinal Cords of Affected Piglets.” *Journal of Comparative Pathology*.

Braun, U., Frei, S., Schweizer, M., Zanoni, R. and Janett, F. (2015) “Short Communication: Transmission of Border Disease Virus to Seronegative Cows Inseminated with Infected Semen.” *Research in Veterinary Science* 100 (June): 297–98.

Brock, K.V. (2003) “The Persistence of Bovine Viral Diarrhoea Virus.” *Biologicals: Journal of the International Association of Biological Standardization* 31 (2): 133–35.

Brockmeier, S.L. and Lager, K.M. (2002) “Experimental Airborne Transmission of Porcine Reproductive and Respiratory Syndrome Virus and Bordetella Bronchiseptica.” *Veterinary Microbiology* 89 (4): 267–75.

Broeders, S., Huber, I., Grohmann, L., Berben, G., Taverniers, I., Mazzara, M., Roosens, N. and Morisset. D. (2014) “Guidelines for Validation of Qualitative Real-Time PCR Methods.” *Trends in Food Science and Technology* 37 (2): 115–26.

Bronsvoort, B.M.C., Alban, L. and Greiner, M. (2008) “Quantitative Assessment of the Likelihood of the Introduction of Classical Swine Fever Virus into the Danish Swine Population.” *Preventive Veterinary Medicine* 85 (3–4): 226–40.

Brooksbank, N. H. (1955) “Trembles in Piglets.” *The Veterinary Record* 67: 576–77.

Buckley, A.C., Falkenberg, S.M., Palmer, M.V., Arruda, P.H., Magstadt, D.R., Schwartz, K.J., Gatto, I.R., Neill, J.D. and Arruda, B.L. (2021) “Distribution and Persistence of Atypical Porcine Pestivirus in Experimentally Inoculated Pigs.” *Journal of Veterinary Diagnostic Investigation: Official Publication of the American Association of Veterinary Laboratory Diagnosticians, Inc*, June.

Burkard, C., Lillico, S.G., Reid, E., Jackson, B., Mileham, A.J., Ait-Ali, T., Whitelaw, C.B.A. and Archibald, A.L. (2017) “Precision Engineering for PRRSV Resistance in Pigs: Macrophages from Genome Edited Pigs Lacking CD163 SRCR5 Domain Are Fully Resistant to Both PRRSV Genotypes While Maintaining Biological Function.” *PLoS Pathogens* 13 (2).

Bustin, S.A. (2010) “Why the Need for QPCR Publication Guidelines?--The Case for MIQE.” *Methods* 50 (4): 217–26.

Bustin, S.A., Benes, V., Garson, J.A., Hellemans, J., Huggett, J., Kubista, M., Mueller, R., Nolan, T., Pfaffl, M.W., Shipley, G.L., Vandesompele, J. and Wittwer, C.T. (2009) “The MIQE Guidelines: Minimum Information for Publication of Quantitative Real-Time PCR Experiments.” *Clinical Chemistry* 55 (4): 611–22.

Bustin, S. and Huggett, J. (2017) “QPCR Primer Design Revisited.” *Biomolecular Detection and Quantification* 14 (December): 19–28.

Cagatay, G. N., Antos, A., Meyer, D., Maistrelli, C., Keuling, O., Becher, P. and Postel, A. (2018) “Frequent Infection of Wild Boar with Atypical Porcine Pestivirus (APPV).” *Transboundary and Emerging Diseases* 65 (4): 1087–93.

Cagatay, G. N., Antos, A., Suckstorff, O., Isken, O., Tautz, N., Becher, P. and Postel, A. (2021) “Porcine Complement Regulatory Protein CD46 Is a Major Receptor for Atypical Porcine Pestivirus but Not for Classical Swine Fever Virus.” *Journal of Virology* 95 (9).

Cagatay, G.N., Meyer, D., Wendt, M., Becher, P. and Postel, A. (2019) “Characterization of the Humoral Immune Response Induced after Infection with Atypical Porcine Pestivirus (APPV).” *Viruses* 11 (10).

Chae, C. (2005) “A Review of Porcine Circovirus 2-Associated Syndromes and Diseases.” *Veterinary Journal (London, England: 1997)* 169 (3): 326–36.

Chapman, A. B. (1956) “Anomalies in Pigs.” *Veternary Science News* 10 (20).

Charpin, C., Mahé, S., Keranflec’h, A., Belloc, C., Cariolet, R., Le Potier, M-F and Rose, N. (2012) “Infectiousness of Pigs Infected by the Porcine Reproductive and Respiratory Syndrome Virus (PRRSV) Is Time-Dependent.” *Veterinary Research* 43 (October): 69.

Chen, F., Knutson, T.P., Braun, E., Jiang, Y., Rossow, S. and Marthaler, D.G. (2019) “Semi-Quantitative Duplex RT-PCR Reveals the Low Occurrence of Porcine Pegivirus and Atypical Porcine Pestivirus in Diagnostic Samples from the United States.” *Transboundary and Emerging Diseases* 66 (3): 1420–25.

Choe, S., Kim, J. H., Kim, K. S., Song, S., Kang, W. C., Kim, H. J., Park, G. N., Cha, R. M., Cho, I. S., Hyun, B. H., Park, B. K., and An, D. J. (2019). Impact of a Live Attenuated Classical Swine Fever Virus Introduced to Jeju Island, a CSF-Free Area. *Pathogens* 8(4), 251.

Choe, S., Park, G-N., Cha, R.M., Hyun, B-H., Park, B-K. and An, D-J. (2020) “Prevalence and Genetic Diversity of Atypical Porcine Pestivirus (APPV) Detected in South Korean Wild Boars.” *Viruses* 12 (6): 680.

Colom-Cadena, A., Ganges, L., Muñoz-González, S., Castillo-Contreras R., Bohórquez, J.A., Rosell, R., Segalés, J., Marco, I. and Cabezon, O. (2018) “Atypical Porcine Pestivirus in Wild Boar (Sus Scrofa), Spain.” *The Veterinary Record* 183 (18): 569.

Coronado, L., Perera, C. L., Rios, L., Frías, M. T., and Pérez, L. J. (2021). A Critical Review about Different Vaccines against Classical Swine Fever Virus and Their Repercussions in Endemic Regions. *Vaccines*, 9(2), 154.

Curtis, J. and Bourne, F.J. (1971) “Immunoglobulin Quantitation in Sow Serum, Colostrum and Milk and the Serum of Young Pigs.” *Biochimica et Biophysica Acta* 236 (1): 319–32.

Dall Agnol, A.M., Alfieri, A.F. and Alfieri, A.A. (2020) “Pestivirus K (Atypical Porcine Pestivirus): Update on the Virus, Viral Infection, and the Association with Congenital Tremor in Newborn Piglets.” *Viruses* 12 (8).

De Groof, A., Deijs, M., Guelen, L., Van Grinsven, L., Van OS-Galdos, L., Vogels, W., Derks, C., Cruijsen, T., Geurts, V., Vrijenhoek, M., Suijskens, J., Van Doorn, P., Van Leengoed, L., Schrier, C. and Van Der Hoek, L. (2016) “Atypical Porcine Pestivirus: A Possible Cause of Congenital Tremor Type A-II in Newborn Piglets.” *Viruses* 8 (10): 271.

Dénes, L., Biksi, I., Albert, M., Szeredi, L., Knapp, D.G., Szilasi, A., Bálint, Á. and Balka, G. (2018) “Detection and Phylogenetic Characterization of Atypical Porcine Pestivirus Strains in Hungary.” *Transboundary and Emerging Diseases* 65 (6): 2039–42.

Department for Enviroment, Food and Rural Affairs (2021) *Farming Statistics-Livestock Populations at 1 December 2020, UK*. Available at: https://assets.publishing.service.gov.uk/government/uploads/system/uploads/attachment_data/file/928464/structure-june20-eng-21oct20.pdf (Accessed: 13 July 2021).

Dessureault, F.G., Choinière, M., Provost, C. and Gagnon, C.A. (2018) “First Report of Atypical Porcine Pestivirus in Piglets with Congenital Tremor in Canada.” *The Canadian Veterinary Journal. La Revue Veterinaire Canadienne* 59 (4): 429–32.

Dial, G.D., Hull, R.D., Olson, C.L., Hill, H.T. and Erickson, G.A. (1990) “Mystery Swine Disease: Implications and Needs of the North American Swine Industry.” *Prof Mystery Swine Dis Committee*, 3–6.

Díaz de Arce, H., Núñez, J.I., Ganges, L., Barreras, M., Teresa Frías, M. and Sobrino, F. (1999) “Molecular Epidemiology of Classical Swine Fever in Cuba.” *Virus Research* 64 (1): 61–67.

Díaz, I., Gimeno, M., Darwich, L., Navarro, N., Kuzemtseva, L., López, S., Galindo, I., Segalés, J., Martín, M., Pujols, J. and Mateu, E. (2012) “Characterization of Homologous and Heterologous Adaptive Immune Responses in Porcine Reproductive and Respiratory Syndrome Virus Infection.” *Veterinary Research* 43 (April): 30.

Doeschl-Wilson, A.B., Kyriazakis, I., Vincent, A., Rothschild, M.F., Thacker, E. and Galina-Pantoja, L. (2009) “Clinical and Pathological Responses of Pigs from Two Genetically Diverse Commercial Lines to Porcine Reproductive and Respiratory Syndrome Virus Infection.” *Journal of Animal Science* 87 (5): 1638–47.

Done, J.T. 1968. “Congenital Nervous Diseases of Pigs: A Review.” *Laboratory Animals* 2 (2): 207–18.

Done S.H, Paton D.J. and White M.E. (1996) “Porcine reproductive and respiratory syndrome (PRRS): a review, with emphasis on pathological, virological and diagnostic aspects. ” British Veterinary Journal. 152(2):153-74.

Dräger, C., Petrov, A., Beer, M., Teifke, J. P., and Blome, S. (2015) Classical swine fever virus marker vaccine strain CP7_E2alf: Shedding and dissemination studies in boars. *Vaccine*, 33(27), 3100–3103.

Dräger, C., Schröder, C., König, P., Tegtmeyer, B., Beer, M., and Blome, S. (2016) Efficacy of Suvaxyn CSF Marker (CP7_E2alf) in the presence of pre-existing antibodies against Bovine viral diarrhea virus type 1. *Vaccine*, 34(39), 4666–4671.

Duan, X., Nauwynck, H.J. and Pensaert, M.B. (1997) “Virus Quantification and Identification of Cellular Targets in the Lungs and Lymphoid Tissues of Pigs at Different Time Intervals after Inoculation with Porcine Reproductive and Respiratory Syndrome Virus (PRRSV).” *Veterinary Microbiology* 56 (1–2): 9–19.

Dutia, B.M., Entrican, G. and Nettleton, P.F. (1990) “Cytopathic and Non-Cytopathic Biotypes of Border Disease Virus Induce Polypeptides of Different Molecular Weight with Common Antigenic Determinants.” *The Journal of General Virology* 71 (Pt 5) (May): 1227–32.

Edwards, M.J. and Mulley, R.C. 1986. “Genetic, Developmental, and Neoplastic Diseases.” https://agris.fao.org/agris-search/search.do?recordID =US8903380.

European Commision (2002) ‘Commission decision of February 2002 approving a diagnostic manual establishing diagnostic procedures, sampling methods and criteria for evaluation of the laboratory tests for the confirmation of classical swine fever (2002/106/EC)’, *OJEC*, Chapter VII, pp. 71–88.

European Medicines Agency (EMA). (2018a). “Advasure.” European Medicines Agency. Available at: https://www.ema.europa.eu/en/medicines/ veterinary/EPAR/advasure. (Accessed: 13 March 2022).

European Medicines Agency (EMA). (2018b). “Porcilis Pesti.” European Medicines Agency. Available at: https://www.ema.europa.eu/en/medicines/veterinary/EPAR/porcilis-pesti. (Accessed: 13 March 2022).

European Medicines Agency (EMA). (2018c). “Suvaxyn CSF Marker.” European Medicines Agency. Available at: https://www.ema.europa.eu/en/medicines/veterinary/EPAR/suvaxyn-csf-marker. (Accessed: 13 March 2022).

Evans, S.S., Repasky, E.A. and Fisher, D.T. (2015) “Fever and the Thermal Regulation of Immunity: The Immune System Feels the Heat.” *Nature Reviews. Immunology* 15 (6): 335–49.

Farez, S. and Morley, R.S. (1997) “Potential Animal Health Hazards of Pork and Pork Products.” *Revue Scientifique et Technique de l’OIE*.

Feliziani, F., Blome, S., Petrini, S., Giammarioli, M., Iscaro, C., Severi, G., Convito, L., Pietschmann, J., Beer, M., and De Mia, G. M. (2014). First assessment of classical swine fever marker vaccine candidate CP7_E2alf for oral immunization of wild boar under field conditions. *Vaccine*, 32(18), 2050–2055.

Fernandez, A., Hewicker, M., Trautwein, G., Pohlenz, J. and Liess, B. (1989) “Viral Antigen Distribution in the Central Nervous System of Cattle Persistently Infected with Bovine Viral Diarrhoea Virus.” *Veterinary Pathology* 26 (1): 26–32.

Fernández-Sainz, I. J., Largo, E., Gladue, D. P., Fletcher, P., O’Donnell, V., Holinka, L. G., Carey, L. B., Lu, X., Nieva, J. L. and Borca, M. V. (2014) “Effect of Specific Amino Acid Substitutions in the Putative Fusion Peptide of Structural Glycoprotein E2 on Classical Swine Fever Virus Replication.” *Virology* 456–457 (May): 121–30.

Finlaison, D.S. and Kirkland, P.D. (2020) “The Outcome of Porcine Foetal Infection with Bungowannah Virus Is Dependent on the Stage of Gestation at Which Infection Occurs. Part 2: Clinical Signs and Gross Pathology.” *Viruses* 12 (8).

Folgueiras-González, A., van den Braak, R., Simmelink, B., Deijs, M., van der Hoek, L. and de Groof, A. (2020) “Atypical Porcine Pestivirus Circulation and Molecular Evolution within an Affected Swine Herd.” *Viruses* 12 (10).

Frossard, J-P., Grierson, S., Cheney, T., Steinbach, F., Choudhury, B. and Williamson, S. (2017) “UK Pigs at the Time of Slaughter: Investigation into the Correlation of Infection with PRRSV and HEV.” *Viruses* 9 (6).

Frydas, I.S., and Nauwynck, H.J. (2016) “Replication Characteristics of Eight Virulent and Two Attenuated Genotype 1 and 2 Porcine Reproductive and Respiratory Syndrome Virus (PRRSV) Strains in Nasal Mucosa Explants.” *Veterinary Microbiology* 182 (January): 156–62.

Frydas, I.S., Verbeeck, M., Cao, J. and Nauwynck, H.J. (2013) “Replication Characteristics of Porcine Reproductive and Respiratory Syndrome Virus (PRRSV) European Subtype 1 (Lelystad) and Subtype 3 (Lena) Strains in Nasal Mucosa and Cells of the Monocytic Lineage: Indications for the Use of New Receptors of PRRSV (Lena).” *Veterinary Research* 44 (1): 1–14.

Ganges, L., Crooke, H.R., Bohórquez, J.A., Postel A., Sakoda, Y., Becher, P. and Ruggli, N. (2020) “Classical Swine Fever Virus: The Past, Present and Future.” *Virus Research* 289 (November): e198151.

Gatto, I.R.H., Arruda, P.H., Visek, C.A., Victoria, J.G., Patterson, A.R., Krull, A.C., Schwartz, K.J., de Oliveira, L.G. and Arruda, B.L. (2018a) “Detection of Atypical Porcine Pestivirus in Semen from Commercial Boar Studs in the United States.” *Transboundary and Emerging Diseases* 65 (2): e339–43.

Gatto, I.R.H., Harmon, K., Bradner, L., Silva, P., Linhares, D.C.L., Arruda, P.H., de Oliveira L.G. and Arruda, B. L. (2018b) “Detection of Atypical Porcine Pestivirus in Brazil in the Central Nervous System of Suckling Piglets with Congenital Tremor.” *Transboundary and Emerging Diseases*.

Gatto, I.R.H., Sonálio, K. and de Oliveira, L.G. (2019) “Atypical Porcine Pestivirus (APPV) as a New Species of Pestivirus in Pig Production.” *Frontiers in Veterinary Science* 6 (February): 35.

Givens, M.D. (2018) “Review: Risks of Disease Transmission through Semen in Cattle.” *Animal: An International Journal of Animal Bioscience* 12 (s1): s165–71.

Gong, Y., Trowbridge, R., Macnaughton, T. B., Westaway, E. G., Shannon, A. D., and Gowans, E. J. (1996) “Characterization of RNA Synthesis during a One-Step Growth Curve and of the Replication Mechanism of Bovine Viral Diarrhoea Virus.” *The Journal of General Virology* 77 (Pt 11) (11): 2729–36.

Graham, S. P., Everett, H. E., Haines, F. J., Johns, H. L., Sosan, O. A., Salguero, F. J., Clifford, D. J., Steinbach, F., Drew, T. W., and Crooke, H. R. (2012) Challenge of pigs with classical swine fever viruses after C-strain vaccination reveals remarkably rapid protection and insights into early immunity. *PloS one*, 7(1), e29310.

Grahofer, A., Zeeh, F. and Nathues, H. (2020) “Seroprevalence of Atypical Porcine Pestivirus in a Closed Pig Herd with Subclinical Infection.” *Transboundary and Emerging Diseases*, May. e13636.

Griebel, P.J. (2015) “BVDV Vaccination in North America: Risks versus Benefits.” *Animal Health Research Reviews / Conference of Research Workers in Animal Diseases* 16 (1): 27–32.

Grooms, D.L. (2004) “Reproductive Consequences of Infection with Bovine Viral Diarrhoea Virus.” *The Veterinary Clinics of North America. Food Animal Practice* 20 (1): 5–19.

Grummer, B., Grotha, S. and Greiser-Wilke, I. (2004) “Bovine Viral Diarrhoea Virus Is Internalized by Clathrin-Dependent Receptor-Mediated Endocytosis.” Journal of Veterinary Medicine. B, *Infectious Diseases and Veterinary Public Health* 51 (10): 427–32.

Guo, Z., Wang, L., Qiao, S., Deng, R. and Zhang, G. (2020) “Genetic Characterization and Recombination Analysis of Atypical Porcine Pestivirus.” *Infection, Genetics and Evolution: Journal of Molecular Epidemiology and Evolutionary Genetics in Infectious Diseases* 81 (July): e104259.

Haiwick, G., Hermann, J., Roof, M., Fergen, B., Philips, R. and Patterson, A. (2018) “Examination of Viraemia and Clinical Signs after Challenge with a Heterologous PRRSV Strain in PRRS Type 2 MLV Vaccinated Pigs: A Challenge-Dose Study.” *PloS One* 13 (12): e0209784.

Halbur, P.G., Paul, P.S., Frey, M.L., Landgraf, J., Eernisse, K., Meng, X.J., Lum, M.A., Andrews, J.J. and Rathje, J.A. (1995) “Comparison of the Pathogenicity of Two US Porcine Reproductive and Respiratory Syndrome Virus Isolates with That of the Lelystad Virus.” *Veterinary Pathology* 32 (6): 648–60.

Halbur, P.G., Andrews, J.J., Huffman, E.L., Paul, P.S., Meng, X-J. and Niyo, Y. (1994) “Development of a Streptavidin-Biotin Immunoperoxidase Procedure for the Detection of Porcine Reproductive and Respiratory Syndrome Virus Antigen in Porcine Lung.” *Journal of Veterinary Diagnostic Investigation: Official Publication of the American Association of Veterinary Laboratory Diagnosticians, Inc* 6 (2): 254–57.

Hansmann, D., Postel, A., Bächlein, C., Fischer, N., Alawi, M., Grundhoff, A., Derking, S., Tenhündfeld, J., Pfankuche, V.M., Herder, V., Wendt, M., Becher, P. and Baumgärtner, W. (2017) “Detection of a New Pestivirus in the Central Nervous System of Piglets with Congenital Tremors.” *Journal of Comparative Pathology* 1 (156): 59.

Harding, J.D., Done, J.T. and Darbyshire, J.H. (1966) “Congenital Tremors in Piglets and Their Relation to Swine Fever.” *The Veterinary Record* 79 (14): 388–90.

Harding, J.D., Done, J.T., Harbourne, J.F., Randall, C.J. and Gilbert, F.R. (1973) “Congenital Tremor Type A 3 in Pigs: An Hereditary Sex-Linked Cerebrospinal Hypomyelinogenesis.” *The Veterinary Record* 92 (20): 527–29.

Hardstaff, J., Hunt, H., Tugwell, L., Thomas, C., Elattar, L., Brownlie, J. and Booth, R. (2020). “Serological Survey of Wild Cervids in England and Wales for Bovine Viral Diarrhoea Virus.” *The Veterinary Record* 187 (7): e47.

Hause, B.M., Collin, E.A., Peddireddi, L., Yuan, F., Chen, Z., Hesse, R.A., Gauger, P.C., Clement, T., Fang, Y. and Anderson, G. (2015) “Discovery of a Novel Putative Atypical Porcine Pestivirus in Pigs in the USA.” *The Journal of General Virology* 96 (10): 2994–98.

Hause, B.M., Duff, J.W., Scheidt, A. and Anderson, G. (2016). “Virus Detection Using Metagenomic Sequencing of Swine Nasal and Rectal Swabs.” *Journal of Swine Health and Production* 24 (6): 304–8.

Hemmink, J.D., Morgan, S.B., Aramouni, M., Everett, H., Salguero, F.J., Canini, L., Porter, E., Chase-Topping, M., Beck, K., MacLoughlin, R., Carr, B.V., Brown, I.H., Bailey, M., Woolhouse, M., Brookes, S.M., Charleston, B. and Tchilian, E. (2016) “Distinct Immune Responses and Virus Shedding in Pigs Following Aerosol, Intra-Nasal and Contact Infection with Pandemic Swine Influenza A Virus, A (H1N1) 09.” *Veterinary Research* 47 (1): 1–15.

Henke, J., Carlson, J., Zani, L., Leidenberger, S., Schwaiger, T., Schlottau, K., Teifke, J. P., Schröder, C., Beer, M., and Blome, S. (2018). Protection against transplacental transmission of moderately virulent classical swine fever virus using live marker vaccine "CP7_E2alf". *Vaccine*, 36(29), 4181–4187.

Hewicker, M., Wöhrmann, T., Fernandez, A., Trautwein, G., Liess, B. and Moennig, V. (1990) “Immunohistological Detection of Bovine Viral Diarrhoea Virus Antigen in the Central Nervous System of Persistently Infected Cattle Using Monoclonal Antibodies.” *Veterinary Microbiology* 23 (1–4): 203–10.

Hines, R.K. and Lukert, P.D. (1994) “Porcine Circovirus as a Cause of Congenital Tremors in Newborn Pigs.” In *Proceedings of the American Association of Swine Practitioners*, 25:344–45.

Hou, Y., Zhang, H., Miranda, L. and Lin, S. (2010). “Serious Overestimation in Quantitative PCR by Circular (Supercoiled) Plasmid Standard: Microalgal Pcna as the Model Gene.” *PloS One* 5 (3): e9545.

Houben, S., van Reeth, K. and Pensaert, M.B. (1995) “Pattern of Infection with the Porcine Reproductive and Respiratory Syndrome Virus on Swine Farms in Belgium.” *Zentralblatt Fur Veterinarmedizin. Reihe B. Journal of Veterinary Medicine. Series B* 42 (4): 209–15.

Huang, Y. L., Deng, M. C., Wang, F. I., Huang, C. C., and Chang, C. Y. (2014) The challenges of classical swine fever control: modified live and E2 subunit vaccines. *Virus research*, 179, 1–11.

Jacobson, R. H. (1998) 'Validation of serological assays for diagnosis of infectious diseases', *Revue scientifique et technique (International Office of Epizootics)*. O.I.E (World Organisation for Animal Health), 17(2), pp. 469–526.

Jericho, K.W. and Langford, E.V. (1982) "Aerosol Vaccination of Calves with Pasteurella Haemolytica against Experimental Respiratory Disease." *Canadian Journal of Comparative Medicine* 46 (3): 287–92.

Ji, W., Guo, Z., Ding N.Z., He C.Q. (2015) "Studying classical swine fever virus: making the best of a bad virus." *Virus Research*. 2;197:35-47.

Jo, W.K., van Elk, C., van de Bildt, M., van Run, P., Petry, M., Jesse, S.T., Jung, K., Ludlow, M., Kuiken, T. and Osterhaus, A. (2019) "An Evolutionary Divergent Pestivirus Lacking the Npro Gene Systemically Infects a Whale Species." *Emerging Microbes and Infections* 8 (1): 1383–92.

Kasahara-Kamiie, M., Kagawa, M., Shiokawa, M., Sunaga, F., Fukase, Y., Aihara, N., Shiga, T., Kamiie, J., Aoki, H. and Nagai, M. (2021) "Detection and Genetic Analysis of a Novel Atypical Porcine Pestivirus from Piglets with Congenital Tremor in Japan." *Transboundary and Emerging Diseases*, 14149 (May).

Kaufmann, C., Stalder, H., Sidler, X., Renzullo, S., Gurtner, C., Grahofer, A. and Schweizer, M. 2019. "Long-Term Circulation of Atypical Porcine Pestivirus (APPV) within Switzerland." *Viruses*, 11 (7) 653

Keffaber, K.K. (1989) "Reproduction Failure of Unknown Etiology." *Am. Assoc. Swine Pract. Newsl.* 1: 1–9.

Keffaber, K., Stevenson, G., Van Alstine, W., Kanitz, C., Harris, L., Gorcyca, D., Schlesinger, K., Schultz, R., Chladek, D. and Morrison, R. (1992) "SIRS Virus Infection in Nursery/Grower Pigs." *American Association of Swine Practitioners Newsletter* 4 (4): 38–40.

Kennedy, J., Pfankuche, V.M., Hoeltig, D., Postel, A., Keuling, O., Ciurkiewicz, M., Baumgärtner, W., Becher, P. and Baechlein, C. (2019) "Genetic Variability of Porcine Pegivirus in Pigs from Europe and China and Insights into Tissue Tropism." *Scientific Reports* 9 (1): 8174.

Kennedy, S., Segalés, J., Rovira, A., Scholes, S., Domingo, M., Moffett, D., Meehan, B., O'Neill, R., McNeilly, F. and Allan, G. (2003). "Absence of Evidence of Porcine Circovirus Infection in Piglets with Congenital Tremors." *Journal of Veterinary Diagnostic Investigation: Official Publication of the American Association of Veterinary Laboratory Diagnosticians, Inc* 15 (2): 151–56.

Kernkamp, H.C.H. (1950). "Myoclonia Congenita; a Disease of Newborn Pigs." *Veterinary Medicine* 45 (5): 189–90.

Krey, T., Thiel, H. J., and Rümenapf, T. (2005). "Acid-resistant bovine pestivirus requires activation for pH-triggered fusion during entry." *Journal of virology*, 79(7), 4191–4200.

Khodakaram-Tafti, A., and Farjanikish, G.H. (2017). "Persistent Bovine Viral Diarrhoea Virus (BVDV) Infection in Cattle Herds." *Iranian Journal of Veterinary Research* 18 (3): 154–63.

Kidd, A.R., Done, J.T., Wrathall, A.E., Pampiglione, G. and Sweasey, D. (1986) "A New Genetically-Determined Congenital Nervous Disorder in Pigs." *The British Veterinary Journal* 142 (3): 275–85.

Kim, S-C., Jeong, C-G., Yoon, S-M., Lee, K-H., Yang, M-S., Kim, B., Lee, S-Y., Kang, S-J. and Kim, W-Il. (2017) "Detection of atypical porcine pestivirus (APPV) from a case of congenital tremor in Korea." *Korean Journal of Veterinary Service* 40 (3): 209–13.

King, A.M.Q., Lefkowitz, E., Adams, M.J. and Carstens, E.B. (2011). *Virus Taxonomy: Ninth Report of the International Committee on Taxonomy of Viruses*. Elsevier.

Kinsley, A.T. (1922) "Dancing Pigs." *Veterinary Medicine* 17 (123).

Kirkland, P.D., Richards, S.G., Rothwell, J.T. and Stanley, D.F. (1991) "Replication of Bovine Viral Diarrhoea Virus in the Bovine Reproductive Tract and Excretion of Virus in Semen during Acute and Chronic Infections." *The Veterinary Record* 128 (25): 587–90.

Kirkland, P.D., Le Potier, M-F. and Finlaison, D. (2019) "Pestiviruses." *Diseases of Swine*. Wiley.

Kitikoon, P., Vincent, A.L., Jones, K.R., Nilubol, D., Yu, S., Janke, B.H., Thacker, B.J. and Thacker, E.L. (2009) 'Vaccine efficacy and immune response to swine influenza virus challenge in pigs infected with porcine reproductive and respiratory syndrome virus at the time of SIV vaccination', *Veterinary microbiology*. Elsevier BV, 139(3–4), pp. 235–244.

Klinge, K.L., Vaughn, E.M., Roof, M.B., Bautista, E.M. and Murtaugh, M.P. (2009) “Age-Dependent Resistance to Porcine Reproductive and Respiratory Syndrome Virus Replication in Swine.” *Virology Journal* 6 (October): 177.

Knox, B., Askaa, J., Basse, A., Bitsch, V., Eskildsen, M., Mandrup, M., Ottosen, H.E., Overby, E., Pedersen, K.B. and Rasmussen, F. (1978) “Congenital Ataxia and Tremor with Cerebellar Hypoplasia in Piglets Borne by Sows Treated with Neguvon Vet. (Metrifonate, Trichlorfon) during Pregnancy.” *Nordisk Veterinaermedicin* 30 (12): 538–45.

Krakowka, S., Ellis, J.A., Meehan, B., Kennedy, S., McNeilly, F. and Allan, G. (2000) “Viral Wasting Syndrome of Swine: Experimental Reproduction of Postweaning Multisystemic Wasting Syndrome in Gnotobiotic Swine by Co-infection with Porcine Circovirus 2 and Porcine Parvovirus.” *Veterinary Pathology* 37 (3): 254–63.

Kralik, P. and Ricchi, M. (2017). “A Basic Guide to Real Time PCR in Microbial Diagnostics: Definitions, Parameters, and Everything.” *Frontiers in Microbiology* 8 (February): 108.

Kritas, S.K., Alexopoulos, C., Kyriakis, C.S., Tzika, E. and Kyriakis, S.C. (2007) “Performance of Fattening Pigs in a Farm Infected with Both Porcine Reproductive and Respiratory Syndrome (PRRS) Virus and Porcine Circovirus Type 2 Following Sow and Piglet Vaccination with an Attenuated PRRS Vaccine.” *Journal of Veterinary Medicine. A, Physiology, Pathology, Clinical Medicine* 54 (6): 287–91.

Kulcsár, G., Soós, P., Kucsera, L., Glávits, R. and Pálfi, V. (2001). “Pathogenicity of a Bovine Viral Diarrhoea Virus Strain in Pregnant Sows: Short Communication.” *Acta Veterinaria Hungarica* 49 (1): 117–20.

Kumar, N., Sharma, S., Barua, S., Tripathi, B.N. and Rouse, B.T. (2018) “Virological and Immunological Outcomes of Co-infections.” *Clinical Microbiology Reviews* 31 (4).

Labarque, G.G., Nauwynck, H.J., Van Reeth, K. and Pensaert, M.B. (2000). “Effect of Cellular Changes and Onset of Humoral Immunity on the Replication of Porcine Reproductive and Respiratory Syndrome Virus in the Lungs of Pigs.” *The Journal of General Virology* 81 (Pt 5): 1327–34.

Lamontagne, L., Pagé, C., Larochelle, R., and Magar, R. (2003) “Porcine Reproductive and Respiratory Syndrome Virus Persistence in Blood, Spleen, Lymph Nodes, and Tonsils of Experimentally Infected Pigs Depends on the Level of CD8high T Cells.” *Viral Immunology* 16 (3): 395–406.

Lamp, B., Schwarz, L., Högler, S., Riedel, C., Sinn, L., Rebel-Bauder, B., Weissenböck, H., Ladinig, A. and Rümenapf, T. (2017) “Novel Pestivirus Species in Pigs, Austria, 2015.” *Emerging Infectious Diseases* 23 (7): 1176–79.

Lanyon, S.R. and Reichel, M.P. (2013) “Understanding the Impact and Control of Bovine Viral Diarrhoea in Cattle Populations.” *Springer Science Reviews* 1 (1): 85–93.

Larsson, E.L. (1955) “Trembling in Piglets.” *Svenska Svinavelsforen Tidskr* 149.

Leforban, Y., Vannier, P. and Cariolet, R. (1992) “Protection of Piglets Born from Ruminant Pestivirus Experimentally Infected Sows, and Their Contacts, to the Challenge with Hog Cholera Virus.” *Annales de Recherches Veterinaires. Annals of Veterinary Research* 23 (1): 73–82.

Leveringhaus, E., Cagatay, G. N., Hardt, J., Becher, P., and Postel, A. (2022) "Different impact of bovine complement regulatory protein 46 (CD46bov) as a cellular receptor for members of the species Pestivirus H and Pestivirus G." *Emerging microbes and infections*, 11(1), 60–72.

Li, Z., He, Y., Xu, X., Leng, X., Li, S., Wen, Y., Wang, F., Xia, M., Cheng, S. and Wu, H. (2016) “Pathological and Immunological Characteristics of Piglets Infected Experimentally with a HP-PRRSV TJ Strain.” *BMC Veterinary Research* 12 (1): 230.

Liu, H., Shi, K., Sun, W., Zhao, J., Yin, Y., Si, H., Qu, S. and Lu, W. (2020) “Development a Multiplex RT-PCR Assay for Simultaneous Detection of African Swine Fever Virus, Classical Swine Fever Virus and Atypical Porcine Pestivirus.” *Journal of Virological Methods* 287 (October): 114006.

Liu, J., Li, Z., Ren, X., Li, H., Lu, R., Zhang, Y. and Ning, Z. (2019) “Viral Load and Histological Distribution of Atypical Porcine Pestivirus in Different Tissues of Naturally Infected Piglets.” *Archives of Virology* 164 (10): 2519–23.

Liu, J., Zhang, P., Chen, Y., Zhong, W., Li, B., Pi, M. and Ning, Z. (2021) “Vaccination with Virus-like Particles of Atypical Porcine Pestivirus Inhibits Virus Replication in Tissues of BALB/c Mice.” *Archives of Virology*, July.

Lunney, J.K., Fang, Y., Ladinig, A., Chen, N., Li, Y., Rowland, B. and Renukaradhya, G.J. (2016) “Porcine Reproductive and Respiratory Syndrome Virus (PRRSV): Pathogenesis and Interaction with the Immune System.” *Annual Review of Animal Biosciences* 4: 129–54.

Luo, Y., Li, S., Sun, Y., and Qiu, H. J. (2014). "Classical swine fever in China: a minireview". *Veterinary microbiology*, 172(1-2), 1–6.

Madson, D., Arruda, P. and Arruda, B. (2019) “Nervous and Locomotor System.” In *Diseases of Swine*, edited by Zimmerman, J., Karriker, L., Ramirez, A., Schwartz, K., Stevenson, G. and Zhang, J., 11:339–72. John Wiley & Sons, Inc., 111 River Street, Hoboken, NJ 07030, USA: Wiley.

Madera, R., Gong, W., Wang, L., Burakova, Y., Lleellish, K., Galliher-Beckley, A., Nietfeld, J., Henningson, J., Jia, K., Li, P., Bai, J., Schlup, J., McVey, S., Tu, C., and Shi, J. (2016) "Pigs immunized with a novel E2 subunit vaccine are protected from subgenotype heterologous classical swine fever virus challenge". *BMC veterinary research*,12(1), 197.

Martinez, D., Mari, B., Aumont, G. and Vidalenc, T. (1993) “Development of a Single Dilution ELISA to Detect Antibody to Dermatophilus Congolensis in Goat and Cattle Sera.” *Veterinary Microbiology* 34 (1): 47–62.

Mechler, M.L., Gomes, F.D.S., Nascimento, K.A., Souza-Pollo, A., Pires, F.F.B., Samara, S.I., Pituco, E.M. and Oliveira, L.G. (2018) “Congenital Tremor in Piglets: Is Bovine Viral Diarrhoea Virus an Etiological Cause?” *Veterinary Microbiology* 220 (July): 107–12.

Meuwissen, M.P., Horst, S.H., Huirne, R.B. and Dijkhuizen, A.A. (1999) “A Model to Estimate the Financial Consequences of Classical Swine Fever Outbreaks: Principles and Outcomes.” *Preventive Veterinary Medicine* 42 (3–4): 249–70.

Meyer, D., Fritsche, S., Luo, Y., Engemann, C., Blome, S., Beyerbach, M., Chang, C. Y., Qiu, H. J., Becher, P., and Postel, A. (2017). "The double-antigen ELISA concept for early detection of Erns -specific classical swine fever virus antibodies and application as an accompanying test for differentiation of infected from marker vaccinated animals". *Transboundary and emerging diseases*, 64(6), 2013–2022.

Michelitsch, A., Dalmann, A., Wernike, K., Reimann, I. and Beer, M. (2019) “Seroprevalences of Newly Discovered Porcine Pestiviruses in German Pig Farms.” *Veterinary Science in China* 6 (4).

Mikeska, T. and Dobrovic, A. (2009) “Validation of a Primer Optimisation Matrix to Improve the Performance of Reverse Transcription - Quantitative Real-Time PCR Assays.” *BMC Research Notes* 2 (June): 112.

Moes, L., and Wirth, M. (2007) "The internal initiation of translation in bovine viral diarrhea virus RNA depends on the presence of an RNA pseudoknot upstream of the initiation codon." *Virology journal* 4 (1): 124.

Mokili, J.L., Rohwer, F. and Dutilh, B.E. (2012). “Metagenomics and Future Perspectives in Virus Discovery.” *Current Opinion in Virology* 2 (1): 63–77.

Morgan, S.B., Frossard, J.P., Pallares, F.J., Gough, J., Stadejek, T., Graham, S.P., Steinbach, F., Drew, T.W. and Salguero, F.J. (2016) “Pathology and Virus Distribution in the Lung and Lymphoid Tissues of Pigs Experimentally Inoculated with Three Distinct Type 1 PRRS Virus Isolates of Varying Pathogenicity.” *Transboundary and Emerging Diseases* 63 (3): 285–95.

Mosadeghi, P. and Heydari-Zarnagh, H. (2018) “Development and Evaluation of a Novel ELISA for Detection of Antibodies against HTLV-I Using Chimeric Peptides.” *Iranian Journal of Allergy, Asthma, and Immunology* 17 (2): 144–50.

Mósena, A.C.S., Weber, M.N., da Cruz, R.A.S., Cibulski, S.P., da Silva, M.S., Puhl, D.E., Hammerschmitt, M.E., Takeuti, K.L., Driemeier, D., de Barcellos, D.E.S.N. and Canal, C.W. (2018) “Presence of Atypical Porcine Pestivirus (APPV) in Brazilian Pigs.” *Transboundary and Emerging Diseases* 65 (1): 22–26.

Mósena, A.C.S., Weber, M.N., Cibulski, S.P., Silva, M.S., Paim, W.P., Silva, G.S., Medeiros, A.A., Viana, N.A., Baumbach, L.F., Puhl, D.E., Silveira, S., Corbellini, L.G. and Canal, C.W. (2020) “Survey for Pestiviruses in Backyard Pigs in Southern Brazil.” *Journal of Veterinary Diagnostic Investigation: Official Publication of the American Association of Veterinary Laboratory Diagnosticians, Inc* 32 (1): 136–41.

Mou, C., Pan, S., Wu, H. and Chen, Z. (2021) “Disruption of Interferon-β Production by the Npro of Atypical Porcine Pestivirus.” *Virulence* 12 (1): 654–65.

Muñoz-González, S., Canturri, A., Pérez-Simó, M., Bohórquez, J.A., Rosell, R., Cabezón, O., Segalés, J., Domingo, M. and Ganges, L. (2017) “First Report of the Novel Atypical Porcine Pestivirus in Spain and a Retrospective Study.” *Transboundary and Emerging Diseases*.

Muñoz-González, S., Ruggli, N., Rosell, R., Pérez, L. J., Frías-Leuporeau, M. T., Fraile, L., Montoya, M., Cordoba, L., Domingo, M., Ehrensperger, F., Summerfield, A., and Ganges, L. (2015) “Postnatal Persistent Infection with Classical Swine Fever Virus and Its Immunological Implications.” *PLOS ONE*.

Nakagawa, S., Johnson, P.C.D. and Schielzeth, H. (2017). “The Coefficient of Determination R2 and Intra-Class Correlation Coefficient from Generalized Linear Mixed-Effects Models Revisited and Expanded.” https://doi.org/10.1101/095851.

Nakagawa, S., and Schielzeth, H. (2013) “A General and Simple Method for ObtainingR2from Generalized Linear Mixed-Effects Models.” *Methods in Ecology and Evolution*.

Nazki, S., Khatun, A., Jeong, C.G., Mattoo, S.U.S., Gu, S., Lee, S.I., Kim, S.C., Park, J.H., Yang, M.S., Kim, B., Park, C.K., Lee, S.M. and Kim, W.I. (2020) “Evaluation of Local and Systemic Immune Responses in Pigs Experimentally Challenged with Porcine Reproductive and Respiratory Syndrome Virus.” *Veterinary Research* 51 (1): 66.

Nelson, D.D., Dark, M.J., Bradway, D.S., Ridpath, J.F., Call, N., Haruna, J., Rurangirwa, F.R. and Evermann, J.F. (2008) “Evidence for Persistent Bovine Viral Diarrhoea Virus Infection in a Captive Mountain Goat (Oreamnos Americanus).” *Journal of Veterinary Diagnostic Investigation: Official Publication of the American Association of Veterinary Laboratory Diagnosticians, Inc* 20 (6): 752–59.

Netea, M.G., Kullberg, B.J. and Van der Meer, J.W. (2000) “Circulating Cytokines as Mediators of Fever.” *Clinical Infectious Diseases: An Official Publication of the Infectious Diseases Society of America* 31 Suppl 5 (October): S178-84.

Nettleton, P.F. and Entrican, G. (1995) “Ruminant Pestiviruses.” *The British Veterinary Journal* 151 (6): 615–42.

Nettleton, P.F., Gilray, J.A., Russo, P. and Dlissi, E. (1998) “Border Disease of Sheep and Goats.” *Veterinary Research* 29 (3–4): 327–40.

Nissley, S.M. (1932) “Shivers in Pigs.” *Journal of the American Veterinary Medical Association* 81 (551).

van Oirschot J. T. (2003). Vaccinology of classical swine fever: from lab to field. *Veterinary microbiology*, *96*(4), 367–384.

Oğuzoğlu, T.C. (2012). “A Review of Border Disease Virus Infection in Ruminants: Molecular Characterization, Pathogenesis, Diagnosis and Control.” *Animal Health, Prod and Hyg* 1: 1–9.

Olesen, A.S., Belsham, G.J., Rasmussen, T.B., Lohse, L., Bødker, R., Halasa, T., Boklund, A. and Bøtner, A. (2020) “Potential Routes for Indirect Transmission of African Swine Fever Virus into Domestic Pig Herds.” *Transboundary and Emerging Diseases* 67 (4): 1472–84.

O’Neill, R.G., O’Connor, M. and O’Reilly, P.J. (2004) “A Survey of Antibodies to Pestivirus in Sheep in the Republic of Ireland.” *Irish Veterinary Journal* 57 (9): 525.

Opriessnig, T., Giménez-Lirola, L.G. and Halbur, P.G. (2011) “Polymicrobial Respiratory Disease in Pigs.” *Animal Health Research Reviews / Conference of Research Workers in Animal Diseases* 12 (2): 133–48.

Ouyang, T., Zhang, X., Liu, X. and Ren, L. (2019) “Co-Infection of Swine with Porcine Circovirus Type 2 and Other Swine Viruses.” *Viruses* 11 (2).

Palfi, V., Houe, H. and Philipsen, J. (1993). “Studies on the Decline of Bovine Virus Diarrhoea Virus (BVD V) Maternal Antibodies and Detectability of BVDV in Persistently Infected Calves.” *Acta Veterinaria Scandinavica* 34 (1): 105–7.

Pan, S., Mou, C., Chen, Z. (2019)"An emerging novel virus: Atypical porcine pestivirus (APPV)." *Reviews in Medical Virology*. 29(1):e2018.

Pan, S., Yan, Y., Shi, K., Wang, M., Mou, C. and Chen, Z. (2019) “Molecular Characterization of Two Novel Atypical Porcine Pestivirus (APPV) Strains from Piglets with Congenital Tremor in China.” *Transboundary and Emerging Diseases* 66 (1): 35–42.

Papatsiros, V.G. (2012) “The Splay Leg Syndrome in Piglets: A Review.” *American Journal of Animal and Veterinary Sciences* 7 (2): 80–83.

Patterson, D.S., Done, J.T., Foulkes, J.A. and Sweasey, D. (1976). “Neurochemistry of the Spinal Cord in Congenital Tremor of Piglets (Type AII), a Spinal Dysmyelimogenesis of Infectious Origin.” *Journal of Neurochemistry* 26 (3): 481–85.

Patterson, D.S., Sweasey, D., Brush, P.J. and Harding, J.D. (1973). “Neurochemistry of the Spinal Cord in British Saddleback Piglets Affected with Congenital Tremor, Type A-IV, a Second Form of Hereditary Cerebrospinal Hypomyelinogenesis.” *Journal of Neurochemistry* 21 (2): 397–406.

Pedersen, K., Kristensen, C.S., Strandbygaard, B., Bøtner, A. and Rasmussen, T.B. (2021). “Detection of Atypical Porcine Pestivirus in Piglets from Danish Sow Herds.” *Viruses* 13 (5).

Pepin, B.J., Kittawornrat, A., Liu, F., Gauger, P.C., Harmon, K., Abate, S., Main, R., Garton, C., Hargrove, J., Rademacher, C., Ramirez, A. and Zimmerman, J. (2015) “Comparison of Specimens for Detection of Porcine Reproductive and Respiratory Syndrome Virus Infection in Boar Studs.” *Transboundary and Emerging Diseases* 62 (3): 295–304.

Peterhans, E., Jungi, T.W. and Schweizer, M. (2003) “BVDV and Innate Immunity.” *Biologicals: Journal of the International Association of Biological Standardization* 31 (2): 107–12.

Petry, D.B., Holl, J.W., Weber, J.S., Doster, A.R., Osorio, F.A. and Johnson, R.K. (2005) “Biological Responses to Porcine Respiratory and Reproductive Syndrome Virus in Pigs of Two Genetic Populations.” *Journal of Animal Science* 83 (7): 1494–1502.

Pfankuche, V.M., Hahn, K., Bodewes, R., Hansmann, F., Habierski, A., Haverkamp, A.K., Pfaender, S., Walter, S., Baechlein, C., Postel, A., Steinmann, E., Becher, P., Osterhaus, A., Baumgärtner, W. and Puff, C. (2018) “Comparison of Different In Situ Hybridization Techniques for the Detection of Various RNA and DNA Viruses.” *Viruses* 10 (7).

Pileri, E. and Mateu, E. (2016) “Review on the Transmission Porcine Reproductive and Respiratory Syndrome Virus between Pigs and Farms and Impact on Vaccination.” *Veterinary Research* 47 (1): 108.

Pogranichniy, R.M., Schwartz, K.J. and Yoon, K-J. (2008) “Isolation of a Novel Viral Agent Associated with Porcine Reproductive and Neurological Syndrome and Reproduction of the Disease.” *Veterinary Microbiology* 131 (1): 35–46.

Poole, T. L., Wang, C., Popp, R. A., Potgieter, L. N., Siddiqui, A. and Collett, M. S. (1995) “Pestivirus Translation Initiation Occurs by Internal Ribosome Entry.” *Virology* 206 (1): 750–54.

Pomorska-Mól, M., Podgórska, K., Czyżewska-Dors, E., Turlewicz-Podbielska, H., Gogulski, M., Włodarek, J. and Łukomska, A. (2020) “Kinetics of Single and Dual Simultaneous Infection of Pigs with Swine Influenza A Virus and Porcine Reproductive and Respiratory Syndrome Virus.” *Journal of Veterinary Internal Medicine / American College of Veterinary Internal Medicine* 34 (5): 1903–13.

Possatti, F., Headley, S.A., Leme, R.A., Dall Agnol, A.M., Zotti, E., de Oliveira, T.E.S., Alfieri, A.F. and Alfieri, A.A. (2018a) “Viruses Associated with Congenital Tremor and High Lethality in Piglets.” *Transboundary and Emerging Diseases* 65 (2): 331–37.

Possatti, F., de Oliveira, T.E.S., Leme, R.A., Zotti, E., Dall Agnol, A.M., Alfieri, A.F., Headley, S.A. and Alfieri, A.A. (2018b) “Pathologic and Molecular Findings Associated with Atypical Porcine Pestivirus Infection in Newborn Piglets.” *Veterinary Microbiology* 227 (December): 41–44.

Postel, A., Hansmann, F., Baechlein, C., Fischer, N., Alawi, M., Grundhoff, A., Derking, S., Tenhündfeld, J., Pfankuche, V.M., Herder, V., Baumgärtner, W., Wendt, M. and Becher, P. (2016) “Presence of Atypical Porcine Pestivirus (APPV) Genomes in Newborn Piglets Correlates with Congenital Tremor.” *Scientific Reports* 6 (June): 27735.

Postel, A., Meyer, D., Cagatay, G.N., Feliziani, F., De Mia, G.M., Fischer, N., Grundhoff, A., Milićević, V., Deng, M.C., Chang, C.Y., Qiu, H.J., Sun, Y., Wendt, M. and Becher, P. (2017a) “High Abundance and Genetic Variability of Atypical Porcine Pestivirus in Pigs from Europe and Asia.” *Emerging Infectious Diseases* 23 (12): 2104–7.

Postel, A., Meyer, D., Petrov, A., and Becher, P. (2017b) “Recent Emergence of a Novel Porcine Pestivirus: Interference with Classical Swine Fever Diagnosis?” *Emerging Microbes and Infections* 6 (4): e19.

Potgieter, L.N. (1997) “Bovine Respiratory Tract Disease Caused by Bovine Viral Diarrhoea Virus.” *The Veterinary Clinics of North America. Food Animal Practice* 13 (3): 471–81.

Qu, Y., Berghman, L.R. and Vandesande, F. (1998). “An Electrochemical Enzyme Immunoassay for Chicken Luteinizing Hormone: Extension of the Detection Limit by Adequate Control of the Nonspecific Adsorption.” *Analytical Biochemistry* 259 (2): 167–75.

R Core Team. (2019) “R: A Language and Environment for Statistical Computing.” Vienna, Austria: R Foundation for Statistical Computing. https://www.R-project.org/.

Reed, G.F., Lynn, F. and Meade, B.D. (2002) “Use of Coefficient of Variation in Assessing Variability of Quantitative Assays.” *Clinical and Diagnostic Laboratory Immunology* 9 (6): 1235–39.

Riedel, C., Aitkenhead, H., El Omari, K. and Rümenapf, T. (2021) “Atypical Porcine Pestiviruses: Relationships and Conserved Structural Features.” *Viruses* 13 (5).

Riedel, C., Lamp, B., Hagen, B., Indik, S. and Rümenapf, T. 2017. “The Core Protein of a Pestivirus Protects the Incoming Virus against IFN-Induced Effectors.” *Scientific Reports* 7 (March): 44459.

Riedel, C., Lamp, B., Heimann, M., & Rümenapf, T. (2010). Characterisation of essential domains and plasticity of the classical Swine Fever virus Core protein. *Journal of virology*, 84 (21), 11523–11531.

Rossow, K.D., Bautista, E.M., Goyal, S.M., Molitor, T.W., Murtaugh, M.P., Morrison, R.B., Benfield, D.A. and Collins, J.E. (1994) “Experimental Porcine Reproductive and Respiratory Syndrome Virus Infection in One-, Four-, and 10-Week-Old Pigs.” *Journal of Veterinary Diagnostic Investigation: Official Publication of the American Association of Veterinary Laboratory Diagnosticians, Inc* 6 (1): 3–12.

Rossow, K.D. (1998) ‘Porcine Reproductive and Respiratory Syndrome’, *Veterinary Pathology*, pp. 1–20.

Rovira, A., Clement, T., Christopher-Hennings, J., Thompson, B., Engle, M., Reicks, D., & Muñoz-Zanzi, C. (2007) "Evaluation of the Sensitivity of Reverse-Transcription Polymerase Chain Reaction to Detect Porcine Reproductive and Respiratory Syndrome Virus on Individual and Pooled Samples from Boars". *Journal of Veterinary Diagnostic Investigation*, 19(5), 502–509.

Rümenapf, T., Unger, G., Strauss, J. H., and Thiel, H. J. (1993) “Processing of the Envelope Glycoproteins of Pestiviruses.” *Journal of Virology* 67 (6): 3288–94.

Rychlik, W., Spencer, W.J. and Rhoads, R.E. (1990) “Optimization of the Annealing Temperature for DNA Amplification in Vitro.” *Nucleic Acids Research* 18 (21): 6409–12.

Salguero, F.J., Frossard, J-P., Rebel, J.M.J., Stadejek, T., Morgan, S.B., Graham, S.P. and Steinbach, F. (2015) “Host–Pathogen Interactions during Porcine Reproductive and Respiratory Syndrome Virus 1 Infection of Piglets.” *Virus Research* 202 (April): 135–43.

Sandvik, T. (2014) “Border Disease Virus: Time to Take More Notice?” *The Veterinary Record* 174 (3): 65–66.

Sawyer, M.M. (1992) “Border Disease of Sheep: The Disease in the Newborn, Adolescent and Adult.” *Comparative Immunology, Microbiology and Infectious Diseases* 15 (3): 171–77.

Schirrmeier, H., Strebelow, G., Depner, K., Hoffmann, B. and Beer, M. (2004) “Genetic and Antigenic Characterization of an Atypical Pestivirus Isolate, a Putative Member of a Novel Pestivirus Species.” *The Journal of General Virology* 85 (Pt 12): 3647–52.

Schmeiser, S., Mast, J., Thiel, H. J., and König, M. (2014) "Morphogenesis of pestiviruses: new insights from ultrastructural studies of strain Giraffe-1." *Journal of virology*, 88(5), 2717–2724.

Schumacher, T., Röntgen, M. and Maak, S. (2021) “Congenital Splay Leg Syndrome in Piglets-Current Knowledge and a New Approach to Etiology.” *Frontiers in Veterinary Science* 8 (February): 609883.

Schwarz, L., Riedel, C., Högler, S., Sinn, L.J., Voglmayr, T., Wöchtl, B., Dinhopl, N., Rebel-Bauder, B., Weissenböck, H., Ladinig, A., Rümenapf, T. and Lamp, B. (2017) “Congenital Infection with Atypical Porcine Pestivirus (APPV) Is Associated with Disease and Viral Persistence.” *Veterinary Research* 48 (1): 1.

Scottish Government. (2019) *Scottish BVD Eradication Scheme: guidance*. Available at: https://www.gov.scot/publications/scottish-bvd-eradication-scheme/pages/screening/ (Accessed: 28 June 2021).

Scottish Government. (2020) *Scottish Agricultural Census: final results - June 2020*, *The Scottish Government*. Available at: https://www.gov.scot/publications/scottish-agricultural-census-final-results-june-2020/ (Accessed: 13 July 2021).

Sentsui, H., Nishimori, T., Kirisawa, R. and Morooka, A. (2001) “Mucosal Disease Induced in Cattle Persistently Infected with Bovine Viral Diarrhoea Virus by Antigenically Different Cytopathic Virus.” *Archives of Virology* 146 (5): 993–1006.

Shen, H., Liu, X., Zhang, P., Wang, L., Liu, Y., Zhang, L., Liang, P. and Song, C. (2018) “Identification and Characterization of Atypical Porcine Pestivirus Genomes in Newborn Piglets with Congenital Tremor in China.” *Journal of Veterinary Science* 19 (3): 468–71.

Shi, B. J., Liu, C. C., Zhou, J., Wang, S. Q., Gao, Z. C., Zhang, X. M., Zhou, B., and Chen, P. Y. (2016) "Entry of Classical Swine Fever Virus into PK-15 Cells via a pH-, Dynamin-, and Cholesterol-Dependent, Clathrin-Mediated Endocytic Pathway That Requires Rab5 and Rab7." *Journal of virology*, 90 (20), 9194–9208.

Shi, K., Xie, S., Sun, W., Liu, H., Zhao, J., Yin, Y., Si, H., Qu, S. and Lu, W. (2021) “Evolution and Genetic Diversity of Atypical Porcine Pestivirus (APPV) from Piglets with Congenital Tremor in Guangxi Province, Southern China.” *Veterinary Medicine and Science* 7 (3): 714–23.

Simonet, B.M. (2005) “Quality Control in Qualitative Analysis.” *Trends in Analytical Chemistry: TRAC* 24 (6): 525–31.

Smith, D.B., Meyers, G., Bukh, J., Gould, E.A., Monath, T., Scott Muerhoff, A., Pletnev, A., Rico-Hesse, R., Stapleton, J.T., Simmonds, P. and Becher, P. (2017) “Proposed Revision to the Taxonomy of the Genus Pestivirus, Family Flaviviridae.” *The Journal of General Virology* 98 (8): 2106–12.

Smit, J. M., Moesker, B., Rodenhuis-Zybert, I. and Wilschut, J. (2011). Flavivirus cell entry and membrane fusion. *Viruses*, *3*(2), 160–171.

Sozzi, E., Salogni, C., Lelli, D., Barbieri, I., Moreno, A., Alborali, G.L. and Lavazza, A. (2019) “Molecular Survey and Phylogenetic Analysis of Atypical Porcine Pestivirus (APPV) Identified in Swine and Wild Boar from Northern Italy.” *Viruses* 11 (12).

Stadejek, T., Larsen, L.E., Podgórska, K., Bøtner, A., Botti, S., Dolka, I., Fabisiak, M., Heegaard, P.M.H., Hjulsager, C.K., Huć, T., Kvisgaard, L.K., Sapierzyński, R. and Nielsen, J. (2017) “Pathogenicity of Three Genetically Diverse Strains of PRRSV Type 1 in Specific Pathogen Free Pigs.” *Veterinary Microbiology* 209 (September): 13–19.

Stadejek, T., Oleksiewicz, M.B., Scherbakov, A.V., Timina, A.M., Krabbe, J.S., Chabros, K. and Potapchuk, D. (2008). “Definition of Subtypes in the European Genotype of Porcine Reproductive and Respiratory Syndrome Virus: Nucleocapsid Characteristics and Geographical Distribution in Europe.” *Archives of Virology* 153 (8): 1479–88.

Steinitz, M. (2000). “Quantitation of the Blocking Effect of Tween 20 and Bovine Serum Albumin in ELISA Microwells.” *Analytical Biochemistry* 282 (2): 232–38.

Stenberg, H., Jacobson, M., and Malmberg, M. (2020). “A Review of Congenital Tremor Type A-II in Piglets.” *Animal Health Research Reviews / Conference of Research Workers in Animal Diseases* 21 (1): 84–88.

Stenberg, H, Leveringhaus, E., Malmsten, A., Dalin, A-M., Postel, A. and Malmberg, M. (2021). “Atypical Porcine Pestivirus – a Widespread Virus in the Swedish Wild Boar Population.” *Transboundary and Emerging Diseases*.

Stevenson, G.W., Kiupel, M., Mittal, S.K., Choi, J., Latimer, K.S. and Kanitz. C.L. (2001) “Tissue Distribution and Genetic Typing of Porcine Circoviruses in Pigs with Naturally Occurring Congenital Tremors.” *Journal of Veterinary Diagnostic Investigation: Official Publication of the American Association of Veterinary Laboratory Diagnosticians, Inc* 13 (1): 57–62.

Strong, R., La Rocca, S.A., Paton, D., Bensaude, E., Sandvik, T., Davis, L., Turner, J., Drew, T., Raue, R., Vangeel, I. and Steinbach, F. (2015) “Viral Dose and Immunosuppression Modulate the Progression of Acute BVDV-1 Infection in Calves: Evidence of Long Term Persistence after Intra-Nasal Infection.” *PloS One* 10 (5): e0124689.

Sur, J.H., Cooper, V.L., Galeota, J.A., Hesse, R.A., Doster, A.R., and Osorio, F.A. (1996) “In Vivo Detection of Porcine Reproductive and Respiratory Syndrome Virus RNA by in Situ Hybridization at Different Times Postinfection.” *Journal of Clinical Microbiology* 34 (9): 2280–86.

Suradhat, S., Damrongwatanapokin, S., and Thanawongnuwech, R. (2007). "Factors critical for successful vaccination against classical swine fever in endemic areas." Veterinary microbiology, 119(1), 1–9.

Sutton, K.M., Lahmers, K.K., Harris, S.P., Wijesena, H.R., Mote, B.E., Kachman, S.D., Borza, T. and Ciobanu, D.C. (2019) “Detection of Atypical Porcine Pestivirus Genome in Newborn Piglets Affected by Congenital Tremor and High Preweaning Mortality.” *Journal of Animal Science* 97 (10): 4093–4100.

Tao, J., Liao, J., Wang, Y., Zhang, X., Wang, J. and Zhu, G. (2013). “Bovine Viral Diarrhoea Virus (BVDV) Infections in Pigs.” *Veterinary Microbiology* 165 (3–4): 185–89.

Tarradas, J., de la Torre, M.E., Rosell, R., Perez, L.J., Pujols, J., Muñoz, M., Muñoz, I., Muñoz, S., Abad, X., Domingo, M., Fraile, L. and Ganges, L. (2014) “The Impact of CSFV on the Immune Response to Control Infection.” *Virus Research* 185 (June): 82–91.

Tautz, N., Tews, B. and Meyers, G. (2015) “The Molecular Biology of Pestiviruses.” In *Advances in Virus Research*, edited by M. Kielian, K. Maramorosch, and T. Mettenleiter, 93:47–160. Academic Press.

Terpstra, C. and Wensvoort, G. (1988) “Natural Infections of Pigs with Bovine Viral Diarrhoea Virus Associated with Signs Resembling Swine Fever.” *Research in Veterinary Science* 45 (2): 137–42.

Terpstra, C., and Kroese, A. H. (1996). "Potency control of modified live viral vaccines for veterinary use." *Vaccine*, 14(6), 570–575.

Tian, K., Yu, X., Zhao, T., Feng, Y., Cao, Z., Wang, C., Hu, Y., Chen, X., Hu, D., Tian, X., Liu, D., Zhang, S., Deng, X., Ding, Y., Yang, L., Zhang, Y., Xiao, H., Qiao, M., Wang, B., Hou, L., Wang, X., Yang, X., Kang, L., Sun, M., Jin, P., Wang, S., Kitamura, Y., Yan, J. and Gao, GF. (2007) “Emergence of Fatal PRRSV Variants: Unparalleled Outbreaks of Atypical PRRS in China and Molecular Dissection of the Unique Hallmark.” *PloS One* 2 (6): e526.

Toplu, N., Oguzoglu, T.Ç., Epikmen, E.T. and Aydogan, A. (2011) “Neuropathologic Study of Border Disease Virus in Naturally Infected Fetal and Neonatal Small Ruminants and Its Association with Apoptosis.” *Veterinary Pathology* 48 (3): 576–83.

Tummaruk, P. and Pearodwong, P. (2016) “Porcine Circovirus Type 2 Expression in the Brain of Neonatal Piglets with Congenital Tremor.” *Comparative Clinical Pathology* 25 (4): 727–32.

Valiakos, G., Athanasiou, L.V., Touloudi, A., Papatsiros, V., Spyrou, V., Petrovska, L. and Billinis, C. (2013). West Nile Virus: Basic Principles, Replication Mechanism, Immune Response and Important Genetic Determinants of Virulence. In (Ed.), Viral Replication. IntechOpen. https://doi.org/10.5772/55198

Vannier, P., Plateau, E., and Tillon, J.P. (1981) “Congenital Tremor in Pigs Farrowed from Sows given Hog Cholera Virus during Pregnancy.” *American Journal of Veterinary Research* 42 (1): 135–37.

Wang, Q., Zhou, H., Hao, Q., Li, M., Liu, J. and Fan, H. (2020) “Co-infection with Porcine Circovirus Type 2 and Streptococcus Suis Serotype 2 Enhances Pathogenicity by Dysregulation of the Immune Responses in Piglets.” *Veterinary Microbiology* 243 (April): 108653.

Wang, Y., Xu, W. Maddera, L., Tsuchiya, D., Thomas, N., Yu, C.R. and Parmely, T. (2019) “Alkaline Phosphatase-Based Chromogenic and Fluorescence Detection Method for BaseScope™ In Situ Hybridization.” *Journal of Histotechnology* 42 (4): 193–201.

Weber, M.N., Streck, A.F., Silveira, S., Mósena, A.C.S., da Silva, M.S. and Canal, C.W. (2015) “Homologous Recombination in Pestiviruses: Identification of Three Putative Novel Events between Different Subtypes/Genogroups.” *Infection, Genetics and Evolution: Journal of Molecular Epidemiology and Evolutionary Genetics in Infectious Diseases* 30 (March): 219–24.

Wen, L., Mao, A., Jiao, F., Zhang, D., Xie, J. and He, K. (2018) “Evidence of Porcine Circovirus-like Virus P1 in Piglets with an Unusual Congenital Tremor.” *Transboundary and Emerging Diseases* 65 (2): e501–4.

Wensvoort, G., Terpstra, C., Pol, J.M., ter Laak, E.A., Bloemraad, M., de Kluyver, E.P., Kragten, C., van Buiten, L., den Besten, A. and Wagenaar, F. (1991) “Mystery Swine Disease in The Netherlands: The Isolation of Lelystad Virus.” *The Veterinary Quarterly* 13 (3): 121–30.

Wesley, R.D., Lager, K.M. and Kehrli, M.E. Jr. (2006) “Infection with Porcine Reproductive and Respiratory Syndrome Virus Stimulates an Early Gamma Interferon Response in the Serum of Pigs.” *Canadian Journal of Veterinary Research = Revue Canadienne de Recherche Veterinaire* 70 (3): 176–82.

Williamson, S. (2017) “Congenital Tremor Associated with Atypical Porcine Pestivirus.” *The Veterinary Record* 180 (2): 42–43.

Williamson, S, Frossard, J-P. and Thomson, J. (2018) “PRRS Diagnoses in Great Britain 2016/17.” *The Veterinary Record* 182 (5): 133–35.

Wood, S. and Scheipl, F. (2017) “Package’gamm4’: Generalized Additive Mixed Models Using’mgcv’and’lme4’.” *Version 0. 2-5. Published* 25 (07): 2017.

World Organisation for Animal Health (2021) *Animal Diseases*. Available at: https://www.oie.int/en/what-we-do/animal-health-and-welfare/animal-diseases/?_paged=3 (Accessed: 26 August 2021).

Wu, S., Wang, Z., Zhang, W. and Deng, S. (2018) “Complete Genome Sequence of an Atypical Porcine Pestivirus Isolated from Jiangxi Province, China.” *Genome Announcements* 6 (24). https://doi.org/10.1128/genomea .00439-18.

Wu, Z., Ren, X., Yang, L., Hu, Y., Yang, J., He, G., Zhang, J., Dong, J., Sun, L., Du, J., Liu, L., Xue, Y., Wang, J., Yang, F., Zhang, S. and Jin, Q. (2012) “Virome Analysis for Identification of Novel Mammalian Viruses in Bat Species from Chinese Provinces.” *Journal of Virology*. https://doi.org/10.1128/jvi.0139-12.

Wu, Z., Liu, B., Du, J., Zhang, J., Lu, L., Zhu, G., Han, Y., Su, H., Yang, L., Zhang, S., Liu, Q. and Jin, Q. (2018) “Discovery of Diverse Rodent and Bat Pestiviruses With Distinct Genomic and Phylogenetic Characteristics in Several Chinese Provinces.” *Frontiers in Microbiology* 9 (October): 2562.

Xie, Y., Wang, X., Su, D., Feng, J., Wei, L., Cai, W., Li, J., Lin, S., Yan, H. and He, D. (2019) “Detection and Genetic Characterization of Atypical Porcine Pestivirus in Piglets With Congenital Tremors in Southern China.” *Frontiers in Microbiology* 10 (June): 1406.

Yan, X.L., Li, Y.Y., He, L.L., Wu, J.L., Tang, X.Y., Chen, G.H., Mai, K.J., Wu, R.T., Li, Q.N., Chen, Y.H., Sun, Y. and Ma, J.Y. (2019) “12 Novel Atypical Porcine Pestivirus Genomes from Neonatal Piglets with Congenital Tremors: A Newly Emerging Branch and High Prevalence in China.” *Virology* 533 (July): 50–58.

Yang, C., Wang, L., Shen, H., Zheng, Y., Bade, S.A., Gauger, P.C., Chen, Q., Zhang, J., Guo, B., Yoon, K.J., Harmon, K.M., Main, R.G. and Li, G. (2018) “Detection and Genetic Characterization of Porcine Pegivirus in Pigs in the United States.” *Transboundary and Emerging Diseases* 65 (3): 618–26.

Yarnall, M.J. and Thrusfield, M.V. (2017) “Engaging Veterinarians and Farmers in Eradicating Bovine Viral Diarrhoea: A Systematic Review of Economic Impact.” *The Veterinary Record* 181 (13): 347.

Yin, Y., Shi, K., Sun, W. and Mo, S. (2019) “Complete Genome Sequence of an Atypical Porcine Pestivirus Strain, GX01-2018, from Guangxi Province, China.” *Microbiology Resource Announcements* 8 (6). https://doi.org/10.1128/ MRA.01440-18.

Yoon, I.J., Joo, H., Christianson, W.T., Morrison, R.B. and Dial, G.D. (1993) “Persistent and Contact Infection in Nursery Pigs Experimentally Infected with Porcine Reproductive and Respiratory Syndrome (PRRS) Virus.” *Swine Health Prod* 1 (4): 5–8.

Yuan, F., Feng, Y., Bai, J., Liu, X., Arruda, B., Anbalagan, S. and Peddireddi, L. (2021) “Genetic Diversity and Prevalence of Atypical Porcine Pestivirus in the Midwest of US Swine Herds during 2016-2018.” *Transboundary and Emerging Diseases*, February.

Yuan, J., Han, Z., Li, J., Huang, Y., Yang, J., Ding, H., Zhang, J., Zhu, M., Zhang, Y., Liao, J., Zhao, M. and Chen, J. (2017) “Atypical Porcine Pestivirus as a Novel Type of Pestivirus in Pigs in China.” *Frontiers in Microbiology* 8 (May): 862.

Zhang, H., Wen, W., Hao, G., Hu, Y., Chen, H., Qian, P. and Li, X. (2018a) “Phylogenetic and Genomic Characterization of a Novel Atypical Porcine Pestivirus in China.” *Transboundary and Emerging Diseases* 65 (1): e202–4.

Zhang, H, Wen, W., Hao, G., Chen, H., Qian, P., and Li, X. (2018b) “A Subunit Vaccine Based on E2 Protein of Atypical Porcine Pestivirus Induces Th2-Type Immune Response in Mice.” *Viruses* 10 (12).

Zhang, K., Wu, K., Liu, J., Ge, S., Xiao, Y., Shang, Y. and Ning, Z. (2017) “Identification of Atypical Porcine Pestivirus Infection in Swine Herds in China.” *Transboundary and Emerging Diseases* 64 (4): 1020–23.

Zheng, G., Li, L. F., Zhang, Y., Qu, L., Wang, W., Li, M., Yu, S., Zhou, M., Luo, Y., Sun, Y., Munir, M., Li, S., and Qiu, H. J. (2020) "MERTK is a host factor that promotes classical swine fever virus entry and antagonizes innate immune response in PK-15 cells." *Emerging microbes and infections*, 9(1), 571–581.

Zhou, K, Yue, H., Tang, C., Ruan, W., Zhou, Q. and Zhang, B. (2019) “Prevalence and Genome Characteristics of Atypical Porcine Pestivirus in Southwest China.” *The Journal of General Virology* 100 (1): 84–88.